



UNIVERSITAT DE  
BARCELONA

## CPT1AM overexpression in BAT from HFD-treated mice prevents the induction of obesity and associated diabetes

Marianela Pía Bastías Pérez

**ADVERTIMENT.** La consulta d'aquesta tesi queda condicionada a l'acceptació de les següents condicions d'ús: La difusió d'aquesta tesi per mitjà del servei TDX ([www.tdx.cat](http://www.tdx.cat)) i a través del Dipòsit Digital de la UB ([diposit.ub.edu](http://diposit.ub.edu)) ha estat autoritzada pels titulars dels drets de propietat intel·lectual únicament per a usos privats emmarcats en activitats d'investigació i docència. No s'autoritza la seva reproducció amb finalitats de lucre ni la seva difusió i posada a disposició des d'un lloc aliè al servei TDX ni al Dipòsit Digital de la UB. No s'autoritza la presentació del seu contingut en una finestra o marc aliè a TDX o al Dipòsit Digital de la UB (framing). Aquesta reserva de drets afecta tant al resum de presentació de la tesi com als seus continguts. En la utilització o cita de parts de la tesi és obligat indicar el nom de la persona autora.

**ADVERTENCIA.** La consulta de esta tesis queda condicionada a la aceptación de las siguientes condiciones de uso: La difusión de esta tesis por medio del servicio TDR ([www.tdx.cat](http://www.tdx.cat)) y a través del Repositorio Digital de la UB ([diposit.ub.edu](http://diposit.ub.edu)) ha sido autorizada por los titulares de los derechos de propiedad intelectual únicamente para usos privados enmarcados en actividades de investigación y docencia. No se autoriza su reproducción con finalidades de lucro ni su difusión y puesta a disposición desde un sitio ajeno al servicio TDR o al Repositorio Digital de la UB. No se autoriza la presentación de su contenido en una ventana o marco ajeno a TDR o al Repositorio Digital de la UB (framing). Esta reserva de derechos afecta tanto al resumen de presentación de la tesis como a sus contenidos. En la utilización o cita de partes de la tesis es obligado indicar el nombre de la persona autora.

**WARNING.** On having consulted this thesis you're accepting the following use conditions: Spreading this thesis by the TDX ([www.tdx.cat](http://www.tdx.cat)) service and by the UB Digital Repository ([diposit.ub.edu](http://diposit.ub.edu)) has been authorized by the titular of the intellectual property rights only for private uses placed in investigation and teaching activities. Reproduction with lucrative aims is not authorized nor its spreading and availability from a site foreign to the TDX service or to the UB Digital Repository. Introducing its content in a window or frame foreign to the TDX service or to the UB Digital Repository is not authorized (framing). Those rights affect to the presentation summary of the thesis as well as to its contents. In the using or citation of parts of the thesis it's obliged to indicate the name of the author.



UNIVERSITAT DE  
BARCELONA

UNIVERSITAT DE BARCELONA  
FACULTAT DE FARMÀCIA I CIÈNCIES DE L'ALIMENTACIÓ

**CPT1AM overexpression in BAT from HFD-treated mice  
prevents the induction of obesity and associated diabetes**

Marianela Pía Bastías Pérez

2022





UNIVERSITAT DE  
BARCELONA

FACULTAT DE FARMÀCIA I CIÈNCIES DE L'ALIMENTACIÓ  
Programa de doctorat en Biotecnologia

**CPT1AM overexpression in BAT from HFD-treated mice  
prevents the induction of obesity and associated diabetes**

Memòria presentada per Marianela Pía Bastías Pérez per optar al títol de  
doctor per la Universitat de Barcelona

Laura Herrero Rodríguez

Dolors Serra Cucurull

Marianela Pía Bastías Pérez

Barcelona, 2022



# **AGRADECIMIENTOS**

**“Nada en la vida es para ser temido, es sólo para ser comprendido. Ahora es el momento de entender más, de modo que podamos temer menos”**

Marie Curie (1867 – 1934)

Ésta es sin duda la parte más difícil de la tesis, redactar en un par de hojas, los agradecimientos y sentimientos relacionados a las personas y lugares, que fueron parte importante en este desafío de vida, el cual fue mi doctorado. El doctorado fue un desafío que comenzó incluso antes de iniciar mi formación de grado como Nutricionista, en Chile. Cuando entré a la Universidad siempre supe que quería especializarme y continuar estudios de postgrado. Quería ser profesora universitaria, dedicarme a la investigación científica y a la docencia, y para entrar a la academia debía perseguir dicha meta. Esta historia comienza en mis ganas de volar y salir del nido, conocer nuevas experiencias de vida, realidades, aventuras, desafíos, conocer gente hermosa en el camino que sin duda dejan huellas en el corazón y contribuyen al crecimiento personal.

Mis ganas de migrar comenzaron mientras estudié en la UBB (Universidad del Bío-Bío), en la ciudad de Chillán, decimosexta región de Chile, la región de Ñuble. Allí tuve mi primer acercamiento con la académica, la UBB me dio muchas oportunidades con las cuales adquirí mis primeras experiencias laborales realizando ayudantías que comprendían parte de docencia en la Universidad. Posteriormente, me dieron una beca para realizar una estancia en España, aquí tuve la primera oportunidad de ir a España, lugar que elegí para vivir posteriormente. La UBB ha sido muy importante para mí, considerando que me ha entregado conocimiento, experiencia y oportunidades, por tanto, comienzo agradeciendo a esta Institución que me formó como una Nutricionista Integral, con la capacidad de seguir lo que yo quisiera, me entregó conocimiento con los cuales me he podido defender en las grandes ligas y ahora a punto de doctorarme, valoro y reconozco que ha sido parte importante en mi formación y en quién soy como profesional.

Como siempre supe que quería ser investigadora y docente, cuando acabé mis estudios de grado, decidí aplicar a las becas del Estado de Chile, Becas Chile de Magister en el Extranjero, otorgadas por ANID (Agencia Nacional de Investigación y Desarrollo). Cuando recibí esta beca, sentí que me había ganado

la lotería. ANID me pagaba para vivir en Barcelona y para estudiar un Master, haciendo algo que me encanta hacer, estudiar. En mi TFM me limitaron las hojas por tanto nunca pude agradecer a ANID por dicha oportunidad de continuar mis estudios de Master. Por ello, aprovecho estas líneas para agradecer dicha oportunidad que fue un peldaño para continuar.

Mientras acababa mis estudios de Master apliqué a las mismas becas, pero para estudios de Doctorado. Debo decir que a estas alturas ya tenía algo de miedo, intriga e incertidumbre de sí sería o no capaz. Nuevamente fui beneficiaria de becas Chile, donde nuevamente sentí que me gané la lotería, pero esta vez era diferente. Esta vez serían cuatro años, no solo uno, como en el Master. Esto implicaba estar cinco años fuera de Chile, lejos de mis padres, lejos de mi novio (que ahora es mi marido), lejos de mi hermano, lejos de mis amigos de la vida. Aquí la historia cambiaría, por muchas razones. Estaría lejos de todos mis seres queridos por más tiempo, estaría sola en otro país, haciendo un doctorado que por cierto fue un desafío de principio a fin.

Y así continuó la historia posterior al Master...

Me había ganado una beca para estar cuatro años en Barcelona, realizando mi doctorado en Biotecnología, (sí, yo misma, Nutricionista estudiando Biotecnología). Muchos no creyeron que fuera capaz, incluso yo misma. Otros apostaron por mí en todo momento, me apoyaron e incentivaron a continuar y no decaer.

El primer año sufrí, estudiando cosas nuevas para mí, diferentes a mi área de estudio y superando mi fobia a los ratoncitos. Leí y leí y leí mucho para tratar de ponerme al nivel de mis compañeros de grupo, que por cierto son excelente científicos. El grupo Betaoxi que esta liderado por las mejores, Laura y Dolors, dos mujeres grandes, sabias y científicas de Elite, mujeres ejemplo en la formación científica, lejos las mejores científicas que yo he tenido la oportunidad de conocer.

En mi grupo, parto agradeciendo a mis dos jefas Laura Herrero y Dolors Serra, ellas fueron las primeras en apostar por mí, en España. Siempre supieron que mi formación era diferente al trabajo en laboratorio, sin embargo, valoraron otros aspectos de mí y mi formación, creyeron que podría contribuir en el grupo



y me dieron la oportunidad de crecer, aprender de ellas y crecer como científica. Por ello, a mis jefas les agradezco y les digo: Gracias por creer en mí y darme las oportunidades que me dieron en cada momento.

A mis compañeros que estuvieron cuando llegué, Sebastián, Mari Carmen, Kevin y Paula, les agradezco por ayudarme en un comienzo con todo lo experimental. Kevin, tu me viste de comienzo a final y gracias por ayudarme cada vez que podías, por tu buena disposición y solidaridad para compartir conocimientos, siempre con disposición a ayudar. Posteriormente llegó al grupo más gente linda, Marjorie, Ivonne, Roberto, Marc, Júlia, Vaso y todos los estudiantes de Master y Erasmus que pasaron por el lab, durante mi estadía. Con algunos compartí más que con otros, pero agradezco su paso y contribución en nuestro grupo mientras estuve, porque aprendí de cada uno de ustedes. Marjorie, me encantaba escuchar chileno en el lab, me hiciste sentir en casa muchas veces. Gracias por todo tu conocimiento, tu amistad y apoyo. Gracias por estar en los días buenos y malos, durante mi estancia y gracias por llegar al lab. Espero tener tu amistad por muchos años y estar para ti siempre que lo necesites. Al resto de mis compañeros gracias por ser parte de esta bella etapa, llena de desafíos. Al Departamento de Bioquímica y Fisiología, de la Facultad de Farmacia y Ciencias de los Alimentos, de la Universidad de Barcelona. Gracias a cada uno, a los jefes de cada grupo, a los técnicos, a las secretarias, a los compañeros de otros grupos, a cada persona que fue parte de esta etapa, en el laboratorio, todos estuvieron siempre dispuestos a colaborar y resolver dudas. Todos fueron siempre muy amables conmigo he hice grata mi estancia en el laboratorio y en el Departamento durante todo el desafío.

Agradezco a ANID, que costeo toda mi estancia en Barcelona, me dieron la posibilidad, no solo de crecer como investigadora, si no también me dieron la experiencia de vida, de vivir en el extranjero, en un lugar mejor que me enseñó muchas cosas.

Barcelona..., ¡Me encanta Barcelona! Un lugar donde he vivido cosas buenas y cosas malas. Pero siempre me sentí segura y tranquila de vivir ahí. Barcelona es una ciudad que cautiva. Bello lugar, ahora te extraño desde Chile, pero se que volveré, más pronto que tarde y sé que cuando vuelva otra vez,

sentiré que estoy en casa. Barcelona a parte de ser un lugar hermoso para mí, me entrego muchas personas bellas en la vida. Partiendo por mis amigas que adoro, Roxy, Ale, Maite, Fer y Cathi. Mis amiguitas cuanto las extraño, ellas lejos superaron las expectativas de los que es ser amigas, mientras estuve en Barcelona. Han sido mi familia y estuvieron en mi etapa de doctorado de principio a fin. Siempre me hicieron sentir buena en lo que hacía, me admiraban como científica y a pesar de no saber nada de ciencia, siempre me hicieron sentir que mi trabajo era muy bacán y que jera la científica del grupo! Estuvieron conmigo en mis etapas de estrés, cuando estuve enferma, cuando tenia ganas de llorar, cuando quería celebrar, cada vez que las necesité. Gracias por estar siempre, aunque ahora es a la distancia. Las adoro y se que nos volveremos a ver, en Chile o en España o en cualquier playa por ahí, como siempre. Se que están para mí, aunque estemos lejos y ustedes saben que yo aquí estoy para ustedes. Gracias a todos los amigos que estuvieron de paso. En la vida hay amigos para reír, para llorar, para ir de fiesta, para celebrar, y amigos que están de paso por tu vida y te dejan alguna enseñanza. Toda persona deja huella que contribuye a nuestra evolución personal. Todos aportamos algo en la vida del otro y en Barcelona conocí personas geniales que hicieron de mí una persona feliz y con una vivencia increíble.

En Barcelona también conocí a Cristian, mi actual marido. Con él viví un gran desafío, la relación a distancia. De los cuatro años de doctorado, estuvimos tres a distancia, viajando cada seis meses cada uno. Nos gastamos la vida en tanto viaje, pero valió la pena. Mi amor, estuviste en cada momento conmigo, horas y horas al teléfono. La verdad para el amor que nos tenemos, nunca fue difícil la distancia, los más terrible fue extrañarnos demasiado, pero por lo demás nunca tuvimos problemas. Nos comunicábamos muchísimo por teléfono, esta fue la forma de mantener la relación, y tu siempre estuviste para mí, me apoyaste en todo momento, estuviste para mí cada vez que lo necesité. Escucharte me subía el ánimo cada vez que no me salían los experimentos, y me incentivaste a seguir, me hiciste sentir que yo sí podía y que ésta sería solo una etapa difícil en mi vida, pero necesaria. Me ayudaste a creerme el cuento, y a sentir que, sí era científica, una nutricientífica. Gracias por acompañarme en mi último año de doctorado en Barcelona, gracias por darme el abrazo que necesite por tres años y por escucharme hablar del laboratorio, los experimentos y la

Cpt1a. Bueno probablemente Cristian también pueda darles una charla de obesidad, Cpt1a y tejido adiposo marrón, que el me escuchó exponer muchas veces antes de presentar esta tesis. Amor, gracias por estar conmigo en cada momento y por apoyarme en mi crecimiento profesional, que seguro fue difícil para los dos. Te amo y espero me sigas acompañando toda la vida en mis ocurrencias.

A mis padres, Marianela Pérez y Jaime Bastías y a mi hermano, el Jaimito, para mí sigue siendo mi Jaimito, aunque tenga 27 años. Mi mamá que siempre me incentivó a seguir estudiando, yo creo que eso lo heredé de ella. Mujer luchadora, estudiosa, responsable, profesional y hermosa, te amo mamita, gracias por estar en cada momento, por preocuparte de mí, por ir a verme cuando lo necesité, por envalentonarte y viajar sola al otro lado del océano para ver a tu hija, por preocuparte de si estaba alimentándome bien o si estaba descansando bien. Gracias por creer en mí y por enviarme siempre tus buenas energías y deseos. A mi papá, que también ha estado en cada momento junto a mi mamá, gracias por estar orgullosos de mí y por estar siempre para mí cuando los necesito. A ustedes podría agradecerles una vida entera, porque me han dado la vida, me formaron, me educaron y luego nos incentivaron a seguir el camino que nosotros eligiéramos seguir. A mi hermano y a mí nos dieron todas las herramientas para ser exitosos en la vida y nosotros hemos intentado aprovechar esas herramientas. A mi hermano gracias por estar ahí cuando lo necesité, por ser mi confidente y por apoyarme en cada decisión que tome, por guardar el secreto las veces que llegue de sorpresa a Chillán. Ustedes han sido fundamental en mi formación y en lo que yo soy hoy día.

Gracias a todos los familiares y amigos que estuvieron pendientes de mí, en la etapa de pandemia, cuando me tocó estar sola en el piso, encerrada por cuatro meses, en Barcelona. Si pudiera nombrar a cada uno de las personas que conocí en esta bella etapa, me faltarían hojas, pero todos han sido importantes en esta etapa de vida. Los que estuvieron del principio hasta los que estuvieron de paso. En Barcelona tuve muchos angelitos que estuvieron para mí y que fueron sumamente importantes.

Hoy decidí volver a Chile, intentaré buscar oportunidades aquí, si no resulta, se que Barcelona es mi otro hogar y que seguro estarán las mismas personas que hoy día extraño. Ahora, llegar a Chile ha sido el desafío siguiente, volver a insertarme a nuestro sistema. Buscar oportunidades y retribuir lo aprendido. Decidí volver a Chile, porque tengo la esperanza de generar un cambio, para aportar con un pequeño granito de arena, a través de la ciencia e investigación. Retribuir con ganas y entusiasmo, aplicando todo lo aprendido para poder ser un aporte a la ciencia, a la investigación y a las nuevas generaciones en formación. Por ahora decido estar donde más se necesita en mi Chile lindo y querido.

Hoy día me siento grande, una nutricionista y científica, casi doctora (porque me falta defender). Creo que me falta mucho por aprender y eso me gusta, pero también estoy feliz de haber concluido esta bella y difícil etapa en Barcelona con gente tan genial, llena de conocimientos nuevos, desafíos, y me siento aún más segura de mí misma en mi área, en mis conocimientos, como científica, investigadora y persona. Espero ser una persona entregada a la ciencia y solidaria con mis conocimientos, porque de eso se trata, de seguir adelante contribuyendo al cambio, disfrutando de los desafíos que nos pone la vida, de seguir creciendo y seguir buscando la felicidad haciendo lo que más me gusta.



## **ABSTRACT**

Obesity and its associated metabolic diseases are currently a priority research topic. The increase in global prevalence at different ages is having a huge economic and health impact. Genetic and environmental factors play a crucial role in the development of obesity, and diet is one of the main factors that directly contributes to the genetic obese phenotype. Scientific evidence has shown that increased fat intake is associated with increased body weight that triggers obesity. Rodent animal models have been extremely useful in the study of obesity, as weight gain can be easily induced by a high-fat diet [1].

Thermogenesis is a process that our body uses to produce heat. Studies show that the body uses a variety of mechanisms to produce this effect, demonstrating that brown adipose tissue (BAT) is one of the main effector organs [2]. In general, adipose tissue is the organ where energy is stored in the form of fat (triacylglycerols), while BAT, in particular, owes its name to the color that characterizes the presence of a large number of mitochondria, which have a high concentration of uncoupling proteins (UCP), in addition to a good number of  $\alpha$  and  $\beta$  adrenergic receptors and high vascularization [3]. BAT is located in specific areas of the body such as the cervical area of the neck, armpits, associated with the ribs, around the heart and kidneys, showing a greater distribution in fetuses and newborns compared to adults [4].

Understanding the activity of adipose tissue is important because of the involvement of this organ in the pathophysiology of obesity.

Mitochondria burn fuels such as fatty acids and glucose into useful energy, consuming oxygen in the process [5]. In addition, BAT has a high concentration of the protein UCP1 (uncoupling protein 1). This protein bypasses the respiratory chain, so instead of generating useful energy, it dissipates energy as heat. This function, known as non-shivering thermogenesis, is crucial in infants to maintain body temperature [6]. BAT has emerged as an important regulator of energy expenditure in obesity by controlling thermogenesis. Carnitine palmitoyltransferase 1A (CPT1A), a key enzyme in fatty acid oxidation (FAO), has been implicated in the control of energy homeostasis. However, the specific role of CPT1A in modulating BAT metabolism to control food intake and obesity is still highly unknown. The aim of this research work was to find new approaches to reduce obesity by activating CPT1A, and thus FAO, in BAT.

For peripheral activation of FAO in BAT, the mutated and permanently active form (CPT1AM) was expressed. This was done in mice *in vivo* using adeno-associated (AAV) vectors. As a result, activation of CPT1A in BAT activated thermogenesis and reduced weight gain, identifying new strategy for potential therapy against obesity and its associated metabolic diseases, such as diabetes.

In addition, our results showed that expression of CPT1AM in BAT increased lipolysis FAO and thermogenesis in BAT. The increase FAO in BAT prevented the increase in the content of triglycerides, cholesterol and insulin in the blood, and the expression of markers of obesity and inflammation in the tissues, caused by HFD. Our results show that FAO is critical in supplying fuel for BAT-generated thermogenesis, which may be

a good strategy to increase energy expenditure through thermogenesis and thus avoid obesity and its associated diseases resulting from HFD.

## ABBREVIATIONS

<b>AAV</b>	Adeno-associated viruses
<b>ACC</b>	Acetyl-CoA carboxylase
<b>AMP</b>	Adenosine monophosphate
<b>AMPK</b>	AMP-activated protein kinase
<b>Apo C-II</b>	Apoprotein C-II
<b>APS</b>	Acid products soluble
<b>AT</b>	Adipose tissue
<b>ATGL</b>	Adipose triglyceride lipase
<b>ATP</b>	Adenosine triphosphate
<b>BAT</b>	Brown adipose tissue
<b>BCA</b>	Bicinchoninic acid
<b>BMI</b>	Body mass index
<b>BMR</b>	Basal metabolic rate
<b>CD3</b>	T cells
<b>cDNA</b>	Complementary cDNA
<b>CEEA</b>	Ethical Committee for Animal experimentation
<b>CPT1A</b>	Carnitine palmitoyltransferase 1A
<b>CPT1AM</b>	Malonil-CoA-insensitive carnitine palmitoyltransferase I mutant
<b>CRP</b>	C-reactive protein
<b>CVD</b>	Cardiovascular disease
<b>DNA</b>	Desoxirribonucleic acid
<b>DIO</b>	Diet-induced obesity
<b>DIT</b>	Diet-induced thermogenesis
<b>ER</b>	Endoplasmic reticulum
<b>FAO</b>	Fatty acid oxidation
<b>FAs</b>	Fatty Acids
<b>FFA</b>	Free fatty acid
<b>FGF</b>	Fibroblast growth factor
<b>GLUT</b>	Glucose transporter
<b>GTT</b>	Glucose Tolerance Test
<b>gWAT</b>	Gonadal White adipose tissue
<b>hCPT1AM</b>	human carnitine palmitoyltransferase 1A mutant



<b>HDL</b>	High-density lipoprotein
<b>HFDs</b>	High-fat diets
<b>HOMA</b>	Homeostasis evaluation model
<b>IDL</b>	Intermediate density lipoproteins
<b>IHC</b>	Immunohistochemistry
<b>iWAT</b>	Inguinal White adipose tissue
<b>KRBH</b>	Krebs-Ringer Bicarbonate Hepes
<b>LCFA</b>	Long Chain Fatty Acid
<b>LDL</b>	Low-density lipoprotein
<b>LPL</b>	Lipoprotein lipase
<b>mRNA</b>	Messenger ribonucleic acid
<b>NAFLD</b>	Non -alcoholic fatty liver
<b>NASH</b>	Non -alcoholic steatohepatitis
<b>NEFA</b>	Non-esterified fatty acid
<b>NCD</b>	Normocaloric diet
<b>PA</b>	Physical activity
<b>PPi</b>	Inorganic pyrophosphatase hydrolyzes
<b>PPAR</b>	Peroxisome proliferator activated receptor
<b>qRT-PCR</b>	Quantitative real-time polymerase chain reactive
<b>rBA</b>	Rat brown adipocyte
<b>SCFA</b>	Short-chain fatty acids
<b>SDS</b>	Sodium dodecyl sulfate
<b>sWAT</b>	Subcutaneous White adipose tissue
<b>T2DM</b>	Type 2 diabetes mellitus
<b>TAG</b>	Hepatic triacylglycerol
<b>TG</b>	Triglyceride
<b>TGF</b>	Transforming growth factor
<b>TNF<math>\alpha</math></b>	Tumor necrosis factor alpha
<b>TRL</b>	Triglyceride-rich lipoproteins
<b>TSH</b>	thyroid-stimulating hormone
<b>UCP</b>	Uncoupling Protein
<b>WAT</b>	White adipose tissue
<b>WB</b>	Western Blot
<b>VEGF</b>	Vascular endothelial growth factor
<b>VLDL</b>	Very low-density lipoproteins
<b>vWAT</b>	Visceral WAT

# INDEX

<b>1</b>	<b>INTRODUCTION.....</b>	<b>1</b>
1.1	<i>Obesity.....</i>	1
1.1.1	Implication of diet in the development of obesity.....	2
1.1.2	Assessment of Diet-Induced Obesity .....	2
1.1.3	Diet and animal models in the study of obesity.....	7
1.1.4	Insulin resistance in the progression of obesity.....	11
1.2	<i>Adipose tissue.....</i>	13
1.2.1	Types of adipose tissues.....	13
1.2.2	Effects of obesity on adipose tissue .....	21
1.2.3	Cellular inflammation in obesity .....	23
1.2.4	Secretory profile of adipose tissue.....	25
1.3	<i>BAT thermogenesis and activity in humans and mice.....</i>	26
1.3.1	Brown adipose tissue activity is decreased in obesity and diabetes .....	30
1.4	<i>Lipid metabolism .....</i>	32
1.4.1	Lipolysis/ lipogenesis .....	33
1.4.2	Fatty acids degradation .....	34
1.4.3	Cholesterol metabolism .....	35
1.5	<i>Mitochondrial bioenergetics.....</i>	36
1.5.1	Fatty acid oxidation .....	36
1.6	<i>Importance of lipid metabolism and fatty acid oxidation .....</i>	39
1.7	<i>Gene therapy .....</i>	39
1.7.1	Adeno-associated viral vectors .....	42
1.8	<i>CPT1 as a therapeutic protein .....</i>	44
1.8.1	Carnitine palmitoyl transferase 1A mutant.....	48

1.9	<i>In vivo expression of CPT1AM in BAT</i> .....	51
<b>2</b>	<b>HYPOTHESIS</b> .....	<b>55</b>
<b>3</b>	<b>AIMs</b> .....	<b>59</b>
3.1	<i>General AIM</i> .....	59
3.1.1	<i>Specific AIMs</i> .....	59
<b>4</b>	<b>MATERIALS AND METHODS</b> .....	<b>63</b>
4.1	<i>Animal model</i> .....	63
4.1.1	<i>Obesity reversal experiment</i> .....	64
4.1.2	<i>Obesity prevention experiment</i> .....	65
4.1.3	<i>Prevention experiment under thermoneutrality conditions in male mice</i> ..	65
4.1.4	<i>Prevention experiment under thermoneutrality conditions in female mice</i>	66
4.2	<i>Diet</i> .....	66
4.3	<i>Viral vectors of adeno-associated viruses</i> .....	67
4.4	<i>Procedure in animals</i> .....	68
4.4.1	<i>Animal identification</i> .....	68
4.4.2	<i>Administration of viral vectors with CPT1AM in el BAT</i> .....	69
4.4.3	<i>Viral vector dilution</i> .....	71
4.4.4	<i>Accommodation of animals in thermoneutrality with acute cold stimulation</i> .....	72
4.4.5	<i>Body weight monitoring</i> .....	74
4.4.6	<i>Monitoring glucose levels</i> .....	74
4.4.7	<i>Intake control</i> .....	74
4.4.8	<i>iBAT thermographic estimation</i> .....	75
4.4.9	<i>Glucose Tolerance Test</i> .....	76
4.4.10	<i>Open Field Test</i> .....	77

4.4.11	Fecal Extraction .....	77
4.4.12	Sacrifice and sample collection .....	78
4.5	<i>Laboratory Techniques</i> .....	79
4.5.1	Blood determinations .....	79
4.5.2	Determination of cholesterol in feces .....	80
4.5.3	Determination of hepatic triglycerides .....	81
4.5.4	RNA extraction and quantification .....	81
4.5.5	Collection, quantification and measurement of protein in tissues.....	85
4.5.6	Western Blot.....	86
4.5.7	Histological analysis.....	90
4.5.8	Immunohistochemistry .....	90
4.5.9	FAO assay.....	91
4.5.10	Bioinformatic and statistical analyzes .....	92
<b>5</b>	<b>RESULTS</b> .....	<b>95</b>
5.1	<i>CPT1AM expression in BAT of obese and hyperglycemic male mice at room temperature conditions. Reversion studies.</i> .....	95
5.1.1	Validation of the administration of CPT1AM in BAT of mice by AVVs viral vectors.....	95
5.2	<i>CPT1AM expression in healthy male mice treated with HFD under room temperature conditions. Prevention studies.</i> .....	98
5.2.1	CPT1AM-expressing mice under HFD are resistant to diet-induced obesity.....	98
5.2.2	BAT-specific CPT1AM overexpression in HFD-treated mice prevented HFD-induced hepatic steatosis and adipose tissue hypertrophy.....	103
5.2.3	Overexpression of CPT1AM in BAT from HFD-treated mice under room temperature conditions alters tissue metabolism .....	105
5.3	<i>CPT1AM expression in healthy male mice under thermoneutrality conditions</i> .....	114

5.3.1	Mice treated with CPT1AM and HFD under thermoneutrality conditions are resistant to diet-induced obesity .....	114
5.3.2	CPT1AM-expressing mice under thermoneutrality conditions are protected against HFD-induced adipose tissue hypertrophy and hepatic steatosis .	120
5.3.3	Food and water intake of mice treated with CPT1AM and HFD under thermoneutrality conditions .....	122
5.3.4	CPT1AM-expressing mice under HFD and thermoneutrality conditions show an increase in BAT browning and a reduction in adipose tissue immune cell infiltration and apoptosis .....	123
5.3.5	Overexpression of CPT1AM in BAT from HFD-treated mice under thermoneutrality conditions alters tissue metabolism.....	127
5.4	<i>CPT1AM expression in healthy female mice under thermoneutrality conditions .....</i>	<i>136</i>
5.4.1	CPT1AM-expressing female mice under HFD and at thermoneutrality conditions are resistant to diet-induced obesity .....	136
5.4.2	Mice treated with HFD under thermoneutrality conditions and with acute cold stimulation prevented hypertrophy in adipose tissue and hepatic steatosis.....	142
5.4.3	Overexpression of CPT1AM in BAT from HFD-treated mice under thermoneutrality conditions with acute cold stimulation increases fatty acid oxidation and affects metabolism in BAT .....	144
5.4.4	Gene expression and protein levels in iWAT, gWAT and liver of HFD-treated mice under thermoneutrality conditions with acute cold stimulation .....	147
5.5	<i>Efficiency of obesity induction through HFD and gene therapy with cpt1am.....</i>	<i>153</i>
5.5.1	Impact of chronic cold in the induction of obesity and treatment with CPT1AM in BAT .....	153
5.5.2	Impact of sexual dimorphism on obesity induction and treatment with CPT1AM in BAT .....	155

<b>6</b>	<b>DISCUSSION .....</b>	<b>159</b>
6.1	<i>Overexpression of CPT1AM in obese and hypoglycemic mice under room temperature conditions failed to reverse HFD-induced obesity derangements.....</i>	<i>159</i>
6.2	<i>Overexpression of CPT1AM prevents obesity and diet-induced hyperglycemia. ....</i>	<i>161</i>
6.2.1	Temperature influences the efficiency of dietary obesity induction and the efficiency of CPT1AM gene therapy. ....	166
6.2.2	Sexual dimorphism impacts the efficiency of obesity induction through diet and the efficiency of gene therapy with CPT1AM.....	167
6.3	<i>Overexpression of CPT1AM modifies food and water intake.....</i>	<i>169</i>
6.4	<i>Overexpression enhances hepatic steatosis and adipose tissue hypertrophy... ..</i>	<i>171</i>
6.5	<i>CPT1AM overexpression modifies tissue metabolism in BAT, iWAT, gWAT, and Liver. ....</i>	<i>172</i>
6.6	<i>Overexpression of CPT1AM increases browning in BAT and reduces immune cell infiltration and apoptosis in adipose tissue. ....</i>	<i>174</i>
6.7	<i>CPT1AM overexpression increases steatorrhea due to cholesterol excretion from HFD.....</i>	<i>175</i>
6.8	<i>Overexpression of CPT1AM increases fatty acid oxidation in BAT.....</i>	<i>175</i>
6.9	<i>Gene therapy for treatment and prevention of obesity.....</i>	<i>177</i>
<b>7</b>	<b>CONCLUSIONS.....</b>	<b>181</b>
<b>8</b>	<b>REFERENCES.....</b>	<b>185</b>
<b>9</b>	<b>SCIENTIFIC PRODUCTION.....</b>	<b>215</b>

## LIST OF FIGURES

Figure 1 Selection of the animal model and diet for the study of obesity. ....	11
Figure 2 Origin of adipocytes. ....	15
Figure 3 Representation of adipose tissue distribution in rodents and humans. .....	20
Figure 4 Alterations in WAT and immunometabolic effects. ....	22
Figure 5 Metabolic and physiological differences in mice under chronic cold or at thermoneutrality.....	30
Figure 6 CPT system. ....	38
Figure 7 Grace Therapy Foundation. ....	41
Figure 8 Carnitine palmitoyltransferase system 1 and CPT2 catalyze the reversible transesterification of acyl-CoA and carnitine to form acyl-carnitine and coenzyme A. ....	48
Figure 9 Used mice and boxes in negative pressure units.....	64
Figure 10 Diet used for the study and induction of obesity. ....	67
Figure 11 Animal identification by ear piercing.....	69
Figure 12 Illustration of a mouse with an open incision in the scapular area. ....	70
Figure 13 Photos of the surgery and its evolution. ....	71
Figure 14 Mice housed in the climatic chamber under thermoneutrality condition.....	73
Figure 15 Intake control.....	75
Figure 16 Thermographic photo made with infrared camera. ....	76
Figure 17 Experimental design and phenotype of obese mice treated with HFD and AVVs viral vectors with CPT1AM or Null control. ....	97
Figure 18 CPT1A protein levels are increased in CPT1AM-expressing mice. ...	98

<b>Figure 19 Experimental design of the prevention studies.</b> .....	99
<b>Figure 20 HFD CPT1AM mice are resistant to HFD-induced weight gain.</b> .....	99
<b>Figure 21 Thermography and GTT CPT1AM-expressing mice under HFD.</b> .....	100
<b>Figure 22 Fasting blood glucose levels and weight of iWAT, gWAT and liver.</b> .....	101
<b>Figure 23 Serum insulin, HOMA-IR, triglycerides, cholesterol and NEFAs levels in CPT1AM-expressing mice under NCD and HFD.</b> .....	102
<b>Figure 24 Food and water intake</b> .....	103
<b>Figure 25 HFD CPT1AM mice show reduced iWAT and gWAT hypertrophy.</b> .....	105
<b>Figure 26 mRNA and protein expression levels in BAT.</b> .....	107
<b>Figure 27 mRNA and protein expression levels in iWAT.</b> .....	109
<b>Figure 28 mRNA and protein expression levels in gWAT.</b> .....	111
<b>Figure 29 mRNA and protein expression levels in liver.</b> .....	113
<b>Figure 30 Experimental design of CPT1AM expression in vivo carried out at thermoneutrality conditions.</b> .....	114
<b>Figure 31 Body weight, interscapular temperature and fasting blood glucose levels of CPT1AM-expressing mice under HFD at thermoneutrality conditions.</b> .....	115
<b>Figure 32 Glucose tolerance test and area under the curve of CPT1AM- expressing mice under HFD at thermoneutrality conditions.</b> .....	116
<b>Figure 33 Mice overexpressing CPT1AM, at 10 weeks under thermoneutrality conditions, were resistant to diet-induced hyperglycemia, hyperinsulinemia, hypercholesterolemia, and hypertriglyceridemia.</b> .....	117
<b>Figure 34 CPT1AM-expressing mice at thermoneutrality improved HFD- induced decrease in the distance travelled.</b> .....	118



Figure 35 At the time of sacrifice following acute cold challenge, CPT1AM-expressing mice were resistant to HFD-induced hyperglycemia, hyperinsulinemia, insulin resistance, and hypercholesterolemia.....	119
Figure 36 CPT1AM-expressing mice under thermoneutrality conditions are protected against HFD-induced adipose tissue hypertrophy and hepatic steatosis.....	121
Figure 37 Measurement of food and water intake of mice under thermoneutrality conditions.....	123
Figure 38 CPT1AM-expressing mice under thermoneutrality conditions show an increase in BAT browning. ....	124
Figure 39 CPT1AM-expressing mice under HFD at thermoneutrality conditions show a reduction of T cell infiltration in BAT and iWAT.....	125
Figure 40 CPT1AM-expressing mice under HFD at thermoneutrality conditions show a reduction of macrophage infiltration in BAT, iWAT and gWAT.....	126
Figure 41 CPT1AM-expressing mice under HFD at thermoneutrality conditions show a reduction of apoptosis in iWAT and gWAT. ....	127
Figure 42 CPT1AM-expressing mice under HFD and at thermoneutrality conditions show altered BAT metabolism, inflammation and are resistant to HFD-induced increase in leptin and ER stress. ....	129
Figure 43 CPT1AM-expressing mice under HFD and at thermoneutrality conditions show altered iWAT metabolism.....	131
Figure 44 CPT1AM-expressing mice under HFD and at thermoneutrality conditions show altered gWAT metabolism. ....	133
Figure 45 CPT1AM-expressing mice under HFD and at thermoneutrality conditions show altered liver metabolism.....	135
Figure 46 Experimental design of mice treated with CPT1AM and with HFD under thermoneutrality conditions.....	137

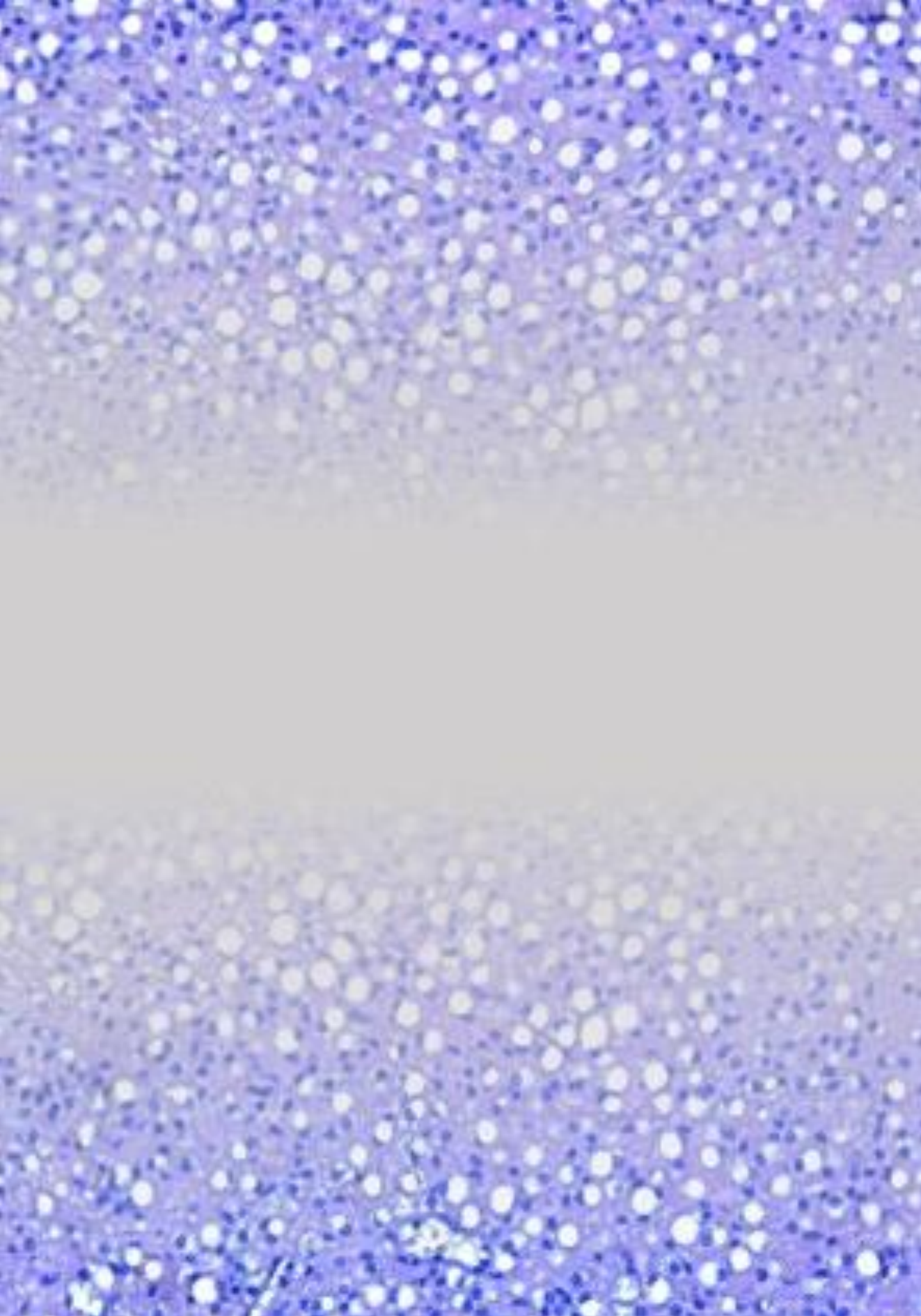
<b>Figure 47 Under thermoneutrality conditions, were resistant to HFD-induced obesity. ....</b>	<b>138</b>
<b>Figure 48 Under thermoneutrality conditions, excreted more cholesterol and were resistant to hyperglycemia, insulin resistance, and hypertriglyceridemia caused by HFD. ....</b>	<b>140</b>
<b>Figure 49 CPT1AM-expressing female mice under HFD and thermoneutrality conditions show a reduction in cumulative food intake. ....</b>	<b>141</b>
<b>Figure 50 Under conditions of thermoneutrality with acute cold stimulation, were resistant to adipose tissue hypertrophy and hepatic steatosis. ....</b>	<b>143</b>
<b>Figure 51 Under conditions of thermoneutrality with acute cold stimulation, oxidizes more fatty acids, alters lipid and glucose metabolism, inflammation, hormones and ER, being resistant to alterations caused by the HFD. ....</b>	<b>146</b>
<b>Figure 52 Gene expression and protein levels in iWAT, from mice treated with CPT1AM intraBAT, under conditions of thermoneutrality with acute cold stimulus. ....</b>	<b>148</b>
<b>Figure 53 Gene expression and protein levels in gWAT of mice treated with CPT1AM intraBAT, under conditions of thermoneutrality with acute cold stimulus. ....</b>	<b>150</b>
<b>Figure 54 Gene expression and protein levels in the liver of mice treated with CPT1AM intraBAT, under conditions of thermoneutrality with acute cold stimulation. ....</b>	<b>152</b>

## LIST OF TABLES

<b>Table 1 Nutritional status category according to BMI in adults. ....</b>	<b>4</b>
<b>Table 2 Types of diets used to study obesity. ....</b>	<b>7</b>
<b>Table 3 Isoforms of CPT1.....</b>	<b>47</b>
<b>Table 4 Quantitative RT-PCR oligonucleotides. ....</b>	<b>84</b>
<b>Table 5 Primary antibodies used in western blot. ....</b>	<b>89</b>
<b>Table 6 Secondary antibodies used in Western Blot. ....</b>	<b>89</b>
<b>Table 7 Obesity induction with HFD therapy was more efficient in mice under thermoneutrality conditions.....</b>	<b>154</b>
<b>Table 8 Female mice were more resistant to obesity induction by HFD than male mice. ....</b>	<b>156</b>



# **Introduction**



# **1 INTRODUCTION**

## **1.1 Obesity**

Overweight and obesity have increased alarmingly in recent years. Current public policies and interventions have failed to stop its global prevalence. It is known that obesity occurs when there is an imbalance between energy intake and expenditure. A positive energy balance triggers the overflow of lipids that accumulate particularly in adipocytes, increasing their number (hyperplasia) and size (hypertrophy). Both genetic and environmental factors play a crucial role in the development of obesity, and diet is undoubtedly one of the main environmental factors involved [1]. The fat content of the diet is often considered the main factor responsible for increased adiposity. Human studies have shown that high-fat diets with more than 30% of total daily energy intake from fat can readily induce obesity [7].

Obesity is a multifactorial chronic disease characterized by excessive fat accumulation. When intake is greater than energy expenditure, an imbalance is produced that is reflected in excess weight. The growing number of new cases has led to its classification as an epidemic, a fact that reflects the need to know the triggering causes in order to work on modifiable factors and the establishment of correct instruments for the detection and assessment of this pathology. [8] One of the most important factors in the development of obesity is the individual's own lifestyle. This will be favored in the presence of a diet defined by a frequent consumption of foods with a high energy density and glycemic index, a consumption greater than the needs, habits related to the size of the portions or the number of intakes throughout the day.

There is a relationship with other factors such as the alteration of the circadian system by suppressing the rhythm of melanocortin, responsible for the

expression and secretion of leptin and adiponectin [9]. Complex interactions between the genome and environmental factors can modulate the expression of genes involved in the metabolism that determine the susceptibility to developing chronic pathologies such as obesity, which has been mentioned as a new future in treatment circles, particularly in obesity and in the prevention of chronic pathologies.

### **1.1.1 Implication of diet in the development of obesity**

Body weight is determined by a complex interplay of various factors such as appetite, intake control, nutrient absorption, neuroendocrine regulators, forms of energy storage and total energy expenditure [10]. Consumption has two phases: Short Term, various enzymatic and hormonal modifications guarantee rapid adaptation of the body to a certain intake; and in the long term, the adaptation that is necessary in the face of increased intakes can only be guaranteed by regulating the genetic expression of the various metabolic pathways that modify the oxidative balance of substrates and thermogenesis. [11] Various nutrients participate directly in this regulation through specific interactions with genes that encode various critical enzymes in the metabolism of lipids and carbohydrates.

In response to high-fat diets, it has been shown in rodents to have a long-term effect on the methylation status of genes related to the regulation of food intake, such as leptin in adipose tissue or melanocortin 4 receptor in the brain [12], which contributes to changes in gene expression.

### **1.1.2 Assessment of Diet-Induced Obesity**

There are different parameters to assess obesity. Too much body fat can lead to weight-related diseases and other health problems. Being underweight



is also a health risk. Evaluation of an overweight or obese patient should include clinical and laboratory studies. This combined information makes it possible to characterize the type and severity of obesity, to determine the patient's health risk and to provide a basis for the choice of treatment. For the diagnosis of obesity, it is necessary to measure weight, height and calculate body mass index (BMI) as part of the basic exploration of any patient. The calculation of the BMI (weight in kilograms/height squared in meters) is the first step in determining the degree of overweight. In addition, in patients with a BMI between 25 and 35 kg/m<sup>2</sup>, abdominal circumference should also be measured [13]. Body mass index is easy to calculate and correlates well with body fat percentage. BMI and waist circumference are screening tools to estimate weight status in relation to potential disease risk. However, they are not disease risk diagnostic tools.

Obesity is considered when the percentage of fat mass is greater than 25% in men and 33% in women. When this parameter cannot be determined, the BMI will be used, considering obesity values  $\geq 30$  kg/m<sup>2</sup>, or waist circumference. Abdominal obesity is considered when the measurement taken on the iliac crest is  $\geq 102$  cm in men and  $\geq 88$  cm in women [14]. Other indices also used to assess obesity are the waist-to-height ratio and the waist-to-hip ratio [15]. Its origin arises from the assumption that the cardiometabolic risk due to the accumulation of abdominal fat depends on the size of the individual. The waist-hip ratio classifies obesity in android, when the fat accumulates mainly in the abdominal area or gynoid if it is located mainly in the buttocks, hips and thighs. This index results from the fraction of the waist circumference divided by the hip circumference [16].

**Table 1 Nutritional status category according to BMI in adults.**

Nutritional condition	BMI
extremely low weight	< 14,0
Low weight	14,1 – 18,4
Normal	18,5 – 24,9
Overweight	25 – 29,9
Obesity I or mild	30 – 34,9
Obesity II or moderate	35 – 40
Obesity III or severe	>40

Obese mice (*ob/ob*) are the most widely used and well-known animal model of genetic obesity. These animals, in addition to the obesity that characterizes them, show alterations similar to those that appear in the human metabolic syndrome. *ob/ob* mice exhibit a mutation in the leptin receptor, which is the molecular basis of their unique phenotype [17]. Leptin is a hormone produced by adipose tissue and important in the central regulation of energy balance [18]. This hormone is released into the bloodstream and the amount released is proportional to the amount of stored lipids. It acts on leptin receptors in the brain, resulting in decreased food intake and increased energy expenditure [19]. Lack of leptin signaling is a cause of obesity in several animal models, and mice are one such model. These mice have a recessive mutation in the leptin receptor gene (*lepr*) [17].

The obesity appears in animals at an early age and is associated with hyperphagia, impaired thermogenesis and lipid deposition in adipose tissue. The aforementioned deficiency leads to a significant change in the neuropeptidergic state of the brain areas involved in the regulation of body weight [20]. It actually produces a dysregulation of ordemanding peptides such as neuropeptide Y, galanin, orexins, melanin concentrating hormone and ghrelin [21]. A direct or

indirect consequence of the loss of leptin receptor-mediated regulation is that mice have large circulating amounts of this hormone compared to their controls [22].

Mice develop adipocyte hyperplasia and hypertrophy [23]. Studies on the adipose tissue of these animals indeed show that their adipocytes increase in number and in size. The greatest increase in adipocytes is observed in the deposition of subcutaneous fatty tissue. Lipogenesis is higher in young mice. In adulthood, the body weight of homozygous animals exceeds the weight of a normal animal by 60%. In addition to the obesity that characterizes them, the mice present various endocrine abnormalities. These animals are, in fact, a very widespread experimental model of insulin resistance, which presents characteristics very similar to those which characterize the human metabolic syndrome. Indeed, in addition to resistance to the metabolic actions of insulin, the animals exhibit dyslipidemia, mild glucose intolerance and hyperinsulinemia [24].

On the other hand, most investigations the HFD, provided *ad libitum*, to early obesity. These diets are generally composed of 60 % fat, 22 % carbohydrates and 18 % protein. [25]. The goal of this diet in which most of the calories come from fat is to cause obesity, as well as insulin resistance and liver damage [26]. However, the results obtained can be very variable in the degree of steatosis, inflammation and fibrosis. The final result will depend on the strain and the species, the specific fat content of the diet, the composition of that same fat and the duration of the treatment [27].

One way to improve outcomes is to increase fat intake in the diet by implanting a gastrostomy tube. This method has been used in male mice C57BL/6 on a diet containing 37% fat (corn oil), 24.5% protein (lactalbumin hydrolyzate), 38.5% carbohydrate (dextrose), vitamins and minerals. After 9

weeks of treatment, we observe how the mice become progressively obese, reaching a higher body weight of 71% and developing inflammation and pericellular fibrosis. Additionally, hyperglycemia, hyperinsulinemia, hyperleptinemia, glucose intolerance, and insulin resistance occur [28].

With a pellet-shaped HFD, for a long time, the same results are obtained. In a study a diet was used that is made up of 22 % saturated fatty acids and 77 % unsaturated fatty acids and supplied to male mice C57BL/6J. The result was an increase in body weight, liver weight gain, insulin levels and fasting leptin. Adiponectin levels, on the contrary, decreased, and the effect of insulin was altered to lower glucose levels. At 30 weeks of treatment, lipogenic genes were expressed, and at 60 weeks an enlarged liver was observed with typical NASH (non -alcoholic steatohepatitis) characteristics. In different stages of progression and gene expression of cytokines and oxidative stress. In addition, in week 60, tumors were observed in 54 % of mice. This reflects the natural progression of NAFLD (non -alcoholic fatty liver) [29].

The composition of the diet can also be varied, for example, with 42% fat, 0.1% cholesterol and the addition of a high fructose-glucose solution to consume *ad libitum* in this way, the development of obesity, insulin resistance, hypertriglyceridemia and increased LDL (low-density lipoprotein) cholesterol is achieved. Thus, at 4-8 weeks he sees steatosis, steatohepatitis at 16-24 weeks, and progressive fibrosis and spontaneous hepatocellular cancer from 16 weeks. Summarize the main changes physiological, metabolic and histological findings of NAFLD (Non-alcoholic fatty liver disease) in a shorter time frame [30]. In short, the histopathological features of the disease as well as the altered parameters of metabolism can be reproduced in an HFD model, but the result is a pathology that is much less severe than human NAFLD [26].

**Table 2 Types of diets used to study obesity.**

<b>Description</b>	<b>Product forms available</b>	<b>Nutritional profile of macronutrients</b>	<b>Reported metabolic effect</b>
<b>Diet with 10,2% energy from fat</b>	Pellet yellow for rat or mouse.	18,0% protein, 10,2% fat (ether extract) and 71,8% carbohydrates.	Normal diet used for control group. No evidence of metabolic alterations.
<b>Diet with 60% energy from fat</b>	Pellet blue for rat or mouse.	18,1% protein, 61,6% fat (ether extract) and 35,8% carbohydrates.	After 6 weeks, the body weight increases.
<b>Diet with 45% energy from fat</b>	Pellet red for rat or mouse.	18,1% protein, 46,1% fat (ether extract) and 20,3% carbohydrates.	After 9 weeks, the body weight increases.
<b>Diet containing corn oil, lactalbumin hydrolysate and dextrose</b>	high- fat liquid diet. Implanting a gastrostomy tube.	24,5% protein, 37% fat and 38,5% carbohydrates.	After 9 weeks, the body weight increases 71% and developing inflammation and pericellular fibrosis.
<b>Diet made up of saturated fatty acids and unsaturated fatty acids</b>	Liquid diet.	Diet made up of 22 % saturated fatty acids and 77 % unsaturated fatty acids.	Increase in body weight, liver weight gain, insulin levels and fasting leptin. Progression of NAFLD.
<b>Diet containing fat, cholesterol and the addition of a high fructose-glucose solution.</b>	Liquid diet.	42% fat, 0.1% cholesterol and high fructose-glucose solution.	the main changes physiological, metabolic and histological findings of NAFLD in a shorter time frame.

**1.1.3 Diet and animal models in the study of obesity**

In laboratory tests and teaching, the most commonly used animals are mice, rats, rabbits, hamsters, dogs, and monkeys, among others [31]; among them, mice are the most used (50.9%) [32]. Thus, the laboratory animal is any animal species generated and maintained in an environment with controlled conditions, which has genetic and microbiological baggage, and which is used as

an instrument of scientific experimentation to obtain data which will be used as information [31]. The advantages of using mice are their small size, ease of maintenance and handling, low maintenance costs, good adaptation to life in pet stores, the fact that they are prolific animals throughout long the year [32], their efficient reproduction and their short generation time, and to have a short life, favoring its use in toxicology, microbiology and other tests. However, the disadvantages of its use are related to the difficulty of harvesting the biological material, the administration of drugs and the application of surgical techniques.

The standard for a model of diet-induced obesity is the mouse. The mouse only develops an obese phenotype when it has access to a HFD, whereas with a low-fat diet it remains normal. When the mice are compared to other strains, they are relatively resistant to the effect of giving them a HFD. Obesity in mice is the result of adipocyte hypertrophy and hyperplasia. Accumulated fat is selectively deposited in the mesentery. Mice show greater weight gain per unit of ingested energy (food efficiency ratio) and the ability of ingested energy to be metabolized (metabolic efficiency) [33]. The weight gain observed in mice therefore cannot be fully explained by increased energy intake, but is also caused by a reduced metabolic rate. In addition to the typical obese features developed in mice on a high-fat diet, they progressively develop insulin resistance, glucose intolerance, mild to moderate hyperglycemia, dyslipidemia, hypoadiponectinemia, resistance to leptin/hyperleptinemia and hypertension. With respect to central adiposity, the progression of diabetes development, as well as the interaction of nutritional components and genetic variables in mice, closely parallels the progression of common forms of the disease in humans [33].

Typically, mice are fed a HFD containing 40-60% calories from fat (control diet 5-10% fat), for 8-16 weeks. The diabetic phenotype in mice is evident after one month of consumption of a high-fat diet: basal plasma glucose

and insulin are elevated, and glucose tolerance tests show a decrease in glucose clearance from the blood and impaired insulin secretion. At 16 weeks, the mice develop a fat mass which increases by 93% [34]. Rodent animal models are very useful for the study of obesity. Among the advantages that can be observed, the diet given to the entire sample of the group can be standardized in terms of the percentage distribution of macronutrients. However, although most rodents tend to become obese with HFDs, there can be great variability in body weight gain, glucose tolerance, insulin resistance, blood lipid content, and other voltage-dependent parameters [35]. Some mouse strains are more sensitive to the development of obesity when nourished with an HFD [36]. Under HFD, the two mice strains, C57BL/6J and AKR/J.26 have similar degrees of weight gain. However, C57BL/6J mice are more intolerant to glucose than AKR/J.26 mice. They are therefore privileged C57BL/6J mice to induce obesity with diet. As the C57BL/6 strains of mice are widely used in studies on diet-induced obesity (DIO). In the case of rats, Sprague-Dawley and Wistar strains are widely used as animal models to study the obesity, as they gain weight easily on an HFD. But, these strains are known to have a response of variable weight gain [37].

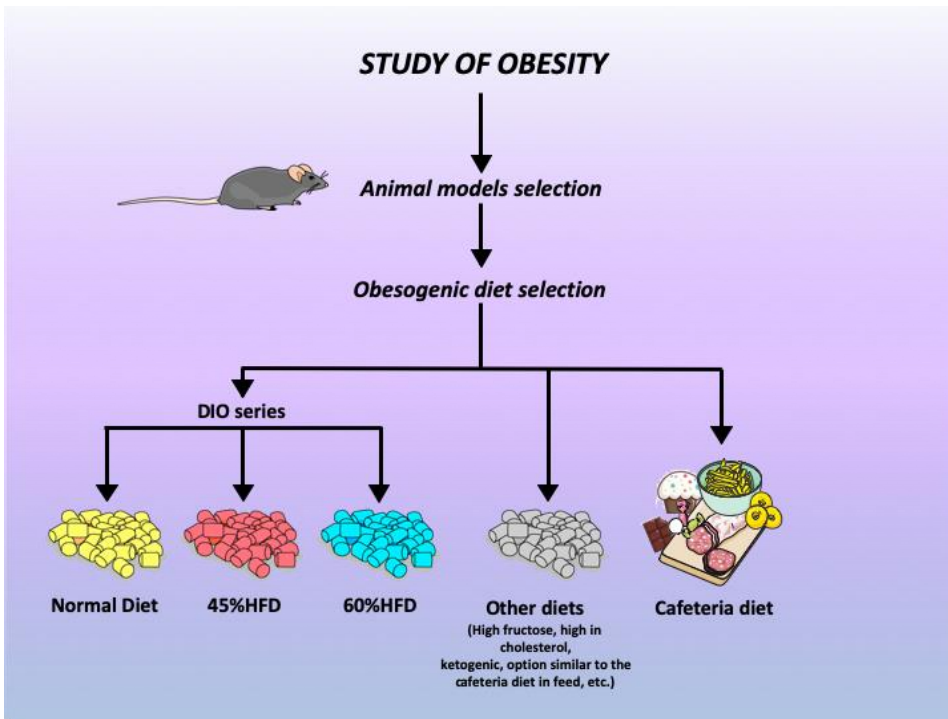
Some animals gain weight quickly, while others gain as much as rats fed with a low -fat diet [38]. In addition, body weight gain in these rats strains is generally similar to 45% or 60% kcal from an HFD. This should be considered in the diet selection process for these strains [39]. But also, this diversity could be interesting, since it could represent what happens in the development of human obesity. Rodent models have been an essential tool in the study of obesity, as they provide a convenient model for the development of drugs and novel dietary interventions [40]. But, compared to humans, there are significant limitations that need to be considered. The main limitation of studies on obesity in rodents is dietary applicability in humans. In animal studies, it has been possible to

control both the exact composition of the ration as quantity of consumption per rodent. However, in humans, it was not possible estimate food intake. In addition, in humans, weight gain and loss will depend on the large individual and genetic variability [41].

To induce obesity, different obesogenic diets can be used, with different chemical composition or even human foods, as is the case of the cafeteria diet, but always the choice of the diet will depend on the research and experimental design objectives previously established to the study [1].



**Figure 1 Selection of the animal model and diet for the study of obesity.**



*In the study of obesity, it is important to make an adequate selection of the animal model and obesogenic diet to respond to the study objectives, established in the experimental design.*

### **1.1.4 Insulin resistance in the progression of obesity**

Insulin resistance is characterized by a decrease in the ability of insulin to perform its normal physiological functions. It usually precedes clearly pathological situations such as type 2 diabetes mellitus or metabolic syndrome and is associated with circumstances such as overweight or obesity [42]. For your research, it is important to consider other aspects, such as age, pregnancy and polycystic ovaries where insulin resistance also plays an important role [43]. Initially, insulin resistance generates compensatory mechanisms, so that over a period of time, insulin hypersecretion keeps blood sugar under control [44]. This period, which could be described as prediabetic, is difficult to detect from a

clinical point of view, precisely because of the maintenance of blood sugar values within normal limits. However, this situation gradually deteriorates when the so-called pancreatic insufficiency occurs, when the beta cells are not only unable to maintain insulin hypersecretion, but also begin to deteriorate, decreasing insulin secretion. It is at this stage that most cases of type 2 diabetes mellitus and metabolic syndrome usually begin to be diagnosed.

The alternative for earlier detection of resistance would be through the analysis of insulin values, either on an empty stomach to calculate the resistance index measured by the homeostasis evaluation model (HOMA) or in the curves glucose tolerance test to detect hyperinsulinemia. The progression of insulin resistance not only leads to type 2 diabetes, but if timely measures are not taken, patients end up dependent on insulin. Although the etiology of the resistance is not yet clearly established, it is considered that there is a polygenic genetic component on which the environment would act. In this sense, lifestyle changes with little physical exercise and constant availability of food in developed and economically emerging countries seem to be responsible for the escalating incidence of insulin resistance-related diseases like type 2 diabetes in recent years. More than 90% of diabetics are classified as type 2. According to the World Health Organization, the number of people affected by this disease in the world would increase from 135 million in 1999 to 299 million in 2025. These forecasts seem to have collapsed and according to the International Diabetes Federation the figures would increase from 246 million in 2007 to 380 million in 2025. If we add to this the progressive aging of the population in developed countries, which increases the prevalence of type 2 diabetes and of the metabolic syndrome, it is clear that we are facing a large-scale health problem that requires maximum attention. Predictions are that almost 30% of the population will experience insulin resistance and its complications throughout their lives [45].

### **1.2 Adipose tissue**

Adipose Tissue (AT) is the body's main energy storage tissue, in addition to being attributed the function of insulation and mechanical protection for some vital organs [46]. For many decades, adipose tissue was considered an inert deposit of triglycerides, recognizing as the only function of the adipocyte, its participation in the regulation of the use of energy reserves by the body via lipogenesis and lipolysis. However, in the mid-1990s, identified leptin, a protein factor produced in adipose tissue with action in the central nervous system, and this gave way to the characterization of a series of factors secreted by this tissue: adipokines [47].

Adipokines have been shown to participate in systemic metabolism, inflammatory processes, coagulation, vascular resistance, and angiogenesis. Some of these cytokines have a local effect, either paracrine or autocrine, while others have important systemic effects. Through these signals, information on energy reserves, appetite, energy expenditure and sensitivity to key metabolism hormones such as insulin, among others, is coordinated. In this way, AT functions are integrated with other organs such as pancreas, digestive tube, liver and brain [47]. In the last decade, the important role of adipocytes in body energy homeostasis, insulin sensitivity, and carbohydrate and lipid metabolism has been recognized [48].

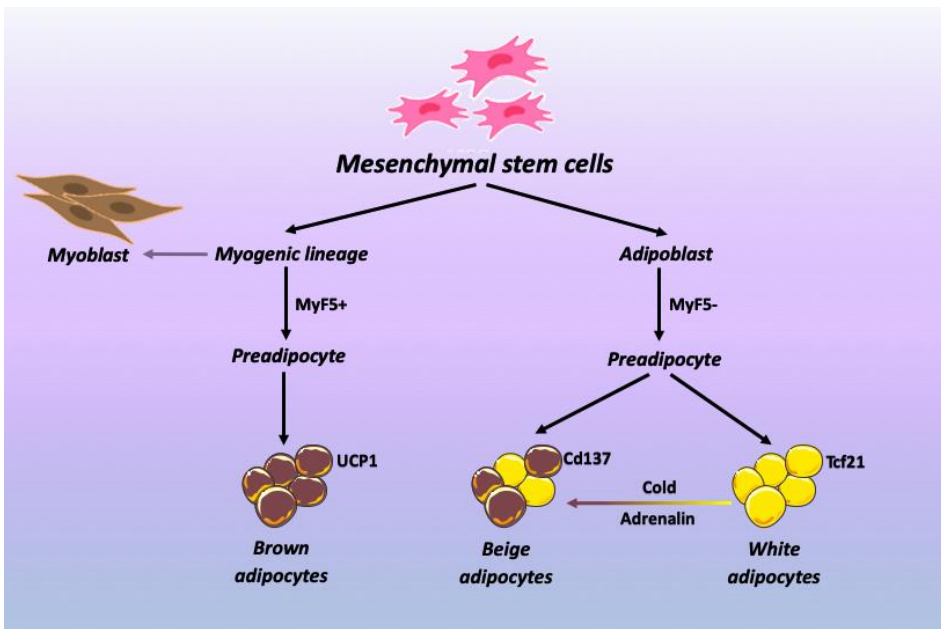
#### **1.2.1 Types of adipose tissues**

Adipose tissue, generally considered a useful appendage to provide protection, heat and energy, has assumed these activities and has positioned itself as an organ with neuroimmuno-endocrine functions, since through the production of molecules such as hormones, antimicrobials, cytokines and

adipokines, participates in the functioning of various cells and organs, which allows it to intervene in the defense and homeostasis of the organism. In addition, it is the organ with the greatest plasticity, since it regenerates after surgery and increases or decreases in size depending on age, physical activity, food intake, endocrine function, genetic predisposition and neonatal programming. Added to this is its capacity for transdifferentiation (transition from one type of adipocyte to another), which can occur in humans [49] and be reversible [50], as well as the ease with which, under certain conditions, such as chronic inflammation, the adipocyte must adopt a phenotype and functions very similar to those of the macrophage [51].

About a tenth of total fat is renewed each year, due to the death of adipocytes and adipogenesis; however, it has been reported that an adipocyte can live for up to nine years. To date, studies aimed at clarifying the origin of adipocytes seem to agree that they come from different lineages derived from mesenchymal stem cells and many different genes have been identified between white and brown adipocytes (Figure 2) [52]. A family of transcription factors essential for the maturation and activation of white, brown and beige adipocytes are the PPARs (peroxisome proliferator activated receptors).

**Figure 2 Origin of adipocytes.**



*Different lineages derived from the mesenchymal stem cell generate different types of adipocytes, depending on the expression of different genes or transcription factors. In humans, they are also caused by the phenomenon of transdifferentiation of white to beige adipocytes, which can be reversible.*

Fat deposits are different from each other, even between those of the same type of fatty tissue. Each is complex, made up of different cells, with different functions and variations in both gene expression [53], and in their response to hormones (the subcutaneous tissue of the thighs responds to sex hormones, the neck, upper back and abdomen to corticosteroids). For example, it is known that during pregnancy, lactation, and post-lactation, subcutaneous white adipocytes convert to milk-producing glands formed by lipid-rich elements which are defined as pink adipocytes [54]. There are also metabolic and replication differences in tissues such as the mesenteric and omental, suggesting that they are not functionally similar and that the different adipose tissue depots

constitute distinct "mini-organs". Regional differences can influence the complications of obesity and the genesis of other pathologies.

### ***1.2.1.1 White adipose tissue***

The adipocyte stores fatty acids and its diameter varies from 20 to 200  $\mu\text{m}$ . It contains a large drop of lipids which moves the nucleus to the periphery, few mitochondria, antibacterial elements, free radicals and nitric oxide, cytokines and adipokines. It has numerous receptors, among others for the recognition of pathogens and lipids, respectively of the toll or scavenger type, as well as for insulin, cytokines and hormones such as TSH (thyroid-stimulating hormone), thyroid, corticosteroids, estrogen and androgens [55].

Exposure to cold and large amounts of norepinephrine for a long time, as well as irisin and meteorin, myokines released during exercise, have been reported to be responsible for the change from white adipocytes to beige and brown adipocytes [56]. In the deposits of this tissue, it has been observed that the density of sympathetic nerve fibers is positively correlated with the development of beige fat; [57] in this regard, histochemical studies show that chronic exposure to cold increases noradrenergic nerve fibers. Transdifferentiation has also been observed in patients with prolonged burn stress [58], in cancer cachexia and in bariatric surgery [59], as well as direct conversion of white to brown adipose tissue in patients with pheochromocytoma, a tumor secreting catecholamines [60].

White adipose tissue (WAT) is the most abundant, it is distributed throughout the body and has several storage areas:

Subcutaneous: corresponds to 80% of the total and shows marked differences between men and women. It provides thermal insulation and is less

linked to metabolic damage secondary to obesity; however, it has recently been associated with venous thrombosis [61] and progenitor cell dysfunction [62].

Perivascular: Provides protection and structural support and influences vascular wall contractility and homeostasis [61].

Visceral: it is divided into omental or omental and mesenteric. It occupies the spaces between the abdominal organs and holds them in place; It has lymph nodes and more blood vessels and adrenergic receptors than the rest of the white tissue. Adipocytes in visceral tissue also express a greater number of receptors for corticosteroids and in obesity the enzyme 11 beta-hydroxysteroid dehydrogenase is overexpressed, which generates active glucocorticoids from inactive glucocorticoids, which stimulate the adipogenesis and increase visceral fat [63]. Visceral adipose tissue is most closely linked to the genesis of metabolic syndrome and obesity-associated pathology [63].

The appearance of obesity in an individual can be understood as the result of the interaction between his genetic heritage and environmental influences, among which the level of physical activity and his food choices, both in quantity (energy intake) and quality (nutrients and other food components). The number of genes involved in the regulation of energy homeostasis and appetite, body weight and adiposity, with possible importance in the etiology of obesity, is enormous.

Multiple mutations have been described in the same gene associated with obesity, including the genes on which the greatest number of replicated studies are specifically those involved in energy metabolism, adipogenesis and cell signaling, genes that code for adipocytokines and other factors involved in the regulation of appetite and intake, genes involved in the regulation of thermogenesis and energy expenditure (uncoupling proteins, mitochondrial genes, UCP1, UCP2 and UCP3, genes of the  $\beta$ -adrenergic receptor family, ADRB3,

ADRB2) and others of unknown function (fat mass and obesity associated ted gene, FTO7).

In mammals, WAT is dispersed throughout the body. In mice as in humans, its anatomical distribution is quite similar. Two major deposits can be found depending on their anatomical location: the visceral WAT (vWAT) and the subcutaneous WAT (sWAT); although there are also differences in adipocyte size, vascularization, glucose and fatty acid (FA) uptake, insulin response or lipolytic capacity, among others. On the one hand, vWAT is located around the abdomen and the whole visceral organs. This group includes omental, mesenteric, retroperitoneal, perirenal, and gonadal WAT (gWAT) deposits. In contrast, deposits located in the buttocks, thighs, and abdomen correspond to sWAT in humans. However, they are classified as suprascapular, anterior and posterior in mice. The posterior deposition includes the thoracolumbar, gluteal and inguinal WAT (iWAT) regions [64]. Generally, sWAT is composed of smaller adipocytes which are more insulin sensitive than vWAT. In addition, these deposits have less lipolytic activity and insulin-stimulated glucose uptake and are considered to have a protective role against obesity.

In contrast, vWAT is commonly associated with metabolic disorders, such as type 2 diabetes mellitus (T2DM) and cardiovascular disease (CVD) [65]. Energy homeostasis is maintained by the deposits described above which make up nearly 100% of fat throughout the body. However, there are other small reservoirs with mechanical or damping functions. These can be found in the retroorbital space, on the face or extremities, as well as in the spinal cord [66].

### ***1.2.1.2 Brown adipose tissue***

Considered tissue thermogenic, this tissue is made up of cells that are smaller than white, they contain multiple (multilocular) lipid droplets, and the



color reflects the cytochromes present in their many mitochondria. These organelles have abundant peak and *sui generis* activity, due to the role of the UCP1, initially known as thermogenin, which modifies oxidative phosphorylation. This modification allows you to decrease the production of ATP (Adenosine triphosphate) and increase the amount of energy dissipated in the form of heat [67]. This mechanism increases the oxidation of fatty acids and glucose, improves insulin sensitivity. It is activated by darkness, cold, stress (norepinephrine) and thyroid hormones. When activated, this tissue reduces high cholesterol and prevents the development of atherosclerosis [68].

The brown tissue has numerous blood capillaries and noradrenergic nerve endings involved in regulating its development and thermogenesis, functions in which the sensory neurons also participate, located between the cells that make up this tissue [69].

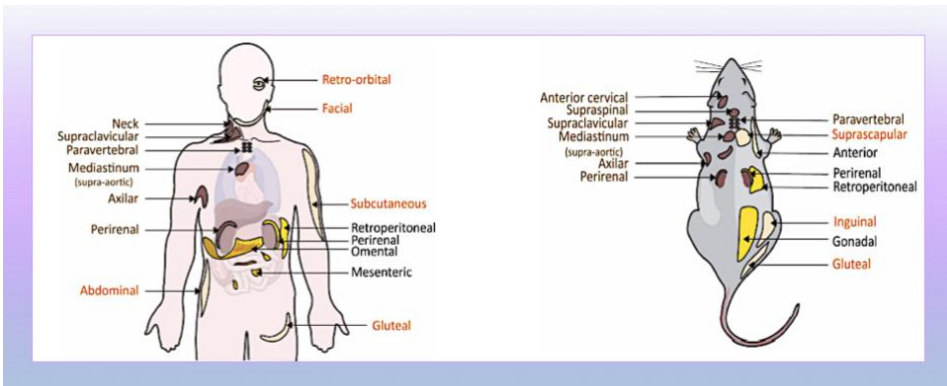
It predominates in the newborn, mainly in the interscapular, perirenal and inguinal regions. In adults, studies based on glucose uptake, by positron emission tomography and [59] f-fluorodeoxyglucose, have detected it in the neck, dispersed in the white tissues and in the interscapular and supraclavicular regions. It is almost absent in obese and elderly subjects [70]. BAT has the ability to perform adaptive thermogenesis, metabolic homeostasis, and secretion of bathokines.

Adaptive Thermogenesis: Regulates body temperature and has been called the "hibernation gland".

Metabolic homeostasis: decreases circulating triglycerides and glucose storage.

Secretion: prostaglandins, nitric oxide, adiponin, cytokines and bathokines [70].

**Figure 3 Representation of adipose tissue distribution in rodents and humans.**



Adipose compartments are grouped into sWAT (light brown), gWAT (yellow), and BAT (dark brown) and are similarly distributed in humans and mice. Adapted from the PhD thesis of M. Carmen Soler, 2021.

### 1.2.1.3 Beige adipose tissue

The cells have a size intermediate between that observed in the components of the white tissue and those of the brown; they develop in the capillary beds of adipose tissue [71]. Only when stimulated do they express in the mitochondria the characteristic thermogenic components (UCP1) of the brown adipocyte, [72] with which they respond to stimuli such as cold and certain cytokines [73]. In humans, as they age it prevents the formation of beige adipocytes due to cold [74].

In addition to the factors indicated in the paragraph corresponding to the WAT, certain elements of the immune system also take part in the transdifferentiation of the beige adipocyte. Thus, it has been observed that IL33 secreted by adipose tissue cells activates innate lymphocytes, which thanks to elements such as the peptide met-enkephalin and cytokines promote differentiation into beige adipocytes [74].

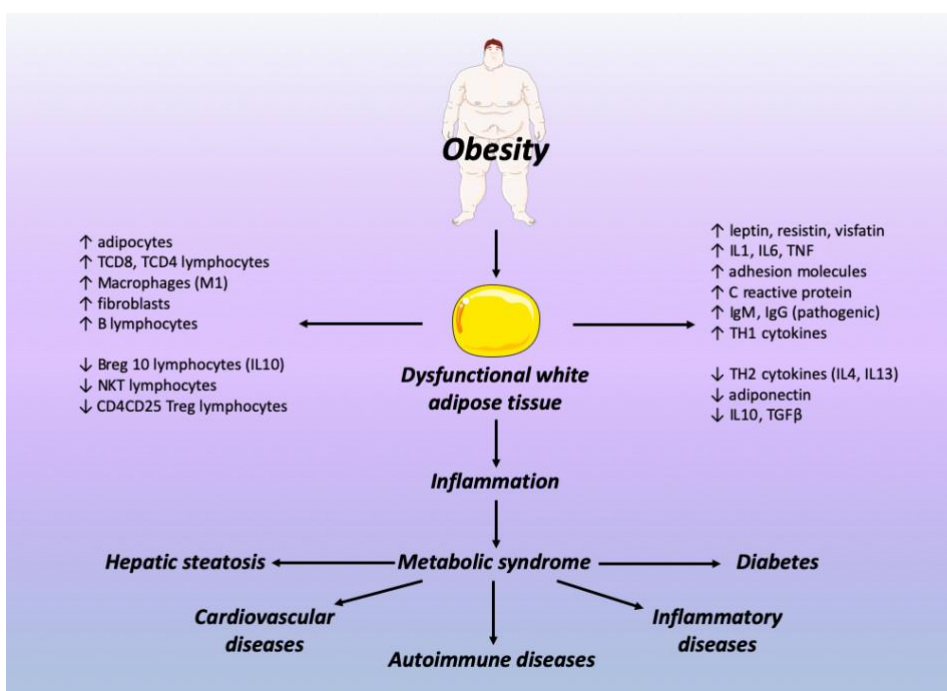
2s secrete IL5 and IL13, which activate IL4-producing eosinophils; this cytokine activates the catecholamine-secreting macrophage M2 and PDGFR $\alpha$ + cell precursors to differentiate into beige adipocytes [75]. These highlight the important participation of Th2 type cytokines (IL4, IL5, IL13) in the genesis of this adipocyte. On the contrary, TGF (transforming growth factor)  $\beta$  inhibits it.

Its flexible phenotype allows it to store or eliminate energy based on environmental or physiological changes and only expresses the UCP1 component when stimulated [72]. Creatine metabolism which, in response to cold or adrenergic activation, uses energy and produces calories [76]. Recent research indicates that preactivated beige tissue can improve glucose tolerance when transplanted into obese mice [71].

### **1.2.2 Effects of obesity on adipose tissue**

The function of adipose tissue is modified when there is obesity; the excess of molecules released by the altered adipocytes and by the rest of the local cells and penetrating again into this tissue, causes, among other things, a low but constant level of inflammation (Figure 4) [55]. In addition to white tissue remodeling due to adipocyte hypertrophy and hyperplasia, there is also remodeling of the vascular and extracellular matrix [77].

**Figure 4 Alterations in WAT and immunometabolic effects.**



*In obesity, the number and normal function of cellular tissue components (left column) are altered (right column). The prooxidant and proinflammatory environment that originates in this tissue induces insulin resistance and damage to other organs, which generates alterations that induce the metabolic syndrome.*

In accordance with the above, in sustained obesity there is fibroinflammation, which exacerbates the functional impairment of adipose tissue, there is insulin resistance and promotes the presentation of type II diabetes and cardiovascular disease. It has even been pointed out that BAT can alter its performance and target function. Several mechanisms [78] have been proposed to explain the pathophysiology of obesity-induced metabolic disorders, including:

- Chronic energy imbalance.

- Greater uptake by adipose tissue of endogenous lipids or lipids from food.
- Ectopic fat deposits and increase in normal fat deposits with visceral predominance.
- Exaggerated expansion of adipocytes with angiogenic limitation leading to ischemia and fibrosis.
- Hypoxia.
- Apoptosis or necrosis of adipocytes.
- Lipid-induced toxicity, with damage to cellular components.
- Increase in reactive oxygen species.
- Endoplasmic reticulum oxidative stress and mitochondrial dysfunction.
- Prooxidant environment that recruits cells and induces pro-inflammatory polarization.
- Dysfunction of WAT, with changes in both cell number and function and secreted molecules, which cause immunometabolic alterations and inflammation. This dysfunction prevents fatty tissue from managing body lipids, so they begin to accumulate in non-fatty tissues such as liver, muscle, bone, heart, promoting insulin resistance, inflammation and metabolic dysfunction in them.

### **1.2.3 Cellular inflammation in obesity**

Obesity is currently considered a chronic, mild-to-moderate inflammatory condition [79]. The demonstration of this exacerbated inflammatory state in conditions of excess is at different levels. At the systemic level, it is manifested by an increase in plasma inflammatory mediators such as C-reactive protein, tumor necrosis factor alpha (TNF $\alpha$ ) or circulating leukocytes (quantitative and qualitative changes) [80]. Additionally, there are changes at

the intracellular level in different cell types associated with metabolism, such as fat, liver, musculoskeletal, and pancreatic beta cells. Although adipose tissue contains some inflammatory cells under normal conditions, the tissues of obese people show a significantly increased proportion [81]. In mouse models with specific gene deletions, it has been observed that obese mice that do not increase macrophage infiltration do not exhibit the metabolic alterations typical of obesity [81]. Similarly, lean mice that see increased numbers of macrophages in adipose tissue exhibit the metabolic alterations typical of obese mice [82]. Thus, the presence of macrophages would be of vital importance in the association of obesity and metabolic and cardiovascular diseases.

There are multiple hypotheses as to why these inflammatory cells infiltrate adipose tissue, including tissue hypoxia [83], adipocyte hypertrophy [84], increased expression of chemokines [85], alterations of the extracellular matrix [86], the release of fatty acids [87], the death of adipocytes [88], among others. There is also evidence that circulating mononuclear leukocytes (including monocytes, circulating precursors of tissue macrophages) are in a pro-inflammatory state in conditions of obesity [83]. This conditions a greater susceptibility to react to chemoattractant signals from different tissues, which would explain the infiltration of other organs. The presence of lymphocytes in adipose tissue has recently been described, although the consequences of their presence are not well understood [89]. These results suggest that obesity may not only activate innate immunity, but also adaptive immunity. To date, no particular antigen has been identified that could explain this phenomenon.

In a situation of obesity where there is excess fat, especially at the visceral level, an inflammatory environment is likely to be created, with an increase in leptin, fibrinogen and components of the renin-angiotensin-aldosterone system. This induces and promotes infiltration of visceral adipose

tissue by macrophages in obesity [90]. These inflammatory mediators are not only produced by adipocytes, but also by cells of the reticuloendothelial system and by preadipocytes. The expression of genes that code for the synthesis of inflammatory mediators is increased in adipocyte stromal tissue, in which macrophages and preadipocytes are also found. The latter also synthesize cytokines when stimulated by TNF- $\alpha$ 77. Thus, in this context, changes in the size of adipose tissue induced by weight gain would generate adipocyte secretion of cytokines, which induces the synthesis and release of chemotray factors from cells of the reticuloendothelial system by the tissue. adipocyte stromal. The end result would be the infiltration of the WAT by macrophages and the perpetuation of local inflammation in the WAT itself [91].

### **1.2.4 Secretory profile of adipose tissue**

Several secretory products of adipose tissue have been identified. The list of these factors continues to grow, which is why only a percentage of them have an adequate functional characterization. Most adipokines can be synthesized by any of the cellular components of adipose tissue: adipocytes, preadipocytes, immune system cells, endothelial cells, and fibroblasts, although some are specific products of a single cell type. These secretion products can have local effects (autocrine activity), influence the physiology of adjacent organs such as the heart, blood vessels or others (paracrine effect) or in very distant organs, via the blood (endocrine effect). The secretion profile under normal physiological conditions would have an effect of metabolic homeostasis. Thanks to these signals, information on energy reserves, appetite, energy expenditure, sensitivity to key metabolic hormones such as insulin, among others, are coordinated.

In this way, the functions of adipose tissue are integrated with other organs such as the pancreas, digestive tract, liver and brain. However, in conditions of obesity, this secretion profile is altered, establishing impaired communication between different organs [92]. For example, under conditions of adipose tissue expansion, signals of excess deposition are not correctly detected at the level of the central nervous system, which does not respond with the expected decrease in appetite [93]. On the other hand, adipose tissue secretory products condition lower insulin sensitivity, both locally and systemically [94]. Moreover, the adipokines secreted in the conditions of obesity are pro-inflammatory and prothrombotic, favoring the fundamental conditions of etiopathogenesis of atheromatosis.

The formation of atherosclerotic plaques (previously understood as a simple deposition of cholesterol in the blood vessels) is the product of the interaction between an exacerbated immune system, whose cells actively migrate to the subendothelial space, and alterations metabolic (increase in oxidized LDL). The inflammatory process that occurs there, associated with the procoagulant state, triggers the acute coronary event which constitutes the main morbidity and mortality associated with obesity [95].

### **1.3 BAT thermogenesis and activity in humans and mice**

BAT has the ability to burn off excess energy in a process called mitochondrial uncoupling. This unique response is facilitated by the mitochondrial protein UCP1, which has the ability to uncouple the respiratory chain by regulating the proton gradient in the mitochondrial membrane for re-entry and heat generation in response to cold, increasing significant energy expenditure. It could be a beneficial treatment for obesity and associated metabolic diseases [96]. Mice lacking UCP1 are seriously compromised in their



ability to maintain normal temperature when exposed to cold and they are also likely to become obese. In mice, BAT has been shown to protect against diet-induced obesity, insulin resistance, and type 2 diabetes. This is based on preventing excessive accumulation of triglyceride (TG) in tissues non-fatty such as muscle and liver [97]. The activity and prevalence of BAT are inversely proportional to the BMI, body fat and visceral fat. This suggests that BAT, due to its thermogenic activity, protects against fat accumulation in humans and rodents.

In mice, activation of BAT reduces adiposity and protects against high-fat diet-induced obesity. Thus, both the BAT mass loss and the severe brown lipoatrophy confers susceptibility to obesity in mice. Recently, it has been described that the amount of BAT is inversely proportional to BMI in humans. Additionally, BAT has been seen to protect against age-related diseases. Therefore, people with smaller BAT stores are more likely to accumulate WAT and increase body weight, which increases the risk of developing metabolic and vascular disorders. In addition to thermogenesis, recent studies have shown that BAT may have a prominent role in lipid and carbohydrate metabolism and may be related to the reduction of elevated concentrations of TG lipogenesis [98].

It has been described that the increased activity of BAT during short exposures to cold could control the metabolism of triglyceride-rich lipoproteins (TRL) in mice, regulating the elimination of these lipoproteins and the excessive circulation of lipids and thus decreasing the TG and increased HDL (high-density lipoprotein). Therefore, FAs (fatty acids) are efficiently introduced into BAT due to the metabolic program that drives TRLs to efficiently take up FAs. This process, together with an increase in the expression of vascular endothelial growth factor (VEGF), leads to an increase in lipoprotein permeability, allowing TGs to exit

capillaries. Activation of BAT by NE does not only activates the release of FA from TG, but also increases the expression of LPL [98].

Therefore, LPL degrades TGs and allows FAs to become available to plasma membrane transporters such as CD36. Additionally, it has been observed in humans that activation of BAT by exposure to cold increases oxidative metabolism, reduces TG content and contributes decisively to energy expenditure. So, the activation of BAT might be able to correct hyperlipidemia, ameliorating the deleterious effects of obesity and dyslipidemia such as insulin resistance or the atherogenic process. Therefore, activation of BAT has been reported to reduce plasma TG and cholesterol levels and attenuate the development of diet-induced atherosclerosis in experimental models. On the other hand, it has been described that BAT could regulate CH metabolism. The BAT mitochondria use pyruvate for combustion whenever UCP-1 is activated by FA. In addition, glucose transporters GLUT-1 and GLUT-4 may be involved in glucose uptake by BAT since the activity and expression of both transporters are increased by both cold exposure and DO [99].

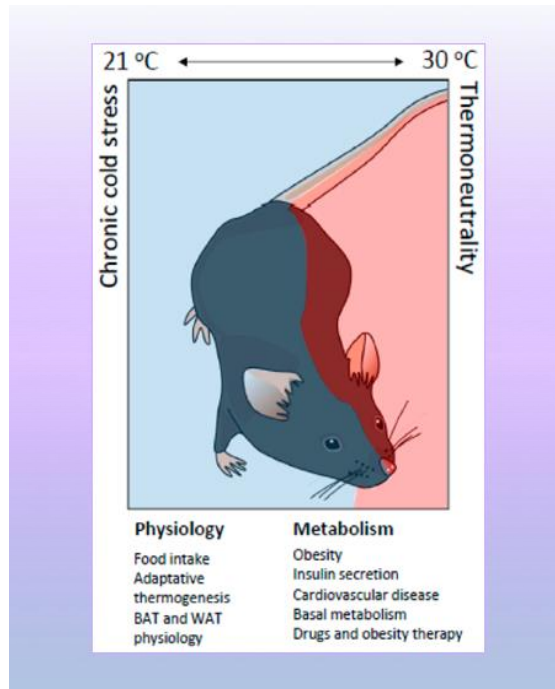
Also, the insulin is responsible for GLUT4-mediated glucose uptake in brown adipose tissue. It has long been thought that the burning of lipids is the primary source of energy for BAT, but it was later shown that upon UCP1 activation, heat production in BAT is the result of both glucose combustion and fat, so in addition to FA, glucose is taken up by BAT and can act as fuel for mitochondrial uncoupling, leading to heat release, weight loss, and lower plasma glucose levels. During cold exposure, FA oxidation occurs to a greater extent, although glucose metabolism is also elevated. Studies in mice have shown that obese and diabetic mice died of hypothermia after being exposed to cold and had only 50% of the thermogenic capacity of BAT. Obese people, but not diabetics, have shown that it is not obesity per se, but accompanied by insulin

resistance, which is partly responsible for the reduction in BAT thermogenesis [98].

In the last decades, brown adipose tissue has become an attractive target to treat obesity. However, environmental variables such as temperature and the dynamics of energy expenditure could influence brown adipose tissue activity. Currently, most metabolic studies are carried out at a room temperature of 21 °C, which is considered a thermoneutral zone for adult humans. However, in mice this chronic cold temperature triggers an increase in their adaptive thermogenesis [100].

In this way, to carry out studies that involve induction of obesity, or others, referring to the development and progression of metabolic changes, it is important to consider the thermogenesis caused by the BAT, and within the variables of studies it is necessary Animals, a key aspect in the conditions of execution of the design and experimental model.

**Figure 5 Metabolic and physiological differences in mice under chronic cold or at thermoneutrality.**



Mouse models used to study metabolic diseases are influenced by environmental temperature. Mice show differences in the metabolic phenotype when housed at a standard temperature (21 °C) vs. thermoneutrality (30 °C). Mice at standard temperatures are subjected to chronic cold. This triggers-controlled hypothermia where energy expenditure is affected by changes in physiology (food intake, BAT and WAT physiology and an increase in adaptive thermogenesis) and in metabolism (basal metabolism, adaptive thermogenesis, diet efficiency, insulin secretion, adipose tissue physiology, inflammation at adipocyte and vascular levels, and the effect of drugs and therapies against obesity).

### 1.3.1 Brown adipose tissue activity is decreased in obesity and diabetes

Adipose tissue plays a crucial role in the study of the mechanisms involved in obesity-related diseases. Adipose tissue is classified into: 1) WAT responsible for storing energy and 2) BAT, which controls thermogenesis by burning fatty acids to produce heat and defend the body against cold. BAT has traditionally received less attention than WAT because it was considered

exclusive to rodents and neonatal humans. However, in the last decade, active BAT has been discovered in adult humans [101]. In addition, it has been seen that the activity of BAT is reduced in obese and diabetic patients [102].

Therefore, BAT has become the focus of attention as any approach capable of increasing BAT mass or activity may be a potential strategy to fight obesity and diabetes. Various factors have been described as activators of "browning" (that is, an increase in the expression and activity of the uncoupling, thermogenic and specific protein of BAT, UCP1) in adipose tissue such as natriuretic peptides, BMP7, norepinephrine or FGF21 among others [101].

Obesity is characterized by a dysregulation between energy intake and energy expenditure. BAT has emerged as an important regulator of energy expenditure in obesity by controlling thermogenesis. CPT1A, a key enzyme in FAO, has been implicated in the control of energy homeostasis. However, the specific role of CPT1A in modulating BAT metabolism to control food intake and obesity is still highly unknown. In rats and mice, the level of dietary fat has been directly linked to an increase in body weight and body fat [103]. Animal models have been widely used in feeding and obesity experiments. In these experiments, a variety of commercial diets have been used to induce obesity [104].

The objective of this research work is to find new approaches to reduce obesity and eating by activating CPT1A, and therefore FAO, in BAT. For peripheral activation of FAO in BAT, the mutated and permanently active form CPT1AM is expressed. This will be done in mice *in vivo* by using adeno-associated virus. As a result, the activation of CPT1A in BAT will activate thermogenesis and reduce food intake, identifying new strategies for a possible therapy against obesity and its associated metabolic diseases such as diabetes.

### **1.4 Lipid metabolism**

Lipoproteins that are substances composed of proteins and fats, perform three main functions: a) transport dietary fats from the intestinal mucosa, where they are absorbed, to the tissues of the animal organism; this role is performed by chylomicrons and chylomicron residues. b) transport triglycerides from the liver to the rest of the body's tissues, to be stored or oxidized for energy. The Responsible for this action are very low-density lipoproteins (very low-density lipoproteins), also known as VLDL. Once triglycerides are released from VLDL into the tissues, the remaining constituents are returned to the liver in the form of intermediate density lipoproteins (IDL), and also as lipoproteins [105], c) act as a mediator in the reverse transport of cholesterol; This task falls to the high-density lipoproteins (HDL), and the LDL, which return to the liver the excess cholesterol formed in the extrahepatic tissues.

Lipids are fats that are absorbed from food or synthesized in the liver. Triglycerides and cholesterol are the lipids most compromised by disease, although all lipids are physiologically important. Cholesterol is a ubiquitous component of all cell membranes, steroids, bile acids, and signaling molecules. Triglycerides primarily store energy in adipocytes and muscle cells. Lipoproteins are hydrophilic spherical structures that have proteins on their surface (apoproteins or apolipoproteins) capable of acting as cofactors and ligands for enzymes responsible for lipid processing. All lipids are hydrophobic and mostly insoluble in blood, thus requiring transport within lipoproteins. Lipoproteins are classified based on their size and density (defined according to the ratio of lipids to proteins) and are important because high concentrations of LDL and low

concentrations of HDL are important risk factors for the development of ischemic heart disease.

Dietary triglycerides are digested in the stomach and duodenum, where they are converted to monoglycerides and free fatty acids by the action of gastric lipase and emulsified as a result of intense gastric peristalsis and the action of pancreatic lipase. Cholesterol esters in the diet are de-esterified to free cholesterol through the mechanisms mentioned. Monoglycerides, free fatty acids, and free cholesterol are then solubilized in the intestine in bile acid micelles, which carry them to the intestinal villi for absorption [105].

Once absorbed into the enterocytes, they reconstitute triglycerides and assemble with cholesterol to form chylomicrons, which are the largest lipoproteins. Chylomicrons transport triglycerides and dietary cholesterol from the interior of enterocytes through lymphatic vessels into the circulation. In the capillaries of adipose and muscle tissues, apoprotein C-II (apo C-II) on the chylomicron activates endothelial lipoprotein lipase (LPL), which converts 90% of the triglycerides within the chylomicrons to fatty acids and glycerol, molecules that are then absorbed by adipocytes and muscle cells for conversion to energy or storage [105].

### **1.4.1 Lipolysis/ lipogenesis**

The adipocyte is a cell that has the appropriate machinery to store a lipid droplet in its cytoplasm, without associated damage. This deposit is not passive, there is a system for regulating lipogenesis (entry into the cell of fatty acids which are esterified by a molecule of glycerol, at the origin of triglycerides). Lipolysis, the release of fatty acids from the fat cell, is also an active phenomenon regulated by different signals. The lipid droplet is covered with different proteins that give it its stability and allow the entry or exit of fatty acids against certain

signals. For example, among the signals that regulate lipogenesis, we have insulin (which stimulates it) and leptin (which inhibits it); among those that modulate lipolysis, catecholamines (prolipolytics) and insulin (antilipolytics) stand out. The excess of circulating fatty acids can lead to their deposition in non-adipose cells, generating insulin resistance through lipotoxicity phenomena [106].

Fat accumulation is determined by the balance between lipid synthesis (lipogenesis) and its breakdown, lipolysis, which is the oxidation of fatty acids. Lipolysis is a metabolic process carried out by adipocytes during times of nutrient deficiency and/or stress, in which the three fatty acids esterified to the glycerol backbone are hydrolyzed from triacylglycerol and released from the cell. Free fatty acids (non-esterified fatty acids with a free carboxyl group) circulate in the blood non-covalently bound to a carrier protein, serum albumin. Impaired lipogenesis in lipogenic tissues is seen in various metabolic diseases including obesity, non-alcoholic fatty liver disease, and metabolic syndrome. Lipogenesis has been reported to be exacerbated in cancerous tissues and in virus-infected cells. These observations suggest that inhibitors of the pathways leading to de novo lipogenesis can be used therapeutically [107].

### **1.4.2 Fatty acids degradation**

Fatty acids are made up of a large hydrocarbon chain that can have between 4 and 33 carbons. However, for them to be oxidized in the Krebs cycle, they must be converted into molecules of smaller molecular size. Therefore, beta-oxidation is a process responsible for the progressive "breaking down" of the long carbon chains of fatty acids and their conversion into smaller molecules. More specifically, beta-oxidation results in the successive removal of two carbon atoms in each cycle of the process, until the fatty acid is completely broken down



into Acetyl-CoA molecules. In addition, during beta-oxidation, reduced coenzymes (NADH and FADH<sub>2</sub>) are also produced that can enter the respiratory chain, so it is a metabolic process that also produces a certain amount of energy [108].

### **1.4.3 Cholesterol metabolism**

Cholesterol is an important lipid molecule used for many biological functions. Cholesterol can be synthesized from endogenous acetyl-CoA or absorbed from food in the gastrointestinal tract. Because cholesterol is lipophilic, it must be transported into the bloodstream via lipoproteins, where it can be taken up by hepatocytes or peripheral tissues. There, cholesterol can be stored, used in cell membranes, or used as a precursor to steroid hormones. The human body cannot break down the ring structure of cholesterol, so the only potential excretion mechanism is the production of bile acids [109].

Cholesterol synthesis is controlled by a feedback mechanism, since the synthesis and activity of this enzyme is inhibited by cholesterol. The activity the enzyme is high in regulation after a period of fasting. Increasing carbohydrates or triacylglycerides in the diet increases cholesterol synthesis from acetyl CoA. Cholesterol administration, although limiting the formation of mevalonic acid, has also been reported to inhibit the conversion of mevalonate administered in cholesterol. A second site of action of the dietary cholesterol feedback mechanism has been suggested to be involved in the cyclization of squalene to lanosterol. Alterations in blood cholesterol levels have been observed in response to changes in the degree of fatty acid saturation in the diet. The higher the level of fatty acid saturation in the diet, the higher the serum cholesterol concentration. The basis for this fact is unknown [109]. The liver plays a major role in the breakdown of cholesterol. The rate of transformation of cholesterol

into its metabolites, including bile acids, will influence the level of excretion of cholesterol by the liver into the bile and therefore on the amount of cholesterol absorbed by the intestine. This cholesterol, like that which comes from food, can influence the rate of synthesis of cholesterol.

### **1.5 Mitochondrial bioenergetics**

#### **1.5.1 Fatty acid oxidation**

Fatty acids are transported in the blood as free fatty acids (FFA), also called non-esterified fatty acids, are fatty acids in the non-esterified state. In plasma the longer chain FFAs are combined with albumin, and in the cell, they are bound to a fatty acid binding protein, so in fact they are never really "free". Shorter chain fatty acids are more soluble in water and exist as a unionized acid or fatty acid anion [110].

The oxidation of fatty acids plays an important role in the production of energy from lipids. During fasting, fatty acids are used for the synthesis of ketone bodies and provide most of the necessary energy. The importance of timely recognition of these defects lies in the fact that their decompensation in most cases can be avoided. Clinically, they are expressed by nonketotic hypoglycemia, acute liver failure, cardiomyopathy, myopathy, and even death triggered by prolonged fasting [111]. Metabolism of fatty acids begins with their release from adipose tissue, where they are deposited as triglycerides, and their subsequent plasma transport coupled to albumin. Once inside the cytosol, the long chain fatty acids (16-18 carbons) that bind coenzyme A cross the carnitine-bound mitochondrial membrane using the carnitine cycle. The various fatty acids coupled with carnitine constitute the so-called acylcarnitine esters. Short and medium chain fatty acids are able to enter the mitochondria directly, without using the carnitine cycle [112].

Within the mitochondrial matrix, the four stages of the  $\beta$ -oxidation cycle sequentially cut fatty acids with two carbon atoms each time by means of two or more specific enzymes for each stage, until the final obtaining of the acetyl-coenzyme A. This, in turn, is used in the liver for the synthesis of the ketone bodies  $\beta$ -hydroxybutyrate and acetoacetate, as well as in other tissues, such as skeletal and cardiac muscles, for the production of (ATP) from the Krebs cycle. Intrahepatic synthesis of  $\beta$ -hydroxybutyrate and acetoacetate ketone bodies provides energy primarily to the brain, thus allowing glucose to be spared in the later stages of fasting. The step called electron transfer transfers some of the energy from  $\beta$ -oxidation to the production of ATP [111].

### **1.5.1.1 Fatty acids are activated before being catabolized**

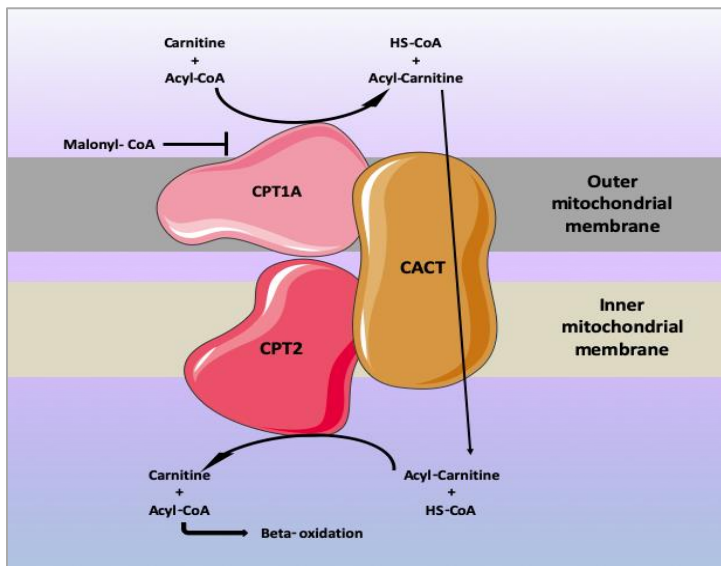
Before fatty acids can be catabolized, they must be converted into an active intermediate; it is the only step in the complete breakdown of a fatty acid that requires energy from ATP. In the presence of ATP and coenzyme A, the enzyme acyl-CoA synthetase (thiokinase) catalyzes the transformation of a fatty acid (or FFA) into an "active fatty acid" or acyl-CoA, using a high-energy phosphate with the formation of adenosine monophosphate (AMP) and Inorganic pyrophosphatase hydrolyzes (PPi). PPi, with loss of another high-energy phosphate, ensuring that the overall reaction continues to completion. Acyl-CoA synthetases are found in the endoplasmic reticulum, peroxisomes, and in and on the outer membrane of mitochondria [113].

### **1.5.1.2 Long-chain fatty acids enter the inner mitochondrial membrane as derivatives of carnitine.**

Carnitine ( $\beta$ -hydroxy- $\gamma$ -trimethylammonium butyrate),  $(\text{CH}_3)_3\text{N}^+-\text{CH}_2-\text{CH}(\text{OH})-\text{CH}_2-\text{COO}^-$ , is widely distributed and particularly abundant in muscle.

Long-chain acyl-CoA (or FFA) cannot penetrate the inner membrane of mitochondria. However, in the presence of carnitine, CPT1, located on the outer mitochondrial membrane, transfers the long-chain acyl group from CoA to carnitine, forming acylcarnitine and releasing CoA. Acylcarnitine is able to penetrate the inner membrane and gain access to the  $\beta$ -oxidation enzyme system via the inner membrane exchange transporter carnitine-acylcarnitine translocase. The transporter binds acylcarnitine and transports it across the membrane in exchange for carnitine. The acyl group is then transferred to CoA, so that acyl-CoA is reformed and carnitine is released. This reaction is catalyzed by carnitine palmitoyltransferase-II, located inside the inner membrane [110].

**Figure 6 CPT system.**



*The long-chain FAs-CoA are transferred from cytoplasm to mitochondrial matrix through CPT system, which includes CPT1, translocase CACT, and CPT2.*

### **1.6 Importance of lipid metabolism and fatty acid oxidation**

Malonyl-CoA, mainly derived from glucose and the first intermediate in fatty acid synthesis, regulates FAO by inhibiting the enzyme carnitine palmitoyltransferase1. Therefore, under high-energy conditions, malonyl-CoA inhibits oxidation by shunting fatty acids for accumulation as triglycerides. There are three CPT1 isoforms with differences in kinetics, malonyl-CoA sensitivity, cellular sublocalization, and tissue expression: CPT1A (liver, brain, pancreas, kidney, and WAT) and CPT1B (BAT, skeletal muscle, heart and WAT) found in the mitochondria and CPT1C (brain) found in the endoplasmic reticulum (ER) [114].

It should be noted that FAO and CPT1 mRNA and protein levels are reduced in obese and diabetic patients [115] [116]. Thus, the fact that CPT1A controls FAO makes it a very attractive target for reducing lipid levels and fighting obesity, as has been shown by our group and by others in white adipocytes and macrophages [117], brown adipocytes [101], liver [118] [119] [120], pancreas [121] [122] y muscle [7]. This effect is even greater when a permanently active mutated form of CPT1A, CPT1AM, which is insensitive to malonyl-CoA, is used [123] no negative effects on lean animals or healthy cells.

### **1.7 Gene therapy**

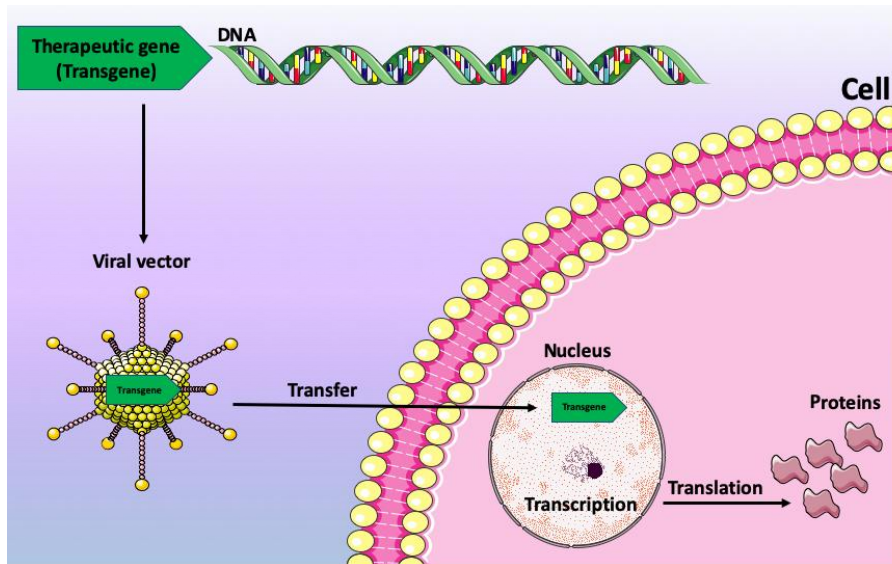
Gene therapy can be defined as the set of techniques that allow fragments of DNA or RNA inside the cell of interest (target cell), with the aim of modulating the expression of certain proteins that are altered by some disease, with this it is possible to reverse the biological disorder that the altered protein produces. It can be used to treat hereditary diseases or acquired diseases. To apply gene therapy, it is first necessary to identify the gene or group of genes causing the alteration [124]. Once the defective gene has been identified, the transfer of the functional copy of the gene is initiated by means of a transporter

capable of entering the nucleus of the cell [125]. The objectives of the transfer in the context of gene therapy: somatic cell and germ cell therapy. The first aims to heal cells in organs and tissues that do not match the germline; the second aims to heal this lineage to impact, in turn, the offspring [126].

While therapy applied to somatic cells tends towards highly predictable results with little impact from the biological domain on the offspring, gene therapy based on the genetic material of the sex chromosomes involves consequences that can be strictly assessed at the time of manipulation. Despite the safety of genetic intervention, an ethical consideration emerges, which although it must be present in any type of therapy, in gene therapy, due to its effectiveness, it becomes relevant [127]. Gene therapy has the advantage of making it possible to achieve sustained circulating levels of the native protein with a single administration of the therapeutic vector, which makes it a very interesting therapeutic strategy.

The most used viral vectors for the realization of the genetic transfer are retrovirus, adenovirus, lentivirus, adenoassociated viruses, and herpes viruses. The choice of each will depend on the therapeutic objective that you want to perform. In this thesis we will focus on the adenoassociated viruses, which are the viral vectors chosen for the transfection of the BAT cells, a procedure that will be detailed later in the chapter of materials and methods.

Figure 7 Grace Therapy Foundation.



*The sequence of the therapeutic gene is introduced into a transporter (vector) that facilitates its transfer to the interior of the cell. The transcription and translation processes of the gene in the cell will lead to the synthesis of the protein that will be corrected to correct the disease.*

There are several AAV serotypes with different tropisms, thus, the choice of a serotype, associated with the use of specific promoters, makes it possible to limit the overexpression of the gene of interest in the target tissue of choice [128].

AAV vectors are genetically modified viruses in which all the viral genes involved in integration and replication mechanisms, and the construct with the therapeutic gene of interest has been added [129]. Moreover, to date, no pathogenic processes in humans have been associated with adeno-associated viruses. Therefore, AAVs maintain the infectivity of the parent virus but are unable to generate new virions. The safety profile of AAVs is excellent and has the ability to provide expression over a large square and variety of tissues, characteristics that make them highly effective vehicles for gene therapy [130].

Therefore, many of the therapeutic strategies for the treatment of genetic diseases in humans by means of *in vivo* gene therapy use AAV technology with very promising results [131].

### 1.7.1 Adeno-associated viral vectors

AAV are very small viruses, belong to the parvovirus family. There are many different types of AAVs. Each type has a different property that allows them to target different cells, ranging from kidney cells to neurons in the brain [132]. AAVs are now widely used in gene therapy strategies to target different diseases depending on the types of organs and tissues they affect [132].

Adeno-associated viral vectors can be used to produce drugs. These vectors are derived from the adeno-associated virus, a single-stranded DNA virus belonging to the Parvoviridae family. AAVs are widely distributed among a large number of animals and humans. It is estimated that approximately 80% of the adult population is seropositive for at least one AAV serotype. Despite the ubiquitous distribution of AAVs and the high frequency of AAV immunity, AAVs do not have not been associated with any pathogenic disease in humans or animals. AAV viruses can only replicate if the cell is co-infected with a helper virus. I know Adenovirus, herpes simplex virus, pseudorabies virus, and human papillomavirus are known to promote the replication of wild-type AAVs. In the presence of a helper virus, AAV generates a productive infection characterized by genome replication, expression of viral genes and production of virions. In the absence of a helper virus in the infected cell, the viral DNA may persist in the host cell nucleus episomally or may integrate into the host cell genome resulting in latent infection [133].

AAVs can infect both dividing and non-dividing cells and can infect a wide range of cell types, although specific serotypes may be associated with more



efficient tissue tropism. Adeno-associated virus particles are non-enveloped and very stable in the environment, even when desiccated [133].

Advances in understanding the molecular basis of obesity and obesity-associated diseases have made gene therapy a vital approach in coping with this world-wide epidemic. Gene therapy for obesity aims to increase or decrease gene product in favor of lipolysis and energy expenditure, leading toward fat reduction and loss of body weight. It involves successful delivery and expression of therapeutic genes in appropriate cells. The ultimate goal of gene therapy is to restore and maintain energy homeostasis [134]. Prevalence of T2DM and obesity is increasing worldwide. Currently available therapies are not suited for all patients in the heterogeneous obese/T2DM population, hence the need for novel treatments. There are currently different published studies that reverse or treat obesity and its associated factors, through gene therapy.

A study finds that the Fibroblast growth factor 21 (FGF21) is considered a promising therapeutic agent for T2DM/obesity. Here, AAVs were used to genetically engineer liver, adipose tissue, or skeletal muscle to secrete FGF21. Treatment of animals under long-term high-fat diet feeding or of ob/ob mice resulted in marked reductions in body weight, adipose tissue hypertrophy and inflammation, hepatic steatosis, inflammation and fibrosis, and insulin resistance for > 1 year. This therapeutic effect was achieved in the absence of side effects despite continuously elevated serum FGF21. This study underscores the potential of FGF21 gene therapy to treat obesity, insulin resistance, and T2DM [135].

Another published study in mice, aimed to revert HFD-induced obesity and NAFLD in mice by enhancing liver FAO. They used adeno-associated virus (AAV) to deliver a permanently active mutant form of human carnitine palmitoyltransferase 1A (hCPT1AM). Expression of hCPT1AM enhanced hepatic

FAO and autophagy, reduced liver steatosis, and improved glucose homeostasis [136].

Another published study aimed to enhance BAT thermogenesis by increasing its FAO rate, in a rat brown adipocyte (rBA) cell line through adenoviral infection. They found that CPT1AM-expressing rBA have increased FAO, lipolysis, UCP1 protein levels and mitochondrial activity. Additionally, enhanced FAO reduced the palmitate-induced increase in triglyceride content and the expression of obese and inflammatory markers. Thus, CPT1AM-expressing rBA had enhanced fat-burning capacity and improved lipid-induced derangements. This indicates that CPT1AM-mediated increase in brown adipocytes FAO may be a new approach to the treatment of obesity-induced disorders [137].

The potential and promise for gene therapy in treating obesity have grown exponentially. Effort made in the past has focused on seeking stable and regulated expression using three different methods of delivery: viral vectors, nonviral vectors, and physical methods. So far, viral vectors remain the most prevalent, despite the safety concerns associated with their *in vivo* applications. Synthetic vectors or physical methods, on the other hand, offer safer, though less efficient, alternatives to viral vectors.

### **1.8 CPT1 as a therapeutic protein**

CPT1 enzyme have acyl-CoA as a substrate and malonyl-CoA as a physiological inhibitor, thus positioning themselves as key enzymes in the regulation of intracellular levels of these metabolites. The CPT1A and B isoforms, located in the outer mitochondrial membrane, are responsible for the internalization of acyl-CoAs in the mitochondria so that they are oxidized. Thus, indeed, the role of hypothalamic CPT1A in the control of appetite and glucose

homeostasis has been demonstrated by several research groups [138]. On the other hand, more recently, in 2002, an exclusively neuronal isoform was discovered, CPT1C, which is located in the endoplasmic reticulum and has similar affinities for acyl-CoA substrate and malonyl-CoA inhibitor, although it has no carnitine palmitoyltransferase activity [139]. Since then, it has been shown that CPT1C modulates the levels of another family of intracellular lipids, ceramides, and that these are necessary for the neuroendocrine action of the hormone's leptin and ghrelin. Moreover, the role of CPT1C in the control of energy homeostasis became evident in several studies showing a hypometabolic phenotype of CPT1C-deficient mice under fasting conditions and on a high-fat diet. Specifically, the function of CPT1C is still not fully understood and the function of CPT1A is to transport FA within the mitochondria for subsequent oxidation.

The function of this enzyme is to help break down certain fats in the food we eat and transform them into energy. It also helps break down fat already stored in the body [139]. This enzyme is essential for the oxidation of fatty acids in the mitochondria. CPT1A links carnitine to long chain fatty acids so that they can cross the inner membrane of mitochondria. Once inside the mitochondria, they can be metabolized to produce energy during periods of fasting, especially in the liver and other tissues. More than 20 mutations [115] in the CPT1A gene have been identified in people with carnitine palmitoyl transferase 1 deficiency. Mutations in the CPT1A gene reduce or they eliminate the activity of CPT1A. Without enough of this enzyme, carnitine does not bind to long chain fatty acids and energy is not produced. This energy depletion leads to hypoketotic hypoglycaemia. Fatty acids can also accumulate in cells and damage the liver, heart and brain. This abnormal accumulation causes the manifestation of other signs and symptoms of the disease.

When the CPT1A enzyme is missing or not working properly, the body cannot break down fat and use it for energy, so it only uses glucose. Although glucose is a good source of energy, there is not enough of it. When it's over, the body tries to use the fats without success. This causes low blood sugar, called hypoglycemia, and harmful substances to build up in the blood. CPT1A deficiency can cause episodes of metabolic crisis disease. Symptoms usually occur if you go several hours without eating. In prolonged periods when food is not eaten, all the glucose in the body is used. This causes hypoglycemia. The body then tries to get energy from fat, which causes harmful substances to build up in the blood. Symptoms are also more likely to appear when a person with CPT1A deficiency gets sick or gets an infection. Prompt emergency treatment in infants and children with CPT1A can help prevent metabolic crises or lessen their severity. [139]

CPT1B is a key enzyme in the beta-oxidation of long-chain fatty acids in skeletal muscle, regulating their entry into the mitochondria, to be oxidized and generate energy [138]. The transport of fatty acids from the cytoplasm to the mitochondria for oxidation takes place thanks to their union with carnitine molecules. This transfer system (CPT) is necessary, because long-chain fatty acids (LCFA) are not capable of penetrating the mitochondrial membrane on their own and do so bound to carnitine. The short-chain fatty acids (SCFA) must be activated in the outer mitochondrial membrane, where they are in the form of Acyl-CoA, but in order to be oxidized once activated, they must reach the mitochondrial matrix. To do this, they must bind to CPT1B, which allows the formation of the carnitine acylCoA complex, which allows the passage of SCFA from the outer membrane to the mitochondrial matrix. Once in the matrix, CPT2B is responsible for reversing the process, separating acyl-CoA from carnitine, thus allowing fatty acid oxidation [138].

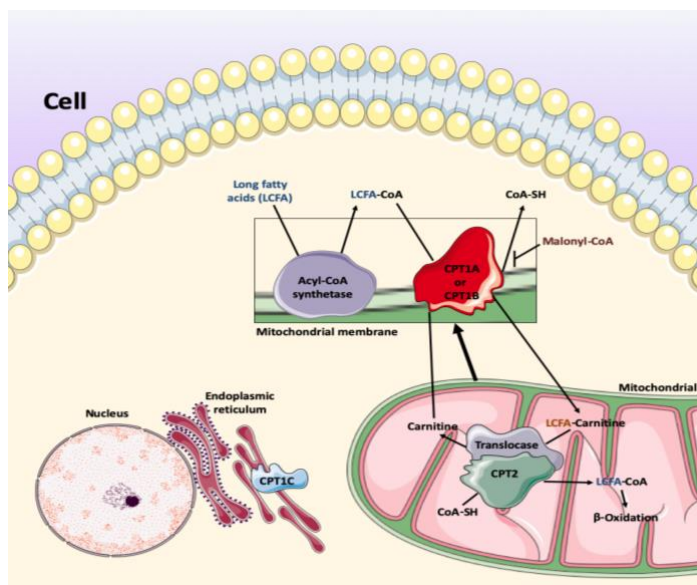
In mammals, three isoforms of CPT1 are expressed, encoded by different genes and with different biochemical properties and tissue distribution:

**Table 3 Isoforms of CPT1.**

Isoforms of CPT1	It is expressed	Function
<b>CPT1A</b>	Liver, brain, pancreas, kidneys and WAT.	Fatty acid oxidation.
<b>CPT1B</b>	BAT, skeletal muscle, heart and WAT.	Is the rate-controlling enzyme of the long-chain fatty acid beta-oxidation pathway in muscle mitochondria.
<b>CPT1C</b>	Brain.	could play a role in the regulation of feeding behavior and whole-body energy homeostasis.

The CPT1A or CPT1L isoform (from the English liver, liver). In rats, it is expressed in the liver, lungs, pancreas, intestine, kidneys, brain and ovaries. It also shows lower expression in heart and WAT and is absent from skeletal muscle and brown adipose tissue [140]. The human CPT1A gene has been mapped to chromosome [141]. The rat CPT1A cDNA encodes a 773 protein with a mass apparent molecular weight of 88 kDa. The activity of this enzyme is inhibited by malonyl-CoA with a sensitivity which can vary according to the physiopathological conditions. CPT1A has a strong affinity for the substrate's carnitine.

**Figure 8 Carnitine palmitoyltransferase system 1 and CPT2 catalyze the reversible transesterification of acyl-CoA and carnitine to form acyl-carnitine and coenzyme A.**



*CPT1A and CPT1B are located in the outer mitochondrial membrane and are specific for long-chain fatty acids (LCFA). The acyl-carnitine transported by the translocases are finally oxidized in the mitochondria. Malonyl-CoA regulates FAO by inhibiting CPT1A and CPT1B, thus being the limiting enzymes of FAO. CPT1C localizes to the ER membrane and has minimal activity detected. Adapted from Casals et al. PLR. 2016.*

### 1.8.1 Carnitine palmitoyl transferase 1A mutant

Long-term overexpression in mouse liver fed a fatty diet of the hepatic isoform of CPT1, CPT1A, or a permanently active mutant, CPT1AM, produces an increase in the oxidation of fatty acids in this tissue and protects against weight gain, the development of obesity and resistance to insulin. In genetically obese mice, a overexpression of CPT1AM in the liver reduces steatosis liver function and blood glucose and insulin levels. For Regarding admission control, CPT1 the hypothalamus may play an important role. He has observed that pharmacological inhibition of CPT1 in hypothalamus of rats leads to a decrease

in intake and weight. While the overexpression of CPT1AM in this organ produces weight gain, hyperphagia, hyperglycemia and hyperinsulinemia. All of this indicates that modulation of CPT1 activity and the oxidation of fatty acids in different tissues can be key to a potential treatment for obesity and associated pathologies [142].

CPT1 is highly regulated by its physiological inhibitor, malonyl-CoA, and represents the main checkpoint of  $\beta$ -oxidation. Malonyl-CoA, derived from glucose, is the first intermediate of lipogenesis and its effect on CPT1 helps maintain a balance between fatty acid synthesis and oxidation processes and signals the relative availability of nutrients in the cell.

To further investigate the role of this enzyme in controlling carbohydrate metabolism, was overexpressed a permanently active isoform of this protein (CPT1AM) in adult male rats.

The enzyme CPT1 catalyzes the entry of LCFA-CoA into the mitochondria and is the main regulator of fatty acid oxidation. Its activity is inhibited by the first intermediate of lipogenesis, malonyl-CoA, which helps maintain the balance between fat synthesis and oxidation.

All members of the malonyl-CoA regulatable carnitine acyltransferase family (CPT1A, CPT1B, and COT) were found to have a methionine at position 593 (M593), while members of the inhibitor-insensitive family (CPT2 and CrAT) have a serine in the same position [143]. By the site-directed mutagenesis technique, the M593 of the rat CPT1A protein was replaced by a serine. This mutation generated an active CPT1A but insensitive to its physiological inhibitor, capable of maintaining 80% of its enzymatic activity regardless of the level of malonyl-CoA [143]. This mutated form of the protein was named CPT1AM.

### ***1.8.1.1 Independent regulation of malonyl-CoA***

In the liver, variations in the insulin/glucagon ratio have been described to produce changes in CPT1 mRNA levels. These changes are associated with low glucose availability and high fatty acid concentrations [144]. In rodents, an increase in CPT1 mRNA has been described during the lactation phase and when fed a high-fat diet. Similarly, diabetic or fasted rats also have higher CPT1A expression and activity in the liver [144]. In the hypothalamus, ghrelin administration has been reported to increase CPT1A expression levels [145]. Despite this, the transcriptional regulation of this enzyme is modest compared to the regulation derived from the concentrations of its substrates or inhibitors.

Likewise, there are post-translational modifications that can alter the catalytic activity of CPT1. Different phosphorylation sites in the CPT1A isoform have been described and the modification of at least two of them alters the kinetic characteristics of the enzyme, in particular its sensitivity to malonyl-CoA [146]. However, it has not been described that these changes are due to variations in physiological state, so they could be constitutive changes [147].

On the other hand, it has been observed that the exposure of cultured hepatocytes to phosphatase 1A inhibitors or adenosine monophosphate-kinase (AMPK) activators activates the enzyme without modifying its sensitivity to malonyl-CoA. This effect is not due to direct protein phosphorylation and disappears when only isolated mitochondria are processed, suggesting that there is some kind of relationship between mitochondria and extra-mitochondrial structure that mediates this effect [148]. In this sense, it has been shown that CPT1A responds to the phosphorylation, by AMPK, of the components of cytoskeleton. This fact could also explain the relationship between cell volume and CPT1 activity [148]. CPT1 is strongly regulated by its physiological inhibitor, malonyl-CoA. For this reason, the mechanisms that



modulate the cytoplasmic concentration of this metabolite are crucial in regulating its activity.

### 1.9 *In vivo* expression of CPT1AM in BAT

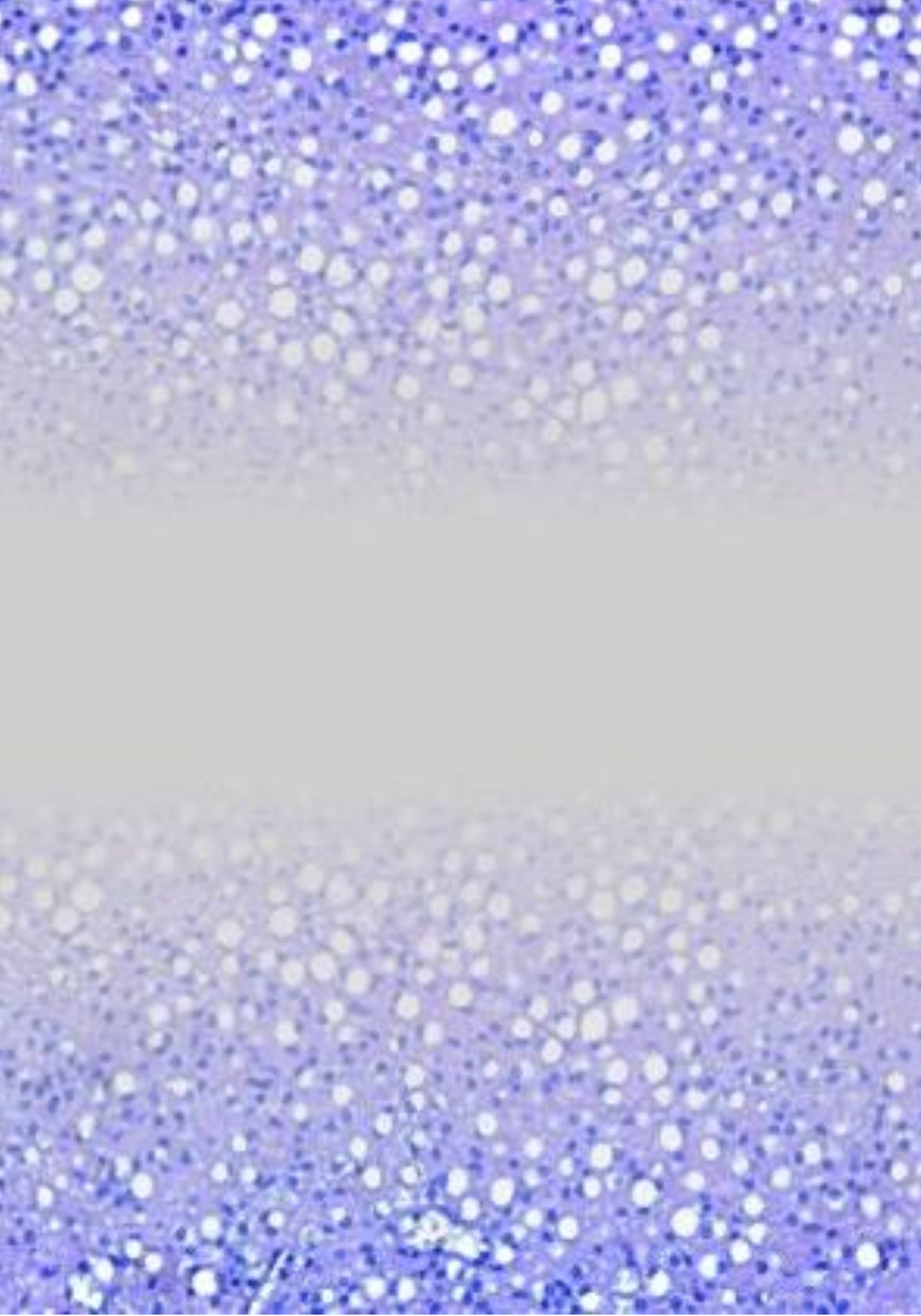
Previous results obtained in our group show that the expression of CPT1AM increases mitochondrial activity and thermogenesis in brown adipocytes *in vitro* [141]. CPT1AM was expressed in a rat brown adipocyte cell line by infection with adenovirus. It was decided to use the CPT1A isoform instead of CPT1B, which is the endogenous form present in BAT, because CPT1A is less sensitive to its inhibitor malonyl-CoA and because it has a higher affinity for the substrate. In addition, the expression of CPT1AM allowed to achieve a permanently active FAO regardless of the levels of malonyl-CoA in the cell.

The results demonstrated that expression of CPT1AM in brown adipocytes increased their FAO, mitochondrial activity, and thermogenesis (lipolysis and UCP1 levels). In addition, the increase in FAO reduced triglyceride content and the expression of obesity and inflammation markers when cells were incubated with palmitate to simulate obesity. This indicates that FAO is critical for fuel provision for thermogenesis and that enhancing FAO in brown adipocytes may be a good strategy in the treatment of obesity [149].

For the *in vivo* study, in collaboration with the group of Dr. Fàtima Bosch (Faculty of Veterinary Medicine, UAB), an AAV was generated specifically CPT1AM in BAT under the control of the UCP1 promoter [130]. This AAV would be drilled directly in the scapular bat of obese and diabetic mice (treated with a high fat diet) and its phenotype will be studied compared to lean controls and treaties with an AAV (Null) control. These studies were carried out to thermoneutrality (30°C), ambient temperature (20°C) or cold (4°C). The project aimed to directly increase thermogenesis in BAT by increasing its ability to FAO.

The mice that express CPT1AM in BAT were expected to show an increase in FAO that leads to an increase in gold and thermogenesis, the reduction of the accumulation of systemic lipids, the decrease in inflammation levels and the best sensitivity to insulin. Therefore, these animals would be protected against diabetes induced by obesity.

# Hypothesis



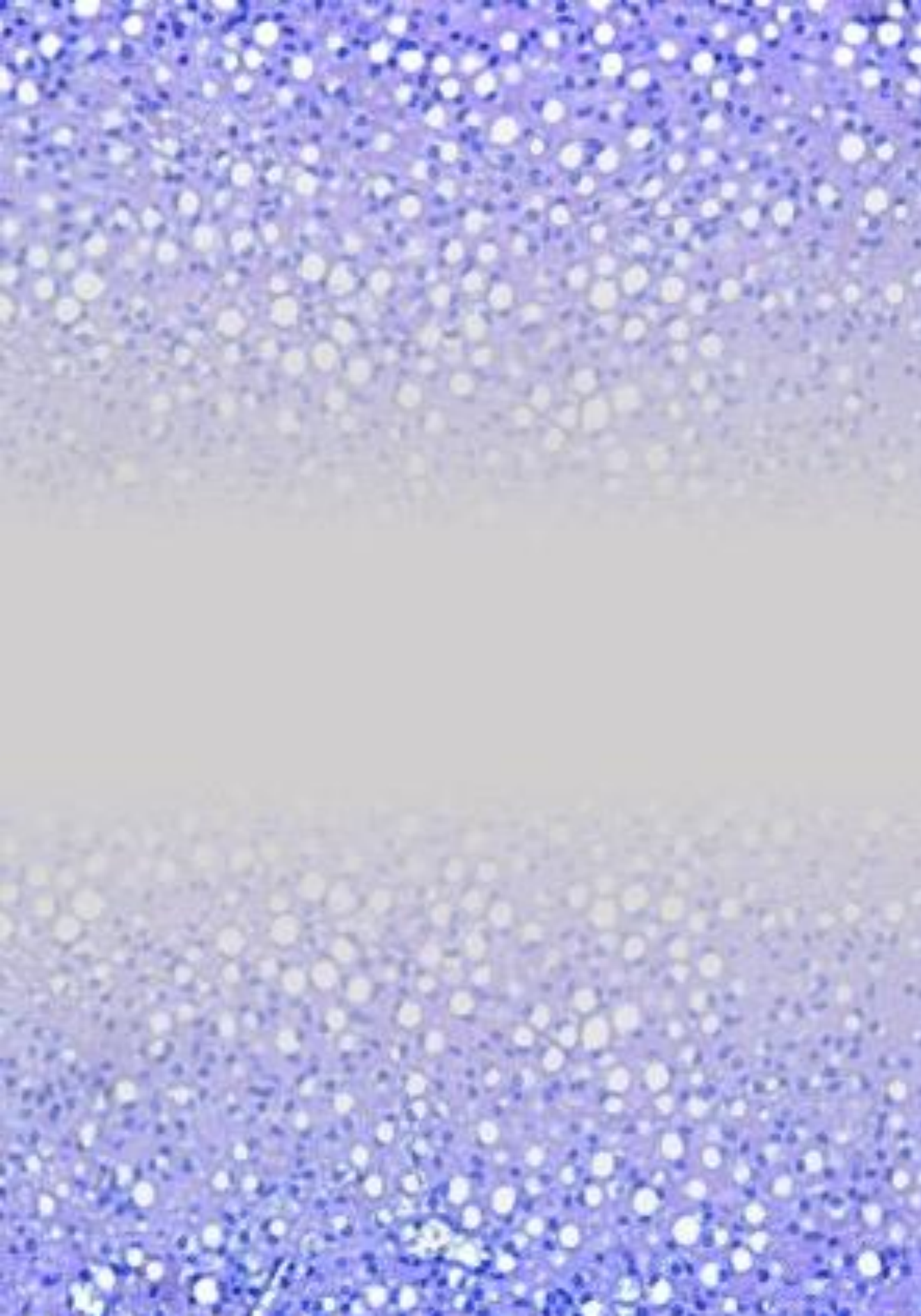
## **2 HYPOTHESIS**

The activation of lipid metabolism by overexpression of CPT1AM in brown adipose tissue reduces obesity and its associated metabolic diseases.





**AIMs**





### **3 AIMs**

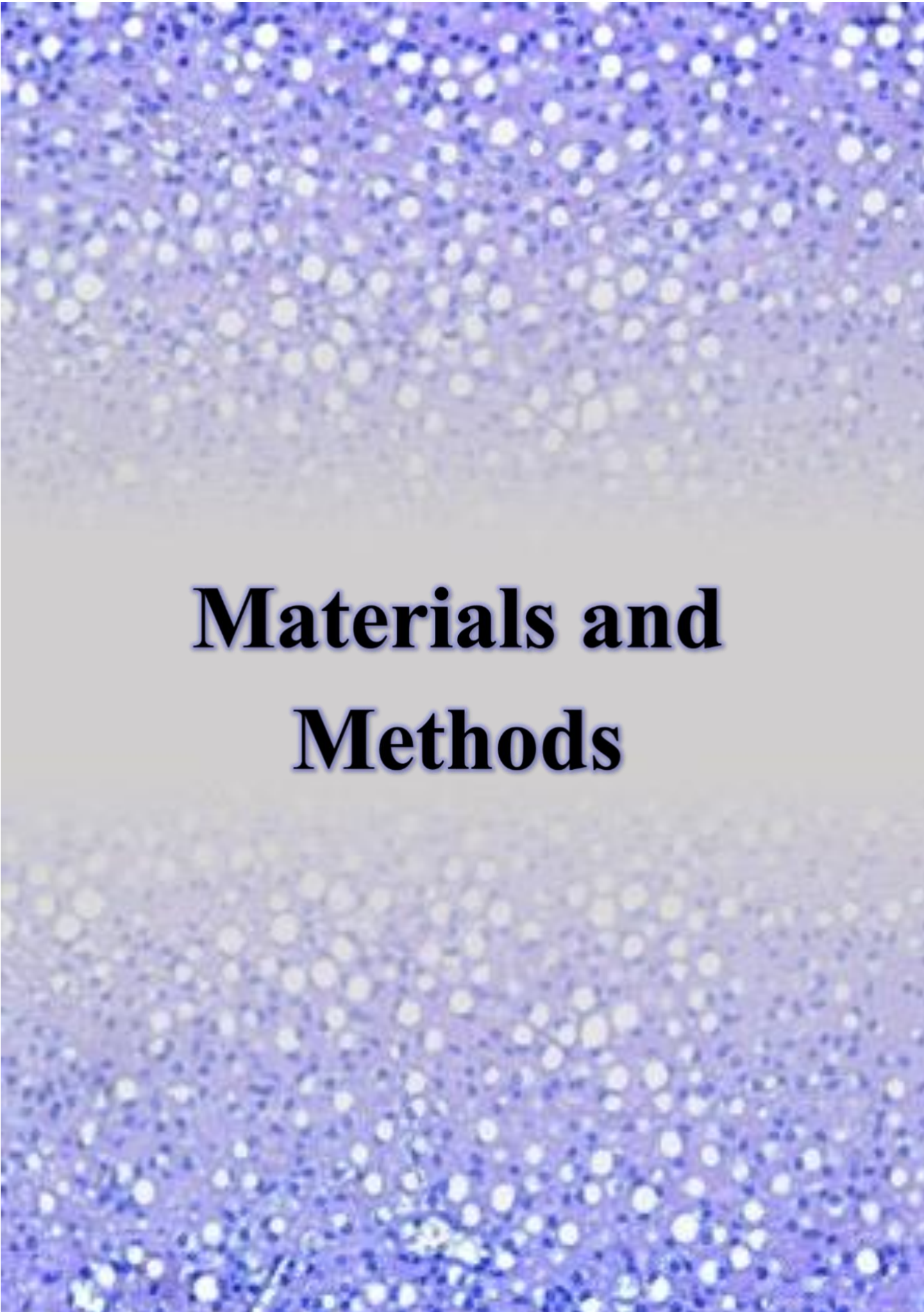
#### **3.1 General AIM**

The main objective of this doctoral thesis is to overexpress CPT1AM in BAT from HFD-treated mice, to prevent and/or treat obesity and associated diabetes. For this purpose, the next specific objectives have been established:

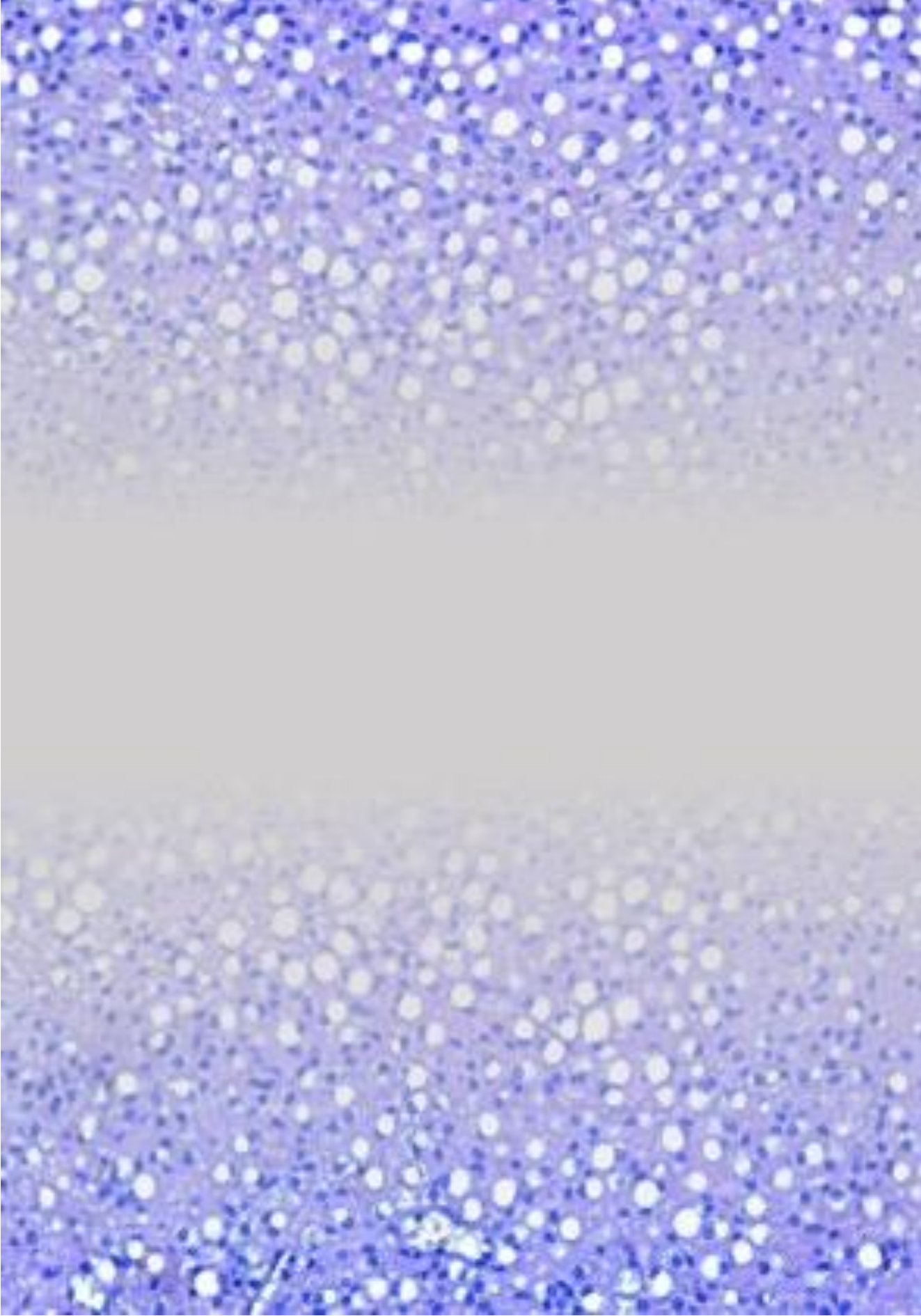
##### **3.1.1 Specific AIMs**

- I. Validation of the administration of CPT1AM in BAT of mice by using AVVs viral vectors.
- II. To analyze the effects of BAT-specific CPT1AM expression in the reversion of diet-induced obesity.
- III. To analyze the effects of BAT-specific CPT1AM expression in the prevention of diet-induced obesity.
- IV. To study the differences in the metabolic phenotype of male and female mice expressing CPT1AM under thermoneutral conditions.
- V. To discern the potential mechanisms involved in the metabolic improvement of CPT1AM-expressing mice.





# **Materials and Methods**



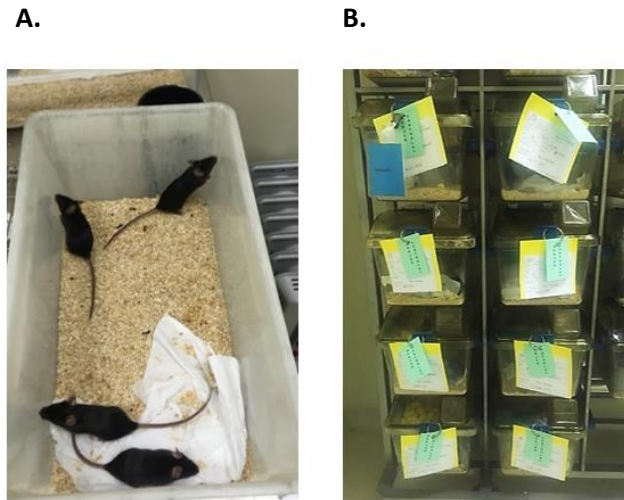
## 4 MATERIALS AND METHODS

### 4.1 Animal model

Male (in cohorts 1, 2 and 3) and female (in cohort 4) mice of the inbred strain C57BL/6J (*Mus Musculus*) were used for this experimental work and were purchased from Janvier Labs, France (ref. no. SC -C57J-M). The mice used are a strain sensitive to the induction of obesity and type II diabetes mellitus by means of a high-fat diet (HFD). In this way, these mice were acquired when they were 7 weeks old, to carry out identification procedures, measurement weight and glucose levels at time zero (before starting the studies).

For this experiment, the animals were kept in the Animal Experimentation Unit of the Faculty of Pharmacy and Food Sciences of the University of Barcelona (reg. no. B-9900030), at  $20 \pm 2$  °C, when they were in the negative pressure, when the viral vectors were punctured. In the case of the animals that were under conditions of thermoneutrality, they were at  $30 \pm 1$  °C, and when acute cold stimuli were performed, the temperature was progressively lowered to  $4 \pm 1$  °C (procedure carried out in the chamber). During the entire procedure they were kept under a 12-h light/dark cycle, at 40-60% humidity and with *ad libitum* access to food and water. All the experimentation protocols and procedures carried out in this study were approved by the Ethics Committee for Animal Experimentation (CEEA) of the University of Barcelona, with procedure number 140/18 P3.

**Figure 9** Used mice and boxes in negative pressure units.



*A) 8-week-old mice. B) Boxes with animals treated with CPT1AM in a negative pressure rack.*

### 4.1.1 Obesity reversal experiment

In the first experiment, when the mice were 8 weeks old, they were put on a normocaloric diet (NCD) (n=16) and HFD (n=16). Once obesity was induced in the HFD mice at 12 weeks, they were treated with the viral vectors, half of the animals with the Null viral vectors (n=8) and the other half with the CPT1AM viral vectors (n= 8), leaving 4 study groups with n=8 (NCD Null, NCD CPT1AM, HFD Null and HFD CPT1AM groups). 20 weeks after viral vector administration, changes in metabolic phenotype and overexpression analysis were observed. This study aimed to reverse HFD-induced morbid obesity through overexpression of CPT1AM in BAT. This experiment was performed on male mice under room temperature conditions at  $20 \pm 2$  °C throughout the procedure, and they were housed 4 animals per cage in the University facilities.



### **4.1.2 Obesity prevention experiment**

In the second experiment, at 9 weeks of age mice were treated with viral vectors, half of the animals with AAVs Null (n=14) and the other half with AAVs CPT1AM (n=15). Immediately after surgery, half of the treated animals underwent NCD (n=7) and HFD (n=7-8), leaving 4 study groups with n=7 and one group with n=8 (HFD CPT1AM). Subsequently, changes in the metabolic phenotype were observed and the overexpression in tissues was analyzed 20 weeks after the administration of AAVs. This study aimed to prevent HFD-induced obesity by overexpressing CPT1AM in BAT. Said experiment was carried out in male mice under conditions of room temperature at  $20 \pm 2$  °C throughout the procedure, like the first cohort of animals, 3 to 4 animals per cage were housed in the University facilities, in the negative pressure room.

### **4.1.3 Prevention experiment under thermoneutrality conditions in male mice**

In the third experiment, at 9 weeks of age, mice were treated with the AAVs, half of the animals with Null (n=16) and the other half with CPT1AM (n=16). Immediately after surgery, half of the treated animals underwent NCD (n=8) and HFD (n=8), leaving the same 4 study groups with n=8. Four animals per cage were housed in the University facilities, in the negative pressure room, during the first week after surgery, and the second week they were transferred to the climatic chamber to subject them to thermoneutrality conditions at  $30 \pm 1$  °C. They were in thermoneutrality throughout the obesity induction process with HFD, and the day before sacrifice, they were subjected to an acute cold stimulus at  $4 \pm 1$  °C for 24 hours to activate BAT. Changes in metabolic phenotype were observed throughout the process and post-sacrifice overexpression was

analyzed 15 weeks after AAV administration. As in the second cohort of animals, HFD-induced obesity was intended to be prevented by overexpression of CPT1AM in BAT. This experiment was performed on male mice.

### **4.1.4 Prevention experiment under thermoneutrality conditions in female mice**

The fourth experiment was similar to the third experiments, but in female mice. At 9 weeks of age, half of the mice were treated with the viral vectors with the Null AAVs (n=20) and the other half with CPT1AM AAVs (n=20). Immediately after surgery, half of the treated animals underwent NCD (n=10) and HFD (n=10), leaving 4 study groups with n=10. Five animals per cage were housed in the University facilities, in the negative pressure room, during the first week after surgery, and the second week they were transferred to the climatic chamber to subject them to thermoneutrality conditions  $30 \pm 1$  °C. Like the male mice, they were in thermoneutrality throughout the obesity induction process with HFD, and the day before sacrifice, they were subjected to an acute cold stimulus at  $4 \pm 1$  °C for 24 hours to activate the BAT. Changes in metabolic phenotype were observed throughout the process and post-sacrifice overexpression was analyzed 15 weeks after AAV administration. As in the second and third cohorts of animals, HFD-induced obesity was intended to be prevented by overexpression of CPT1AM in BAT.

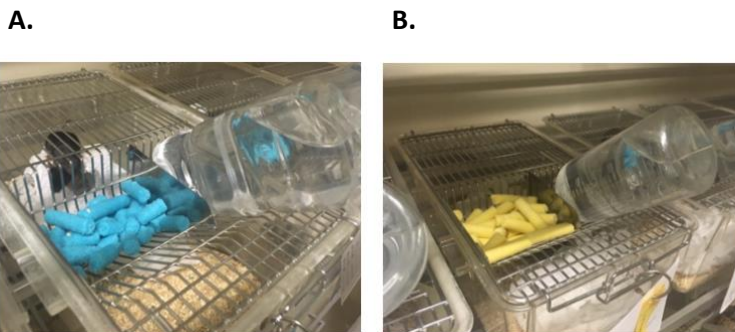
## **4.2 Diet**

For the induction of obesity, two diets from the DIO (diet-induced obesity) series were used, the purified diet for rodents with 10% energy from fat (NCD), yellow color (ref. no. T-58Y2-58124) and the purified rodent diet with 60%



energy from fat (HFD), blue (ref. no. T-58Y1-58126), both diets purchased from International PSL TestDiet. The NCD used is a low-fat formula which was considered a normal or control diet. This diet had a macronutrient caloric distribution equivalent to 10.2% fat, 18% protein, and 71.8% carbohydrate. As for HFD, it was used to induce obesity and insulin resistance in mice, since it had a macronutrient caloric distribution equivalent to 61.6% fat, 18.1% protein, and 20.3% carbohydrates. Both diets have been intended for consumption by rodents in a laboratory and/or experimental environment, for the study of obesity [149].

**Figure 10** Diet used for the study and induction of obesity.



A) Cage of animals with NCD. B) HFD animal cage.

### 4.3 Viral vectors of adeno-associated viruses

AAVs are a simple and non-autonomous virus, which contains single-stranded linear DNA. AAVs are one of the vectors of choice for many *in vivo* gene transfer applications due to their low immunogenicity and safety profile [150].

AAV vectors transduce dividing and non-dividing cells, driving long-term (up to several years) gene expression in small and large animal models of disease in tissues with very low proliferation rates [150]. In this study, AAVs were used as a viral vector for the *in vivo* overexpression of CPT1AM. In collaboration with

the group of Dr. Fàtima Bosch (Faculty of Veterinary Medicine, UAB), a viral vector was generated that expresses CPT1AM specifically in BAT via a UCP1 mini-promoter. The synthesis and production of the AAVs was carried out at the Center for Animal Biotechnology and Gene Therapy (CBATEG) and the production of viral vectors obtained were of serotype 8, due to the transfection efficiency in the BAT [135]. The viral vectors obtained were AAV8-UCP1basal-CPT1AM-WPRE, with a titer of  $5.74 \times 10^{13}$  and AAV8-UCP1basal-NULL-WPRE, as a treatment control, with a titer of  $8.73 \times 10^{13}$ .

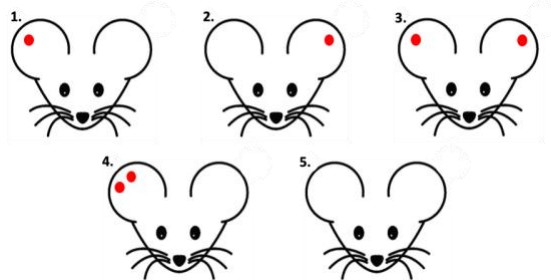
### **4.4 Procedure in animals**

All the mice used for this study were received at 7 weeks of age, in which identification procedures were carried out by ear marking, weight control and glucose levels were measured, before inducing obesity and treating the animals with CPT1AM.

#### **4.4.1 Animal identification**

To identify the animals, ear piercings were performed, immobilizing the mouse and performing the corresponding piercing with an ear piercer (ref. 16543062, FST.). This technique is fast and does not cause damage to the rodent. When four to five animals were housed per cage, five perforation patterns were performed on the mice in each cage, perforating the ears of each mouse, perforating the right, left, right and left ears, two holes on the right and another mouse without drilling.

**Figure 11 Animal identification by ear piercing.**



#### **4.4.2 Administration of viral vectors with CPT1AM in el BAT**

Prior to performing the surgery, the mouse was anesthetized, injecting intraperitoneally, injecting 100 mg/kg of Ketamine (ref. Merial Imagene 100 mg/ml) and 10 mg/kg of Xylazine (ref. Bayer Rompun 20 mg/ml). ml), diluted in a 0.9% NaCl solution. After a few minutes, when the mouse was asleep, the subscapular area was shaved and an incision was made in that area. Once opened, with the help of tweezers, the WAT that is above the BAT was lifted, and when the BAT was located in the shape of a butterfly, four punctures were made with 10 uL of solution with AAVs, by clicking directly on the BAT. This solution was injected with a Hamilton syringe (ref. no. 702, Teknokroma) administering the viral vectors to overexpress CPT1AM in BAT.

**Figure 12** Illustration of a mouse with an open incision in the scapular area.

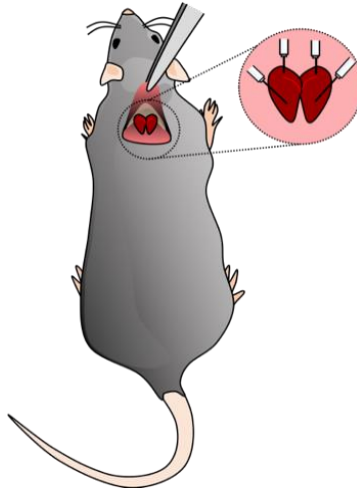
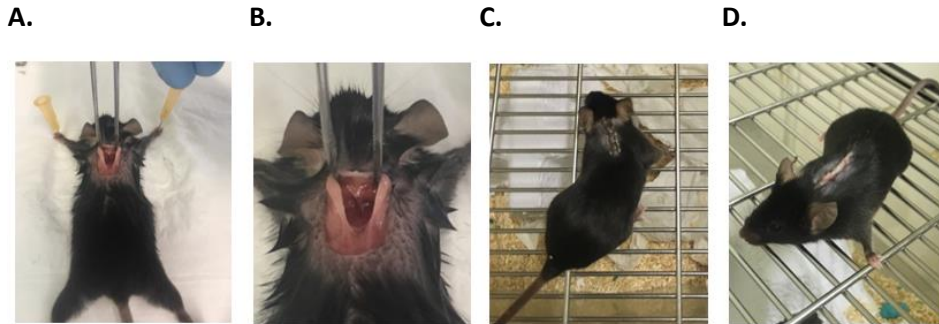


*Illustration of a mouse with an open incision in the scapular area where the butterfly-shaped BAT is located, indicating the areas where the punctures with the viral vectors were made.*

While the surgery was performed on the mice, the solution with the viral vectors was kept on ice at 4 °C. Finally, the incision was closed with two or three staples (cat. no. 120 20-000, FST). Immediately after the mice awoke from anesthesia they had the NCD and HFD ready *ad libitum*, corresponding to each experimental group. Mice were monitored for 5 days post-injection to follow the progress of surgery. After four or five days the staples were removed, when the wound had already healed.

**Figure 13 Photos of the surgery and its evolution.**



A) Photo of the location of the BAT. B) Butterfly-shaped BAT C) Incision with staples 3 days after surgery. D) Incision without staples 5 days after surgery.

**4.4.3 Viral vector dilution**

For AVV dilution, the AAV8-UCP1basal-CPT1AM-WPRE vector is used with an amount of 5.74E+13 vg/mL and the AAV8-UCP1basal-NULL-WPRE vector with an amount of 8.73E+13 vg/mL.

<b>Vector</b>	<b>vg/mL</b>
AAV8-UCP1basal-CPT1AM-WPRE	5.74E+13
AAV8-UCP1basal-NULL-WPRE	8.73E+13

AAV8-UCP1basal-CPT1AM-WPRE (16 mice with CPT1AM)

- Amount of AAV per mouse (40 ul injection):  

$$40 \text{ ul} \times \frac{1 \text{ ml}}{10^3 \text{ ul}} \times \frac{5.74 \times 10^{13} \text{ vg}}{1 \text{ ml}} = 2.296 \times 10^{12} \text{ vg}$$

- 40 ul will be injected, with a total amount of AAV of  $2.296 \times 10^{12}$  vg

### AAV8-UCP1basal-NULL-WPRE (16 mice with Null)

- The same amount of AAV must be administered to all mice. Therefore, since the limiting virus is CPT1AM (because  $2,296 \times 10^{12}$  vg is the maximum amount to be injected), the Null virus must be diluted so  $2.296 \times 10^{12}$  vg will also be injected.
- Total AAV amount (16 mice with NULL= 640 ul): (we will prepare 700 ul just in case)

$$700 \text{ ul} \times \frac{1 \text{ ml}}{8,73 \times 10^{13} \text{ vg}} \times \frac{2.296 \times 10^{12} \text{ vg}}{40 \text{ ul}} = 0.46 \text{ ml} = 460 \text{ ul AAV NULL}$$

- Complete the volume up to 700 ul with 240ul of PBS with 0,001% PBS-pluronic.

#### **4.4.4 Accommodation of animals in thermoneutrality with acute cold stimulation**

The mice of the third and fourth experiments were in thermoneutrality conditions and were subjected to an acute cold stimulus. The following week after surgery, the mice were transferred to the climatic chamber of our research group, which is located in the faculty's animal facility. The HPP750life climatic chamber (Memmert, Biolab), has different applications such as environmental simulations, climatic tests, material tests, stability tests and animal

maintenance. In this experiment, the chamber was kept running at  $30 \pm 1$  °C throughout the experiment. Two days before the acute cold stimulus, the temperature began to be reduced progressively, so that the temperature was lowered from 30 °C to 25 °C in the morning, then from 25 °C to 20 °C in the afternoon. , the next day, it was lowered from 20 °C to 15 °C in the morning, from 15 °C to 10 °C in the afternoon, and at night it was lowered to 4 °C. Once the chamber reached a temperature of  $4 \pm 1$ °C, the 24 hours for subsequent sacrifice began to count. In this way, the entire experiment was carried out under thermoneutrality conditions to avoid prior activation of BAT during the induction of obesity by HFD, and prior to sacrifice, an acute cold stimulus was performed for BAT activation.

**Figure 14 Mice housed in the climatic chamber under thermoneutrality condition.**

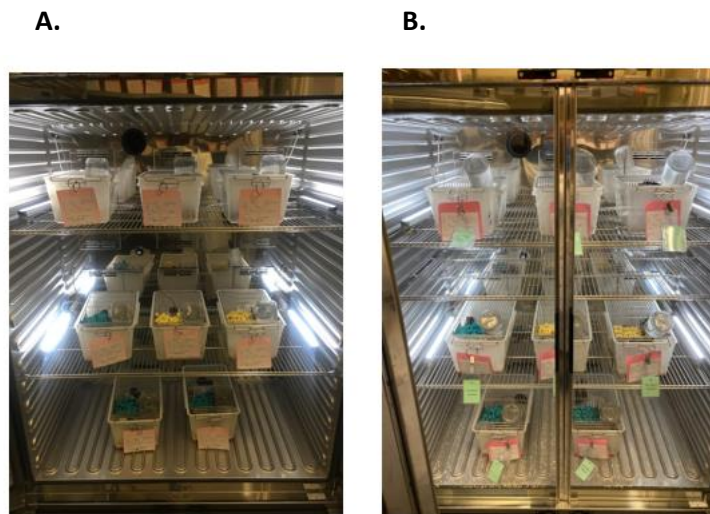


*Photo of the boxes inside the climatic chamber, with the mice grouped into 4 and 5 animals per cage. A) Third cohort of mice. B) Fourth cohort of mice.*

### **4.4.5 Body weight monitoring**

Body weight was recorded weekly, every Wednesday, on a high-precision scale (Mettler Toledo ME54). Regarding weekly weight gain, it was calculated by adding the body weight of each animal, gained or lost over the weeks.

### **4.4.6 Monitoring glucose levels**

Glucose levels were measured monthly, with a previous fast of 6 hours. To measure glucose levels, a drop of blood was obtained from the animal's tail vein and measured in glucose test strips (Bayer, Contour next, ref. 84191389), after seconds the glucometer (Bayer, Contour XT, ref. 83415194), returned the result which was recorded. After the measurement and recording, the tail of the animal was cauterized to avoid further blood loss (ref. no. 18010-00, FST).

### **4.4.7 Intake control**

Intake control was carried out by estimating food and water per cage, on a weekly basis. Changes of diet and water were carried out every week with a quantity sufficient for the 3-5 mice in each cage (according to each experimental cohort). The diet and water were weighed before the change and the following week it was weighed again to record the weekly consumption of food and water per cage, in order to obtain an estimated consumption per animal. Regarding the quantification of food, it was done in grams and in kilocalories. Regarding the measurement of water, it was carried out in milliliters.



**Figure 15 Intake control.**

**A.**



**B.**



*A) food weighing. B) water bottle weighing.*

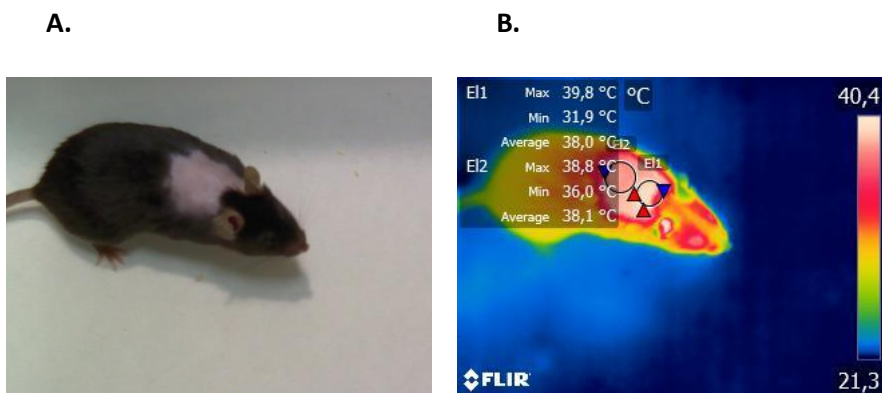
#### **4.4.8 iBAT thermographic estimation**

Thermography is a technique that allows estimating the surface temperature of an object based on the amount of infrared radiation emitted. The day before the measurement, the animals were depilated in the interscapular area with an electric shaver (Oster Golden two speed A5) and then with depilatory cream (Deliplus, depilatory cream for sensitive skin). They were then fasted for 12 hours overnight. The next day, three images of the dorsal area of each mouse were made, which was normalized by the intervertebral area (or back area), these results were calculated by the difference between the interscapular temperature and the dorsal temperature of each animal. To take the photos, an infrared camera (FLIR T420; FLIR Systems, AB, Sweden) was used, which recorded the thermal images made of the mice. To analyze the heat estimation by iBAT, thermal data were extracted and analyzed in the FLIR Tools software (Version 4.1), the maximum temperature of the region of interest (ROI)

drawn around the interscapular area was estimated. The thermographic results were adjusted to the atmospheric temperature of the animal facility and to the reflected temperature (measured with aluminum foil), recorded on the day the photos were taken.

In the third animal cohort, this measurement was made to the previous moment of the sacrifice, but without shaving them the previous day (since they were under stimulus of acute cold) and in fasting conditions for 2 hours, in order to observe changes under said conditions.

**Figure 16 Thermographic photo made with infrared camera.**



*Thermographic photo of a mouse from the second experimental cohort. A) Picture at the visible light. B) Thermographic photo quantified in the area of highest temperature in the BAT, and in the area of the mouse's back.*

### 4.4.9 Glucose Tolerance Test

To study glucose metabolism, the Glucose Tolerance Test (GTT) was performed, measuring glucose levels from blood obtained from the tail vein. Blood glucose was measured at time 0, with a previous fast of 12 hours and

subsequently 20% glucose (Baxter, ref. 2B0124P) was administered by intraperitoneal injection to a final dose of 2 g/kg body weight of each mouse. Finally, glucose was measured using a hand glucometer and its reactive strips, at consecutive times of 15, 30, 60, 90 and 120 minutes after injection. The data were registered in each measurement and after the 120 -minute measurement, the animal's tail was caulked to avoid blood losses once the procedure is finished.

### **4.4.10 Open Field Test**

The open field test is used to assess anxiety and exploratory behaviors in mice. It is based on an animal's natural tendency to explore and protect itself through avoidance, which means that a normal animal spends more time on the periphery of the open field than in the center (the most anxiogenic zone). With this test, parameters such as locomotor activity, exploratory capacity, anxiety and stress can be measured. One week before carrying out this test, the animals were taken to the open field to get used to it and not show biased results due to the stress of being in a new place at the time of the study. The animals were transported to the testing room and left in place for 30 minutes individually. To carry out the test, the animal is placed in the open field and the SMART 3.0 program was used, which is adjusted for the test to be carried out. This monitors the entire Open Field Test by registering it on the camera that is located over the open field. Recording analysis was performed to measure the activity of each mouse in each of the zones at 5 and 10-minute intervals.

### **4.4.11 Fecal Extraction**

In the experiment carried out in female mice (fourth cohort of animals) it was wanted to determine the excreted cholesterol, which was measured in feces. To obtain fecal samples, it was necessary to immobilize the animal and

perform a circular massage in the intestinal area, in a clockwise direction. Three circular massages were performed and the fecal sample was obtained, which were collected directly from the rectum to avoid contamination. They were placed in a 2 ml airtight tube and kept refrigerated until measurement. In the animals that did not obtain feces, after the three massages they were left in their cage and tried again a few minutes later, with a maximum of three attempts so as not to stress the mouse.

### **4.4.12 Sacrifice and sample collection**

In the first and second cohort of animals, a previous fast of 12 hours was carried out, during the night, to study them in basal conditions. In the third and fourth cohort of animals, it was only wanted to normalize the intake, fasting the animals for 2 hours, prior to sacrifice, because it was not expected to study the changes generated by the diet. At the time of sacrifice they were put to sleep with 4% isoflurane (Piramal Healthcare, ref. 60307-120-25) and sacrificed by cervical dislocation. An incision was made in the area of the heart and all the blood was rapidly extracted with a syringe, which was refrigerated in a 1.5 mL tube until centrifuged for phase separation. Tissues (BAT, gWAT, iWAT, liver, heart, pancreas, spleen, and hypothalamus) were then carefully dissected. BAT, gWAT, iWAT and liver tissues were weighed and normalized by the body weight of each mouse. Afterwards, a small part was cut to preserve in 10% formalin solution (Sigma-Aldrich, ref. HT5017) for histological analysis and the rest of the tissues were preserved in liquid nitrogen and then stored in freezers at -80°C.

In the fourth cohort of animals, before sacrifice and after the acute cold stimulus, the FAO assay was performed, after the BAT was dissected and weighed, a quarter of the tissue was obtained to maintain in the prepared

maintenance medium, which kept the tissue oxidizing during the sacrifice until the medium was changed for subsequent incubation, which is detailed later. The maintenance medium was composed of Krebs-Ringer Bicarbonate Hepes (KRBH) supplemented with 2.5 mM Oleate bound to BSA and 25 mM Glucose.

KRBH
KRB 5X + NaHCO <sub>3</sub> 100 mM + HEPES 1M pH 7,4 + H <sub>2</sub> O

### 4.5 Laboratory Techniques

#### 4.5.1 Blood determinations

Blood was collected after 12 on GTT day, and after 2 hours of fasting on the day of the sacrifice. The GTT day was removed from the tail of the tail using capillaries (Deltalab, Ref. 7301) and the day of the sacrifice, the blood was extracted directly from the heart. The collected blood was put in the blood tubes and remained for at least 30 minutes at room temperature. Then they centrifuge for 15 minutes at 3,000 g at 4 ° C. After the blood was separated in phases, the supernatant was obtained and stored in small aliquots at -20 ° C and then determine the levels of metabolites and hormones.

##### 4.5.1.1 Determination of total cholesterol, triglycerides and NEFAs

To determine the concentration of fats in blood, the serum triglyceride determination kit (Sigma-Aldrich, ref. TR0100-1KT), the cholesterol kit (Biosystems, ref. 11505) and the non-esterified fatty acid (NEFA) kit were used (Wako Diagnostic, refs 434-91795, 436-91995, 270-77000) to measure TG,

cholesterol and NEFA levels according to the manufacturer's instructions, respectively.

### **4.5.1.2 Determination of insulin in blood**

Insulin levels were measured using the Ultrasensitive Mouse Insulin ELISA Kit (Crystal Chem Inc, ref. 90080). This is a specific kit for the detection of mouse insulin in small amounts of sample, only 5  $\mu$ l. It also allows measurement of low and high insulin concentrations at the same time because the kit provides a standard curve in a low, wide, or high range.

### **4.5.2 Determination of cholesterol in feces**

For lipid extraction, normal saline solution is added at of powdered feces in a tube and stirred in Vortex. Chloroform is added: mixture of methanol and stir. Then the suspension (around 2,000 rpm) for 10 min at room temperature is centrifuged. Then two liquid phases will be seen that are separated by a solid phase; There may be another small solid phase in the background. The lower liquid phase contains the lipids extracted in chloroform: methanol. Holding the plastic tube on a glass tube, a needle is inserted through the tube wall at the bottom of the two liquid phases; then, the needle is removed.

Then a syringe is connected from air to another needle; The needle is inserted in the upper part of the bottom of the two liquid phases, just below the solid phase, then the tube on the glass tube that is labeled with the mouse number is held and the air is injected carefully; The lower liquid phase will drain from the plastic tube and will be collected in the glass tube. Then comes evaporation, the glass tubes are placed on a support under a smoke bell. The tubes are left alone for 3 to 4 days until all the liquid evaporates. The tubes are weighed in the analytical balance. The weights of the empty tubes of the new

tubes are subtracted to obtain the dough of lipids by of feces. Last multiplies the dough of lipids by the total weight of the feces in grams and is divided by the number of days that the stool was collected to obtain the excretion of average mouse lipids per day.

### **4.5.3 Determination of hepatic triglycerides**

Liver TGs were extracted from 100 mg of tissue by adding 500  $\mu$ l of 0.1% SDS. Tissue was homogenized in a 2 ml tube using beads and a Tissuelyser LT for 3 min at 50 Hz and incubated overnight at room temperature with constant shaking (Heidolph, Reax 2). The next day, 150  $\mu$ l were frozen at -20 °C to measure protein concentration and 350  $\mu$ l were used for TG extraction. Extraction began with the addition of 350  $\mu$ l of methanol and a vigorous vortex was applied to mix. 750  $\mu$ l of chloroform were added, mixed again and incubated for 30 min at 4°C. 48  $\mu$ l of 0.5 M KCl were added and the samples were incubated for 30 min at 4 °C and then centrifuged for 10 min at 2000 rpm at 4 °C. The supernatant and tissue debris were removed to obtain the lower phase containing the TG. 300  $\mu$ l of the lower phase was evaporated in the fume hood overnight. Finally, the product was resuspended in 50  $\mu$ l of 100% ethanol and quantified using the serum triglyceride determination kit (Sigma-Aldrich, ref. TR0100-1KT) according to the manufacturer's instructions.

### **4.5.4 RNA extraction and quantification**

#### ***4.5.4.1 RNA extraction from tissues***

Prior to RNA extraction, all tissues were weighed to extract from the same amount in all samples. In the case of livers, the RNA was extracted conventionally with the trizol reagent (Sigma-Aldrich, Ref. T9424). 70 mg of tissue was obtained, by adding 1 ml of trizol reagent. The fabrics containing lipids

such as Ibat, Gwat and Iwat (50-100 mg) were treated with 1 ml of lysis reagent of the RNeasy Lipid Tissue Mini Kit. After the addition of the appropriate lysis reagent, the tissues were broken using pearls. (Qiagen, Ref. 69989 or Ref. 69997) In the TissueLyser Lt (Qiagen, Ref. 85600) for 3 minutes at 50 Hz. The extraction of RNA was carried out according to the kit's manufacturer protocol and the extraction of RNA according to the protocol according to the protocol Trizol, subsequently the samples were quantified and stored at  $-80^{\circ}\text{C}$ .

#### ***4.5.4.2 cDNA synthesis by reverse transcription***

Reverse transcription was performed from 400 ng of RNA samples with the TaqMan reverse transcription kit (Applied Biosystems, ref. N8080234) using random primers. All reagents were added with RNA. down to a final volume of 20  $\mu\text{l}$ . Then the samples were incubated in the thermal cycler (Analytik Jena, FlexCycler) for 10 minutes at  $25^{\circ}\text{C}$ , 30 minutes at  $48^{\circ}\text{C}$  and 5 minutes at  $95^{\circ}\text{C}$ . The cDNA was diluted by adding 60  $\mu\text{l}$  of nuclease-free water to a concentration of 5 ng/ $\mu\text{l}$ . Finally, the working concentration was 2.5 ng/ $\mu\text{l}$ . All negative control reverse transcriptase without reverse transcriptase and one without RNA samples were included.

#### ***4.5.4.3 Quantitative real-time polymerase chain reaction***

Quantitative real-time polymerase chain reaction (qRT-PCR) is one of the most widely used techniques to quantify gene expression, which uses a fluorophore to detect double-stranded DNA. qRT-PCR. It can be performed with a LightCycler<sup>®</sup> 480 Instrument II in a total volume of 10  $\mu\text{l}$  including 2.5  $\mu\text{l}$  of cDNA working concentration, 5  $\mu\text{l}$  2X SYBR Green PCR Master Mix Reagent Kit, 0.5  $\mu\text{l}$  of primer 10  $\mu\text{M}$  (10  $\mu\text{M}$  forward primer



and 10  $\mu$ M reverse primer) and 2  $\mu$ l of nuclease-free water. qRT-PCR. A negative control without cDNA sample was included. All reactions were performed in duplicate in a 384-well plate and a brief centrifugation was applied before running. The qRT-PCR program included a 5-minute preincubation at 95°C to dehybridize the cDNA strands. The reactions were then denatured for 15 seconds at 95°C, annealed for 10 seconds at 60°C and held for 10 seconds at 72°C for 45 consecutive cycles. The relative quantification was expressed as a fold change from the control group. RNA levels were normalized with a reference gene which showed no statistically significant difference between sample groups.

**Table 4 Quantitative RT-PCR oligonucleotides.**

Oligonucleotides	Forward (5' → 3')	Reverse (5' → 3')
<i>Abca1</i>	CCAGAGAATGTTTCATTGT	GCAGATCAAGCATCCCAACT
<i>Adipoq</i>	GCAGAGATGGCACTCCTGGA	CCCTTCAGCTCCTGTCTTCC
<i>Atgl</i>	TGACCATCTGCCTTCCAGA	TGTAGGTGGCGCAAGACA
<i>Bip</i>	ACTTGGGGACCACCTATTCCT	ATCGCCAATCAGACGCTCC
<i>Bmp8b</i>	ATGCGAGTCCGCTAAACG	GGCCCAGTAGCCATAGGAGT
<i>Catalase</i>	GTGCATGCATGACAACCAG	TGAAGCGTTTCACATCTACAGC
<i>Chop</i>	CCCTGCCTTTACCTTGG	CCGCTCGTTCTCCTGTCTC
<i>Cidea</i>	GCCTGCAGGAATTATCAGC	AGAACTCCTCTGTGTCCACCA
<i>Col4a1</i>	TTAAAGGACTCCAGGGACCAC	CCCCTGAGCCTGTCTCACAC
<i>Cpt1a</i>	GACTCCGCTCGCTCATT	TCTGCCATCTTGAGTGGTGA
<i>Cpt1am</i>	ACAATGGGACATTCCAGGAG	AAAGACTGGCGCTGTCTCA
<i>Fas</i>	CAGATGATGACAGGAGATGGAA	CACTCACACCCACCCAGA
<i>G6p</i>	AGGAAGGATGGAGGAAGGAA	TGGAACCAGATGGGAAAGAG
<i>Glut2</i>	CTATGACGTCAATGGCACAGA	AGAGCAGTAGCAGACTGCA
<i>Glut4</i>	GATGACCGTGGCTCTGCT	GCTCTGCCACAATGAACCA
<i>Hsl</i>	GCGCTGGAGGAGTGTITTT	CGCTCTCCAGTTGAACCAAG
<i>Il-10</i>	GGTTGCCAAGCCTTATCGGA	ACCTGCTCCACTGCCTTGCT
<i>Il-18</i>	GCCCATCCTCTGTGACTCAT	AGGCCACAGTATTTTGTCTG
<i>Il-6</i>	GATGGATGCTACCAAACCTG	CCAGGTAGCTATGGTACTCCAGAA
<i>Ldlr</i>	AGAGGGGTGAACCTGGTGTG	CAGGTAAGTGGCAACCACCAT
<i>Leptin</i>	CAGGATCAATGACATTTACACA	GCTGGTGAAGGACCTGTTGAT
<i>Mgl1</i>	TGAGAAAGGCTTTAAGAAGCTGGG	GACCACCTGTAGTGTGTGGG
<i>Mttp</i>	GTGGAGGAATCCTGATGGTGA	TGATGTTAGGTGTACTTTTGCCC
<i>Pgc1α</i>	GAAAGGGCCAAACAGAGAGA	GTAAATCACACGGCGCTCTT
<i>Plin1</i>	AACGTGGTAGACTGTGGTACA	TCTCGGAATTCGCTCTCG
<i>Ppara</i>	ACGATGCTGTCCTCCTTGATG	GCGTCTGACTCGGTCTTCTT
<i>Pparγ</i>	CGCTGATGCACTGCCTATGA	AGAGGTCCACAGAGCTGATTCC
<i>Resistin</i>	TGCCAGTGTGCAAGGATAGA	TGGAAACCACGCTCACTT
<i>Rpl32</i>	GCTGCCATCTGTTTTACGG	TGACTGGTGCCTGATGAACT
<i>Scd1</i>	TTCCCTCTGCAAGCTCTAC	CAGAGCGCTGGTCTATGTAGT
<i>Tbp</i>	ACCCTTACCAATGACTCCTATG	TGACTGCAGCAAATCGCTTGG
<i>Tgfb</i>	TGGAGCAACATGTGGAATC	CAGCAGCCGGTTACCAAG
<i>Tnfa</i>	CTGTAGCCCACGTCGTAGC	TTTGAGATCCATGCCGTTG
<i>Ucp1</i>	GGCCTCTACGACTCAGTCCA	TAAGCCGGCTGAGATCTTGT
<i>Ucp2</i>	CCGGGCTCTGGAAG	CCCAAGCGGAGAAAGGA

Oligonucleotides were from Sigma-Aldrich.

### **4.5.5 Collection, quantification and measurement of protein in tissues**

#### ***4.5.5.1 Protein extraction from frozen tissue***

Total protein extraction was performed from mouse tissues. Tissues protein extraction was performed by adding 1 ml or 300  $\mu$ l of protein extraction buffer to 30–70 mg of non-fatty tissue or 50–100 mg of fatty tissue, respectively. Tissues were disrupted using beads and a TissueLyser LT for 3 minutes at 50 Hz until complete homogenization. Once the cellular or tissue protein lysates were obtained, they were stored in ice for 20 min with gentle orbital shaking. Lysates were centrifuged for 15 minutes at 13,000 rpm at 4°C. The supernatant was then carefully collected avoiding the cell membrane debris pellet and upper lipid layer commonly present in adipose tissue protein extracts. Finally, the samples were frozen at -80°C for later analysis.

#### ***4.5.5.2 Protein quantification***

Protein quantification was performed by the bicinchoninic acid (BCA) protein assay. It is an accurate colorimetric test that is unaffected by lysis buffer, detergents, or lipids that may be present in samples. A standard curve was produced in a 96-well plate by making dilutions of 2 mg/ml of BSA (0.2, 0.4, 0.8, 1.6, 2 mg/ml) up to a volume final 20  $\mu$ l. The samples were diluted up to 20  $\mu$ l in dH<sub>2</sub>O depending on their origin. The protein assay kit was used by mixing the A: B (50:1) reagents and 200  $\mu$ l of this mixture was added to each well. After the samples were incubated for 30 minutes at 37°C, the purple color emitted by the binding of BCA to the protein was measured at an absorbance of 562 nm at the endpoint at room temperature using the variskan Lux (microplate reader multimode). Standards and samples were quantitated in duplicate.

### **4.5.6 Western Blot**

Western Blot is an analytical technique used for the specific detection of a protein from a mixture of proteins in a sample using a specific antibody. This immunodetection technique is carried out in three steps: the electrophoretic separation of proteins according to their molecular weight, their subsequent transfer to a solid support and the detection of the specific protein by an antibody.

#### **4.5.6.1 Electrophoresis**

After determining the total protein concentration of each sample, protein extracts were prepared for subsequent electrophoretic separation. For this, the samples were adjusted to a stock of 1 µg/µl by adding the proportional part of the DH2 loading buffer distilled O and 6X [Tris-HCl 375 mM pH 6.8, 9% (w/v) dodecylsulfate of sodium (SDS), 50% (v/v) glycerol, 0.03% (w/v) bromophenol blue, 9% (v/v) β-mercaptoethanol]. The proteins were then denatured for 5 min at 95°C in a thermoblock. Finally, the samples were kept on ice or stored at -20°C for later use.

Protein denaturation electrophoresis is performed on a sodium dodecyl sulfate-polyacrylamide (SDS-PAGE) gel system consisting of a stacking gel to concentrate proteins and a separator gel that separates them according to their molecular weight. Gels were prepared with 10% acrylamide, which depends on the molecular weight of the protein to be studied. The composition of the gels was carried out in Mini-PROTEAN® Spacer Plates (Bio-Rad, ref. 1653312) or empty Criterion cassettes (Bio-Rad, ref. 3459901, ref. 3459902 and ref. 3459903). Polymerized gels were overlaid with buffer flow [25 mM Tris-HCl pH 8.8, 192 mM glycine, and 0.1% (w/v) SDS], and 15-30 µg of total protein per well

was been loaded. Depending on the type of tissue, in addition, 7  $\mu$ l of precision Plus Protein™ Dual Color (10-250 kDa) (Bio-Rad, ref. 1610394) was loaded as a molecular weight reference in the first well of each gel. Samples started running at 80 V until they passed the stacking gel, then the intensity was increased to 120 V until the proteins reached the end of the separator. About 90-120 minutes. Electrophoresis was performed with the Mini-PROTEAN® tetravertical electrophoresis cell (Bio-Rad) or the Criterion electrophoresis cell gel.

### ***4.5.6.2 Transfer***

Once the electrophoresis is finalized, the proteins present in the separation gel are transferred to a membrane of nitrocellulose of 0.45  $\mu$ m forming a sandwich with sponges and whatman paper in both sides. A water transfer with recirculation of continuous transfer buffer [25 mM Tris-HCl pH 8.5, glicina 190 mM, SDS al 0.2% (w/v), metanol al 20% (v/v)] using Mini Trans-Blot Cell (BioRad) or Criterion™ Blotter with wire electrodes (Bio-Rad, ref .1704071) by. 90 minutes at 250 mA at 4°C.

After transfer, the membrane was washed once with Tris-buffered saline. (TBST) [10 mM Tris-HCl, pH 7.4, 150 mM NaCl, 0.1% (v/v) Tween 20] and stained for 5 min on an orbital shaker with Ponceau S (Sigma-Aldrich, ref P3504) [0.1% (w/v) Ponceau Red in 5% (v/v) acetic acid] to visualize the protein pattern indicating that the amount of sample loaded and the transfer process was successful. Finally, the membrane was destained with 5% (v/v) acetic acid and washed three times with TBST for 10 min on an orbital shaker.

### ***4.5.6.3 Membrane blockage***

Prior to incubation with antibodies, the membrane was blocked in blocking solution [5% (w/v) Blotto dry skim milk (Santa Cruz Biotechnology, ref.

SC-2325) in TBST] on an orbital shaker for one hour at room temperature. to block non-specific antibody binding sites. Then, the membrane was washed three times for 5 minutes in TBST with shaking and incubated overnight at 4°C with constant shaking with the primary antibody specific for the protein to be detected. Primary antibodies were resuspended in blocking solution or in BSA (Sigma-Aldrich, ref. A9647) [5% (w/v) BSA in TBST] at the indicated dilution. The next day, the nitrocellulose membrane is washed 3 times for 10 min with stirring.

#### ***4.5.6.4 Detection***

Antibody detection was performed by chemiluminescence. The membrane was incubated for 5 minutes in the dark with a mixture of reagents A and B. Western Pierce™ ECL Blot Substrate. Protein detection was performed with ImageQuant LAS 4000 Mini (GE Healthcare, Image Quant LAS 4000 V1.2 Software) to take images of chemiluminescent signals. The acquired images were processed with the Image J program (v1.50b, NIH) which quantifies the average optical density of all the immunoreactive bands.

## Materials and Methods

**Table 5 Primary antibodies used in western blot.**

Antibody	Source	Dilution	Solution	Reference
Anti-pACC (Ser 79)	Rabbit	1:1,000	5% (w/v) BSA in TBST	Cell Signaling, 3661
Anti-ACC	Rabbit	1:1,000	5% (w/v) BSA in TBST	Cell Signaling, 3662
Anti-ATGL	Rabbit	1:1,000	5% (w/v) BSA in TBST	Cell Signaling, 2138S
Anti- $\beta$ -Actin	Rabbit	1:25,000	5% (w/v) BSA in TBST	Sigma-Aldrich, A3854
Anti-CPT1A	Rabbit	1:6,000	5% (w/v) BSA in TBST	Sci Crunch Cat#CPT1A, RRID: AB_2636894
Anti-FAS	Rabbit	1:1,000	5% (w/v) BSA in TBST	Santa Cruz, sc-20140
Anti-pHSL (Ser 660)	Rabbit	1:1,000	5% (w/v) BSA in TBST	Cell Signaling, 4126
Anti-HSL	Rabbit	1:1,000	5% (w/v) BSA in TBST	Cell Signaling, 4107
Anti-PLIN5	Guinea Pig	1:1,000	5% (w/v) milk in TBST	Abcam, ab192749
Anti-UCP1	Rabbit	1:1,000	5% (w/v) milk in TBST	Abcam, ab10983
Anti-VINCULIN	Mouse	1:5,000	5% (w/v) milk in TBST	Santa Cruz, sc-25336

**Table 6 Secondary antibodies used in Western Blot.**

Antibody	Source	Dilution	Solution	Reference
Anti-Guinea Pig, HRP-linked Ab	Goat	1:10,000	5% (w/v) milk in TBST	Abcam, ab97155
Anti-Mouse, HRP-linked Ab	Sheep	1:10,000	5% (w/v) milk in TBST	GE Healthcare, NA931V
Anti-rabbit IgG, HRP-linked Ab	Goat	1:10,000	5% (w/v) milk in TBST	Santa Cruz, sc-2004

### **4.5.7 Histological analysis**

A histological analysis of the tissues involved in the metabolism was carried out to analyze their morphology after the treatments. After the mice were sacrificed, a sample of iBAT, iWAT, gWAT and liver from each mouse was immersed in 10% formalin for 24 h. After this time, the fatty tissues were transferred to 1X DPBS. Finally, they were sent to the histology biobank of Hospital Clinic of Barcelona (IDIBAPS). Samples were embedded in paraffin, cut into 4  $\mu\text{m}$  sections, and stained with hematoxylin and eosin (H&E). Images of the stained samples were taken using the microscope (Leica DMI4000 B and Leica DFC300 FX camera) and processed with Image J program (v1.50b, NIH). Adipocyte area was calculated with the MRI Adipocytes Tool of ImageJ software.

### **4.5.8 Immunohistochemistry**

Immunohistochemistry (IHC) is a procedure that aims to detect, amplify and make visible a specific antigen, which is generally a protein. This technique allows identifying the location of a specific substance at the tissue level. It is based on the use of antibodies that specifically bind to a substance that is to be identified (primary antigen). Like the histological samples, these were processed in the Biobanco of the Clinic Hospital in Barcelona - IDIBAPS. For this detection, different antibody staining was used to identify browning (UCP1), T cells (CD3), macrophages (MAC-2) and apoptosis (CASPASE-3), in BAT, iWAT and gWAT.

For macrophage immunostaining, we used primary monoclonal rat anti-murine antibody to MAC-2 (1/40,000; Cedarlane) combined with a secondary rabbit anti-rat Ig (1/3,000). For browning staining, we used primary polyclonal rabbit anti-murine UCP1 antibody (1/500; Cell Marque). For T cells staining, we



used primary polyclonal rabbit anti-murine CD3 antibody (1/4,000; Cell Marque). For apoptosis, we used monoclonal rabbit anti-murine Caspase3 antibody (1/500; Cell Signaling). Finally, samples were developed with diaminobenzidine and counterstained with hematoxylin. Sections were viewed under a microscope at  $\times 20$  magnification.

### **4.5.9 FAO assay**

To see the fatty acid oxidation of BAT, part of the tissue was removed on the day of sacrifice and kept in the medium detailed above. When the sacrifice of the mice was finished, the BAT pieces that were in the maintenance medium were changed to a new plate with new incubation medium, but previously pre-gassed (with 95% O<sub>2</sub> 5% CO<sub>2</sub>). The pre-gassed medium was composed of KRBH supplemented with 2.5 mM Oleate bound to BSA, 1% bovine serum albumin (fatty acid free-BSA) and 25mM Glucose. With the pre-gassed medium, the tissues were incubated at 37°C for 30 minutes. After incubation, the pre-gassed medium was changed with fresh medium, but this time supplemented with 2.5 mM [1-<sup>14</sup>C] Oleate, radiolabeled. At this stage, the plate with the tissues is sealed, with a Whatman paper in each well of the plate, soaked in 0.1N KOH, which absorbs the CO<sub>2</sub> released by the tissue submerged in the medium with labeled Oleate. An incubation with this medium was carried out for 2 hours at 37°C. After said incubation, the reaction was stopped in each tissue, with 0.5 N H<sub>2</sub>SO<sub>4</sub>, so that the CO<sub>2</sub> released by the tissue would remain retained in the paper. It was left incubating overnight at 37°C and the next day the radioactivity of the papers was measured with CO<sub>2</sub>. The radioactivity of the paper and of the medium that each tissue had, to measure released CO<sub>2</sub> and APS. The

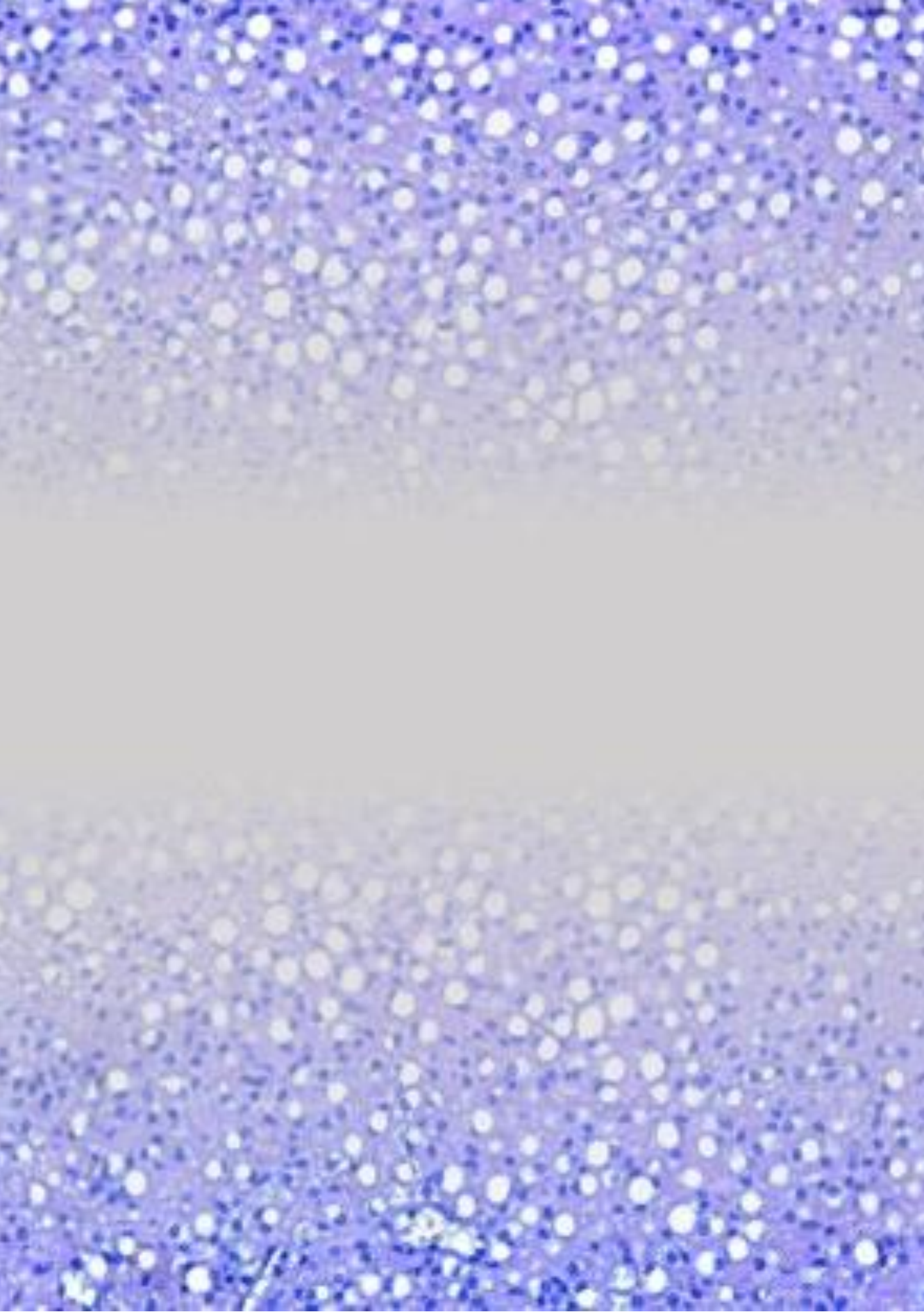
measurement was carried out in the scintillation counter equipment of the Radioactivity Units of the Faculty of Pharmacy of the University of Barcelona.

### **4.5.10 Bioinformatic and statistical analyzes**

The statistical analyzes carried out indicate a comparison between controls and treatments of each experimental model. Statistical analysis of Student's t-test was used when two groups were compared. Statistical analysis of Dunnett's test was performed when various groups were compared with the control group. One-way ANOVA followed by Tukey's post hoc test was used when a variable was compared between more than two groups. To compare all the variables of the different experiments, they were correlated using multivariate analysis tables.

To compare two variables, we performed a two-way ANOVA followed by Šidák's or Tukey's post hoc test to correct for multiple comparisons between two groups or more than two groups, respectively. Statistically significant differences were considered when the confidence level was greater than 95% ( $p$  value < 0.05). Figures represent data expressed as mean  $\pm$  standard error of the mean (SEM). The number of animals and/or samples per group used in each experiment is specified in the legend of each figure. All statistical analyzes and figures were generated with GraphPad Prism 8.0.2 (GraphPad Software, La Jolla, CA, USA). Fiji Image-J1.33 software (NIH; Bethesda, MD, USA) was used to process Western blot images. The adipocyte area was calculated with the MRI\_Adipocytes\_Tools of ImageJ software, as was the quantification of staining in the IHC of the UCP1 and MAC-2 antibodies.

# Results



## 5 RESULTS

The results of this thesis demonstrated that the expression of CPT1AM in brown adipocytes increased their FAO mitochondrial activity and thermogenesis (lipolysis and UCP1 levels). In addition, the increase in FAO reduced triglyceride content and the expression of obesity and inflammation markers when cells were incubated with palmitate to simulate obesity. This indicates that FAO is critical for fuel provision for thermogenesis and that enhancing FAO in brown adipocytes may be a good strategy in the treatment of obesity. These *in vitro* results have been recently published [8] and guarantee the success of the *in vivo* and *ex vivo* project presented.

### 5.1 CPT1AM expression in BAT of obese and hyperglycemic male mice at room temperature conditions. Reversion studies.

#### 5.1.1 Validation of the administration of CPT1AM in BAT of mice by AAVs viral vectors.

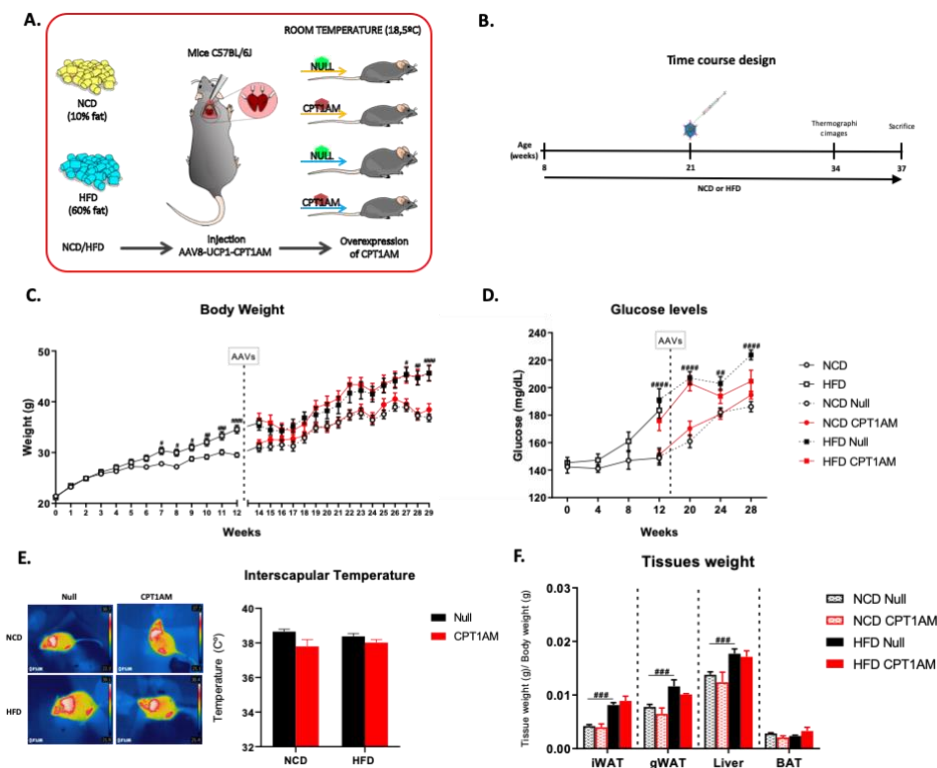
Previous studies in mice have shown that gene therapy through the administration of AAVs vectors has been an efficient strategy to overexpress genes *in vivo* in (BAT) and others [151]. We first asked whether the *in vivo* overexpression of CPT1AM in the BAT of HFD-fed mice would have an effect on their obese phenotype (Figure 17A-B). Obesity was induced with HFD in healthy 8-week-old mice, which were on a diet for 12 weeks, until they reached the obese metabolic phenotype reflected in weight (Figure 17C) and glucose levels (Figure 17D). At week 13 of diet, AAV-CPT1AM or AAV-null as a control were administered to mice. Weight was monitored weekly and glucose levels monthly. No significant differences were observed in the phenotype of the mice

that were injected with AAV-CPT1AM in terms of body weight (Figure 17C), and glucose levels (Figure 17D).

At week 26 of diet, thermographic pictures were taken to evaluate the interscapular temperature of the mice. However, no significant differences were observed (Figure 17E). At 29 weeks of diet, mice were fasted for 12 hours and subsequently sacrificed. BAT, liver, and inguinal (iWAT) and gonadal (gWAT) WAT were extracted to be weighed (Figure 17F) and analyzed. At the time of sacrifice, significant increases in iWAT, gWAT and Liver weight were only observed between the groups of animals with HFD Null (Figure 17F).



**Figure 17 Experimental design and phenotype of obese mice treated with HFD and AAVs viral vectors with CPT1AM or Null control.**

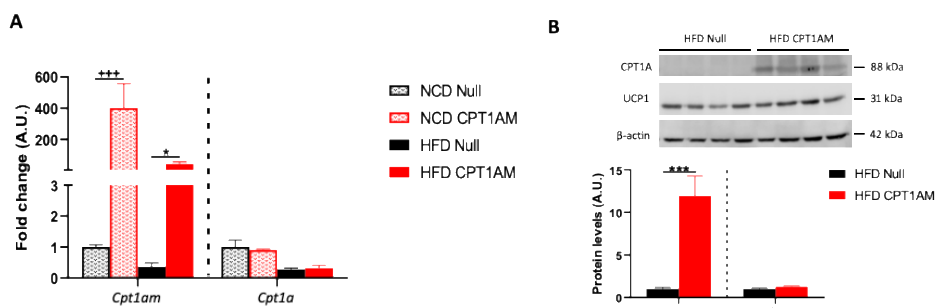


A) Experimental design B) Time course design. C) Body weight. D) Fasting blood glucose levels. E) Thermography. F) iWAT, gWAT, liver and BAT tissue weight, normalized by individual body weight of each mouse.

Although no significant differences were observed in the phenotype of CPT1AM-expressing mice compared to Null controls, the mRNA expression of *Cpt1am* showed a 600-fold and 150-fold increase in the NCD and HFD groups, respectively (Figure 18A). The mouse *Cpt1a* gene expression equivalent to endogenous *Cpt1a* was measured (Figure 18A), and no significant differences were observed. CPT1A protein levels were measured in the BAT of the HFD Null and HFD CPT1AM groups, and a significant increase was observed in the

CPT1AM-expressing mice (Figure 18B). UCP1 protein levels were also measured (Figure 18B), but no significant differences were observed.

**Figure 18 CPT1A protein levels are increased in CPT1AM-expressing mice.**



A) mRNA expression levels of *Cpt1am* and the endogenous *Cpt1a* genes. mRNA levels were normalized by *Rpl32*. B) CPT1A and UCP1 protein levels. Data are expressed as mean  $\pm$  SEM;  $n = 8$ .

## 5.2 CPT1AM expression in healthy male mice treated with HFD under room temperature conditions. Prevention studies.

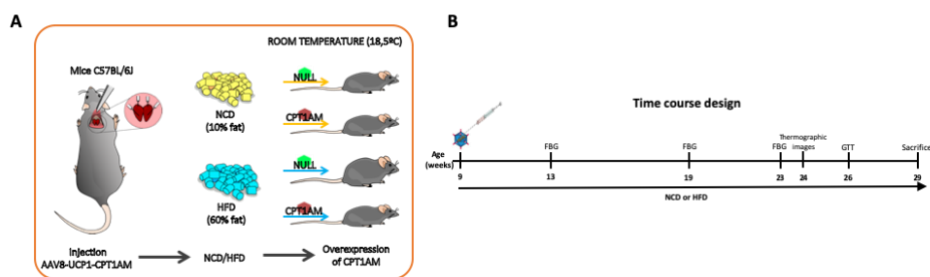
### 5.2.1 CPT1AM-expressing mice under HFD are resistant to diet-induced obesity

At this point we thought that the already established obesity and hyperglycemia might be difficult to overcome by a BAT-specific expression of CPT1AM in reversion studies. Thus, next we decided to study BAT-specific expression of CPT1AM in prevention studies by injecting the viral vectors in lean mice that were fed under NCD or HFD starting the same day of the injection. That is, healthy 9-week-old mice were punctured and immediately after surgery, they underwent NCD and HFD (Figure 19A-B), to study any potential change in



the metabolic phenotype, during the induction of obesity and hyperglycemia by HFD.

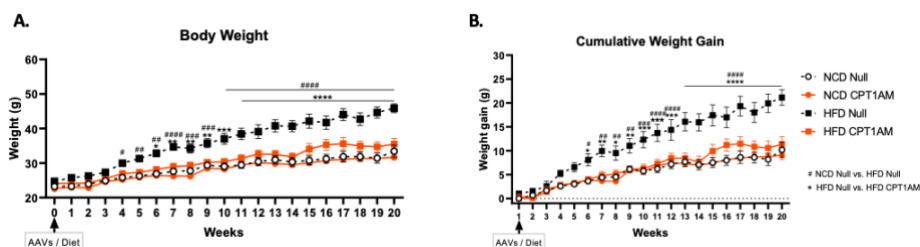
**Figure 19 Experimental design of the prevention studies.**



A) Experimental design. B) Time course design.

Weight was monitored weekly for 20 weeks after the viral vector's injection and NCD or HFD treatment. HFD CPT1AM mice maintained their weight almost in the normal range thus they were resistant to the obesity induced by HFD, and HFD Null mice became obese from the fourth week after the start of the diet (Figure 20A). Differences in weight gain were also observed from the sixth week after the start of treatment, between the HFD Null and HFD CPT1AM groups (Figure 20B).

**Figure 20 HFD CPT1AM mice are resistant to HFD-induced weight gain.**

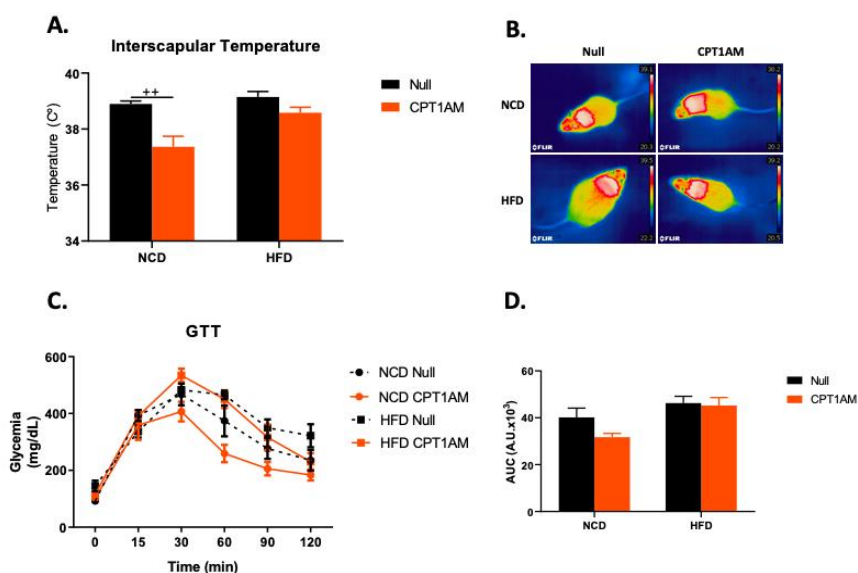


A) Body weight. B) Body weight gain. Data are expressed as mean  $\pm$  SEM; n = 6-7.

To estimate BAT thermogenesis, heat release from the interscapular area of mice was measured 15 weeks after CPT1AM administration and initiation of the diet. A decrease in the interscapular temperature of NCD CPT1AM mice was observed compared to NCD control (Figure 21A-B). No differences were seen between the HFD groups.

To monitor glucose metabolism, at 17 weeks, a GTT was performed under basal conditions in which no significant differences were observed between the groups (Figure 21C-D).

**Figure 21 Thermography and GTT CPT1AM-expressing mice under HFD.**

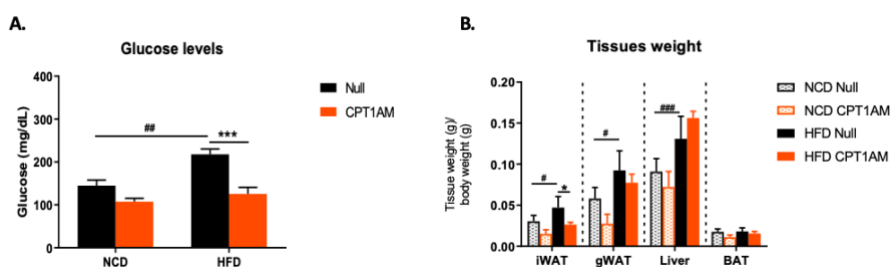


*A) Interscapular temperature. B) Representative images of thermography. C) GTT. D) Area under the curve (AUC) of GTT. Data are expressed as mean  $\pm$  SEM; n = 6-7.*

At 20 weeks after treatment, mice were sacrificed under a 12-hour fast. At this time point, HFD-induced increase in fasting blood glucose levels were restored in CPT1AM-expressing mice (Figure 22A). On the day of sacrifice, iWAT, gWAT, liver and BAT were dissected and the tissue weight was measured. As

expected HFD increased the weight of iWAT, gWAT and liver of the HFD Null group compared to NCD Null (Figure 22B). However, iWAT weight from the HFD CPT1AM group was decreased compared to HFD Null (Figure 22B). No differences were seen in BAT weight.

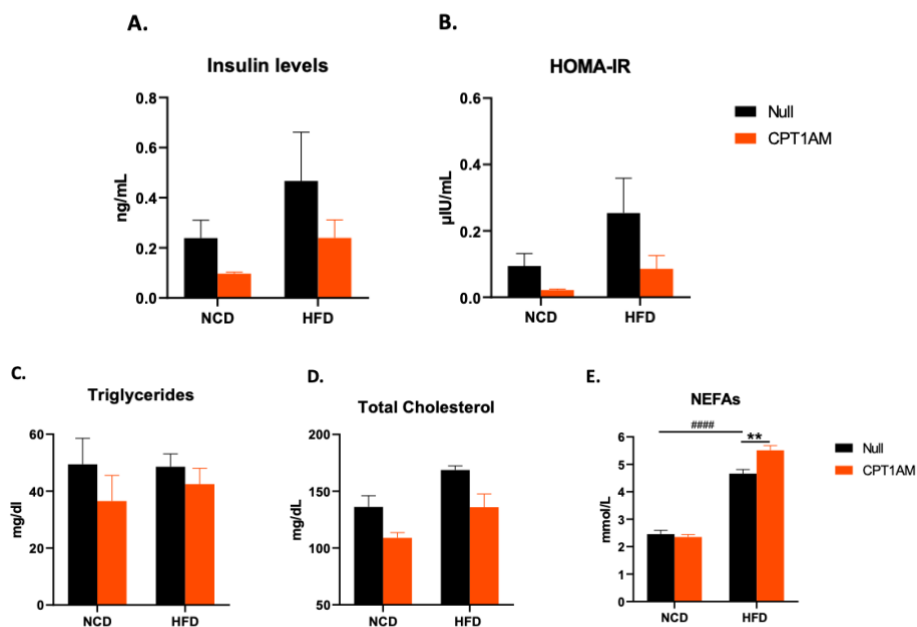
**Figure 22 Fasting blood glucose levels and weight of iWAT, gWAT and liver.**



A) Fasting blood glucose levels. B) Weight of iWAT, gWAT, liver and BAT normalized by body weight of each mouse. Data are expressed as mean  $\pm$  SEM;  $n = 6-7$ .

Next, we measured serum insulin levels and the insulin resistance index (HOMA-IR) (Figure 23B), total triglycerides (Figure 23C), total cholesterol (Figure 23D) and non-esterified fatty acids (NEFAs) (Figure 23E). Although no significant differences were observed when performing these measurements, there was a trend in the HFD CPT1AM group to decrease the HFD-induced increase in insulin levels, HOMA-IR and total cholesterol. HFD-induced increase in NEFA was further enhanced in the HFD CPT1AM group (Figure 23E).

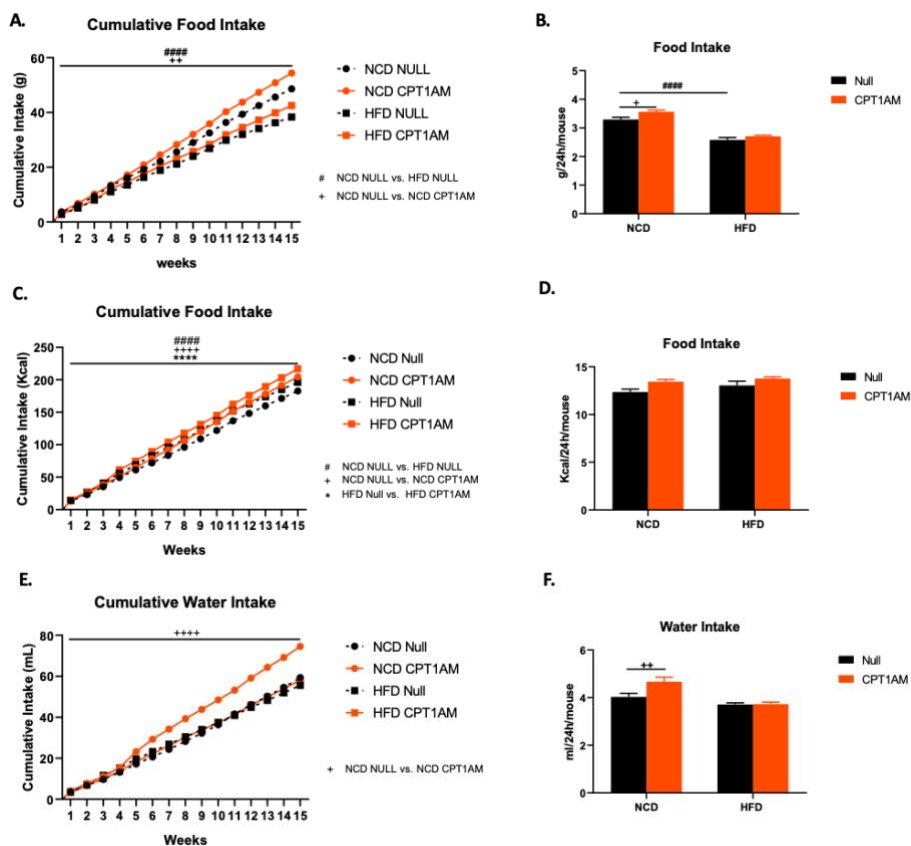
**Figure 23 Serum insulin, HOMA-IR, triglycerides, cholesterol and NEFAs levels in CPT1AM-expressing mice under NCD and HFD.**



A) Insulin levels. B) HOMA-IR. C) Total triglyceride levels. D) Total cholesterol levels. E) NEFAs. Data are expressed as mean  $\pm$  SEM; n = 6-7.

When quantifying water intake, significant differences are only observed in the NCD CPT1AM group, since it has a higher water consumption, in cumulative and daily intake compared to the NCD and HFD Null groups (Figure 24E-F).

Figure 24 Food and water intake.



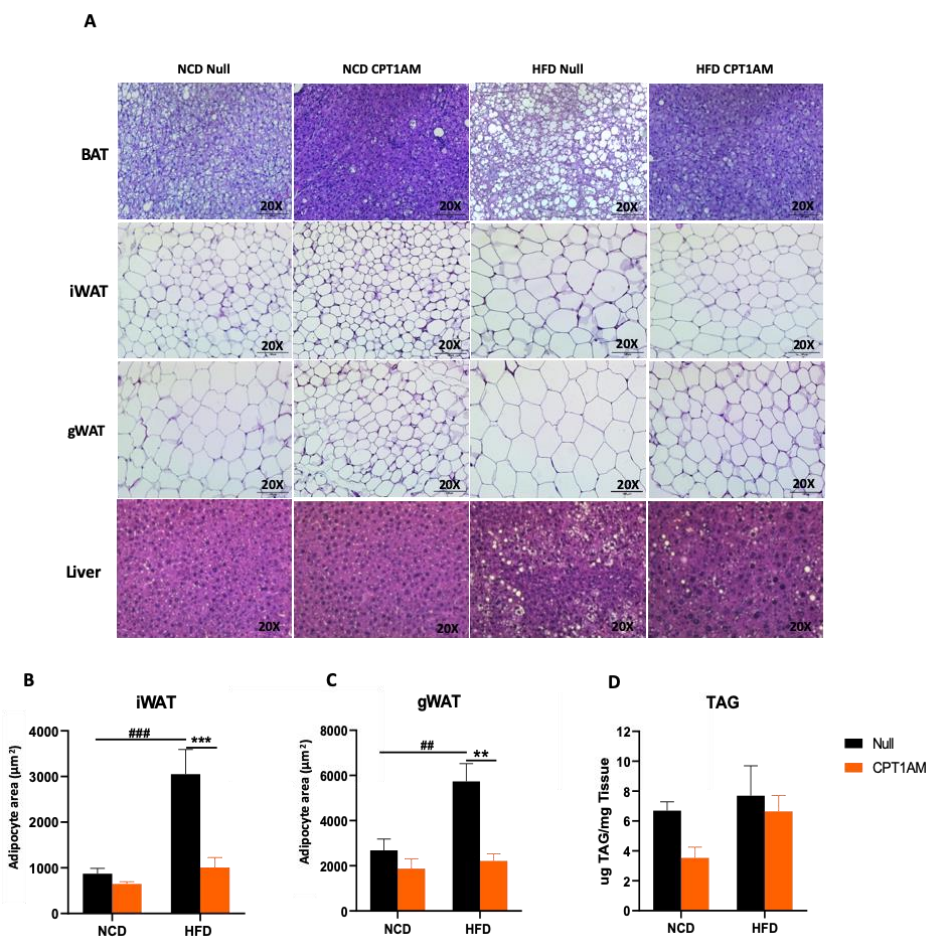
A) Cumulative food intake. B) Daily food intake. C) Cumulative calorie intake. D) Daily calorie intake. E) Accumulated water intake. F) Daily water intake. Data are expressed as mean  $\pm$  SEM; n = 6-7.

### 5.2.2 BAT-specific CPT1AM overexpression in HFD-treated mice prevented HFD-induced hepatic steatosis and adipose tissue hypertrophy

The morphology of BAT, iWAT, gWAT and liver was studied by H&E histology (Figure 25A). In addition, adipocyte area was quantified in iWAT and gWAT (Figure 25B-C), and hepatic triacylglycerol (TAG) content was measured (Figure 25D).

At the histological level, HFD-induced the brown-to-white transformation seen in BAT was partially restored in HFD CPT1AM mice (Figure 25A). Importantly, HFD-induced hypertrophy in iWAT and gWAT was reduced in HFD CPT1AM mice compared to HFD Null controls (Figure 25A). Morphometric analysis revealed that the HFD-induced increase in adipocyte size in iWAT and gWAT was blunted in the HFD CPT1AM group (Figure 25B, C). Regarding hepatic steatosis, no significant differences were observed in the TAG measurement (Figure 25C) while a tendency was observed towards a decrease in the lipid droplets accumulation in the HFD CPT1AM group compared to HFD Null control.

**Figure 25 HFD CPT1AM mice show reduced iWAT and gWAT hypertrophy.**



A) Representative images of H&E-stained BAT, iWAT, gWAT, and livers sections. Scale bar 100  $\mu\text{m}$  (20x magnification). B) Quantification of the size of adipocytes in iWAT. C) Quantification of the size of adipocytes in gWAT. D) Quantification of TAG liver content. Data are expressed as mean  $\pm$  SEM; n = 6-7.

### 5.2.3 Overexpression of CPT1AM in BAT from HFD-treated mice under room temperature conditions alters tissue metabolism

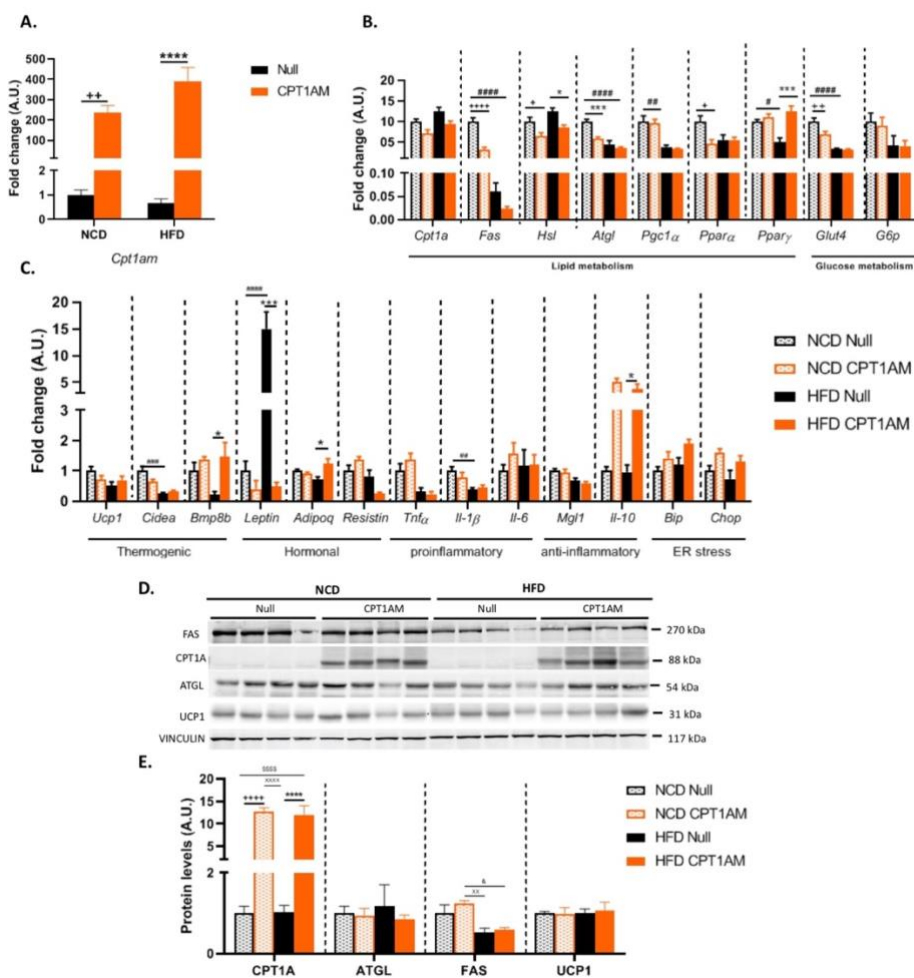
To complement the histological characterization of tissues and the metabolic phenotype, mRNA and protein expression levels were studied by qRT-

PCR and Western Blot (WB), respectively in BAT (Figure 26), iWAT (Figure 27), gWAT (Figure 28) and liver (Figure 29). In BAT, the mRNA expression of *Cpt1am* was evaluated to verify the BAT-specific overexpression by the injection of viral vectors. Some genes involved in lipid metabolism (*Cpt1a*, *Fas*, *Hsl*, *Atgl*, *Pgc1α*, *Pparaα*, and *Pparγ*), glucose metabolism (*Glut4*, and *G6p*), thermogenesis (*Ucp1*, *Cidea*, and *Bmp8b*), hormones (*Leptin*, *Adiponectin*, and *Resistin*), inflammation (*Tnfa*, *Il1β*, *Il6*, *Mgt1*, and *Il10*), and ER stress (*Bip*, and *Chop*) were studied (Figure 26).

A significant increase in the *Cpt1am* mRNA expression was observed in CPT1AM-expressing mice both under NCD and HFD, corroborating the efficiency of the viral therapy (Figure 26A). Quantification of protein levels (FAS, CPT1A, ATGL, UCP1) normalized by the VINCULIN protein was also performed (Figure 26D-E). CPT1A protein levels were increase in both NCD CPT1AM and HFD CPT1AM groups compared to Null controls (Figure 26D-E). No changes were seen in the protein levels of ATGL, FAS and UCP1 between CPT1AM-expressing mice compared to Null controls (Figure 26E).



Figure 26 mRNA and protein expression levels in BAT.

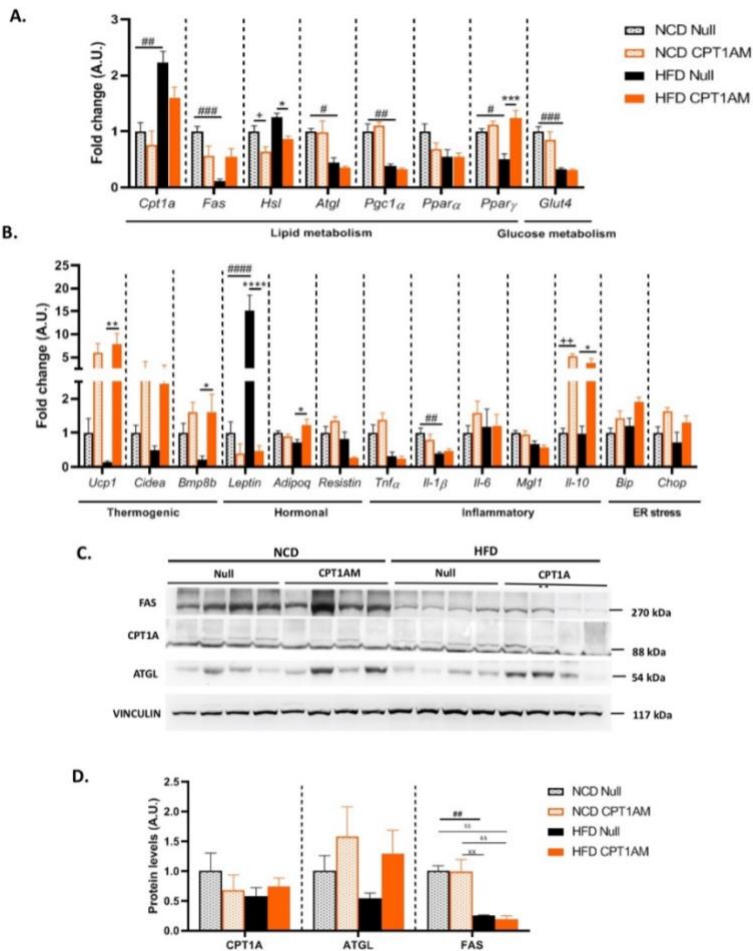


RNA expression levels of *Cpt1am* (A) and genes involved in lipid metabolism (*Cpt1a*, *Fas*, *Hsl*, *Atgl*, *Pgc1α*, *Pparaα*, and *Pparγ*) (B), glucose metabolism (*Glut4*, and *G6p*) (B), and thermogenesis (*Ucp1*, *Cidea*, and *Bmp8b*), hormones (*Leptin*, *Adiponectin*, and *Resistin*), inflammation (*Tnfα*, *Il1β*, *Il6*, *Mgt1*, and *Il10*), and ER stress (*Bip*, and *Chop*) (C). mRNA levels were normalized by *Rpl32*. (D) Representative WB and (D) Quantification of CPT1A, ATGL, FAS and UCP1 normalized by VINCULIN. Data are expressed as mean ± SEM; n = 6-7.

In iWAT, genes involved in lipid metabolism (*Cpt1a*, *Fas*, *Hsl*, *Atgl*, *Pgc1α*, *Pparaα*, and *Pparγ*) and (*Glut4*) were studied (Figure 27A), in addition to

thermogenic genes (*Ucp1*, *Cidea*, *Bmp8b*), hormones (*Leptin*, *Adiponectin*, *Resistin*), inflammatory (*Tnfa*, *Il1b*, *Il6*, *Mgt1*, *Il10*), and ER (*Bip*, *Chop*) (Figure 27B). Likewise, it was observed that the mice that overexpressed CPT1AM under HFD conditions were resistant to the increase in *Leptin* caused by the diet (Figure 27C). Similarly, an increase in the thermogenic genes *Ucp1* and *Bmp8b* is seen. No differences were seen in the protein levels of CPT1A, ATGL, and FAS between CPT1AM-expressing mice compared to Null control (Figure 27C-D).

Figure 27 mRNA and protein expression levels in iWAT.



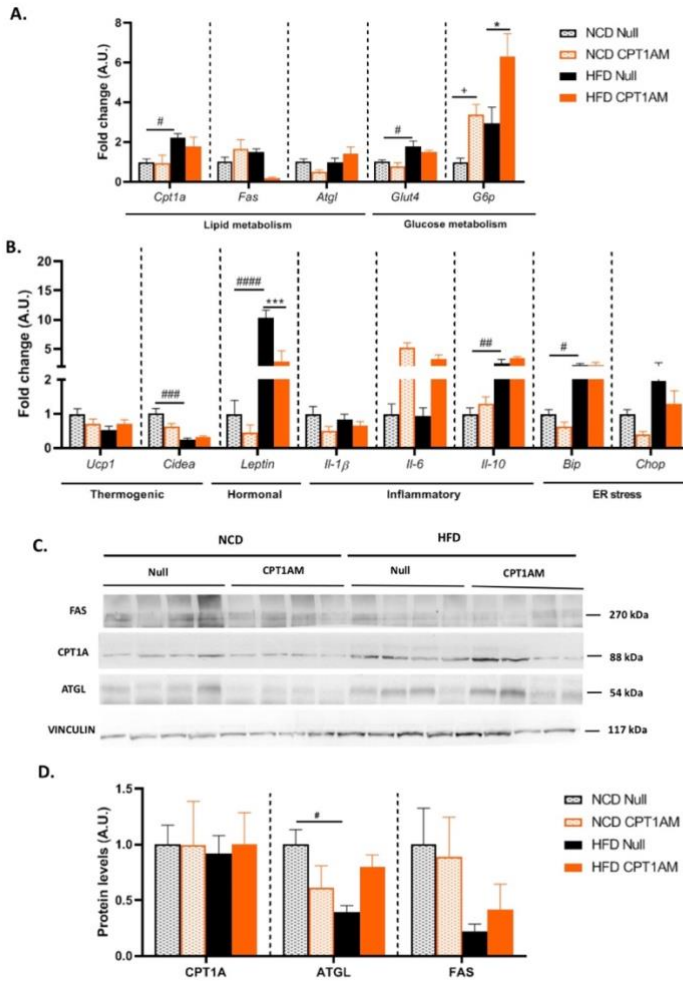
A) qRT-PCR analysis of the *Cpt1a*, *Fas*, *Hsl*, *Atgl*, *Pgc1 $\alpha$* , *Ppara $\alpha$* , *Ppara $\gamma$*  and *Glut4* genes. B) qRT-PCR analysis of the genes *Ucp1*, *Cidea*, *Bmp8b*, *Leptin*, *Adipoq*, *Resistin*, *Tnfa*, *Il-1 $\beta$* , *Il-6*, *Mgl1*, *Il-10*, *Bip* and *Chop*. mRNA levels were normalized by *Rpl32* (A-B). C) Representative WB. D) Quantification of CPT1A, ATGL and FAS, normalized by VINCULIN. Data are expressed as mean  $\pm$  SEM; n = 6-7.

In gWAT, gene expression was also measured and WB was performed to observe protein levels (Figure 28A-D), the measured lipid metabolism genes (*Cpt1a*, *Fas*, *Atgl*), glucose metabolism (*Glut4*, *G6p*) (Figure 28A), thermogenic

genes (*Ucp1*, *Cidea*), the hormone *Leptin*, inflammatory genes (*Il1 $\beta$* , *Il6*, *Il10*), and ER genes (*Bip*, *Chop*) (Figure 28B). In gWAT, changes in *G6p* of glucose metabolism, were observed, and as in BAT and iWAT, resistance to the increase in *Leptin* caused by HFD was observed. (Figure 28B).

In the quantification of protein levels (FAS, CPT1A, ATGL) no significant differences were observed (Figure 28C-D).

**Figure 28 mRNA and protein expression levels in gWAT.**

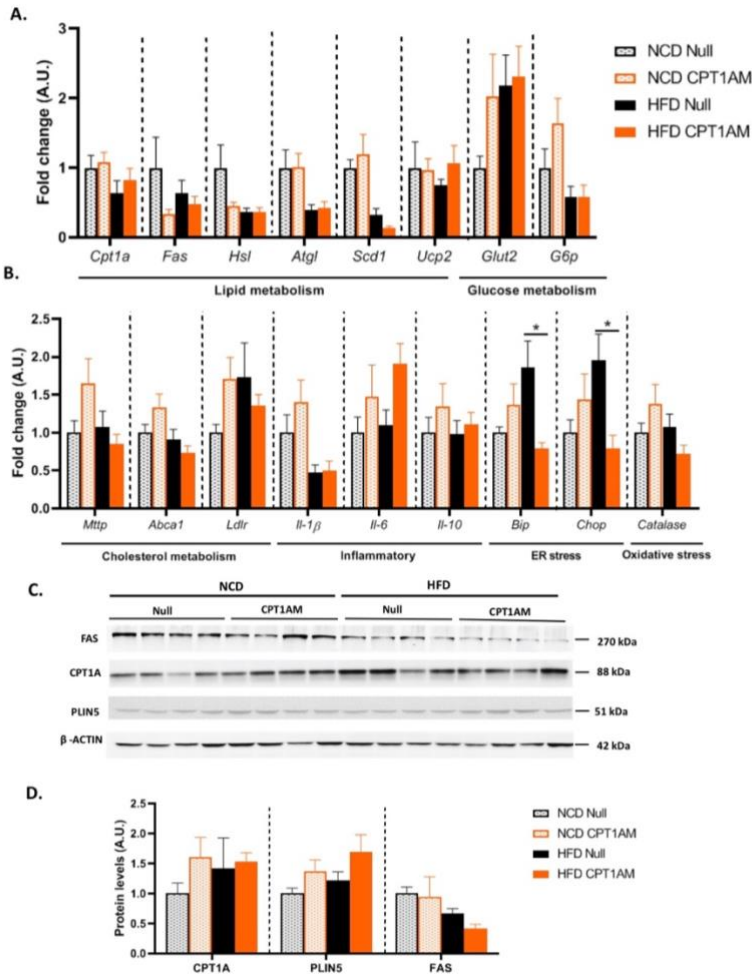


A) qRT-PCR analysis of the *Cpt1a*, *Fas*, *Atgl*, *Glut4* and *G6p* genes. B) qRT-PCR analysis of the *Ucp1*, *Cidea*, *Leptin*, *Il-1 $\beta$* , *Il-6*, *Il-10*, *Bip* and *Chop* genes. mRNA levels were normalized by *Rpl32* (A-B). C) Representative WB. D) Quantification of CPT1A, ATGL and FAS, normalized by VINCULIN. Data are expressed as mean  $\pm$  SEM; n = 6-7.

Finally, in this experiment, gene expression was observed and protein levels were observed in the liver (Figure 29A-D), in which lipid metabolism genes

(*Cpt1a*, *Fas*, *Hsl*, *Atgl*, *Scd1*, *Ucp2*) were analyzed, of the glucose metabolism (*Glut2*, *G6p*) (Figure 29A). Cholesterol metabolism genes (*Mttp*, *Abca1*, *Ldlr*), inflammatory genes (*Il1b*, *Il6*, *Il10*), ER (*Bip*, *Chop*) and oxidative stress genes (*Catalase*) were also studied (Figure 29B). Of the genes studied, only significant differences were seen in ER, since mice that overexpressed CPT1AM decreased reticulum stress caused by HFD (Figure 29B). In the quantification of lipid metabolism protein levels (FAS, CPT1A, PLIN5), which were normalized by the  $\beta$ -ACTIN protein, no significant differences were observed (Figure 29C-D).

Figure 29 mRNA and protein expression levels in liver.



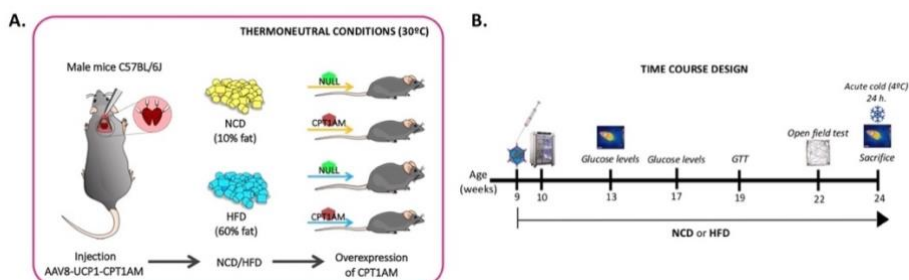
A) qRT-PCR analysis of the *Cpt1a*, *Fas*, *Hsl*, *Atgl*, *Scd1*, *Scd2*, *Glut2* and *G6p* genes. B) qRT-PCR analysis of the *Mttp*, *Abca1*, *Ldlr*, *Il-1β*, *Il-6*, *Il-10*, *Bip*, *Chop* and *Catalase* genes. mRNA levels were normalized by *Tbp* (A-B). C) Representative WB. D) Quantification of CPT1A, PLIN5 and FAS, normalized by β-ACTIN. Data are expressed as mean ± SEM; n = 6-7.

### 5.3 CPT1AM expression in healthy male mice under thermoneutrality conditions

#### 5.3.1 Mice treated with CPT1AM and HFD under thermoneutrality conditions are resistant to diet-induced obesity

To evaluate whether the maintenance of the animals under thermoneutrality conditions might affect the outcome of the HFD and CPT1AM expression, next we carried out similar experiments keeping the animals inside a thermoneutrality chamber throughout the experimental process. We expect that under thermoneutrality conditions the chronic cold-induced BAT activation would be avoided. Thus, in these experiments, CPT1AM was overexpressed in the BAT of healthy 9-week-old mice, which were subjected to NCD and HFD, but under thermoneutrality conditions, to observe changes in the metabolic phenotype, during the induction of obesity with the HFD, and the changes in the overexpression after an acute cold stimulus in the BAT, to increase the thermogenic activity at the time of sacrifice.

**Figure 30 Experimental design of CPT1AM expression in vivo carried out at thermoneutrality conditions.**

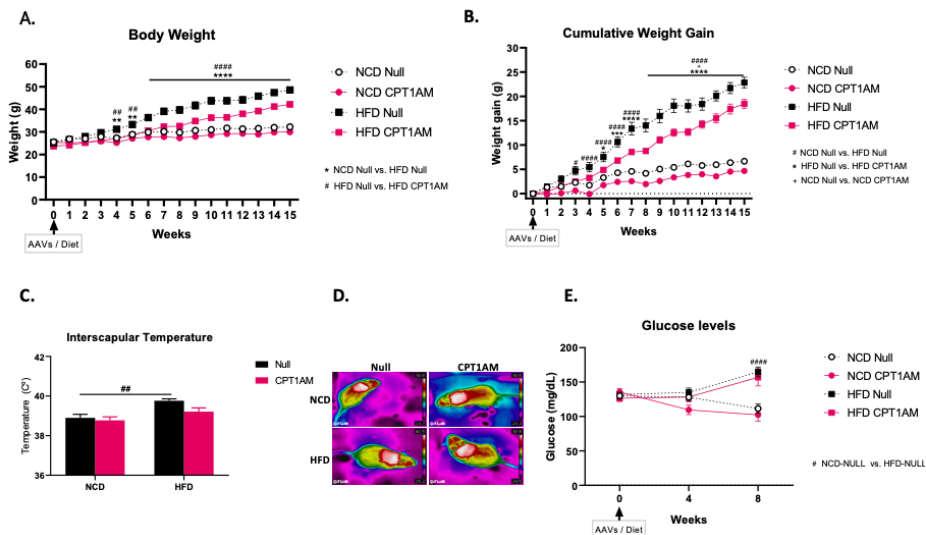


A) Figure of the experimental design carried out under thermoneutrality conditions. B) Time course design.



Weekly monitoring of weight and weight gain was carried out during the 15 weeks that they were in treatment with CPT1AM and with HFD. HFD CPT1AM mice maintained their weight almost in the normal range, thus, they were resistant to obesity induction by diet, and HFD Null mice became obese from week 4 post-diet (Figure 31A). Differences in weight gain from 6 weeks post-treatment were also seen between the HFD Null and HFD CPT1AM groups (Figure 31B). Regarding interscapular temperature. Glucose levels at 4 and 8 weeks were also monitored, but no significant changes were observed in HFD CPT1AM mice compared to HFD Null controls (Figure 31E).

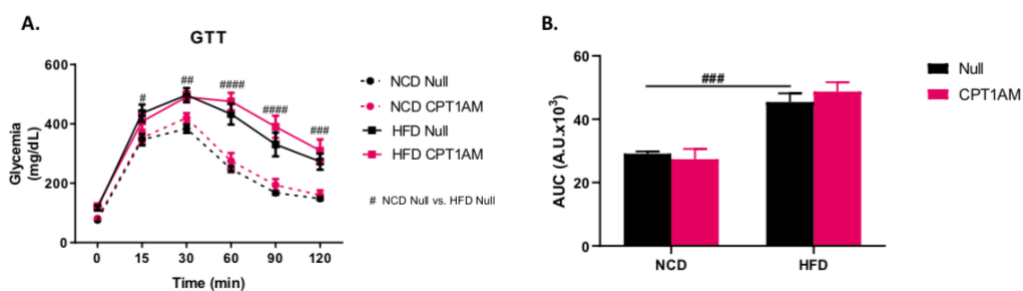
**Figure 31** Body weight, interscapular temperature and fasting blood glucose levels of CPT1AM-expressing mice under HFD at thermoneutrality conditions.



A) Weekly monitoring of body weight. B) Weekly monitoring of body weight gain. C) Thermography. D) Representative photos of thermography. E) Monthly monitoring of glucose levels. Data are expressed as mean  $\pm$  SEM;  $n = 8$ .

To monitor glucose metabolism, 10 weeks after treatment with CPT1AM and HFD, a GTT was performed in which significant differences were observed between the NCD and HFD groups, evidencing the induction of obesity through diet (Figure 32A- B). No differences were seen between the CPT1AM and Null groups either under NCD or HFD.

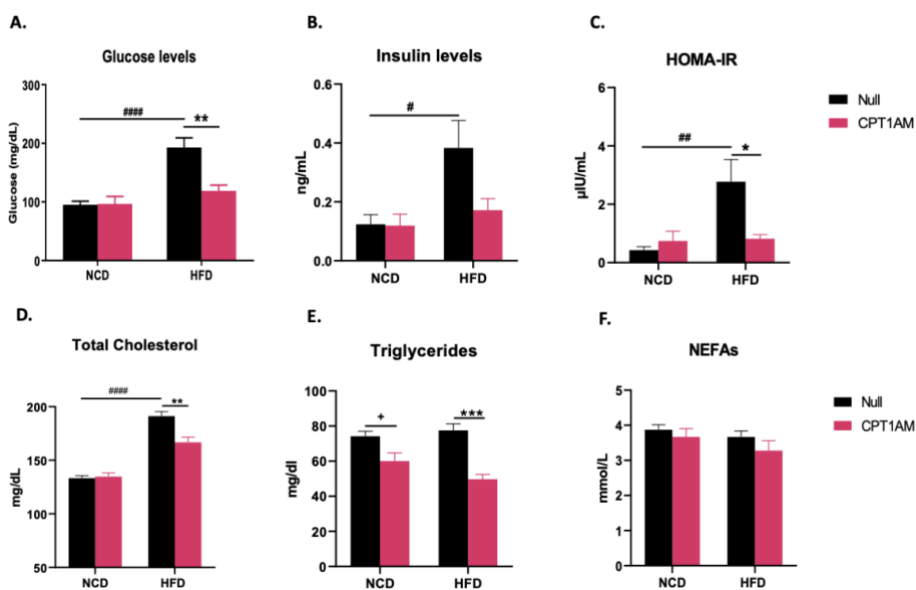
**Figure 32** Glucose tolerance test and area under the curve of CPT1AM-expressing mice under HFD at thermoneutrality conditions.



A) GTT. B) AUC of GTT. Data are expressed as mean  $\pm$  SEM;  $n = 8$ .

In addition, at 10 weeks, serum fasting blood glucose and insulin levels (Figure 33A-B), HOMA-IR (Figure 33C), total cholesterol (Figure 33D), triglycerides (Figure 33E) and NEFAs (Figure 33F) were measured. Despite the HFD-induced impaired glucose tolerance evidenced in the GTT (Figure 33A-B), HFD CPT1AM mice had glucose and HOMA-IR levels in near normal ranges (Figure 33A and C). HFD-induced increase in cholesterol levels was reduced in the HFD CPT1AM group (Figure 33D). Likewise, mice that overexpress CPT1AM, with NCD and HFD, have reduced triglyceride levels (Figure 33E). No differences were seen in serum NEFAs levels (Figure 33F).

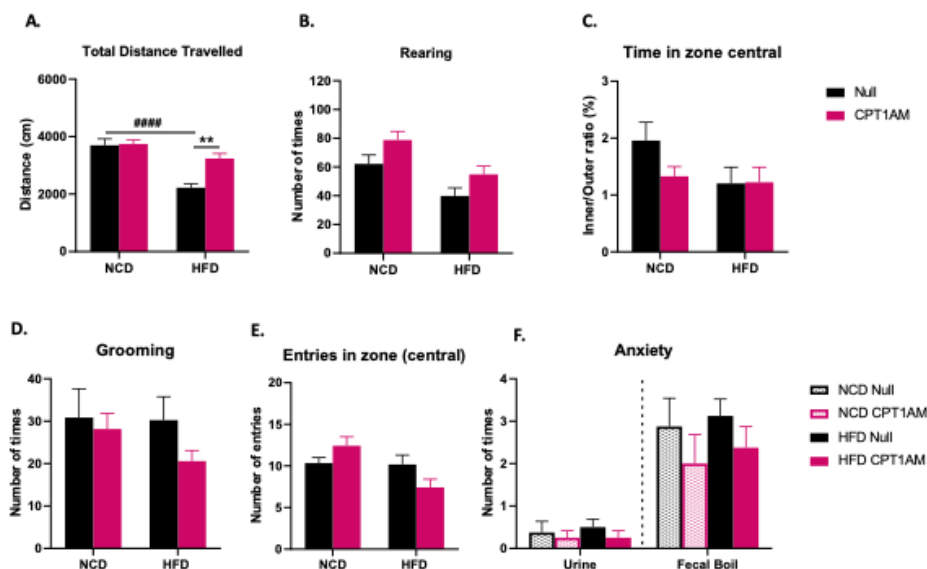
**Figure 33 Mice overexpressing CPT1AM, at 10 weeks under thermoneutrality conditions, were resistant to diet-induced hyperglycemia, hyperinsulinemia, hypercholesterolemia, and hypertriglyceridemia.**



A) Glucose levels. B) Insulin levels. C) HOMA-IR. D) Total Cholesterol Levels. E) Triglycerides levels. F) NEFAs levels. Data are expressed as mean  $\pm$  SEM; n = 8.

At 13 weeks after treatment with CPT1AM and NCD/HFD, the mice were subjected to the Open Field test to assess animal movement, anxiety and stress levels (Figure 34A-F). In the test carried out, a significant decrease in the distance traveled by the HFD Null mice compared to NCD control was observed, which is reflected in a greater sedentary lifestyle caused by the HFD. Importantly, this decrease was blunted in the HFD CPT1AM mice (Figure 34A). Regarding anxiety and stress levels, no significant changes were observed (Figure 34B-F).

**Figure 34 CPT1AM-expressing mice at thermoneutrality improved HFD-induced decrease in the distance travelled.**



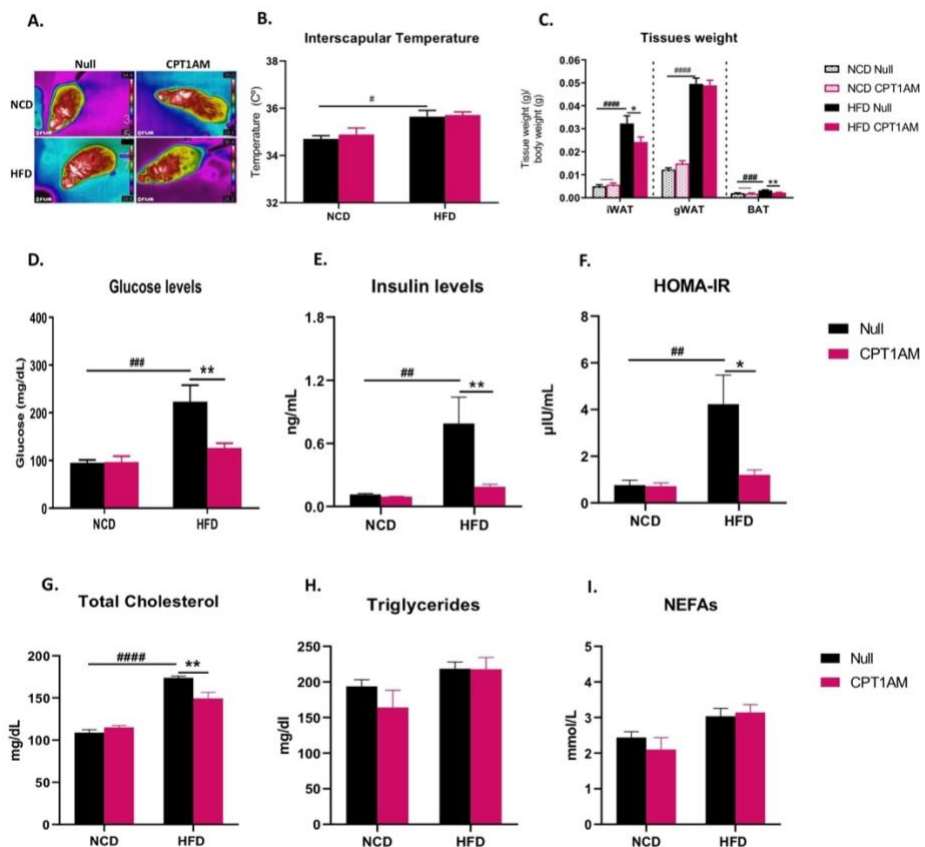
Measurements performed with the Open Field test. A) Total distance travelled. B) Rearing. C) Time in zone central. D) Grooming. E) Entries in zone (central). F) Anxiety (number of times the animals urinate and defecate). Data are expressed as mean  $\pm$  SEM;  $n = 8$ .

After 15 weeks of treatment with CPT1AM and NCD/HFD, mice were sacrificed under fasting conditions (2 hours) and after an acute cold stimulus (4°C) for 24 hours. The interscapular temperature was measured, and an increase was seen in both Null and CPT1AM groups treated with HFD compared to the NCD groups (Figure 35A-B). iWAT, gWAT and BAT were dissected and weighted (Figure 35C). The HFD CPT1AM group showed a reduction in the iWAT and BAT weight compared to HFD Null mice (Figure 35C).

Also, glucose levels (Figure 35D), insulin levels (Figure 35E), HOMA-IR (Figure 35F), total cholesterol (Figure 35G), triglyceride levels (Figure 35H) and NEFAs (Figure 35I) were measured in blood plasma. Significant results were

observed at this time point where HFD-induced alterations in glucose, insulin, HOMA-IR, and cholesterol levels were decreased in HFD CPT1AM mice (Figure 35D-G). Regarding triglycerides and NEFAs, at the time of sacrifice, no significant differences were observed (Figure 35H-I).

**Figure 35** At the time of sacrifice following acute cold challenge, CPT1AM-expressing mice were resistant to HFD-induced hyperglycemia, hyperinsulinemia, insulin resistance, and hypercholesterolemia.



A) Thermography: Representative images. B) Interscapular temperature. C) Weight of iWAT, gWAT and BAT, normalized by the body weight of each mouse. D) Glucose levels. E) Insulin

levels. F) HOMA-IR. G) Total Cholesterol Levels. H) Triglyceride levels. I) Levels of NEFAs. Data are expressed as mean  $\pm$  SEM; n = 8.

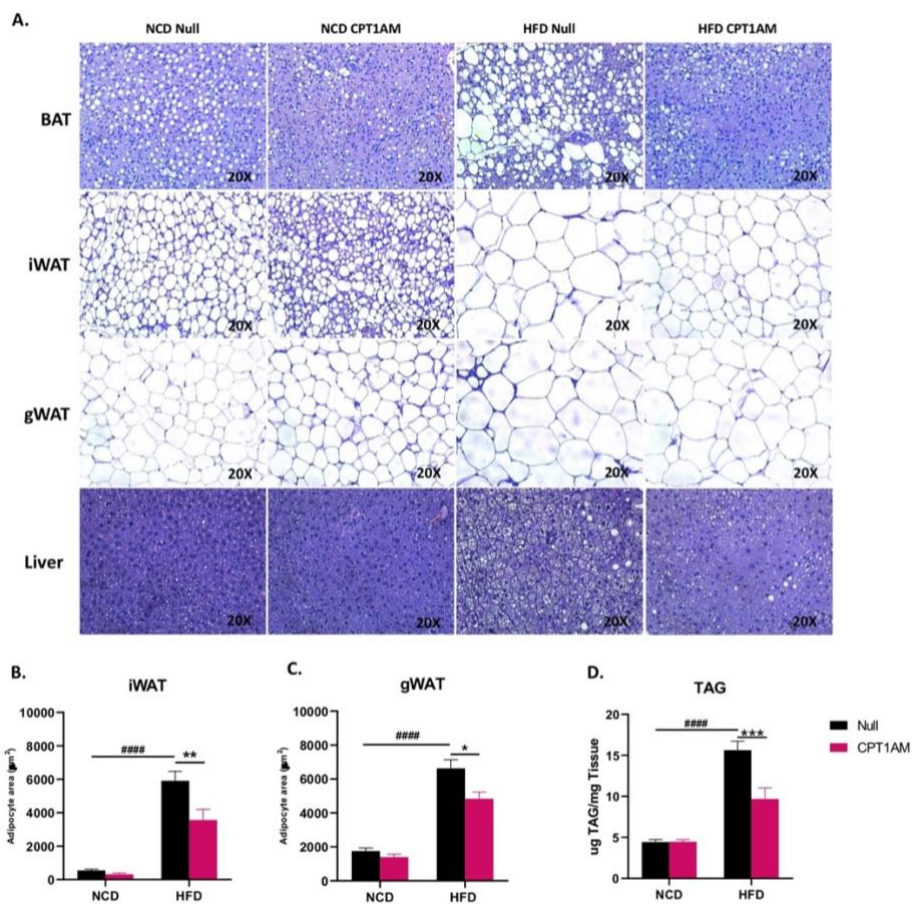
### **5.3.2 CPT1AM-expressing mice under thermoneutrality conditions are protected against HFD-induced adipose tissue hypertrophy and hepatic steatosis**

After sacrifice, histological characterization of BAT, iWAT, gWAT and liver tissue was performed (Figure 36A). In addition, the area of adipocytes in iWAT and gWAT was quantified (Figure 36B-C), and hepatic TAG content was measured (Figure 36D).

In the histological characterization of BAT, the browning of the BAT that were punctured with CPT1AM by means of the viral vectors, with respect to the Null groups, both with NCD and HFD, is visually appreciated (Figure 36A). In iWAT and gWAT of HFD Null mice, increased hypertrophy is observed due to the increase in the size of adipocytes, with respect to the NCD Null and HFD CPT1AM groups. For its part, in the HFD CPT1AM group, adipocytes were observed in iWAT and gWAT, of a similar size to the groups with NCD (Figure 36A-C).

HFD-induced hepatic steatosis was reduced in CPT1AM-expressing mice both at the histological level and TAG content (Figure 36A, D).

**Figure 36** CPT1AM-expressing mice under thermoneutrality conditions are protected against HFD-induced adipose tissue hypertrophy and hepatic steatosis.



**A)** Representative images of H&E-stained BAT, iWAT, gWAT, and liver sections. Scale bar 100 µm (20x magnification). **B)** Quantification of adipocyte area in iWAT. **C)** Quantification of adipocyte area in gWAT. **D)** Quantification of TAG content in liver. Data are expressed as mean ± SEM; n = 8.

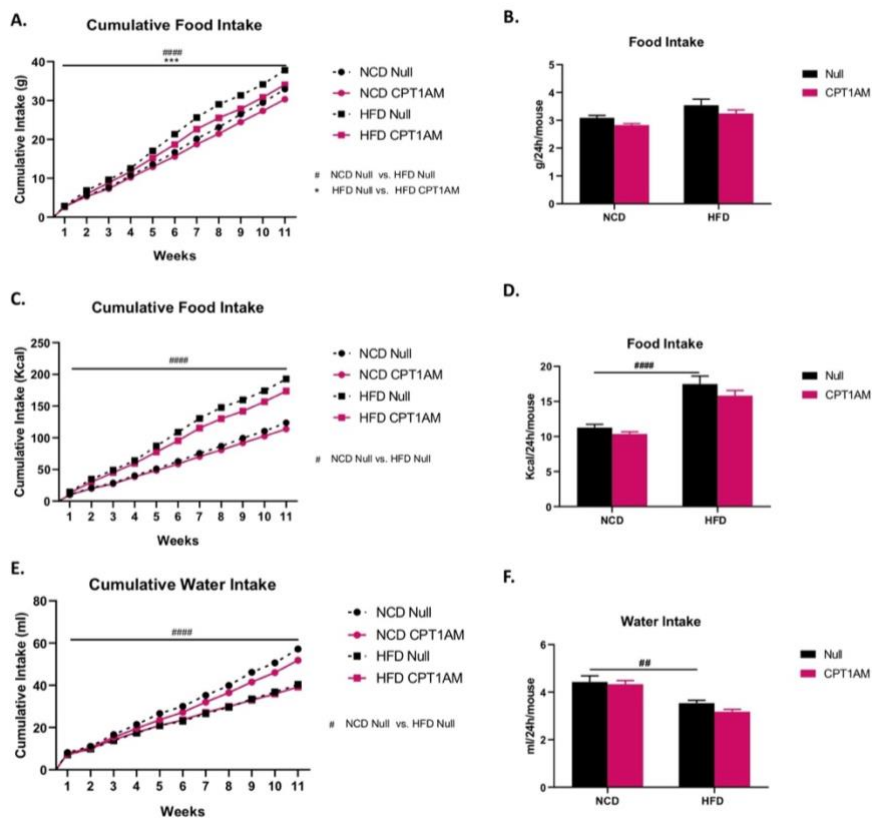
### **5.3.3 Food and water intake of mice treated with CPT1AM and HFD under thermoneutrality conditions**

Similar to the experiments carried out under room temperature conditions, during the induction of obesity by HFD and overexpression of CPT1AM, estimation was made on the control of diet and water intake, which was measured from the week after administration of viral vectors with CPT1AM. Cumulative food intake in grams was monitored. HFD CPT1AM mice had lower food intake compared to HFD Null mice (Figure 37A). When quantifying the daily intake per mouse, no significant differences are shown (Figure 37B). When quantifying the caloric intake (accumulated and daily intake), as expected, a greater consumption of calories is evidenced in the HFD mice compared to the NCD mice (Figure 37C-D).

When quantifying the daily and cumulative intake of water, it is observed that HFD mice consume less water than NCD mice (Figure 37E-F).



**Figure 37 Measurement of food and water intake of mice under thermoneutrality conditions.**



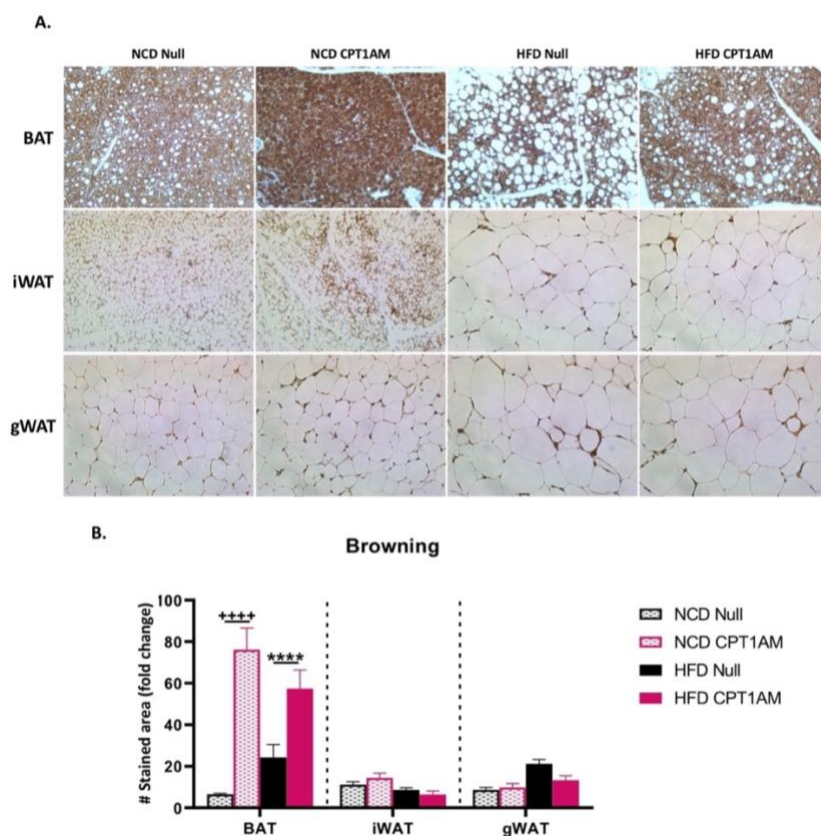
A) Cumulative food intake. B) Daily food intake. C) Cumulative caloric intake. D) Daily caloric intake. E) Accumulated water intake. F) Daily water intake. Data are expressed as mean  $\pm$  SEM; n = 8.

### 5.3.4 CPT1AM-expressing mice under HFD and thermoneutrality conditions show an increase in BAT browning and a reduction in adipose tissue immune cell infiltration and apoptosis

Using the IHC technique, different staining antibodies were used to identify browning (UCP1), T cells (CD3), macrophages (MAC-2) and apoptosis (Caspase-3), in BAT, iWAT and gWAT. When observing the browning in tissues,

an increase in staining is observed, mainly in the BAT of mice with CPT1AM treatment, under NCD and HFD conditions. When quantifying the browning with the stained area, significant differences in BAT are observed. No such differences are observed in iWAT and gWAT (Figure 38A-B).

**Figure 38 CPT1AM-expressing mice under thermoneutrality conditions show an increase in BAT browning.**

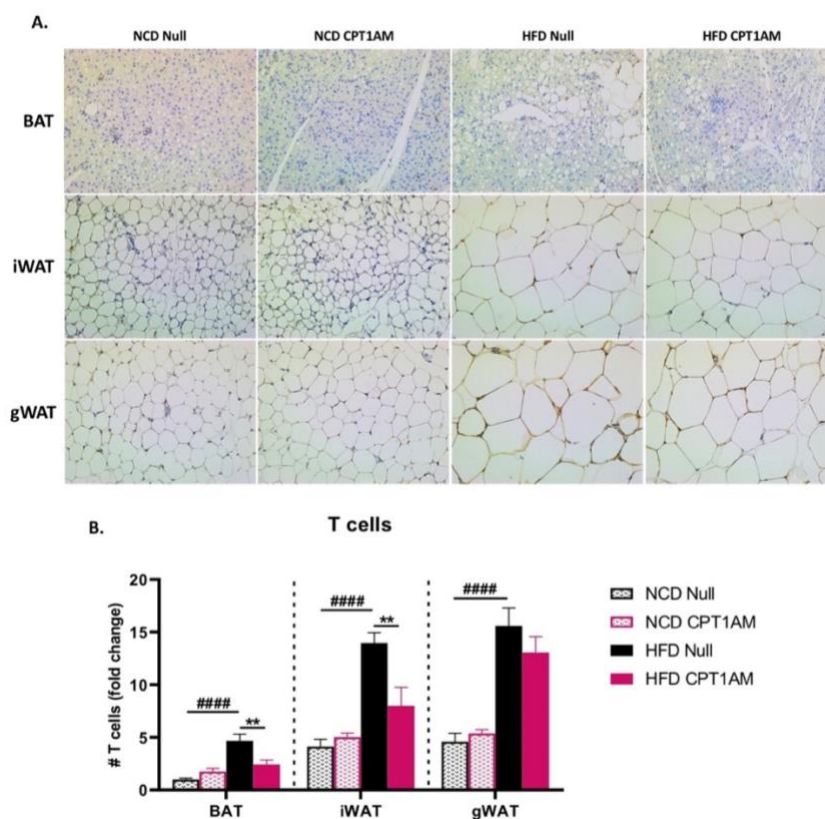


A) Representative images of immunohistochemical localization of UCP1. B) Browning was and expressed as a percentage of the stained area. Data are expressed as mean  $\pm$  SEM;  $n = 8$ .

To analyze immune cell infiltration, T cell quantification was performed. The HFD CPT1AM group showed a reduction of the HFD-induced increase in T

cell infiltration in BAT and iWAT (Figure 39A-B). In gWAT no significant differences were observed (Figure 39A-B).

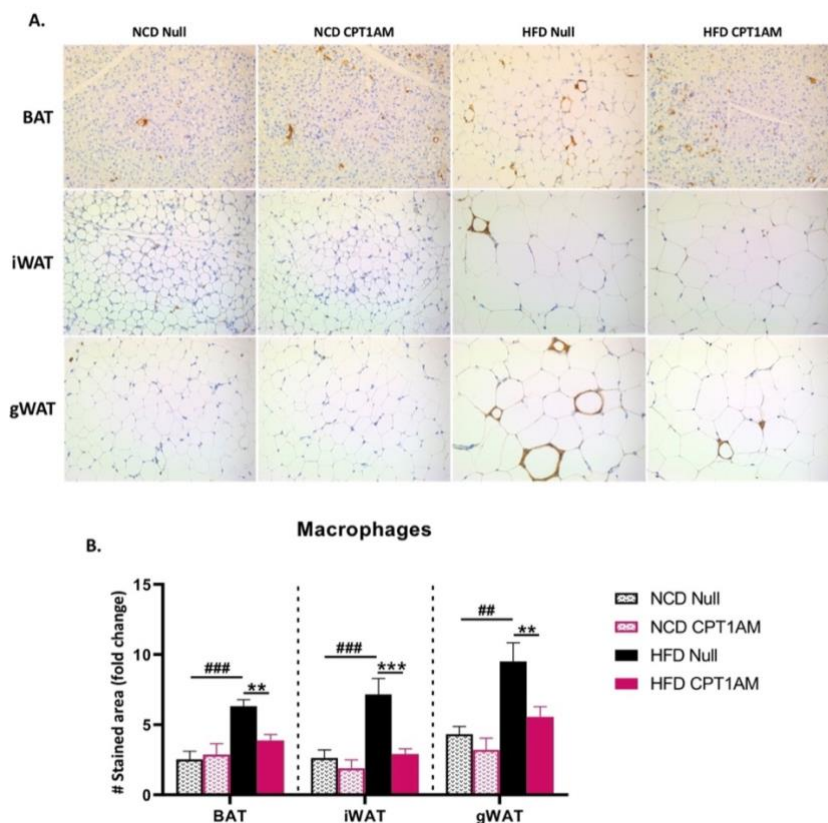
**Figure 39** *CPT1AM*-expressing mice under HFD at thermoneutrality conditions show a reduction of T cell infiltration in BAT and iWAT.



A) Representative images of immunohistochemical localization of CD3. B) T cell infiltration was quantified and expressed as number of stained cells. Data are expressed as mean  $\pm$  SEM;  $n = 8$ .

The quantification of macrophage infiltration was also performed. As well as T cell infiltration, mice overexpressing *CPT1AM* under HFD conditions had less macrophage infiltration caused by HFD (Figure 40A-B).

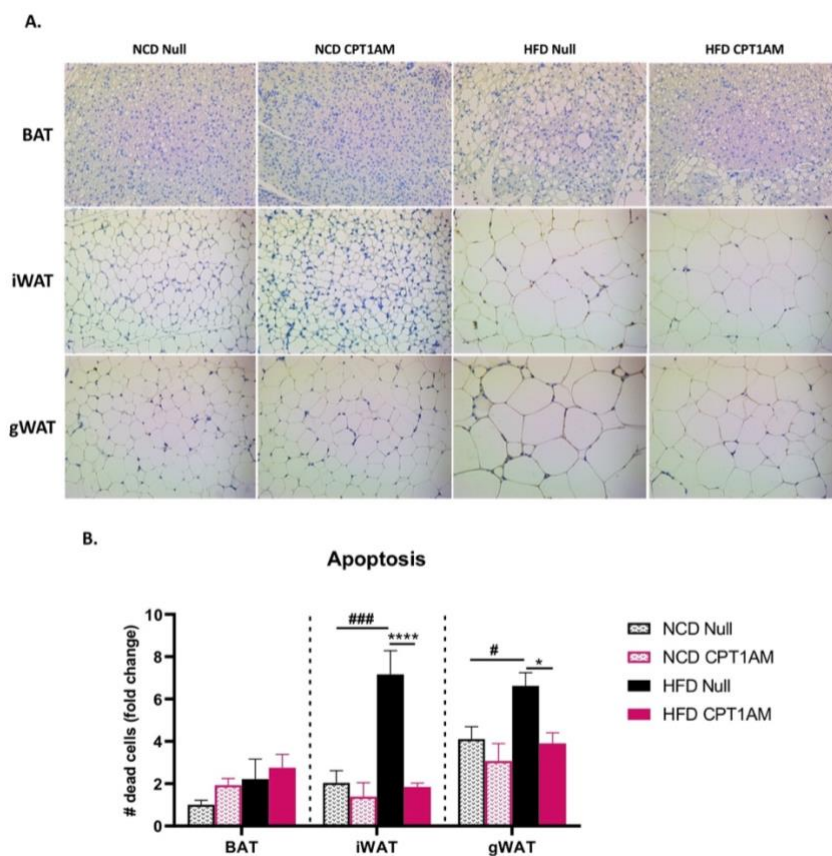
**Figure 40** *CPT1AM*-expressing mice under HFD at thermoneutrality conditions show a reduction of macrophage infiltration in BAT, iWAT and gWAT.



*A)* Representative images of immunohistochemical localization of MAC-2. *B)* Macrophage infiltration was quantified and expressed as a percentage of the stained area. Data are expressed as mean  $\pm$  SEM;  $n = 8$ .

In addition, apoptosis was studied, in which significant differences in iWAT and gWAT were observed. When quantifying the cells staining with Caspase-3, in mice that overexpressed *CPT1AM* under HFD conditions, they presented less infiltration of Caspase-3, preventing apoptosis caused by HFD (Figure 41A-B).

**Figure 41** *CPT1AM*-expressing mice under HFD at thermoneutrality conditions show a reduction of apoptosis in iWAT and gWAT.



A) Representative images of immunohistochemical localization of Caspase-3. B) Apoptosis was quantified and expressed as the number of dead cells. Data are expressed as mean  $\pm$  SEM;  $n = 8$ .

### 5.3.5 Overexpression of CPT1AM in BAT from HFD-treated mice under thermoneutrality conditions alters tissue metabolism

As in the experiment carried out under room temperature conditions, to complement the histological characterization of tissues and the metabolic phenotype, qRT-PCR and WB were performed to measure gene expression and

protein levels, in BAT (Figure 42), iWAT (Figure 43), gWAT (Figure 44), and liver (Figure 45).

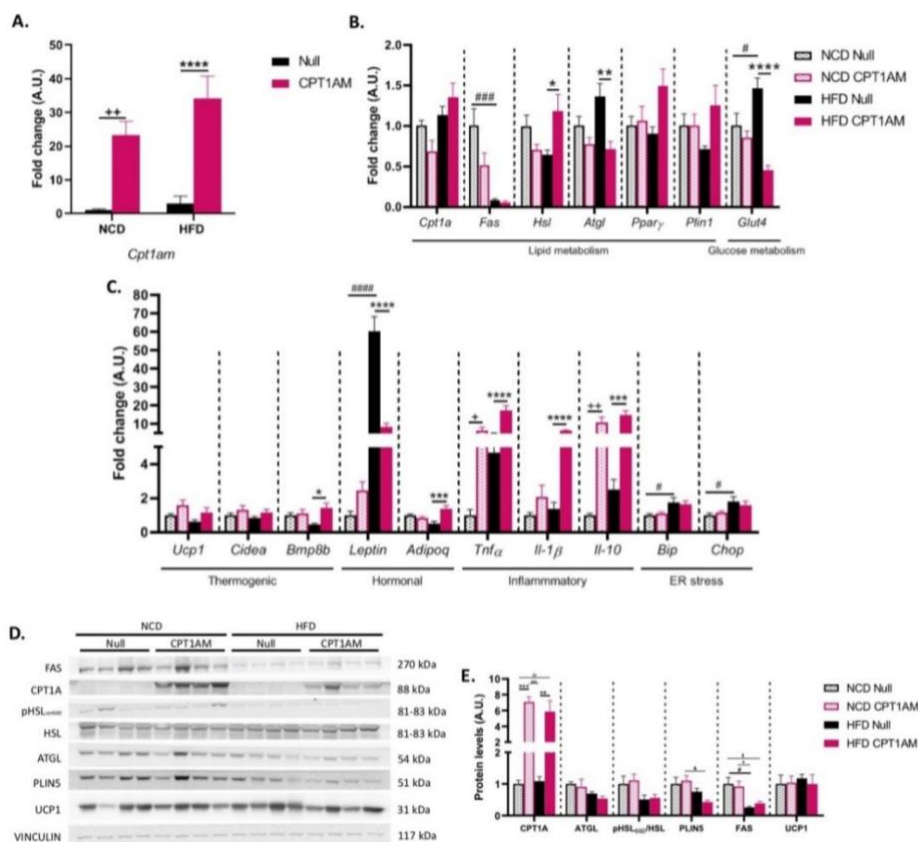
In the qRT-PCR performed in BAT, *Cpt1am* gene was observed (Figure 42A), to verify efficient overexpression by injecting viral vectors. Some lipid metabolism genes (*Cpt1a*, *Fas*, *Hsl*, *Atgl*, *Ppar $\gamma$* , *Plin1*) and glucose metabolism (*Glut4*) were also studied (Figure 42B), as well as thermogenic genes (*Ucp1*, *Cidea*, *Bmp8b*), hormones (*Leptin*, *Adipoq*), inflammatory (*Tnfa*, *Il1b*, *Il10*) and ER stress (*Bip*, *Chop*) (Figure 42C).

An increase of the *Cpt1am* mRNA expression was observed amplifying 35 times more in the mice that were treated with CPT1AM, corroborating the efficient overexpression using the AAVs (Figure 42A).

In the quantification of protein levels by WB, CPT1A, ATGL, HSL, PLIN5, FAS and UCP1, normalized by the VINCULIN protein, were measured (Figure 42D-E). The increase in CPT1A protein levels is visually appreciated (Figure 42D), of the mice that were transduced with CPT1AM, presenting 7 times more protein compared to the Null groups (Figure 42E). In the proteins ATGL, HSL, PLIN5, FAS and UCP1, no significant differences are observed (Figure 42E).



**Figure 42 CPT1AM-expressing mice under HFD and at thermoneutrality conditions show altered BAT metabolism, inflammation and are resistant to HFD-induced increase in leptin and ER stress.**



A) Analysis by qRT-PCR of *Cpt1am* gene. B) Analysis by qRT-PCR of *Cpt1a*, *Fas*, *Hsl*, *Atgl*, *Plin1* and *Glut4* genes. C) Analysis by qRT-PCR of genes *Ucp1*, *Cidea*, *Bmp8b*, *Leptin*, *Adipoq*, *Tnf $\alpha$* , *Il-1 $\beta$* , *Il-10*, *Bip* and *Chop*. mRNA levels were normalized by *Rpl32* (A-C). D) Representative Western blot. E) Quantification of CPT1A, ATGL, HSL, PLIN5, FAS and UCP1, normalized by VINCULIN. Data are expressed as mean  $\pm$  SEM; n = 8 mice. Data were analyzed by two-way repeated measures ANOVA test, followed by Tukey's post hoc test, #p<0.05, ###p<0.001, ####p<0.0001 NCD Null v/s HFD Null (B-C,E), \*p<0.05, \*\*p<0.01, \*\*\*p<0.001, \*\*\*\*p<0.0001 HFD Null v/s HFD CPT1AM (A-C,E), +p<0.05, ++p<0.01, +++p<0.001, NCD Null v/s NCD CPT1AM (A-C,E), &p<0.05 NCD CPT1AM v/s HFD CPT1AM, Xp<0.05, XXXXp<0.0001 NCD CPT1AM v/s HFD Null, \$p<0.05, \$\$p<0.01 NCD Null v/s HFD CPT1AM (E).

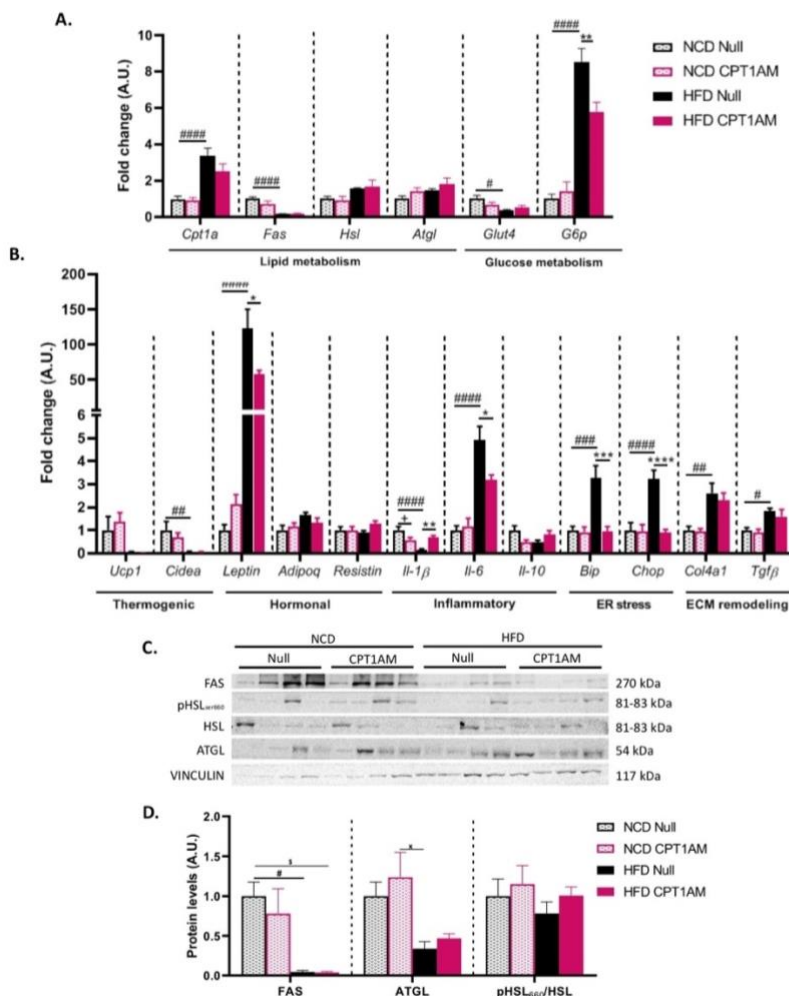
In the qRT-PCR performed in iWAT, some genes involved in lipid metabolism (*Cpt1a*, *Fas*, *Hsl*, *Atgl*) and glucose metabolism (*Glut4*, *G6p*) were studied (Figure 43A), as well as thermogenic genes (*Ucp1*, *Cidea*). Also, hormones (*Leptin*, *Adipoq*), inflammatory (*Tnfa*, *Il1- $\beta$* , *Il-6*, *Il-10*), ER (*Bip*, *Chop*) and extracellular matrix (ECM) remodeling (*Col4a1*, *Tgf $\beta$* ) genes (Figure 43B).

These were also resistant to the increase in *Leptin* caused by HFD (Figure 43B), in addition, they increased the expression of *Il1- $\beta$*  and decreased the expression of *Il-6*, reversing those changes in inflammation caused by HFD. Similarly, a significant decrease in the *Bip* and *Chop* genes is seen, evidencing a decrease in ER in the tissues, of the mice that overexpress CPT1AM, under HFD conditions. No changes in ECM remodeling were observed (Figure 43B).

In the quantification of protein levels of lipid metabolism by WB (CPT1A, ATGL, FAS), no significant differences were observed in protein levels (Figure 43C-D).



**Figure 43 CPT1AM-expressing mice under HFD and at thermoneutrality conditions show altered iWAT metabolism.**



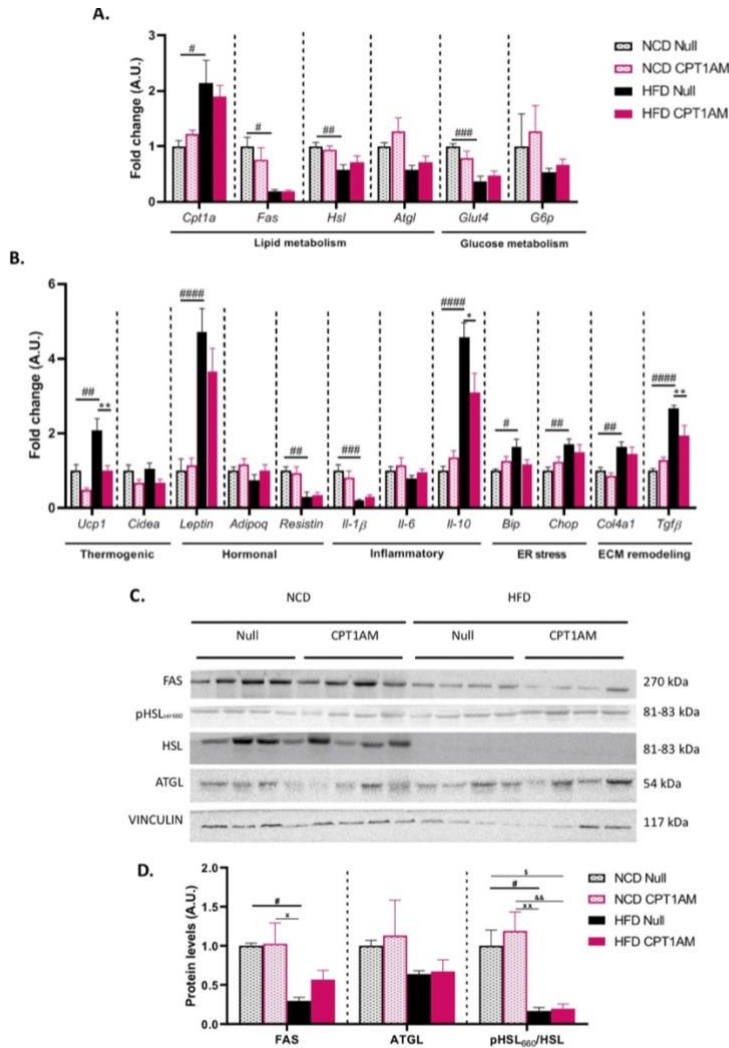
A) Analysis by qRT-PCR of *Cpt1a*, *Fas*, *Hsl*, *Atgl*, *Glut4* and *G6p* genes. B) Analysis by qRT-PCR of genes *Ucp1*, *Cidea*, *Leptin*, *Adipoq*, *Resistin*, *Il-1β*, *Il-6*, *Il-10*, *Bip*, *Chop*, *Col4a1* and *Tgfβ*. mRNA levels were normalized by *Rpl32* (A-B). C) Representative Western blot. D) Quantification of FAS, ATGL and HSL, normalized by VINCULIN. Data are expressed as mean ± SEM; n = 8 mice. Data were analyzed by two-way repeated measures ANOVA test, followed by Tukey's post hoc test, #p<0.05, ##p <0.01, ###p <0.001, ####p <0.0001 NCD Null v/s HFD Null (A-B,D), \*\*p<0.01, \*\*\*p<0.001, \*\*\*\*p<0.0001 HFD Null v/s HFD CPT1AM (A-B), +p<0.05 NCD Null v/s NCD CPT1AM (B), Xp<0.05 NCD CPT1AM v/s HFD Null, §p<0.05 NCD Null v/s HFD CPT1AM (D).

In gWAT, gene expression and WB were also quantified to study protein levels (Figure 44A-D), in which genes were analyzed lipid metabolism (*Cpt1a*, *Fas*, *Hsl*, *Atgl*), glucose metabolism (*Glut4*, *G6p*) (Figure 44A), thermogenic genes (*Ucp1*, *Cidea*), hormones (*Leptin*, *Adipoq*, *Resistin*), inflammatory genes (*Il1-β*, *Il-6*, *Il-10*), ER (*Bip*, *Chop*) and ECM remodeling (*Col4a1*, *Tgfβ*) (Figure 44B).

No changes in glucose and lipid metabolism were seen with CPT1AM treatment (Figure 44A). But a significant decrease in the thermogenic gene *Ucp1* is observed in mice that overexpress CPT1AM, reversing the increase caused by HFD (Figure 44B). A significant decrease in *Il-10* and *Tgfβ*, inflammation and ECM remodeling genes, is also observed, blunting the increase caused by HFD (Figure 44B).

In the quantification of protein levels studying by WB (FAS, ATGL and HSL) no significant differences were observed in the proteins of lipid metabolism (Figure 44C-D).

**Figure 44 CPT1AM-expressing mice under HFD and at thermoneutrality conditions show altered gWAT metabolism.**



A) Analysis by qRT-PCR of *Cpt1a*, *Fas*, *Hsl*, *Atgl*, *Glut4* and *G6p* genes. B) Analysis by qRT-PCR of genes *Ucp1*, *Cidea*, *Leptin*, *Adipoq*, *Resistin*, *Il-1β*, *Il-6*, *Il-10*, *Bip*, *Chop*, *Col4a1* and *Tgfb*. mRNA levels were normalized by *Rpl32* (A-B). C) Representative Western blot. D) Quantification of FAS, ATGL and HSL, normalized by VINCULIN. Data are expressed as mean ± SEM; n = 8 mice. Data were analyzed by two-way repeated measures ANOVA test, followed by Tukey's post hoc test, #p<0.05, ##p<0.01, ###p<0.001, ####p<0.0001 NCD Null v/s HFD Null (A-B,D), \*\*p<0.01, HFD

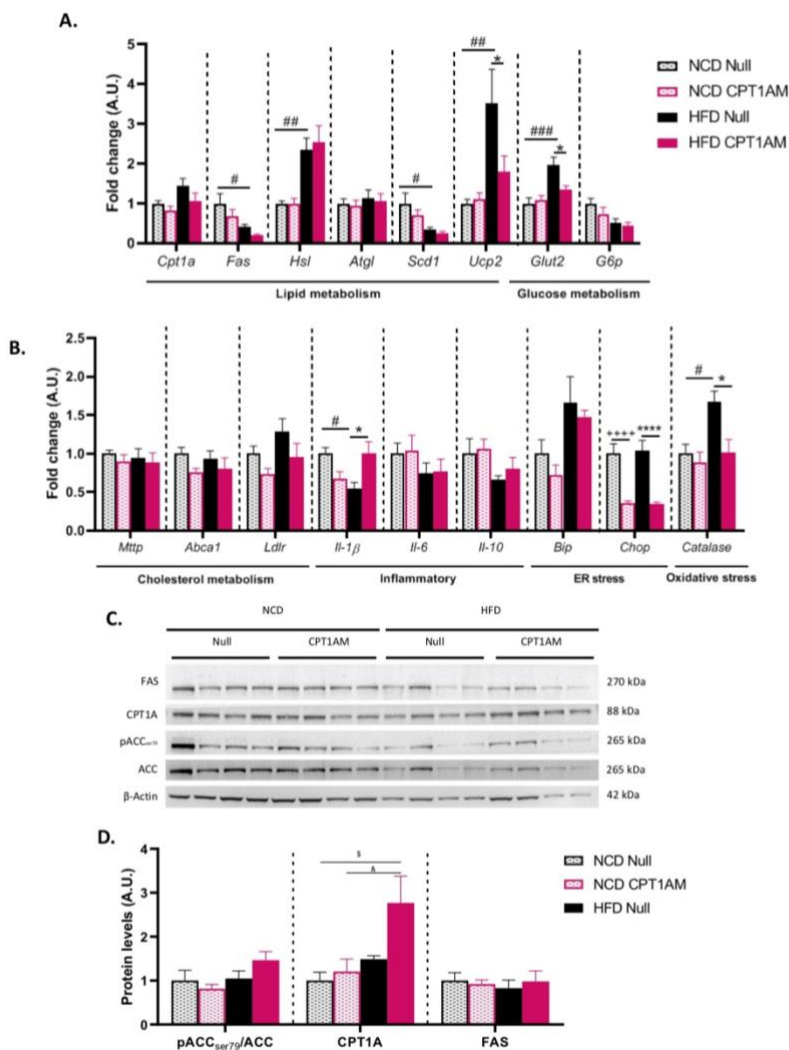
Null v/s HFD CPT1AM (B),  $Xp < 0.05$ ,  $XXp < 0.01$  NCD CPT1AM v/s HFD Null,  $\$p < 0.05$  NCD Null v/s HFD CPT1AM,  $\&\&p < 0.01$  NCD CPT1AM v/s HFD CPT1AM(D).

Finally, in this experiment, gene expression was observed and protein levels were observed in the liver (Figure 45A-D), in which lipid metabolism genes (*Cpt1a*, *Fas*, *Hsl*, *Atgl*, *Scd1*, *Ucp2*), metabolism of glucose (*Glut2*, *G6p*) (Figure 45A). Cholesterol metabolism genes (*Mttp*, *Abca1*, *Ldlr*), inflammatory genes (*Il1- $\beta$* , *Il-6*, *Il-10*), RD (*Bip*, *Chop*) and oxidative stress genes (*Catalase*) were also studied (Figure 45B).

Of the genes studied, significant differences were seen in *Ucp2* and *Glut2*, in lipid and glucose metabolism, respectively, reversing the increase caused by HFD in mice that overexpress CPT1AM (Figure 45A). Likewise, an increase in *Il1- $\beta$*  occurs, preventing the alteration caused by the diet (Figure 45B). In addition, there is a decrease in *Chop* in mice overexpressing CPT1AM with NCD and HFD, decreasing the endoplasmic reticulum stress. Similarly, there is a decrease in oxidative stress in the livers of mice that overexpress CPT1AM under HFD conditions, presenting low levels of *Catalase* (Figure 45B).

In the quantification of protein levels of lipid metabolism (ACC, CPT1A, FAS), which were normalized by the  $\beta$ -ACTIN protein, no significant differences were observed (figure 45C-D).

**Figure 45 CPT1AM-expressing mice under HFD and at thermoneutrality conditions show altered liver metabolism.**



A) Analysis by qRT-PCR of *Cpt1a*, *Fas*, *Hsl*, *Atgl*, *Scd1*, *Ucp2* and *Glut2* genes. B) Analysis by qRT-PCR of genes *Mttp*, *Abca1*, *Ldlr*, *Il-1 $\beta$* , *Il-6*, *Il-10*, *Bip* and *Catalase* mRNA levels were normalized by *Tbp* (A-B). C) Representative Western blot. D) Quantification of CPT1A, ACC and FAS, normalized by  $\beta$ -ACTIN. Data are expressed as mean  $\pm$  SEM;  $n = 10$  mice. Data were analyzed by two-way repeated measures ANOVA test, followed by Tukey's post hoc test,  $\#p < 0.05$ ,  $\#\#p < 0.01$  NCD Null

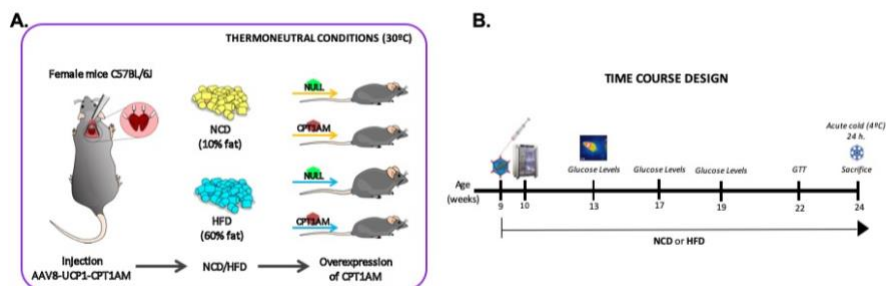
*v/s HFD Null (A,D), +p<0.05 NCD Null v/s NCD CPT1AM, Xp<0.05 NCD CPT1AM v/s HFD Null, \$\$\$p<0.001 NCD Null v/s HFD CPT1AM (D).*

### **5.4 CPT1AM expression in healthy female mice under thermoneutrality conditions**

#### **5.4.1 CPT1AM-expressing female mice under HFD and at thermoneutrality conditions are resistant to diet-induced obesity**

In the experiment carried out in male mice, significant changes were seen in the metabolic phenotype and overexpression in tissues of mice. Therefore, next we aimed at performing similar experiments in female mice, with a larger sample size, under thermoneutrality conditions and with an acute cold stimulus prior the day of the sacrifice. Thus, CPT1AM was overexpressed by AVVs viral vectors in the BAT of healthy 9-week-old female mice, which were subjected to NCD and HFD, under thermoneutrality conditions, to observe changes in the metabolic phenotype, during the induction of obesity with HFD, and to observe the changes in overexpression, after the acute cold stimulus, for the activation of BAT.

**Figure 46 Experimental design of mice treated with CPT1AM and with HFD under thermoneutrality conditions.**



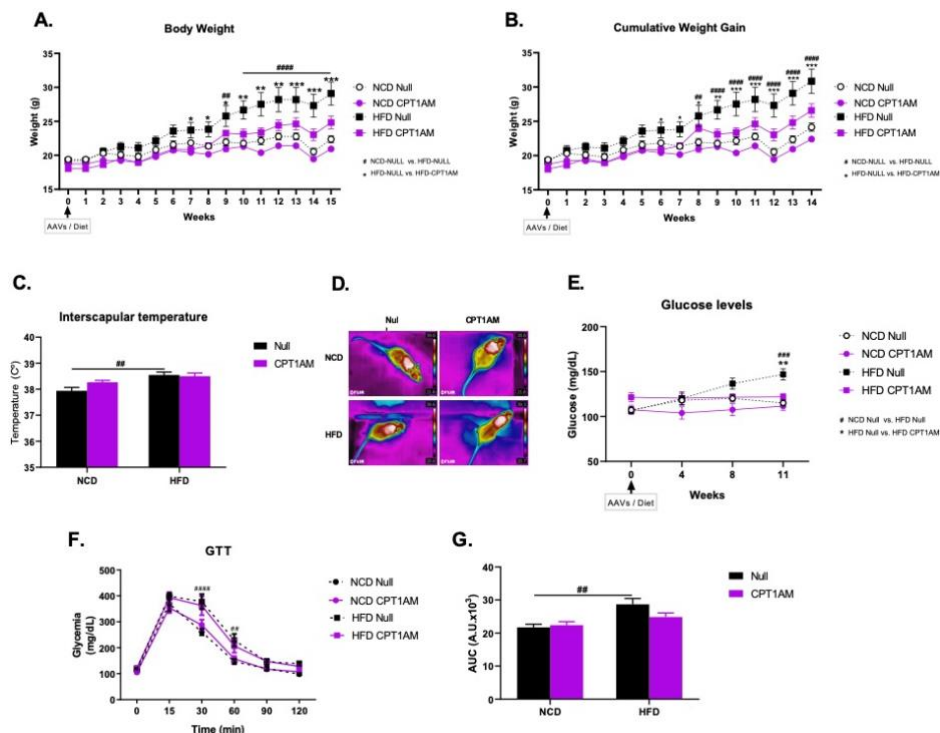
A) Figure of the experimental design carried out under thermoneutrality conditions (30°C). B) Time course design.

As in the third experiment, weekly monitoring of weight and weight gain was carried out during the 15 weeks that they were in treatment with CPT1AM and with HFD. From week 7 after surgery and diet, the HFD Null mice had a significantly higher weight, but the HFD CPT1AM group maintained their weight almost in the normal levels. Therefore, they were resistant to obesity induction by HFD (Figure 47A). The same differences in weight gain were also observed from 6 weeks after treatment and start of diet (Figure 47B).

A significant increase in interscapular temperature was also observed in HFD mice at 4 weeks post-surgery and induction of obesity (Figure 47C-D). Regarding glucose levels that were monitored monthly, significant differences were observed in glucose levels at 11 weeks after surgery and obesity induction by HFD, since the HFD CPT1AM group had glucose levels similar to NCD groups (Figure 47E).

At 13 weeks post-treatment, a GTT was performed, in which an increase in AUC of GTT from HFD Null mice is observed, which is not observed in mice overexpressing CPT1AM (Figure 47F-G).

**Figure 47** Under thermoneutrality conditions, were resistant to HFD-induced obesity.



A) Weekly monitoring of body weight. B) Weekly monitoring of body weight gain. C) Thermography. D) Representative photo of the thermography. E) Monthly monitoring of glucose levels. F) GTT. G) AUC of GTT. Data are expressed as mean  $\pm$  SEM;  $n = 10$ .

Similarly, in the experiment in male mice, 15 weeks after treatment with CPT1AM and HFD, the mice were sacrificed. BAT, iWAT, gWAT and Livers were dissected to be weighed and studied. A significant increase in iWAT, gWAT and liver sizes was observed in the HFD Null group, which was not seen in mice overexpressing CPT1AM on the same diet. Regarding the size of BAT, no significant differences were observed (Figure 48A).

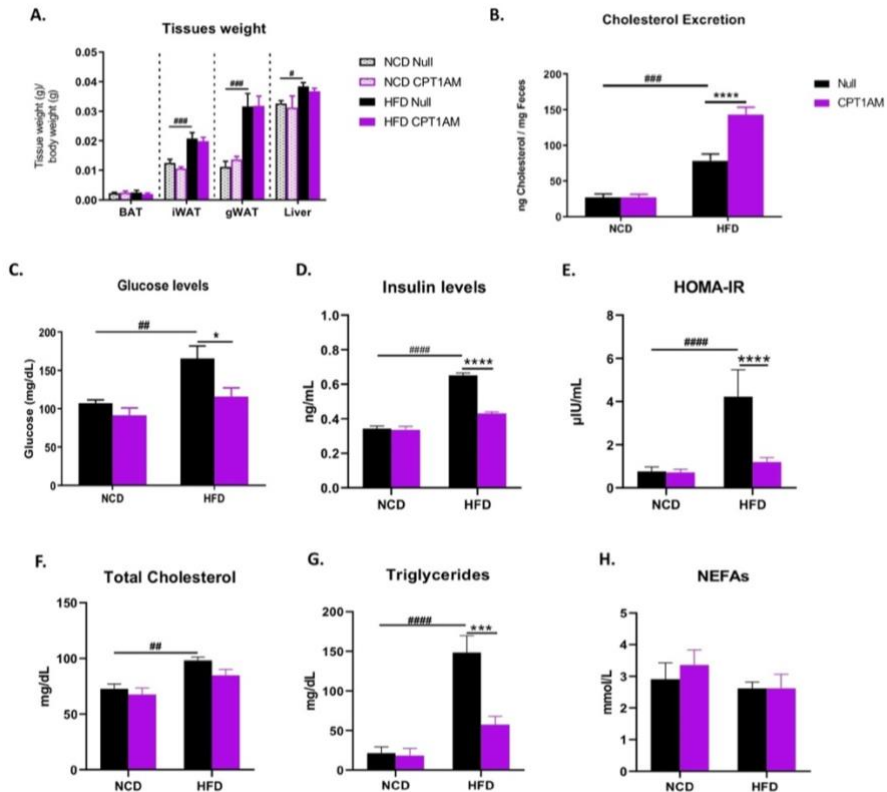
Fecal feces were extracted days before sacrifice to measure excreted cholesterol. Our sample showed a significant increase in cholesterol excretion in



feces under HFD conditions, but in mice overexpressing CPT1AM the excretion is even higher (Figure 48B). In addition, on the day of sacrifice, blood plasma was extracted to measure glucose levels (Figure 48C), insulin levels (Figure 48D), HOMA-IR (figure 48E), total cholesterol levels (Figure 48F), triglyceride levels (Figure 48G), and NEFAs (Figure 48H).

In the blood parameters of glucose, insulin, HOMA-IR, and triglycerides, a significant decrease is observed in the HFD CPT1AM mice compared to the HFD Null mice (Figure 48 C-E, G). No significant differences were observed in total cholesterol and NEFAs levels (Figure 48F, H).

**Figure 48** Under thermoneutrality conditions, excreted more cholesterol and were resistant to hyperglycemia, insulin resistance, and hypertriglyceridemia caused by HFD.



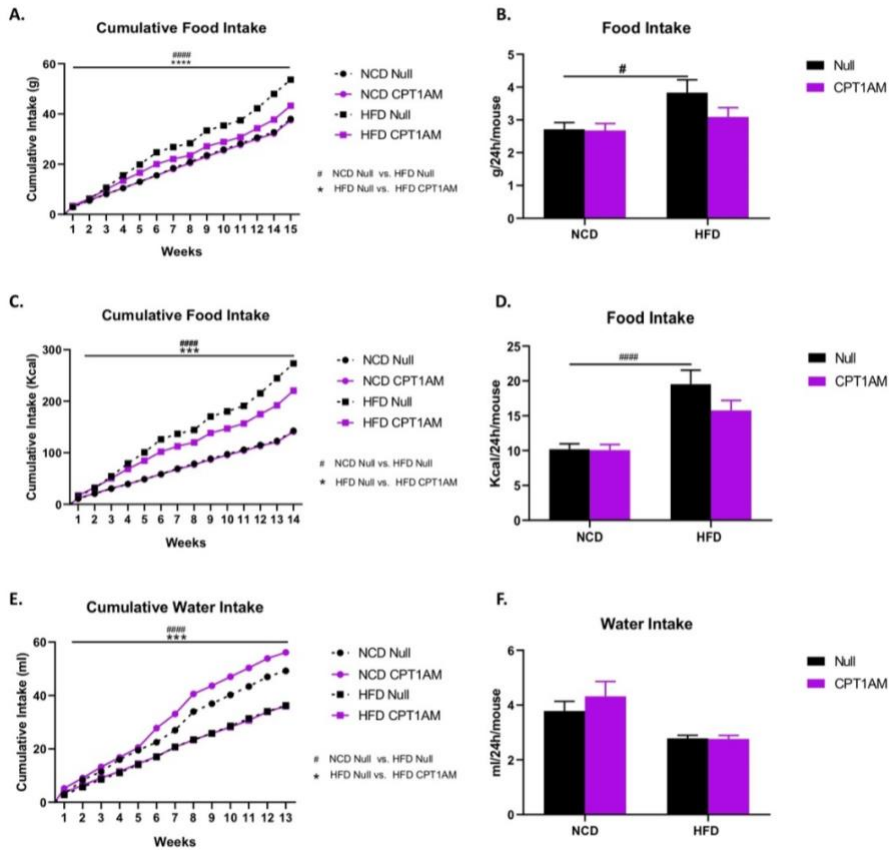
A) Weight of BAT, iWAT, gWAT and liver, normalized by the body weight of each mouse. B) Cholesterol excretion in feces. C) Glucose levels. D) Insulin levels. E) HOMA-IR. F) Total cholesterol levels. G) Triglyceride levels. H) NEFAs. Data are expressed as mean  $\pm$  SEM; n = 10.

During the induction of obesity by HFD and overexpression of CPT1AM, control of diet and water intake was performed, which was measured from the week after administration of viral vectors with CPT1AM (Figure 49A-F), as well as in the previous experiment. The cumulative food intake in grams of the HFD groups was found to be significantly higher than the NCD groups. (Figure 49A). But when quantifying the daily intake per mouse, the HFD CPT1AM group shows

no such increase (Figure 49B). The same happens for cumulative and daily caloric intake (Figure 49C-D).

When estimating the cumulative water intake, it is observed that the HFD mice consume less water than the NCD mice (Figure 49E), however, when estimating the daily water consumption per mouse, no significant differences were observed (Figure 49F).

**Figure 49 CPT1AM-expressing female mice under HFD and thermoneutrality conditions show a reduction in cumulative food intake.**



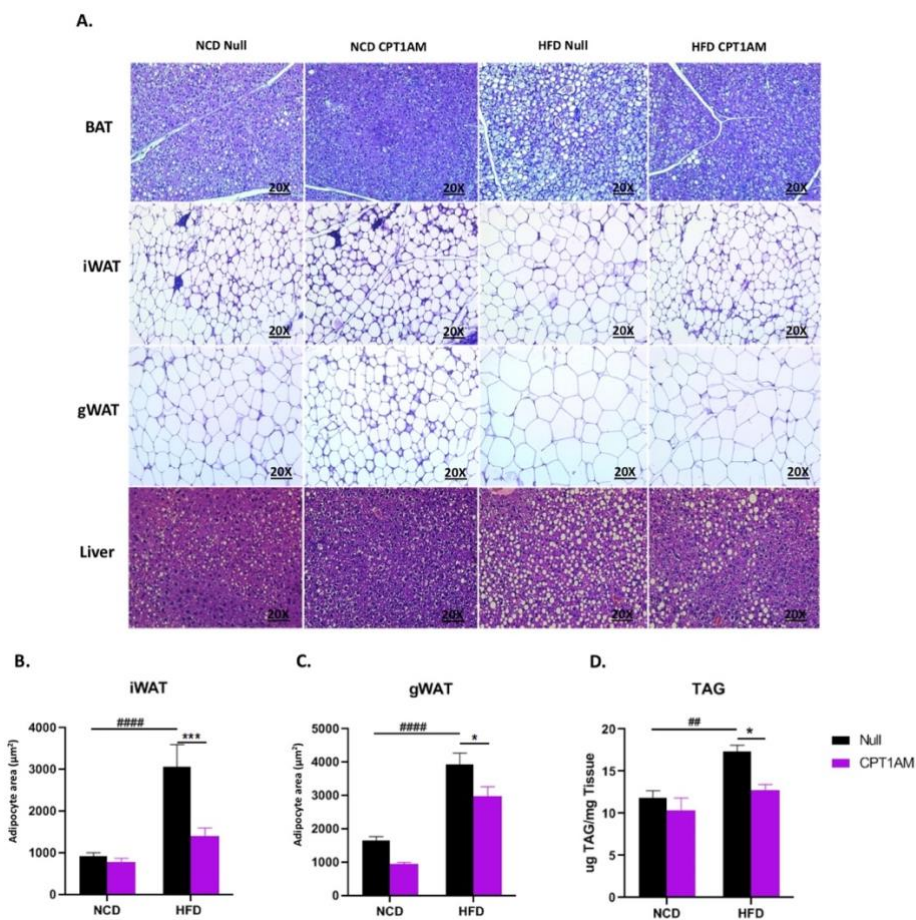
(A) Cumulative food intake. B) Daily food intake. C) Cumulative caloric intake. D) Daily caloric intake. E) Collection of accumulated water. F) Daily water intake. Data are expressed as mean  $\pm$  SEM; n = 10.

### **5.4.2 Mice treated with HFD under thermoneutrality conditions and with acute cold stimulation prevented hypertrophy in adipose tissue and hepatic steatosis**

Histological characterization of BAT, iWAT, gWAT and liver tissue was also performed (figure 50A). In addition, the area of adipocytes in iWAT and gWAT was quantified (figure 50B-C), and hepatic TAG content was measured (figure 50D). As in male mice, in the histological characterization of BAT, greater browning of the BAT that were punctured with CPT1AM by means of the viral vectors is visually appreciated, compared to the Null groups, both with NCD and HFD (figure 50A). When quantifying the size of the adipocytes, it was observed that the iWAT and gWAT of the mice that overexpress CPT1AM under HFD conditions present less hypertrophy than the HFD Null mice (figure 50A-C).

Regarding the content of hepatic TAG, significant differences are observed, since the livers of the HFD CPT1AM group present lower levels of TAG (figure 50D) and fewer lipid droplets than the livers of HFD Null mice (figure 50A), therefore, had less hepatic steatosis, caused by HFD.

**Figure 50** Under conditions of thermoneutrality with acute cold stimulation, were resistant to adipose tissue hypertrophy and hepatic steatosis.



A) Representative images of BAT, iWAT, gWAT and liver sections stained with H&E. 100 µm scale bar (20x magnification). B) Quantification of the size of adipocytes in iWAT. C) Quantification of the size of adipocytes in gWAT. D) Quantification of TAG content in the livers. Data are expressed as mean ± SEM; n = 10.

### 5.4.3 Overexpression of CPT1AM in BAT from HFD-treated mice under thermoneutrality conditions with acute cold stimulation increases fatty acid oxidation and affects metabolism in BAT

At the time of sacrifice, the fatty acid oxidation assay was performed in BAT, with labeled oleate, to measure CO<sub>2</sub> (Figure 51A) and soluble acid products (APS) released by the tissue (figure 51B). In both cases, a significant increase is observed in the tissues that were punctured with CPT1AM, demonstrating increased fatty acid oxidation (FAO) in the tissues of mice overexpressing CPT1AM (Figure 51A-B).

As in the experiment carried out in males, to complement the histological characterization of BAT and the metabolic phenotype of female mice, qRT-PCR and WB were performed to measure gene expression and protein levels in BAT (Figure 51C-G).

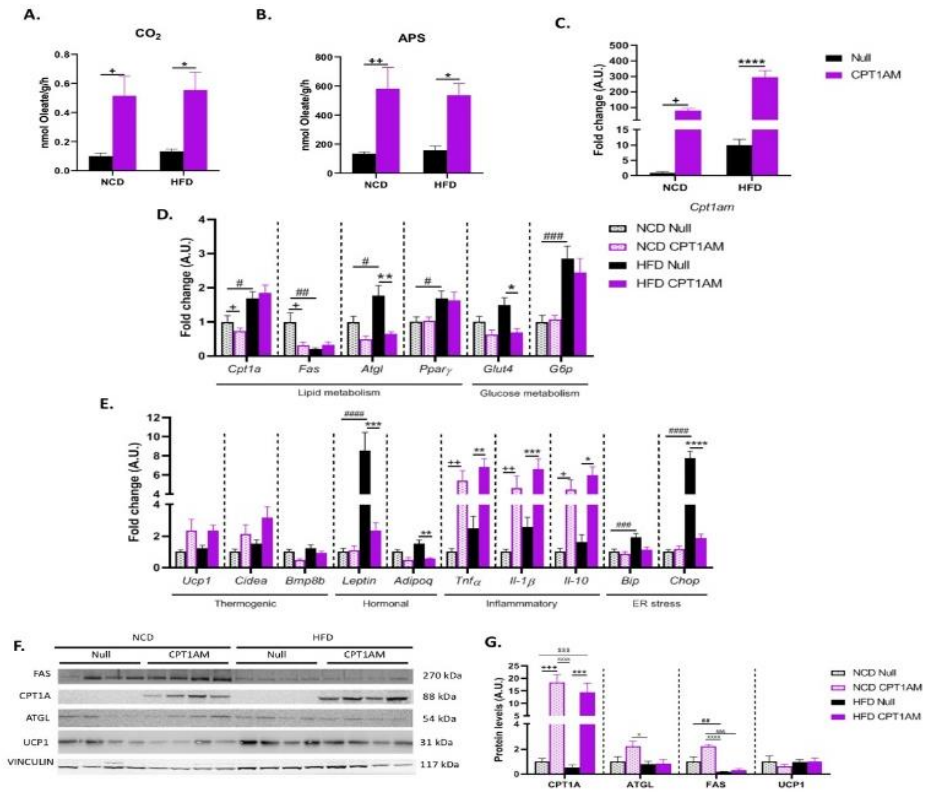
In the qRT-PCR carried out in BAT, *Cpt1am* was observed (Figure 51C), to verify the efficient overexpression, by means of the injection of viral vectors. Some lipid metabolism genes (*Cpt1a*, *Fas*, *Atgl*, *Pparγ*) and glucose metabolism genes (*Glut4*, *G6p*) were also studied (figure 51D), as well as thermogenic genes (*Ucp1*, *Cidea*, *Bmp8b*), hormones (*Leptin*, *Adipoq*), inflammatory (*Tnfα*, *Il1β*, *Il10*) and ER (*Bip*, *Chop*) (Figure 51E).

Significant increase of the *Cpt1am* gene was observed amplifying 100 to 300 times more in the mice that were treated with CPT1AM, corroborating the overexpression (Figure 51C). In addition, significant changes were seen in mice overexpressing CPT1AM under HFD conditions in the *Atgl* genes for lipid metabolism and *Glu4* for glucose metabolism (Figure 51D). Likewise, differences were seen in *Leptin* and *Adipoq*, of the mice that overexpress CPT1AM; being resistant to the hormonal increase caused by HFD. On the other hand, a

significant increase in inflammatory genes *Tnfa*, *Il1b*, and *Il10* was observed in mice overexpressing CPT1AM. Similarly, differences are observed in the *Bip* and *Chop* genes, being resistant to the increase in ER caused by HFD in mice that overexpress CPT1AM (Figure 51E).

In the quantification of protein levels by WB, CPT1A, ATGL, FAS and UCP1, normalized by the VINCULIN protein, were measured (Figure 51F-G). In which the increase in CPT1A protein is visually appreciated (Figure 51F-G), of the mice that were punctured with CPT1AM, presenting 15 to 20 times more protein compared to the Null groups (Figure 51G). In the ATGL, FAS and UCP1 proteins, no significant differences are observed, by means of the WB technique (Figure 51G).

**Figure 51** Under conditions of thermoneutrality with acute cold stimulation, oxidizes more fatty acids, alters lipid and glucose metabolism, inflammation, hormones and ER, being resistant to alterations caused by the HFD



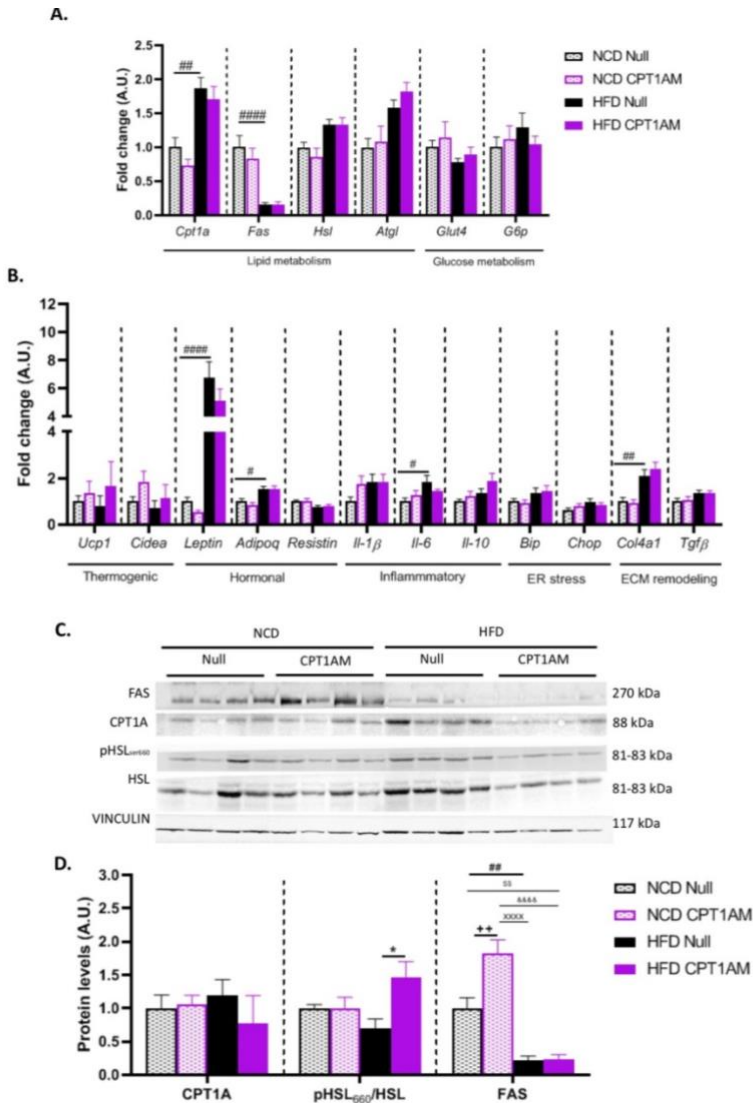
A)  $\text{CO}_2$  released by BAT by FAO assay. B) APS released by BAT by FAO assay. C) qRT-PCR analysis of the *Cpt1am* gene. D) qRT-PCR analysis of the *Cpt1a*, *Fas*, *Atgl*, *Ppar $\gamma$* , *Glut4* and *G6p* genes. E) qRT-PCR analysis of the genes *Ucp1*, *Cidea*, *Bmp8b*, *Leptin*, *Adipoq*, *Tnf $\alpha$* , *Il-1 $\beta$* , *Bip* and *Chop*. mRNA levels were normalized by *Rpl32* (C-E). F) Representative WB. G) Quantification of CPT1A, ATGL, FAS and UCP1, normalized by VINCULIN. Data are expressed as mean  $\pm$  SEM; n = 10.



### 5.4.4 Gene expression and protein levels in iWAT, gWAT and liver of HFD-treated mice under thermoneutrality conditions with acute cold stimulation

qRT-PCR was performed in iWAT to look at some lipid metabolism genes such as *Cpt1a*, *Fas*, *Hsl*, *Atgl* and glucose metabolism genes *Glut4* and *G6p* (Figure 52A), thermogenic genes *Ucp1* and *Cidea*, hormones such as *Leptin*, *Adipoq* and *Resistin*, were also seen, inflammatory *Il1-β*, *Il-6* and *Il-10*, from ER *Bip* and *Chop*, and from ECM, *Col4a1* and *Tgfβ* (Figure 52B). When quantifying gene expression, no significant changes were observed in lipid and glucose metabolism (Figure 52A), nor were changes in thermogenic genes, hormones, inflammation, ER, or ECM remodeling (Figure 52B). In the quantification of protein levels of lipid metabolism by WB of CPT1A, HSL and FAS proteins, no significant differences were observed (figure 52C-D).

**Figure 52 Gene expression and protein levels in iWAT, from mice treated with CPT1AM intraBAT, under conditions of thermoneutrality with acute cold stimulus.**



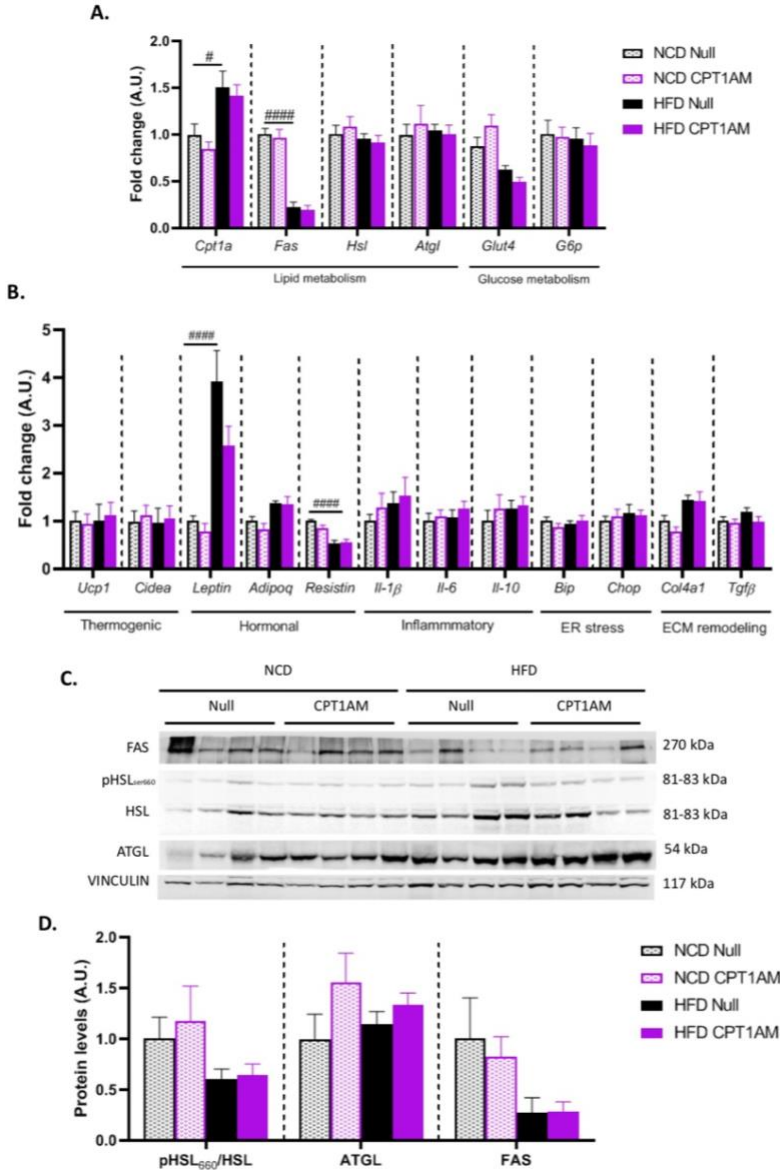
A) Analysis by qRT-PCR of *Cpt1a*, *Fas*, *Hsl*, *Atgl*, *Glut4* and *G6p* genes. B) Analysis by qRT-PCR of genes *Ucp1*, *Cidea*, *Leptin*, *Adipoq*, *Resistin*, *Il-1β*, *Il-6*, *Il-10*, *Bip*, *Chop*, *Col4a1* and *Tgfβ*. mRNA levels were normalized by *Rpl32* (A-B). C) Representative Western blot. D) Quantification of CPT1A, HSL and FAS, normalized by VINCLIN. Data are expressed as mean ± SEM; n = 10 mice. Data were analyzed by two-way repeated measures ANOVA test, followed by Tukey's post hoc test,

# $p < 0.05$ , ## $p < 0.01$ , #### $p < 0.0001$  NCD Null v/s HFD Null (A-B,D), \* $p < 0.05$  HFD Null v/s HFD CPT1AM (D), ++ $p < 0.01$  NCD Null v/s NCD CPT1AM, &&& $p < 0.0001$  NCD CPT1AM v/s HFD CPT1AM, XXXX $p < 0.0001$  NCD CPT1AM v/s HFD Null, \$\$\$ $p < 0.01$  NCD Null v/s HFD CPT1AM (D).

In gWAT, gene expression and WB were also quantified to observe protein levels (Figure 53A-D), in which lipid metabolism genes (*Cpt1a*, *Fas*, *Hsl*, *Atgl*) and of glucose metabolism (*Glut4*, *G6p*) (Figure 53A) were analyzed. Also, thermogenic genes (*Ucp1*, *Cidea*), hormones (*Leptin*, *Adipoq*, *Resistin*), inflammatory genes (*Il1- $\beta$* , *Il-6*, *Il-10*), ER (*Bip*, *Chop*) and ECM remodeling (*Col4a1*, *Tgf $\beta$* ). As in iWAT, no significant changes were seen in the genes studied (Figure 53A-B).

In the quantification of protein levels studying by WB (FAS, ATGL and HSL) no significant differences were observed (Figure 53C-D).

**Figure 53 Gene expression and protein levels in gWAT of mice treated with CPT1AM intraBAT, under conditions of thermoneutrality with acute cold stimulus.**

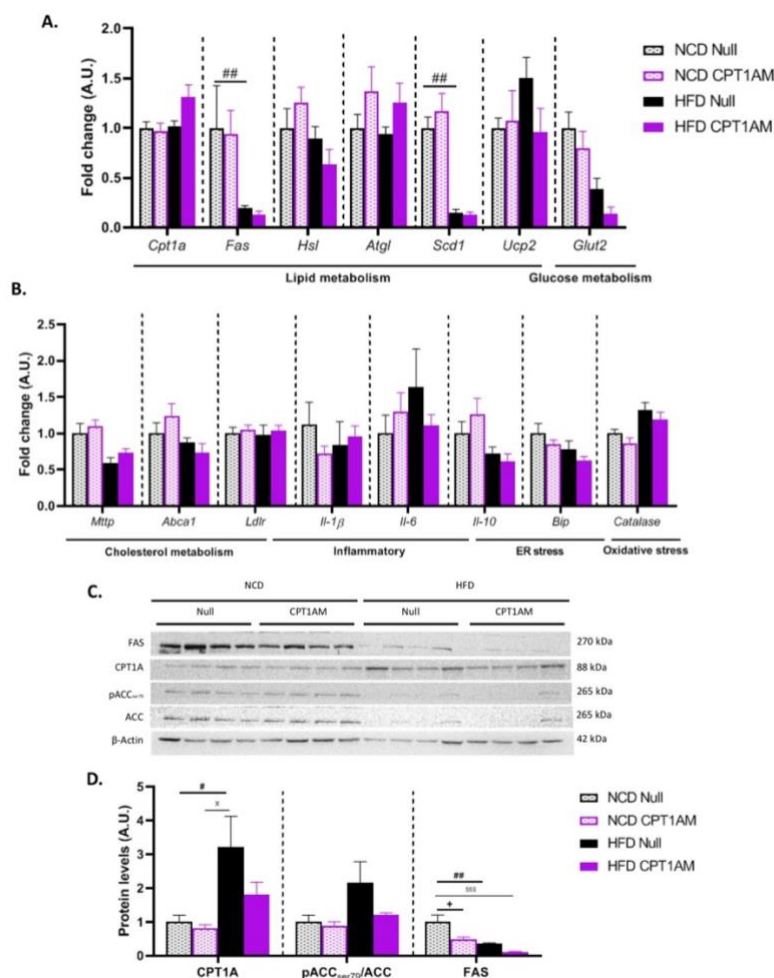


A) Analysis by qRT-PCR of *Cpt1a*, *Fas*, *Hsl*, *Atgl*, *Glut4* and *G6p* genes. B) Analysis by qRT-PCR of genes *Ucp1*, *Cidea*, *Leptin*, *Adipoq*, *Resistin*, *Il-1β*, *Il-6*, *Il-10*, *Bip*, *Chop*, *Col4a1* and *Tgfβ*. mRNA levels were normalized by *Rpl32* (A-B). C) Representative Western blot. D) Quantification of

*HSL, ATGL and FAS, normalized by VINCULIN. Data are expressed as mean  $\pm$  SEM; n = 10 mice. Data were analyzed by two-way repeated measures ANOVA test, followed by Tukey's post hoc test, #p<0.05, ####p <0.0001 NCD Null v/s HFD Null (A-B).*

Finally, in this experiment, gene expression was observed and protein levels were observed in the liver (Figure 54A-D), in which lipid metabolism genes (*Cpt1a, Fas, Hsl, Atgl, Scd1, Ucp2*) and of the glucose metabolism (*Glut2*) (Figure 54A). Cholesterol metabolism genes (*Mttp, Abca1, Ldlr*), inflammatory genes (*Il1- $\beta$ , Il-6, Il-10*), ER (*Bip*) and oxidative stress genes (*Catalase*) were also studied (Figure 49B). As in iWAT and gWAT, no significant changes in gene expression are observed (Figure 49A-B). In the quantification of protein levels of lipid metabolism (CPT1A, ACC and FAS), which were normalized by the  $\beta$ -ACTIN protein, no significant differences were observed (Figure 54C-D).

**Figure 54 Gene expression and protein levels in the liver of mice treated with CPT1AM intraBAT, under conditions of thermoneutrality with acute cold stimulation.**



A) Analysis by qRT-PCR of *Cpt1a*, *Fas*, *Hsl*, *Atgl*, *Scd1*, *Ucp2* and *Glut2* genes. B) Analysis by qRT-PCR of genes *Mtp*, *Abca1*, *Ldlr*, *Il-1β*, *Il-6*, *Il-10*, *Bip* and *Catalase* mRNA levels were normalized by *Tbp* (A-B). C) Representative Western blot. D) Quantification of CPT1A, ACC and FAS, normalized by β-ACTIN. Data are expressed as mean ± SEM; n = 10 mice. Data were analyzed by two-way repeated measures ANOVA test, followed by Tukey's post hoc test, #p < 0.05, ##p < 0.01 NCD Null v/s HFD Null (A,D), +p < 0.05 NCD Null v/s NCD CPT1AM, Xp < 0.05 NCD CPT1AM v/s HFD Null, \$\$\$p < 0.001 NCD Null v/s HFD CPT1AM (D).

### **5.5 Efficiency of obesity induction through HFD and gene therapy with *cpt1am***

In order to assess the degree of efficiency in the induction of obesity and therapy with CPT1AM, the repeated measures ANOVA test was performed correlating the variables under study (Table 7 and 8).

In the analysis, weight gain during the first 14 initial weeks of treatment between experiments 2 and 3 was considered as a dependent variable, to assess the impact of ambient temperature that causes a prior activation of BAT due to chronic cold (experiment 2) and under conditions of thermoneutrality without prior activation of BAT (experiment 3) (Table 7A-B).

On the other hand, we wanted to assess the impact of sexual dimorphism between experiments 3 and 4, to study the changes in the phenotype in males and females (Table 8A-B).

#### **5.5.1 Impact of chronic cold in the induction of obesity and treatment with CPT1AM in BAT**

When looking at Table 7A, in which the variables interact, significant differences can be seen in the induction of obesity, since HFD was more efficient in inducing obesity in thermoneutrality conditions, compared to the room temperature condition. HFD Null mice under room temperature conditions, although they gained weight, the gain was less compared to HFD Null mice under thermoneutrality conditions (Table 7A).

Regarding the efficiency of the treatment with CPT1AM, the same significance difference is observed in conditions of room temperature and thermoneutrality, since the HFD CPT1AM mice gain less weight than the HFD

Null mice, therefore, the treatment was equally efficient in both conditions (Table 7A).

Both CPT1AM treatment and diet have a significant impact on weight gain in mice. However, the induction of obesity by HFD depends on whether or not there is prior activation of BAT by chronic cold (Table 7B).

**Table 7 Obesity induction with HFD therapy was more efficient in mice under thermoneutrality conditions.**

A.

Post Hoc Comparisons - DIET		TRAT	Temp	95% CI for Mean Difference				P <sub>bonf</sub>
			Mean	Lower	Upper	SE	t	
NCD, Null, RoomTemp.	HFD, Null, RoomTemp.		-20,36	-38,85	-1,868	5,6	-3,64	0,018 *
	NCD, CPT1AM, RoomTemp.		-2,177	-20,67	16,315	5,6	-0,39	1
	HFD, CPT1AM, RoomTemp.		-2,157	-19,98	15,662	5,39	-0,4	1
	NCD, Null, Thermoneutrality		-1,228	-18,53	16,07	5,24	-0,24	1
	HFD, Null, Thermoneutrality		-38,84	-56,14	-21,55	5,24	-7,42	<.001 ***
	NCD, CPT1AM, Thermoneutrality		11,807	-5,491	29,104	5,24	2,255	0,801
	HFD, CPT1AM, Thermoneutrality		-22,6	-39,9	-5,307	5,24	-4,32	0,002 **
HFD, Null, RoomTemp.	NCD, CPT1AM, RoomTemp.		18,182	-0,31	36,674	5,6	3,249	0,059
	HFD, CPT1AM, RoomTemp.		18,203	0,383	36,022	5,39	3,375	0,041 *
	NCD, Null, Thermoneutrality		19,132	1,834	36,429	5,24	3,654	0,018 *
	HFD, Null, Thermoneutrality		-18,49	-35,78	-1,187	5,24	-3,53	0,026 *
	NCD, CPT1AM, Thermoneutrality		32,166	14,868	49,464	5,24	6,144	<.001 ***
	HFD, CPT1AM, Thermoneutrality		-2,245	-19,54	15,053	5,24	-0,43	1
NCD, CPT1AM, RoomTemp.	HFD, CPT1AM, RoomTemp.		0,02	-17,8	17,84	5,39	0,004	1
	NCD, Null, Thermoneutrality		0,95	-16,35	18,247	5,24	0,181	1
	HFD, Null, Thermoneutrality		-36,67	-53,97	-19,37	5,24	-7	<.001 ***
	NCD, CPT1AM, Thermoneutrality		13,984	-3,314	31,282	5,24	2,671	0,286
	HFD, CPT1AM, Thermoneutrality		-20,43	-37,72	-3,129	5,24	-3,9	0,008 **
	NCD, Null, Thermoneutrality		0,929	-15,65	17,506	5,02	0,185	1
HFD, CPT1AM, RoomTemp.	HFD, Null, Thermoneutrality		-36,69	-53,26	-20,11	5,02	-7,31	<.001 ***
	NCD, CPT1AM, Thermoneutrality		13,964	-2,613	30,54	5,02	2,783	0,213
	HFD, CPT1AM, Thermoneutrality		-20,45	-37,02	-3,871	5,02	-4,08	0,005 **
	HFD, Null, Thermoneutrality		-37,62	-53,63	-21,6	4,85	-7,76	<.001 ***
	NCD, CPT1AM, Thermoneutrality		13,034	-2,98	29,049	4,85	2,689	0,273
	HFD, CPT1AM, Thermoneutrality		-21,38	-37,39	-5,362	4,85	-4,41	0,002 **
HFD, Null, Thermoneutrality	NCD, CPT1AM, Thermoneutrality		50,651	34,636	66,665	4,85	10,45	<.001 ***
	HFD, CPT1AM, Thermoneutrality		16,24	0,226	32,255	4,85	3,351	0,044 *
NCD, CPT1AM, Thermoneutrality	HFD, CPT1AM, Thermoneutrality		-34,41	-50,43	-18,4	4,85	-7,1	<.001 ***

\* p < .05, \*\* p < .01, \*\*\* p < .001  
 Note. P-value and confidence intervals adjusted for comparing a family of 28 estimates (confidence intervals corrected using the bonferroni method).  
 Note. Results are averaged over the levels of: Semanas



B.

Between Subjects Effects					
Cases	Sum of Squares	df	Mean Square	F	p
DIET	104511,594	1	104511,594	79,44	<.001
TRAT	25137,697	1	25137,697	19,11	<.001
Temp	8393,379	1	8393,379	6,38	0,015
DIET $\square$ TRAT	6814,566	1	6814,566	5,18	0,027
DIET $\square$ Temp	32727,965	1	32727,965	24,88	<.001
TRAT $\square$ Temp	2150,412	1	2150,412	1,635	0,207
DIET $\square$ TRAT $\square$ Temp	3613,108	1	3613,108	2,746	0,104
Residuals	64461,113	49	1315,533		

*Note.* Type III Sum of Squares

*A) Table of Post Hoc Comparisons. B) ANOVA table of repeated measures. Analysis of weight gain data over 14 weeks, after obesity induction with HFD and CPT1AM treatment.*

### **5.5.2 Impact of sexual dimorphism on obesity induction and treatment with CPT1AM in BAT**

As in the previous analysis, in which the variables interacted, significant differences were observed in the induction of obesity, since HFD was more efficient in inducing obesity in male mice, but in females it was not possible to obtain a metabolic phenotype of efficient obesity. Although female HFD Null mice gained weight, the gain was less compared to male HFD Null mice (Table 8A). Regarding the efficiency of treatment with CPT1AM, it is observed that both HFD CPT1AM males and females gain less weight than HFD Null mice, but this difference is greater in male mice (Table 8A). Both sexual dimorphism and diet have a significant impact on weight gain in mice. Treatment with CPT1AM also has an important impact, but this can be seen when obesity induction has been efficient (Table 8B).

**Table 8 Female mice were more resistant to obesity induction by HFD than male mice.**

A.

Post Hoc Comparisons - DIET $\square$ TRAT $\square$ Sex		95% CI for Mean Difference			SE	t	P <sub>Scheffe</sub>
		Mean	Lower	Upper			
NCD, Null, Male	HFD, Null, Male	-37,62	-60,19	-15,05	6,92	-5,43	<.001 ***
	NCD, CPT1AM, Male	13,034	-9,536	35,605	6,92	1,883	0,826
	HFD, CPT1AM, Male	-21,38	-43,95	1,194	6,92	-3,09	0,237
	NCD, Null, Female	9,686	-11,73	31,098	6,57	1,475	0,947
	HFD, Null, Female	-3,688	-25,1	17,724	6,57	-0,56	1
	NCD, CPT1AM, Female	8,539	-12,87	29,951	6,57	1,3	0,973
HFD, Null, Male	HFD, CPT1AM, Female	5,98	-15,43	27,392	6,57	0,911	0,997
	NCD, CPT1AM, Male	50,651	28,08	73,221	6,92	7,316	<.001 ***
	HFD, CPT1AM, Male	16,24	-6,33	38,811	6,92	2,346	0,601
	NCD, Null, Female	47,303	25,89	68,715	6,57	7,202	<.001 ***
	HFD, Null, Female	33,928	12,516	55,341	6,57	5,166	0,002 **
	NCD, CPT1AM, Female	46,155	24,743	67,567	6,57	7,028	<.001 ***
NCD, CPT1AM, Male	HFD, CPT1AM, Female	43,597	22,184	65,009	6,57	6,638	<.001 ***
	HFD, CPT1AM, Male	-34,41	-56,98	-11,84	6,92	-4,97	0,003 **
	NCD, Null, Female	-3,348	-24,76	18,064	6,57	-0,51	1
	HFD, Null, Female	-16,72	-38,14	4,69	6,57	-2,55	0,493
	NCD, CPT1AM, Female	-4,496	-25,91	16,917	6,57	-0,69	1
	HFD, CPT1AM, Female	-7,054	-28,47	14,358	6,57	-1,07	0,991
HFD, CPT1AM, Male	NCD, Null, Female	31,062	9,65	52,475	6,57	4,73	0,006 **
	HFD, Null, Female	17,688	-3,724	39,1	6,57	2,693	0,415
	NCD, CPT1AM, Female	29,915	8,503	51,327	6,57	4,555	0,009 **
	HFD, CPT1AM, Female	27,356	5,944	48,769	6,57	4,165	0,026 *
NCD, Null, Female	HFD, Null, Female	-13,37	-33,56	6,813	6,19	-2,16	0,699
	NCD, CPT1AM, Female	-1,148	-21,34	19,04	6,19	-0,19	1
	HFD, CPT1AM, Female	-3,706	-23,89	16,482	6,19	-0,6	1
HFD, Null, Female	NCD, CPT1AM, Female	12,227	-7,961	32,414	6,19	1,975	0,788
	HFD, CPT1AM, Female	9,668	-10,52	29,856	6,19	1,561	0,928
NCD, CPT1AM, Female	HFD, CPT1AM, Female	-2,559	-22,75	17,629	6,19	-0,41	1

\*p < .05, \*\*p < .01, \*\*\*p < .001  
 Note. P-value and confidence intervals adjusted for comparing a family of 28 estimates (confidence intervals corrected using the bonferroni method).  
 Note. Results are averaged over the levels of: Semanas

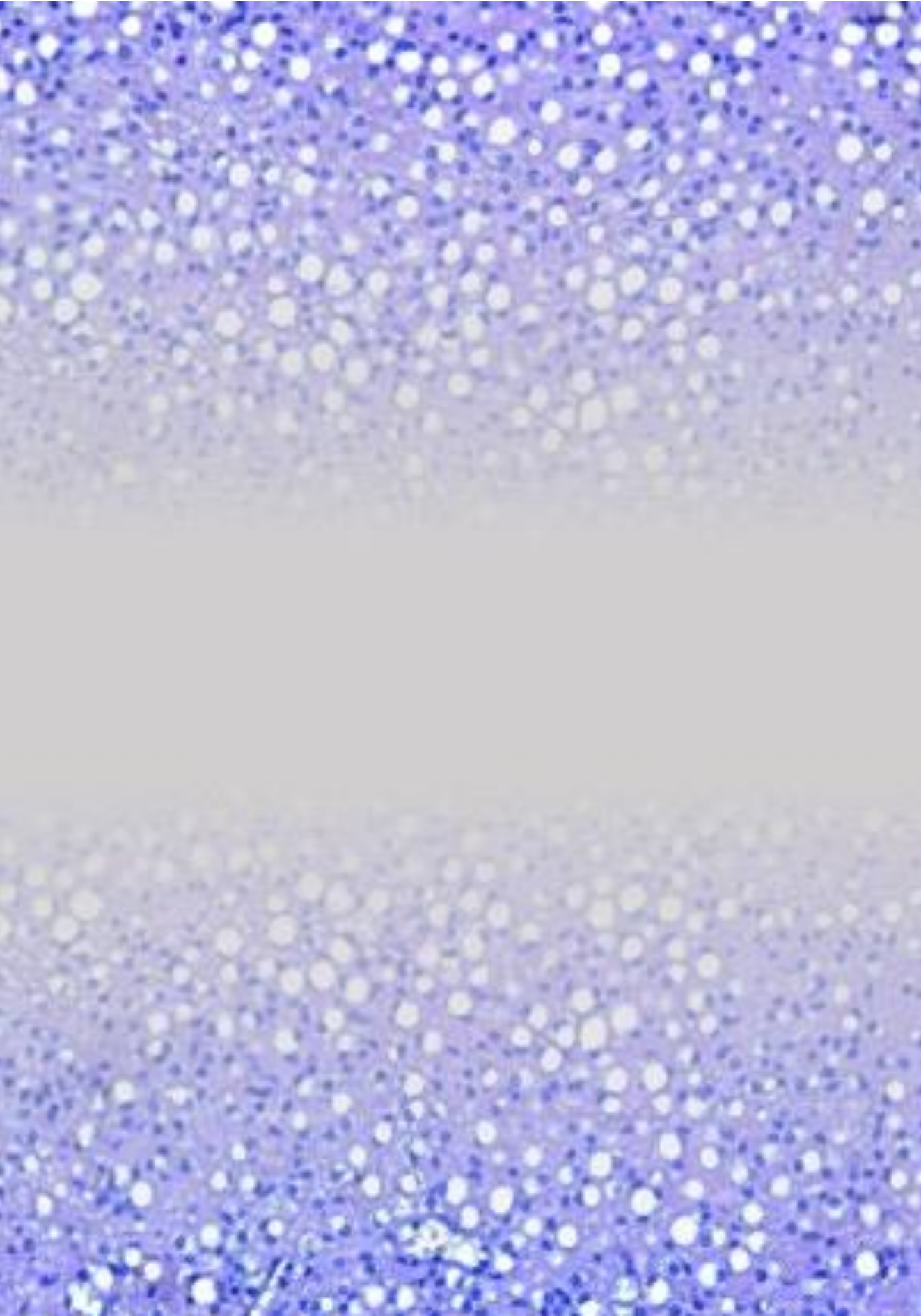
B.

Between Subjects Effects					
Cases	Sum of Squares	df	Mean Square	F	p
DIET	120353,225	1	120353,225	44,84	<.001
TRAT	22220,73	1	22220,73	8,279	0,005
Sex	68739,212	1	68739,212	25,61	<.001
DIET $\square$ TRAT	3058,307	1	3058,307	1,139	0,29
DIET $\square$ Sex	48946,939	1	48946,939	18,24	<.001
TRAT $\square$ Sex	6700,06	1	6700,06	2,496	0,119
DIET $\square$ TRAT $\square$ Sex	900,813	1	900,813	0,336	0,564
Residuals	171775,923	64	2683,999		

Note. Type III Sum of Squares

A) Table of Post Hoc Comparisons. B) ANOVA table of repeated measures. Analysis of weight gain data over 14 weeks, after obesity induction with HFD and CPT1AM treatment.

# **Discussion**



## **6 DISCUSSION**

In this doctoral thesis, CPT1AM has been overexpressed in BAT from mice treated with HFD, to prevent and/or treat obesity and diabetes, the results showed that the expression of CPT1AM in BAT increased lipolysis and mitochondrial through FAO and thermogenesis in the BAT. In addition, the increase of FAO in BAT prevented the increase in blood triglyceride, cholesterol and insulin, and the expression of markers of obesity and inflammation in tissues. When part of the BAT was incubated with oleate to simulate obesity in adipocytes, an increase in FAO was observed, indicating that FAO is critical in supplying fuel for BAT-generated thermogenesis, which may be a good strategy to increase energy expenditure through thermogenesis and thus avoid obesity and its associated diseases resulting from HFD.

### **6.1 Overexpression of CPT1AM in obese and hypoglycemic mice under room temperature conditions failed to reverse HFD-induced obesity derangements.**

In a first pilot experiment, which aimed to reverse HFD-induced obesity through overexpression of CPT1AM in BAT, we first questioned whether *in vivo* overexpression of CPT1AM in the BAT of HFD-fed mice would have an effect on their phenotype.

Obesity was induced with HFD in healthy mice, which were on a diet for 12 weeks, until reaching the obese metabolic phenotype reflected in weight (Figure 17C) and glucose levels (Figure 17D). Subsequently, the overexpression of CPT1AM in BAT was carried out, which was effective, since an increase of *Cpt1am* mRNA in BAT was observed, of 600 and 150 times in the NCD and HFD groups, respectively (Figure 17A). In addition, CPT1A protein levels measured in

BAT in HFD mice showed a 15-fold increase. Despite this, no significant differences were observed in the phenotype of mice injected with CPT1AM viral vectors in terms of body weight (Figure 17C) and glucose levels (Figure 17D), thus, reversal of the phenotype was not achieved. Thus, diet had a greater impact on the phenotype than the same treatment with CPT1AM.

On the one hand, it is known that the 60% fat HFD of the DIO series used in this study generates significant differences in body weight in C57BL/6J mice at 12 weeks [152], therefore, here we are already talking about obesity which reflects changes in glucose metabolism, evidenced in the monthly monitoring of glucose levels (Figure 17D) and possibly changes at the tissue and cellular level.

On the other hand, considering that there is an increase in the thermogenic activity of BAT in these mice that were in room temperature conditions (chronic cold) and with evidence of overexpression of CPT1AM in BAT, it would have been possible to increase only % the total energy expenditure, the energy requirement of a person is related to their energy expenditure and is defined as the energy consumed by an organism, it is represented by the basal metabolic rate (BMR), physical activity (PA) and diet-induced thermogenesis (DIT). The BMR is the minimum amount of energy that an organism requires to be alive and represents 60-70% of the total energy expenditure (TGE), in most sedentary adults. The AF represents between 25-75% of the TGE and the TID represents about 10% of the TGE [153].

Therefore, reversing obesity from the thermogenic dynamics of BAT is more difficult when there is already metabolic damage associated with tissue and cellular dysfunction, which causes HFD. In this experiment, it should be considered that when these mice were operated on, they already presented this tissue dysfunction not only at the organism level, but also at the BAT level.



Finally, in this experiment there were technical limitations of air conditioning in the animal facility. Due to the length of the experimental design, the mice spent 3 months to induce the diet and 3 months to see the effects. During the last 3 months, these mice were in the animal facility in the summer season in July and August, where there was ambient humidity of up to 85%, for this reason the diet had to be changed up to 3 times a week, due to that the same humidity formed fungi in the diet, on a recurring basis. In this way, the increase in environmental humidity affected the adequate intake of the diet in mice, which is evidenced in the variation of weight from week to week.

Furthermore, the temperature requirements for mice are 20 to 25 °C and the ambient relative humidity between 40 and 70%. The environmental conditions in which the animals are raised and experimented decisively influence the responses to the different treatments. If standardized responses are required, the conditions in which the animals are kept must be fixed [154].

### **6.2 Overexpression of CPT1AM prevents obesity and diet-induced hyperglycemia.**

The high incidence of obesity and related diseases have made it a priority to study the mechanisms for controlling caloric intake and expenditure. In recent years, multiple studies have tried to delve into the molecular mechanisms that, in the hypothalamus, control the expression of neuropeptides and neuromodulators responsible for regulating food intake [155]. As a result, the key role played by fatty acid metabolism in these processes has been demonstrated. The enzyme CPT1 is the main regulator of fatty acid oxidation. First, a permanently active isoform of the enzyme (CPT1AM) has been overexpressed in the BAT ventromedial nucleus of the hypothalamus. The

results obtained show that the overexpression of CPT1AM in the hypothalamus initially causes hyperphagia and, in a later state, insulin resistance, glucose intolerance and hyperglycemia [155].

On the other hand, a previous study demonstrates that long-term activation of hepatic fatty acids (FAO) mediated by AAV may be a successful strategy for reversing already established obesity with associated hyperglycemia. This through the use of CPT1AM. As a result, enhanced hepatic FAO through CPT1AM-mediated gene therapy was shown to reduce diet-induced weight gain and hepatic steatosis and improve hepatic insulin signaling in obese mice [136].

Also, in a study, transplants with CPT1AM were performed in mice, as a result an improvement in glucose tolerance and insulin was shown. The transplant was able to prevent hepatic steatosis and restore the expression of genes involved in glucose and cholesterol metabolism. In addition, mice transplanted with CPT1AM showed a reduction in HFD-induced hyperglycemia and glucose intolerance [156].

In this thesis work, significant changes were seen in the metabolic phenotype and overexpression in mouse tissues. HFD-induced obesity was intended to be prevented by overexpression of CPT1AM in BAT. HFD CPT1AM mice maintained their weight almost in the normal range thus they were resistant to HFD and HFD-induced obesity. Null mice became obese from the fourth week after initiation of the diet (Figure 20A). Differences in weight gain were also observed from the sixth week after the start of treatment, between the HFD Null and HFD CPT1AM groups (Figure 20B).

On the other hand, mice treated with CPT1AM and HFD under room temperature conditions are resistant to diet-induced obesity, overexpression of



CPT1AM in BAT from mice treated with HFD under room temperature conditions prevented hypertrophy in adipose tissue and hepatic steatosis. During HFD induction of obesity, control of diet and water intake was measured from one week after administration of AVV with CPT1AM. Cumulative food intake in grams was monitored, NCD Null mice have a higher intake compared to HFD Null and NCD mice. CPT1AM mice have a higher intake compared to NCD Null mice. When quantifying by caloric intake, in the cumulative caloric intake, a higher caloric intake of the HFD mice is evidenced.

When quantifying the daily caloric intake per mouse, no significant differences are shown. When it comes to quantifying water intake, significant differences are only observed in the NCD CPT1AM group, since it has a higher water consumption, in accumulated form and daily intake compared to the NCD and HFD Null groups. Furthermore, overexpression of CPT1AM in BAT from HFD-treated mice under room temperature conditions affects tissue metabolism. As in the experiment carried out under room temperature conditions, during the induction of obesity by HFD and overexpression of CPT1AM under thermoneutrality conditions, an estimate was made on the control of diet and water intake, which was measured from the following week administration of viral vectors with CPT1AM. Cumulative food intake in grams was monitored, in which HFD CPT1AM mice had lower food intake than HFD Null mice, reducing polyphagia caused by HFD. When quantifying the daily intake per mouse, no significant differences were shown. Overexpression of CPT1AM in BAT from HFD-treated mice under the thermoneutrality conditions with acute cold stimulation also affects tissue metabolism.

Compared with the two environments, the impact of chronic cold in the induction of obesity and treatment with CPT1AM in BAT, when observing (Table

7A), in which the variables interact, differences in the induction of obesity are appreciated, since the HFD was more efficient in inducing obesity under thermoneutrality conditions, compared to room temperature. HFD Null mice under room temperature conditions gained weight, the gain was less compared to HFD Null mice under thermoneutrality conditions (Table 7A). Regarding the efficiency of the treatment with CPT1AM, in the same significance the difference is observed in conditions of room temperature and thermoneutrality, since the HFD CPT1AM mice gain less weight than the HFD Null mice, therefore, the treatment was equally efficient in both conditions (Table 7A). Both CPT1AM treatment and diet have a significant impact on weight gain in mice however, obesity induction by HFD is dependent on whether or not there is prior BAT activation by chronic cold (Table 7B).

On the other hand, HFD CPT1AM mice maintained their weight almost in the normal range, thus they were resistant to HFD-induced obesity. Null mice became obese from the fourth week after initiation of the diet (Figure 20A). Differences in weight gain were also observed from the sixth week after the start of treatment, between the HFD Null and HFD CPT1AM groups (Figure 20B). In the measurement of glucose levels, a significant increase was observed in HFD Null mice and HFD mice. CPT1AM maintained glucose levels similar to NCD Null mice. In addition to a significant increase in the size of iWAT, gWAT and livers was observed in the HFD Null group, but a significant decrease in iWAT was only observed in the HFD CPT1AM mice with respect to HFD Null.

Also, in iWAT and gWAT from HFD Null mice, an increase in hypertrophy was observed per adipocyte area, compared to NCD Null mice and CPT1AM mice. The HFD CPT1AM group presented adipocytes of similar size to the groups with NCD. Regarding hepatic steatosis, no significant differences were observed

in the TAG measurement, however, it was observed in the histological representation of the liver that the HFD CPT1AM group presented fewer lipid droplets than the HFD Null group.

Differences in weight gain were also observed from 6 weeks post-treatment between HFD Null and HFD CPT1AM groups. Regarding interscapular temperature, no increase in interscapular temperature, caused by HFD, was observed. Glucose levels at 4 and 8 weeks were also monitored, but there were no significant results. Changes were seen in HFD CPT1AM mice, as they had elevated glucose levels as a result.

In the prevention experiment carried out under chronic cold conditions, significant results were not reflected in many of the parameters studied in the metabolic phenotype and gene expression, however, there was a statistical trend, which shows a reduction in the effects acquired by the HFD. This is the case of blood insulin levels (Figure 23A). Here, no significant differences are evident, but there is a clear statistical trend, which might have been demonstrated with a larger number in each group (greater than eight mice). On the other hand, there is more variability in the HFD Null group, because the animals had fasted for at least twenty hours at the time of sacrifice and blood samples were obtained, therefore, the insulin levels of the HFD Null group had dropped considerably at the twenty hours fast. Considering that the researcher cannot know for sure how many hours before the fast, the mouse had stopped eating. That is why there is also this variability in the levels of the control group.

Thus, it was necessary to carry out a subsequent study, under thermoneutrality conditions to avoid prior activation of BAT, with a larger number of samples per group. For blood measurements, it was considered to

subject them to for only two hours to normalize intake and have at least a known range, to observe the parameters under diet conditions.

### **6.2.1 Temperature influences the efficiency of dietary obesity induction and the efficiency of CPT1AM gene therapy.**

Animals keep their body temperature constant in the face of environmental variations by producing heat, a phenomenon called thermogenesis. In this they differ from poikilothermic animals, whose body temperature varies according to the outside temperature. An individual's energy expenditure has several components. Within each component there is a part that is mandatory and another that is variable and adjustable by various hormonal effectors. Temperature and protein levels are higher in the liver of CPT1AM mice, indicating increased energy dissipation [155].

Observing Table 7A, in which the variables interact, differences in the induction of obesity can be seen, since the HFD was more efficient in inducing obesity in thermoneutrality conditions, compared to the room temperature condition. Thermoneutrality they became more obese with the diet, but it seems that the CPT1AM therapy took longer to take effect. The same had significant changes avoiding obesity and hyperglycemia. Regarding the efficiency of CPT1AM treatment, the same significant difference is observed in room temperature and thermoneutrality conditions, since HFD CPT1AM mice gain less weight than HFD null mice, therefore, the treatment was equally effective in both. conditions (Table 7A). Both CPT1AM treatment and diet have a significant impact on weight gain in mice. However, the induction of obesity by HFD is dependent on whether or not there is prior activation of BAT by chronic cold (Table 7B).

### **6.2.2 Sexual dimorphism impacts the efficiency of obesity induction through diet and the efficiency of gene therapy with CPT1AM.**

Sexual dimorphism manifests itself in different ways. First, the sex roles of males and females may place each in a different relationship to the environment, causing different selection and response. Thus, since females produce numerous gametes, the difference in question is associated with body size; hence the larger size observed in a high number of species. Studies have been carried out [157] about the influence of sex on alterations in mitochondrial function and WAT biogenesis, both in a control situation and in response to a kissogenic lipid-rich diet. Likewise, the relationship between mitochondrial function and the development of insulin resistance during the obese state and the role of sex hormones in the development of sex differences were investigated.

From the results obtained [157], it was shown that mitochondrial function and WAT biogenesis depend on sex, deposition and food ingested, and that sexual dimorphism manifests at early ages. The female rats presented a retroperitoneal deposit with a more abundant but less differentiated mitochondrial population than that of the males. All this translates into a better profile of insulin sensitivity in this sex, both at a systemic level and at a tissue level, since females present a more active signaling pathway towards insulin than males. Ovarian hormones are thought to be partly responsible for this sexual dimorphism, with the gonadal depot being more sensitive to estrogen regulation, thereby binding estrogen to a greater degree of mitochondrial differentiation and adiponectin expression.

Furthermore, studies carried out [157] have revealed the existence of a sexual dimorphism both at the level of morphology and mitochondrial functionality. Results obtained in skeletal muscle [158], liver [159], brown adipose tissue [159], heart [158] and brain [160] indicate that female rats have a more differentiated mitochondrial population with greater oxidative capacity. Moreover, specifically in the TAM, the existence of larger mitochondria and with a density of cristae higher than that of males has been corroborated [161]. However, there is hardly any information on the possible sexual dimorphism in BAD and, where appropriate, on the factors responsible for said dimorphism.

On the other hand, to better understand why mice lacking *Cpt1a* reduced body weight gain, a study [162] measured food intake in mice. Interestingly, the mice showed a sexual dimorphism in caloric intake. While the male reduced food intake, no changes were observed. This result measured by weekly food intake agrees with those measured by the TSE system, confirming and reinforcing the difference between male and female mice.

Most food intake studies are conducted on male mice, and little is known about caloric intake in female mice. Despite this, it is quite logical to assume a relationship based on sex, differences in food consumption, and dietary intake. Males and females have different patterns of metabolic regulation, including food control, which contributes to sexual differences in metabolic development. Sex-based differences in mammalian feeding behavior have been attributed exclusively to the effects of gonadal hormones, especially estrogens and androgens, which regulate food intake and energy metabolism by acting on the brain and various peripheral tissues.

In this thesis, females have a harder time inducing obesity through diet than males, but CPT1AM therapy appears to be more effective. In the

experiment carried out in male mice, significant changes were observed in the metabolic phenotype and overexpression in mouse tissues, for which the experimental design was replicated in female mice, there is an impact of sexual dimorphism in the induction of obesity and treatment with CPT1AM in BAT. As in the analysis in which the variables interacted, differences were observed in the induction of obesity, since the HFD was more efficient in inducing obesity in male mice, but in females it was not possible to obtain a metabolic index of the phenotype of obesity. efficient obesity. Although female HFD Null mice gained weight, the gain was less compared to male HFD Null mice (Table 8A). Regarding the efficiency of CPT1AM treatment, it is observed that both HFD CPT1AM males and females gain less weight than HFD Null mice, but the difference is greater in male mice (Table 8A).

### **6.3 Overexpression of CPT1AM modifies food and water intake.**

Although studies suggest that the amount of food water that mice consume is modulated by environmental variables such as the number of responses to obtain the food or by characteristics of the food such as taste or caloric content, there are other variables that can modify the amount of food. food consumed [163]. In addition, the interval between meals and access to food, as potential integrators of some of the results in eating behavior, open the possibility of generating new lines of basic research. These lines of research, in addition to integrating findings from nominally different areas, for example motivation theory and behavior analysis, will focus on creating an experimental animal model that helps explain, predict and perhaps prevent some of the problems of food in humans. In this sense, the need for new research on dietary intake and its associated variables is suggested.

Some examples of cases of eating behavior in humans that can be included in the animal model are obesity and diabetes. In this thesis, when quantifying water intake, significant differences were only observed in the NCD CPT1AM group, since it has a higher water consumption, in accumulated and daily intake compared to the NCD and HFD Null groups. When estimating the cumulative water intake, it is observed that the HFD mice consume less water than the NCD mice (Figure 49E), however, when the daily water consumption per mouse is estimated, there are no significant differences.

Similar to the experiments performed at room temperature, during HFD induction of obesity and CPT1AM overexpression, an estimation was made on dietary control and water intake, which was measured from the week after the delivery of viral vectors with CPT1AM. Cumulative food intake in grams was monitored. HFD CPT1AM mice had lower food intake compared to HFD Null mice. When quantifying the daily intake per mouse, no significant differences are shown. Quantifying caloric intake (cumulative and daily intake), there is evidence of higher caloric intake in HFD mice compared to NCD mice (Figure 49C-D). When quantifying daily and cumulative water intake, HFD mice consume less water than NCD mice.

In order to have more accurate and concrete data, it would have been necessary to subject the animals to metabolic cages, so that it would have been possible to verify exactly what they ingested in terms of food and water. In addition, it would have been possible to quantify the energy expenditure and compare the total energy expenditure between the groups, in this way an increase in the adaptive thermogenesis of BAT could have been associated with the total energy expenditure, finally triggering an increase in it.



In this way, clear data would also have been obtained on caloric intake and thus have obtained concrete conclusions on the changes in intake caused by CPT1AM.

In this study, the metabolic cages were a limitation of the study, because the mice were inside the climatic chamber during all the time at 30°C in thermoneutrality and at 4°C when the acute cold stimulus was performed. The ideal would have been to subject the animals to the metabolic cage under these temperature conditions, in order to observe changes associated with ambient temperature in energy expenditure.

#### **6.4 Overexpression enhances hepatic steatosis and adipose tissue hypertrophy.**

The increase in adipose tissue has been related to an increased production of proinflammatory cytokines that, together with fatty acids, seem to be responsible for the development of insulin resistance, hepatic steatosis, and adipose tissue hypertrophy. Thus, the greater or lesser expansibility or capacity of adipose tissue to store lipids also seems to play an important role in the development of hepatic steatosis, since exceeding this capacity, variable in each case, would be at the origin of lipid leakage to other tissues where they could interfere with the insulin signal. That is why in this thesis several molecular mechanisms related to the development of hepatic steatosis and its relationship with the extensibility of adipose tissue and obesity are reviewed.

Hepatic steatosis has been shown to improve with the use of CPT1AM. Transplantation of CPT1AM-expressing adipocytes reduces hepatic steatosis, liver TG content in HFD-fed mice, and hypertrophy in iWAT of HFD-fed mice

[156]. Taken together, these results point towards a restoration of iWAT functionality, including reduction of hypertrophy.

Another study carried out also showed that the overexpression of CPT1AM improved hepatic FAO and reduced hepatic steatosis. [136]. Studies that have increased short-term CPT1A activity in the liver have shown a decrease in hepatic triglyceride content [164]. Furthermore, a long-term increase in CPT1A and an insensitive CPT1AM isoform [158] has been shown to prevent steatosis and the development of obesity in mice fed a HFD [136].

In this thesis, the histological characterization of BAT, iWAT, gWAT and liver tissue was performed (Figures 25, 36, 50). In addition, the area of adipocytes in iWAT and gWAT was quantified, and hepatic TAG content was measured. In the histological characterization of the BAT, the browning of the BAT that were punctured with CPT1AM by means of the viral vectors, null groups are observed, both with NCD and with HFD (Figures 25, 36, 50A). In iWAT and gWAT of HFD Null mice, an increase in hypertrophy due to increased adipocyte size is observed, with respect to the NCD Null and HFD CPT1AM groups. On the other hand, in the HFD CPT1AM group adipocytes were observed in iWAT and gWAT, similar in size to the NCD groups (Figures 24, 35, 49A-C). HFD-induced hepatic steatosis was reduced in mice expressing CPT1AM both at the histological level and TAG content (Figures 35, 49A, D).

### **6.5 CPT1AM overexpression modifies tissue metabolism in BAT, iWAT, gWAT, and Liver.**

In recent years, BAT has become a key player in the control of energy metabolism as an active endocrine organ. Obesity-associated WAT fibrosis, inflammation, oxidative damage, apoptosis, and mitochondrial dysfunction

contribute to dysregulation of WAT metabolism and the development of metabolic diseases such as insulin resistance and type 2 diabetes [165]. CPT1A regulates the rate-limiting step in mitochondrial oxidation of FA and thus plays a central role in lipid metabolism [160]. Furthermore, CPT1AM expression in the liver increases hepatic autophagy and modulates cholesterol metabolism in HFD-fed mice. [136].

In this study, gene expression was also observed in the liver in which the lipid metabolism genes (Cpt1a, Fas, HSL, Atgl, Scd1, Ucp2) and glucose metabolism (Glut2, G6p) were analyzed. Cholesterol metabolism genes (Mttp, Abca1, Ldlr), inflammatory genes (Il1 $\beta$ , Il6, Il10), Emergencies (beep, itch) and oxidative stress genes (Catalase) were also studied. Of the genes studied, only significant differences were observed in ER, since mice that overexpressed CPT1AM decreased reticulum stress caused by HFD. In the quantification of lipid levels of metabolic proteins (FAS, CPT1A, PLIN5) no differences observed.

Furthermore, overexpression of CPT1AM in BAT from HFD-treated mice under thermoneutrality conditions alters tissue metabolism. As in the experiment performed under room temperature conditions, to complement the histological characterization of tissues and metabolic phenotype analysis, qRT-PCR and WB were performed to measure gene expression and protein levels, in BAT, iWAT, gWAT and liver. On the day of sacrifice, iWAT, gWAT, liver and BAT were dissected and tissue weight was measured. As expected HFD increased iWAT, gWAT and liver weight of HFD Null group compared to NCD Null. However, iWAT weight of the HFD CPT1AM group decreased compared to HFD Null with no differences observed in BAT weight.

### **6.6 Overexpression of CPT1AM increases browning in BAT and reduces immune cell infiltration and apoptosis in adipose tissue.**

Current cases of obesity generate a constant need to develop new therapeutic strategies to restore energy balance. For this reason, the concept of activating brown adipose tissue to increase energy expenditure has been revived. Research in recent years has significantly increased understanding of the mechanisms involved in BAT activation and WAT dimming. They also allowed the identification of critical molecules and critical steps of both processes and thus many new therapeutic targets [166]. Various non-pharmacological approaches, as well as chemical compounds targeting WAT darkening induction and BAT activation, have been tested *in vitro* and in animal models of genetically determined and/or diet-induced obesity. The therapeutic potential of some of these strategies has also been tested in humans.

CPT is responsible for fatty acid oxidation in brown adipocytes that plays a key role in mitochondrial oxidative phosphorylation. Therefore, the anti-obesity properties of CPT1 are based on both the ability to inhibit lipogenesis and the induction of thermogenesis and darkening of adipose tissue.

Infiltration of immune cells such as macrophages and T cells was increased in BAT from obese mice, although to a lesser extent than in eWAT and iWAT. [152] Looking at tissue browning, increased staining is observed, mainly in BAT from CPT1AM-treated mice, under NCD and HFD conditions. By quantifying the darkening with the stained area, significant differences in BAT are observed. No such differences are observed in iWAT and gWAT (Figure 38A-B).

Regarding immune cell infiltration and apoptosis, a reduction in immune cell infiltration (Figures 39 and 40) and apoptosis (Figure 41) was observed in the

WAT of mice that overexpressed CPT1AM compared to Null and were resistant to tissue changes caused by HFD.

### **6.7 CPT1AM overexpression increases steatorrhea due to cholesterol excretion from HFD.**

Steatorrhea is associated with malabsorption syndrome and is defined by the loss of fat by storage, although when there is pancreatic insufficiency the absorption of all nutrients is compromised; however, carbohydrates and proteins can be absorbed in part by other enzyme systems, such as salivary amylase and stomach proteases, while lipases are only produced in the pancreas. Malabsorption can be parietal or luminal. In the first, patients have a disorder of the intestinal wall, either in the wall itself or in the lymphatic vessels that constitute the drainage system of the intestine. In the second, the intestine is healthy, but the enzymes of the pancreas are missing, so it is really a problem of luminal maldigestion.

In both cases there is steatorrhea, which is clinically manifested by the presence of oily stools and can be confirmed with a fairly simple test, which is the observation of neutral fats. In this study, our sample showed a significant increase in fecal cholesterol excretion under HFD conditions, but in mice overexpressing CPT1AM the excretion is even higher (Figure 48B). Thus, mice overexpressing CPT1AM shed more cholesterol in the feces from excess dietary fat.

### **6.8 Overexpression of CPT1AM increases fatty acid oxidation in BAT.**

Studies [137] have shown that increasing the rate of fatty acid oxidation improves BAT thermogenesis. Thus, CPT1AM, a permanently active mutant form

of CPT1A, has been expressed in a mouse brown adipocyte cell line via adenoviral infection. Mice expressing CPT1AM were found to have increased FAO, lipolysis, UCP1 protein levels, and mitochondrial activity. In addition, enhanced FAO reduced the palmitate-induced increase in triglyceride content and the expression of inflammatory and obesity markers. Thus, mice expressing CPT1AM had enhanced fat-burning ability and improved lipid-induced disorders. This indicates that CPT1AM-mediated augmentation of brown adipocytes may be a new approach for the treatment of obesity-induced disorders.

On the other hand, although it is clear that fatty acid oxidation is a critical and fundamental metabolic endpoint in humans [167] and rodents, it is unclear how adipocyte fatty acid oxidation affects whole-body metabolism autonomously. Thus, a conditional loss-of-function allele has been generated for CPT2 [168], an obligate step in mitochondrial long-chain fatty acid beta-oxidation that is encoded by a single gene. We show that fatty acid oxidation of adipose tissue is not only required for acute cold adaptation, but also for the induction of thermogenic genes in BAT. Loss of adipose fatty acid oxidation alters adiposity in a diet-dependent manner.

Secondly, excessive CPT1 activity increases fatty acid oxidation, without affecting glucose oxidation. Thus, overexpression of CPT1 increases the rate of fatty acid oxidation at high and low glucose concentrations [122]. The first published studies [169] described how the sensitivity of the inhibition of fatty acid oxidation or "external" CPT activity of rat liver isolated from mitochondria by malonyl-CoA was markedly reduced in fasting preparations in diabetic rats. In this thesis, the fatty acid oxidation assay was performed in BAT, where there is a significant increase observed in the tissues that were punctured with

CPT1AM, demonstrating an increase in FAO in the BATs of mice that overexpress CPT1AM (Figure 51A-B).

### **6.9 Gene therapy for treatment and prevention of obesity**

Family studies have shown that genetic factors play a significant role in the pathogenesis of obesity. Rare mutations in humans and model organisms have provided insights into multiple pathways that may lead to obesity. Studies of candidate genes indicate that some genes involved in pathways regulating energy expenditure and food intake play a critical role in the predisposition of obesity. In obesity cases where the genetic defect is clearly identified, transfer of copies of a functional gene to diseased cells will provide a cure similar to monogenic diseases applicable in gene therapy [134].

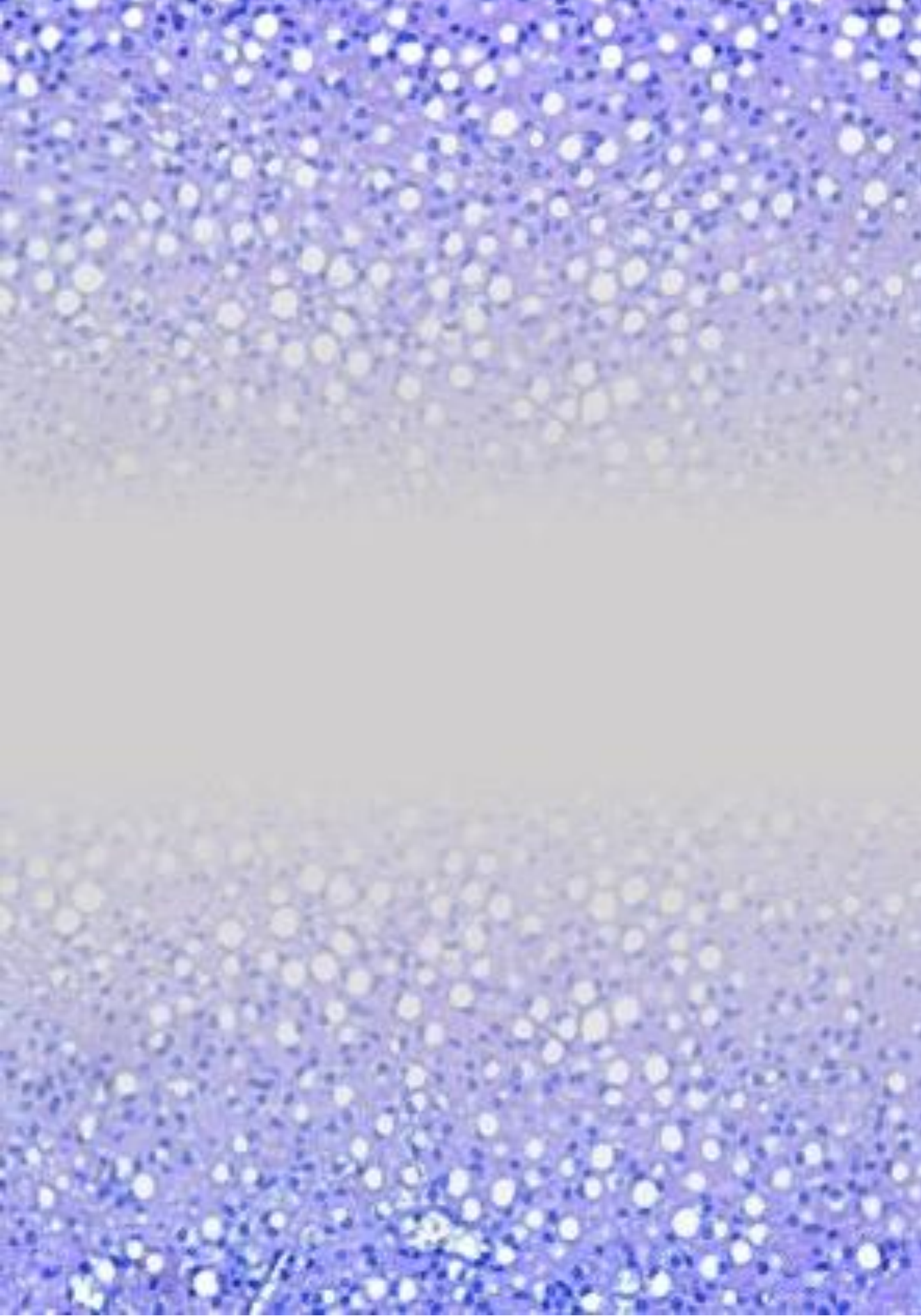
In addition to its genetic link, obesity is also considered a “modern” disease caused by changes in lifestyle and diet structure. Excess food intake, especially foods enriched with fat and high calories, and sedentary lifestyle are also considered a major cause of obesity. In principle, fat accumulation, a result of an increase in lipogenesis can be inhibited by decreasing the amount and activity of involved enzymes by overexpressing a transcription factor to selectively suppress transcription of genes responsible for lipogenesis and fat accumulation. Introduction of genes capable of enhancing energy expenditure may reduce fat accumulation and weight loss.

In fact, recent animal studies [170] [171] [172] have shown that gene transfer to obese mice was effective in reducing fat mass and alleviating insulin resistance and fatty liver, providing direct evidence in support of the gene therapy approach in re-establishing and maintaining the metabolic homeostasis. Although the potential of gene therapy in treating obesity appears evident,

additional safety studies involving pharmacokinetics, biodistribution, and toxicity should be accurately evaluated in large animal models before clinical trials might proceed.



# **Conclusions**



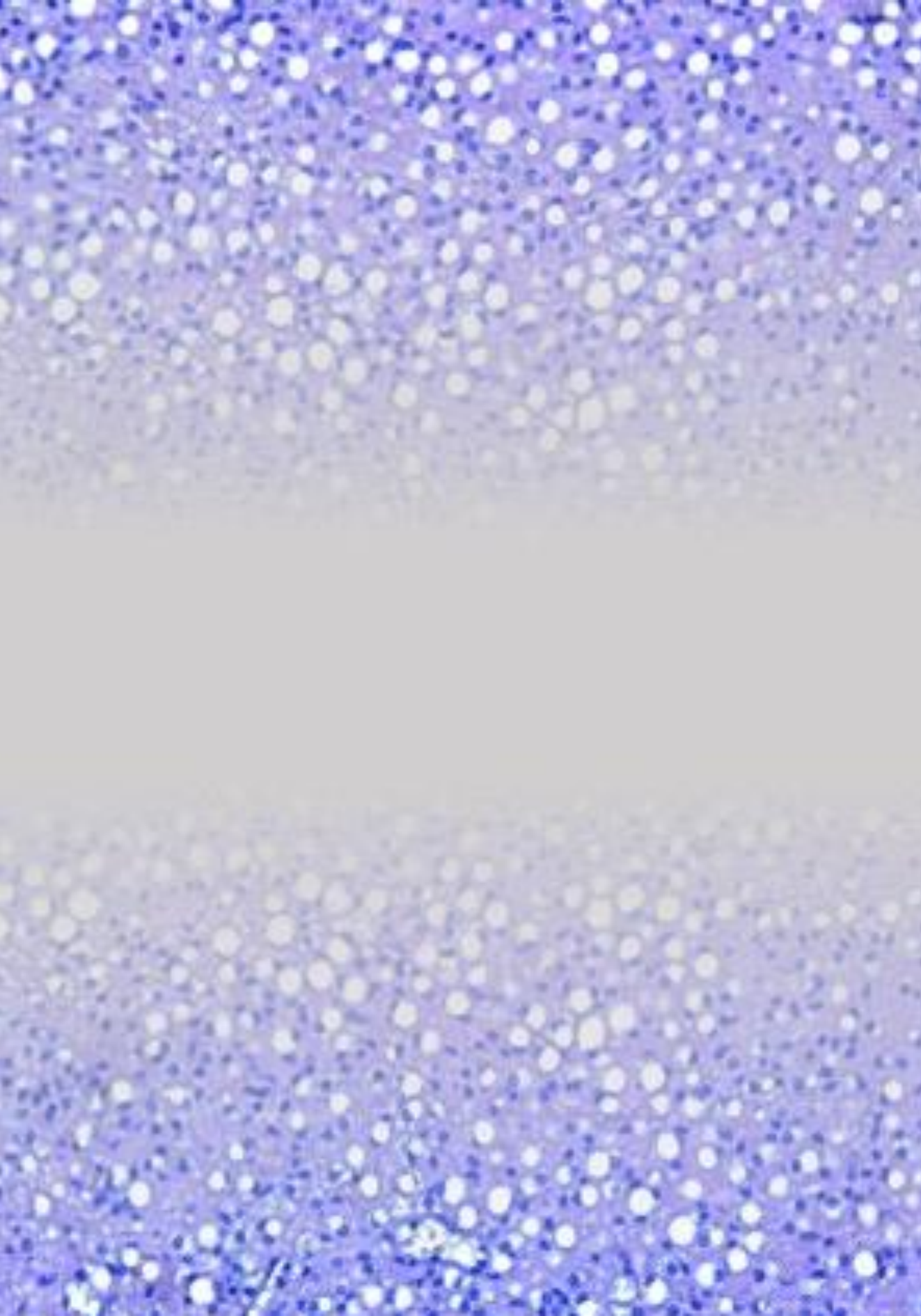
### 7 CONCLUSIONS

- I. The BAT-specific injection of AAVs carrying the expression of CPT1AM is an efficient technique for the specific gene therapy approach in this tissue.
- II. The BAT-specific overexpression of CPT1AM is able to prevent HFD-induced obesity under conditions of room temperature (chronic cold) and thermoneutrality.
- III. The overexpression of CPT1AM in mouse BAT prevented adipose tissue hypertrophy and hepatic steatosis.
- IV. CPT1AM-expressing mice showed altered adipose tissue and liver metabolism, with main changes seen in leptin, G6p, Bip and Chop gene expression.
- V. CPT1AM therapy and BAT activation are more effective at thermoneutral conditions followed by acute cold stimulation than at room temperature conditions (chronic cold).
- VI. HFD-induced obesity at thermoneutrality is more efficient in male than in female mice.
- VII. BAT-specific CPT1AM therapy is more efficient in female than in male mice.
- VIII. The overexpression of CPT1AM in mouse BAT is correlated with a higher FAO in BAT.
- IX. BAT-specific overexpression of CPT1AM produces higher steatorrhea compared to HFD control group (HFD Null).
- X. Both sexual dimorphism and diet have a significant impact on weight gain in mice.





# References



### 8 REFERENCES

- [1] M. Bastías-Pérez, D. Serra and L. Herrero, "Dietary Options for Rodents in the Study of Obesity," *Nutrients*, vol. 3234-12, pp. 2-19, 2020.
- [2] K. Townsend and Y. Tseng, "Brown fat fuel utilization and thermogenesis.," *Trends Endocrinol Metab*, vol. 25, pp. 168-177, 2014.
- [3] B. Cannon and J. Nedergaard, "Brown adipose tissue: Function and physiological significance," *Physiol Rev.*, vol. 84, pp. 277- 359, 2004.
- [4] M. Saito, "Brown adipose tissue as a regulator of energy expenditure and body fat in humans," *Diabetes Metab J*, vol. 37, pp. 22-29, 2013.
- [5] J. Fisler and C. Warden, "Uncoupling proteins, dietary fat and the metabolic syndrome," *Nutr Metab (Lond)*, vol. 3, p. 38, 2006.
- [6] Universitat de Barcelona, "Nueva técnica para medir la actividad del tejido adiposo marrón, un órgano clave en el desarrollo de la obesidad," 06 Junio 2017.[Online].Available:[https://www.ub.edu/web/ub/es/menu\\_eines/noticies/2017/06/007.html](https://www.ub.edu/web/ub/es/menu_eines/noticies/2017/06/007.html). [Accessed 19 Junio 2020].
- [7] Clinton R. Andrew J. Hoy; Nigel Turner; Matthew J. Watt; Tamara L. Allen; Kevin Carpenter; Gregory J. Cooney; Mark A. Febbraio; Edward W. Kraegen "Overexpression of Carnitine Palmitoyltransferase-1 in Skeletal Muscle Is Sufficient to Enhance Fatty Acid Oxidation and Improve High-Fat Diet–Induced Insulin Resistance", 2009, vol. 58(3), pp. 550–558.
- [8] S. Fruh, "Obesity: Risk factors, complications, and strategies for sustainable long-term weight management," *J Am Assoc Nurse Pract*, vol. 29, no. 1, p. S3–S14, 2017.
- [9] L. O' Connor, S. Brage, S. Griffin, N. Wareham and N. Forouhi , "The cross-sectional association between snacking behaviour and measures of

- adiposity: the Fenland Study," UK. *Brit J Nutr*, vol. 114, no. 8, pp. 1286-96, 2015.
- [10] A. Paulo, E. Serra, M. Bonet and C. Picó, "Obesity: Molecular bases of a multifactorial problem," *European Journal of Nutrition*, vol. 39, pp. 127-144, 2000.
- [11] J. G. Gutiérrez Reyes, G. Meléndez Mie, A. Zúñiga Rivera and A. Serralde Zúñiga, "Genómica nutricional y obesidad," *Revista de Endocrinología y Nutrición*, vol. 14, no. 4, pp. 247-256, 2006.
- [12] S. Widiker, S. Karst, A. Wagener and A. Brockmann, "High-fat diet leads to a decreased methylation of the Mc4r gene in the obese BFM1 and the lean B6 mouse lines. *J. Appl. Genet*," vol. 2, no. 51, p. 193–197, 2010.
- [13] F. Gasca, "Limitations of body mass index," Amigho, 2020.
- [14] A. Lecube, S. Monereo, M. A. Rubio, P. Martínez-de-Icaya, A. Martí and J. Salvador, "Prevención, diagnóstico y tratamiento de la obesidad. Posicionamiento de la Sociedad Española para el estudio de la Obesidad de 2016," *Endocrinol Nutr*, vol. 64, no. 1, pp. 15-22, 2016.
- [15] M. Ashwell, P. Gunn and S. Gibson, "Waist-to-height ratio is a better screening tool than waist circumference and BMI for adult cardiometabolic risk factors: systematic review and meta-analysis," *Obes Rev*, vol. 13, pp. 275-86, 2012.
- [16] World Health Organization (WHO), "Waist circumference and waist-hip ratio. Report of a WHO Expert Consultation," Geneva: WHO, 2011.
- [17] S. Chua, X. Chung, W. Wupeng, Y. Zhang, S. Liu and L. Tartaglia, "Phenotypes of mouse diabetes and rat fatty due to mutations in the OB (leptin) receptor," *Science*, vol. 271, pp. 994-996, 1996.



- [18] Y. Zhang, R. Proenca, M. Maffei, M. Barone, L. Leopold and J. Friedman, "Positional cloning of the mouse obese gene and its human homologue," *Nature*, vol. 372, pp. 425-432, 1994.
- [19] R. Ahima and J. Flier, "Leptin," *Annu Rev Physiol*, vol. 62, pp. 413-437, 2000.
- [20] B. Beck, "Neuropeptides and obesity," *Nutrition*, vol. 16, pp. 916-923, 2000.
- [21] B. Beck, A. Bulet, J. Nicolas and C. Bulet, "Hyperphagia in obesity is associated with a central peptidergic dysregulation in rats," *J Nutr*, vol. 120, pp. 806-811, 1990.
- [22] L. Hardie, D. Rayner, S. Holmes and P. Trayhurn, "Circulating leptin levels are modulated by fasting, cold exposure and insulin administration in lean but not Zucker (fa/fa) rats as measured by ELISA," *Biochem Biophys Res Commun*, vol. 223, pp. 660-665, 1996.
- [23] P. Johnson, L. Zucker, J. Cruce and J. Hirsch, "Cellularity of adipose depots in the genetically obese Zucker rat," *J Lipid Res*, vol. 12, pp. 706-714, 1971.
- [24] J. Stern, P. Johnson, M. Greenwood, L. Zucker and J. Hirsch, "Insulin resistance and pancreatic insulin release in the genetically obese Zucker rat," *Proc Soc Exp Biol Med*, vol. 139, pp. 66-69, 1972.
- [25] S. Ibrahim, P. Hirsova, H. Malhi and G. Gores, "Animal Models of Nonalcoholic Steatohepatitis: Eat, Delete, and Inflammation," *Dig Dis Sci*, vol. 61, no. 15, pp. 1325-36, 2016.
- [26] L. Hebbard and J. George, "Animal models of nonalcoholic fatty liver disease," *Nat Rev Gastroenterol Hepatol*, vol. 8, no. 1, pp. 35-44, 2011.
- [27] G. Kanuri and I. Bergheim, "In vitro and in vivo models of non-alcoholic fatty liver disease (NAFLD)," *Int J Mol Sci*, vol. 14, no. 6, pp. 11963-8, 2013.

- [28] Q. Deng, H. She and J. Cheng, "Steatohepatitis induced by intragastric overfeeding in mice," *Hepatology*, vol. 42, no. 4, pp. 905-14, 2005.
- [29] A. Nakamura and Y. Terauchi, "Lessons from Mouse Models of High-Fat Diet-Induced NAFLD," *Int J Mol Sci*, vol. 14, no. 11, pp. 21240-57, 2013.
- [30] A. Asgharpour, S. Cazanave, T. Pacana, M. Seneshaw, R. Vincent, B. Banini, D. Kumar, K. Daita, H. Min, F. Mirshahi, P. Bedossa, X. Sun, Y. Hoshida, S. Koduru, D. Contaifer, U. Warncke, D. Wijesinghe and A. Sanyal, "A diet-induced animal model of non-alcoholic fatty liver disease and hepatocellular cancer," *J Hepatol*, vol. 65, no. 3, pp. 579-88, 2016.
- [31] F. Fuentes, R. Mendoza, A. Rosales and R. Cisneros, "Instituto Nacional de Salud, Ministerio de Salud," *Guía de manejo y cuidado de animales de laboratorio: ratón*. Ministerio de Salud, Lima, 2008.
- [32] G. Pérez, "Fundamentos del trabajo con animales de laboratorio en proyectos de investigación," *Revista del Hospital J.M*, 2007.
- [33] Y. Tanja, "Diet-induced models for obesity and type 2 diabetes," *Drug Discovery Today: Disease Models*, vol. 4, no. 1, pp. 3-8, 2007.
- [34] M. Sörhede Winzell and A. Bo, "The High-Fat Diet–Fed Mouse. A Model for Studying Mechanisms and Treatment of Impaired Glucose Tolerance and Type 2 Diabetes," *Diabetes*, vol. 53, no. 3, pp. s215-s219, 2004.
- [35] A. Gajda, "High-Fat Diets for Diet-Induced Obesity (DIO) Models," *Res. Diets*, vol. 4, p. 1–4, 2008.
- [36] M. Rossmeisl, J. Rim, R. Koza and L. Kozak, "Variation in type 2 diabetes—Related traits in mouse strains susceptible to diet-induced obesity," *Diabetes*, vol. 52, p. 1958–1966, 2003.

- [37] T. Lauterio, J. Bond and E. Ulman, "Development and Characterization of a Purified Diet to Identify Obesity-Susceptible and Resistant Rat Populations," *J. Nutr.*, vol. 124, p. 2172–2178, 1994.
- [38] C. Farley, J. Cook, B. Spar, T. Austin and T. Kowalski, "Meal Pattern Analysis of Diet-Induced Obesity in Susceptible and Resistant Rats," *Obes. Res.*, vol. 11, p. 845–851, 2003.
- [39] T. Kondoh and K. Torii, "MSG intake suppresses weight gain, fat deposition, and plasma leptin levels in male Sprague–Dawley rats," *Physiol. Behav.*, vol. 95, p. 135–144, 2008.
- [40] J. Suleiman, M. Mohamed and A. Abu Bakar, "A systematic review on different models of inducing obesity in animals: Advantages and limitations," *J. Adv. Veter. Anim. Res.*, vol. 7, p. 103–114, 2019.
- [41] P. Even, S. Virtue, N. Morton, G. Fromentin and R. Semple, "Editorial: Are Rodent models fit for investigation of human obesity and related diseases?," *Front. Nutr.*, vol. 4, p. 58, 2017.
- [42] H. Mokdad, B. Bowman, E. Ford, F. Vinicor, J. Marks and J. Koplan, "The continuing epidemics of obesity and diabetes in the United States," *Jama*, vol. 286, pp. 1195-1200, 2001.
- [43] F. Facchini, N. Hua, F. Abbasi and G. Reaven, "Insulin resistance as a predictor of age-related diseases," *J Clin Endocrinol Metab*, vol. 86, pp. 3574-3578, 2001.
- [44] G. Reaven, "The insulin resistance syndrome: definition and dietary approaches to treatment," *Annu Rev Nutr*, vol. 25, pp. 391-406, 2005.
- [45] M. Ros Pérez and G. Medina-Gómez, "Obesity, adipogenesis and insulin resistance," *Elsevier*, vol. 58, no. 7, pp. 360-369, 2011.

- [46] M. Esteve Ràfols , "Tejido adiposo: heterogeneidad celular y diversidad funcional," *Endocrinología y Nutrición*, 2014.
- [47] M. Reyes , "Características biológicas del tejido adiposo: el adipocito como célula," *Rev Méd Clín Las Condes*, vol. 5, no. 2, pp. 136-144, 2012.
- [48] D. García Torres, M. Castellanos González, R. Cedeño Morales , M. Benet Rodríguez and I. Ramírez Arteaga , "Adipose tissue as an endocrine gland: Pathophysiological implications," *Rev Finlay*, vol. 1, no. 2, pp. 131-151, 2011.
- [49] V. Barquissau , D. Beuzelin , D. Pisani , G. Beranger, A. Mairal and A. Montagner, "White-to-brite conversion in human adipocytes promotes metabolic reprogramming toward fatty acid-anabolic and catabolic pathways," *Mol Metab*, vol. 5, no. 5, pp. 352-365, 2016.
- [50] S. Cinti, " Adipose Organ Development and Remodeling," *Compr Physiol*, vol. 14, no. 8(4), pp. 1357-1431, 2018.
- [51] G. Charriere , B. Cousin, E. Arnaud, M. André , F. Bacou and L. Penicaud, "Preadipocyte conversion to macrophage evidence of plasticity," *J Biol Chem*, vol. 278, no. 11, pp. 9850-9855, 2003.
- [52] J. Timmons, K. Wennmalm, O. Larsson, T. Walden, T. Lassmann and N. Petrovic, "Myogenic gene expression signature establishes that Brown and White adipocytes originate from distinct cell lineages," *Proc Natl Acad Sci U S A*, vol. 104, no. 11, pp. 4401-4406, 2007.
- [53] M. Vohl, R. Sladek, J. Robitaille, S. Gurd, P. Marceau and D. Richard, "A survey of genes differentially expressed in subcutaneous and visceral adipose tissue in men," *Obes Res*, vol. 12, no. 8, pp. 1217-1222, 2004.
- [54] Cinti S, "Pink Adipocytes," *Trends Endocrinol Metab*, vol. 9, pp. 651-666, 2018.

- [55] G. B. Vega-Robledo and M. G. Rico-Rosillo, "Adipose tissue: immune function and obesity-induced alterations," *Rev. alerg. Méx.* , vol. 6, no. 3, 2020.
- [56] M. Jedrychowski, C. Wrann, J. Paulo, K. Gerber, J. Szpyt and M. Robinson, "Detection and quantitation of circulating human irisin by tandem mass spectrometry," *Cell Metab*, vol. 22, no. 4, pp. 734-740, 2015.
- [57] Q. Wang, C. Tao, R. Gupta and P. Scherer, "Tracking adipogenesis during white adipose tissue development, expansion and regeneration," *Nat Med*, vol. 19, pp. 1338-1344, 2013.
- [58] L. Sidossis and S. Kajimura, "Brown and beige fat in humans: thermogenic adipocytes that control energy and glucosa homeostasis," *J Clin Invest*, vol. 125, no. 2, pp. 478-486, 2015.
- [59] S. Kajimura, B. Spiegelman and P. Seale, "Brown and beige fat: physiological roles beyond heat generation.," *Cell Metab*, vol. 22, no. 4, pp. 546-559, 2015.
- [60] A. Frontini, A. Vitali, J. Peregrini , I. Murano and C. Romiti, "Ricquier D, et al. White-to-brown transdifferentiation of omental adipocytes in patients affected by pheochromocytoma," *Biochim Biophys Acta*, vol. 1831, no. 5, pp. 950-959, 2013.
- [61] G. Vilahur, S. Ben-Aicha and L. Badimon, "New insights into the role of adipose tissue in thrombosis.," *Cardiovascular Res*, vol. 113, no. 9, pp. 1046-1054, 2017.
- [62] G. Pachón-Peña, C. Serena, M. Ejerque, J. Petriz, X. Durán and W. Oliva-Olivera, "Obesity determines the immunophenotypic profile and functional characteristics of human mesenchymal stem cells from adipose tissue," *Stem Cells Transl Med*, vol. 5, no. 4, pp. 464-475, 2016.

- [63] G. Wolf, "Glucocorticoids in adipocytes stimulate visceral obesity," *Nutr Rev*, vol. 60, no. 5 Pt 1, pp. 148-151, 2002.
- [64] D. Chusyd, D. Wang, T. Huffman and T. Nagy, "Relationships between rodent white adipose fat pads and human white adipose fat depots. *Front*," *Nutr*, vol. 3, 2016.
- [65] E. Rosen and B. Spiegelman, "What we talk about when we talk about fat.," *Cell*, vol. 156, p. 20–44, 2014.
- [66] R. Zwick, C. Guerrero-Juarez and V. Horsley, "Plikus. Anatomical, physiological, and functional diversity of adipose tissue," *Cell Metab*, vol. 27, p. 68–83, 2018.
- [67] A. Fedorenko, P. Lishko and Y. Kirichok, "Mechanism of fatty-acid-dependent UCP1 uncoupling in brown fat mitochondria," *Cell*, vol. 151, no. 2, pp. 400-413, 2012.
- [68] J. Berbée, M. Boon, P. Khedoe, A. Bartelt, C. Schlein and A. Worthmann, "Brown fat activation reduces hypercholesterolaemia and protects from atherosclerosis development," *Nat Commun*, vol. 6, p. 6356, 2015.
- [69] C. Vaughan and T. Bartness, "Anterograde transneuronal viral tract tracing reveals central sensory circuits from brown fat and sensory denervation alters its thermogenic responses," *Am J Physiol Regul Integr Comp Physiol*, vol. 302, pp. R1049-R1058, 2012.
- [70] K. Svensson, J. Long, M. Jedrychowski, P. Cohen, J. Lo and S. Serag, "A secreted Slit2 fragment regulates adipose tissue thermogenesis and metabolic function," *Cell Metab*, vol. 23, pp. 454-466, 2016.
- [71] S. Min, J. Kady, M. Nam, R. Rojas-Rodríguez, A. Berkenwald and J. Kim, "Human "brite/beige" adipocytes develop from capillary networks, and

- their implantation improves metabolic homeostasis in mice," *Nat Med*, vol. 22, no. 3, pp. 312-318, 2016.
- [72] J. Wu, P. Boström, L. Sparks, L. Ye, J. Choi and A. Giang, "Beige adipocytes are a distinct type of thermogenic fat cell in mouse and human," *Cell*, vol. 150, no. 2, pp. 366-376, 2012.
- [73] M. Lee, J. Odegaard, L. Mukundau, Y. Qiu, A. Molofsky and J. Nussbaum, "Activated type 2 innate lymphoid cells regulate beige fat biogenesis," *Cell*, vol. 160, pp. 74-87, 2015.
- [74] D. Berry, Y. Jiang, R. Arpke, E. Close, A. Uchida and D. Reading, "Cellular aging contributes to failure of cold induced beige adipocyte formation in old mice and humans," *Cell*, vol. 25, no. 1, pp. 166-181, 2017.
- [75] Y. Qiu, K. Nguyen, J. Odegaard, X. Cui, X. Tian and R. Locksley, "Eosinophils and type 2 cytokine signaling in macrophages orchestrate development of functional beige fat," *Cell*, vol. 157, no. 6, pp. 1292-1308, 2014.
- [76] L. Kazak, E. Chouchani, M. Jedrychowski, B. Erickson, K. Shinoda and P. Cohen, "A creatine-drivers substrate cycle enhances energy expenditure and thermogenesis in beige fat," *Cell*, vol. 163, no. 3, pp. 643-655, 2015.
- [77] V. Pellegrinelli, S. Carobbio and A. Vidal-Puig, "Adipose tissue plasticity: how fat depots respond differently to pathophysiological cues," *Diabetologia*, vol. 59, no. 6, pp. 1075-1088, 2016.
- [78] G. Hotamisligil, "Inflammation, metaflammation and immunometabolic disorders," *Nature*, vol. 542, pp. 177-185, 2017.
- [79] M. Reyes, "Características inflamatorias de la obesidad," *Rev Chil Nutr*, vol. 37, pp. 498-504, 2010.
- [80] J. Danesh, R. Collins, P. Appleby and R. Peto, "Association of fibrinogen, C-reactive protein, albumin, or leukocyte count with coronary heart

- disease: meta-analyses of prospective studies," *Jama*, vol. 279, pp. 1477-1482, 1998.
- [81] S. Weisberg, D. Hunter and R. Huber, "CCR2 modulates inflammatory and metabolic effects of high-fat feeding," *J Clin Invest*, vol. 116, pp. 115-124, 2006.
- [82] J. Odegaard, R. Ricardo-Gonzalez and M. Goforth, "Macrophage-specific PPAR gamma controls alternative activation and improves insulin resistance," *Nature*, vol. 447, pp. 1116-1120, 2007.
- [83] H. Ghanim, A. Aljada, D. Hofmeyer, T. Syed, P. Mohanty and P. Dandona, "Circulating mononuclear cells in the obese are in a proinflammatory state," *Circulation*, vol. 110, pp. 1564-1571, 2004.
- [84] J. Smith, M. Al-Amri, P. Dorairaj and A. Sniderman , "The adipocyte life cycle hypothesis," *Clin Sci (Lond)*, vol. 110, pp. 1-9, 2006.
- [85] N. Halberg, I. Wernstedt-Asterholm and P. Scherer, "The adipocyte as an endocrine cell," *Endocrinol Metab Clin North Am*, vol. 37, pp. 753-768, 2008.
- [86] S. Wozniak, L. Gee, M. Wachtel and E. Frezza, "Adipose tissue: the new endocrine organ? A review article," *Dig Dis Sci*, vol. 54, pp. 1847-1856, 2009.
- [87] A. Kosteli, E. Sugaru and G. Haemmerle, "Weight loss and lipolysis promote a dynamic immune response in murine adipose tissue," *J Clin Invest*, vol. 120, no. 3466-79.
- [88] S. Cinti, G. Mitchell and G. Barbatelli, "Adipocyte death defines macrophage localization and function in adipose tissue of obese mice and humans," *J Lipid Res*, vol. 46, pp. 2347-2355, 2005.



- [89] D. Kaminski and T. Randall, "Adaptive immunity and adipose tissue biology," *Trends Immunol*, vol. 31, pp. 384-90.
- [90] S. Weisberg, D. McCann, M. Desai, M. Rosenbaum, R. Leibel and A. Ferrante, "Obesity is associated with macrophage accumulation in adipose tissue," *J Clin Invest*, vol. 112, pp. 1796-1808, 2003.
- [91] A. Gómez-Hernández, L. Perdomo, Ó. Escribano and M. Benito, "Papel del tejido adiposo blanco en las complicaciones vasculares asociadas a la obesidad," *Clínica e Investigación en Arteriosclerosis*, vol. 25, no. 1, pp. 27-35, 2013.
- [92] N. Halberg, I. Wernstedt-Asterholm and P. Scherer, "The adipocyte as an endocrine cell," *Endocrinol Metab Clin North Am*, vol. 37, pp. 753-768, 2008.
- [93] J. Friedman, "Leptin and the regulation of body weigh," *Keio J Med*, vol. 60, pp. 1-9.
- [94] S. De Ferranti and D. Mozaffarian, "The perfect storm: obesity, adipocyte dysfunction, and metabolic consequences," *Clin Chem*, vol. 54, pp. 945-955, 2008.
- [95] P. Libby, "Inflammation in atherosclerosis," *Nature*, vol. 420, pp. 868-874, 2002.
- [96] E. Broeders, D. Nicole, D. Bouvy, D. Wouter and M. Van Lichtenbelt, "Endogenous ways to stimulate brown adipose tissue in humans," *Annals of Medicine (AnnMed)*, vol. 43, p. 123–132, 2005.
- [97] S. Kim and J. Plutzky, "Brown Fat and Browning for the Treatment of Obesity and Related Metabolic Disorders," *Diabetes & Metabolism Journal (dmj)*, vol. 40, pp. 12-21, 2016.

- [98] C. Kuminev Cruz, "Nuevas terapias en el tratamiento de la obesidad y sus complicaciones metabólicas asociadas," pp. 1-20, 2017.
- [99] A. Gómez-Hernández, "Differential Role of Adipose Tissues in Obesity and Related Metabolic and Vascular Complications," *International Journal of Endocrinology*, vol. 15, 2016.
- [100] M. Bastías-Pérez, S. Zagnutt, M. Soler-Vázquez, P. Mera, D. Serra and M. Herrero., "Impact of Adaptive Thermogenesis in Mice on the Treatment of Obesity," *Cells*, vol. 9, no. 2, 2020.
- [101] M. Calderon-Dominguez, D. Sebastián, R. Fucho, M. Weber, J. Mir, E. García-Casarrubios, M. J. Obregón, A. Zorzano, Á. Valverde, D. Serra and L. Herrero , "Carnitine Palmitoyltransferase 1 Increases Lipolysis, UCP1 Protein Expression and Mitochondrial Activity in Brown Adipocytes," *Plos One*, vol. 11, no. 7, 2015.
- [102] A. Cypess, S. Lehman, G. Williams, I. Tal, D. Rodman, A. Goldfine, F. Kuo, E. Palmer, Y.-H. Tseng, A. Doria, G. Kolodny and R. Kahn, "Identification and Importance of Brown Adipose Tissue in Adult Humans," *N Engl J Med*, vol. 360, pp. 1509-1517, 2009.
- [103] A. Sclafani and D. Springer, "Dietary obesity in adult rats: Similarities to hypothalamic and human obesity syndromes.," *Physiol. Behav*, vol. 17, p. 461–471, 1976.
- [104] R. Buettner, J. Schölmerich and L. Bollheimer, "High-fat diets: Modeling the metabolic disorders of human obesity in rodents.," *Obesity*, vol. 15, p. 798–808, 2007.
- [105] M. Davidson, "Generalidades sobre el metabolismo de los lípidos," no. <https://www.msmanuals.com/es-co/professional/trastornos-endocrinol> 2019.

- [106] K. Jaworski, E. Sarkadi-Nagy, R. Duncan, M. Ahmadian and H. Sul , "Regulation of triglyceride metabolism IV. Hormonal regulation of lipolysis in adipose tissue," *Am J Physiol Gastrointest Liver Physiol*, vol. 293, pp. G1-G4, 2007.
- [107] B. Sánchez Salazar, "Vías de señalización que participan en la regulación de la lipólisis en adipocitos," *REB*, vol. 25, no. 3, pp. 80-84, 2006.
- [108] S. Houten, S. Violante, F. Ventura and R. Wanders, "The biochemistry and physiology of mitochondrial fatty acid  $\beta$ -oxidation and its genetic disorders," *Annu. Rev. Physiol*, vol. 78, p. 23–44, 2016.
- [109] M. Molina, C. Vázquez and V. Ruíz Gutiérrez, "Metabolismo del colesterol su regulación a nivel hepático e intestinal," *Grasas y Aceites*, vol. 42, no. Fase. 4 , pp. 298-308, 1991.
- [110] K. Botham and P. Mayes, *CAPÍTULO 22: Oxidación de ácidos grasos: cetogénesis*, Lange, 2005.
- [111] E. Raimann and V. Cornejo, "Fatty acid oxidation defects produce nonketotic hypoglycemia in childhood," *Rev Chil Nutr* , vol. 34, no. 1, 2007.
- [112] B. Burton, "Inborn errors of metabolism in Infancy: A guide to diagnosis," *Pediatrics*, vol. 102, pp. 69-73, 1998.
- [113] T. Grevengoed, E. Klett and R. Coleman, "Acyl-CoA Metabolism and Partitioning," *Annu Rev Nutr*, vol. 34, pp. 1-30, 2014.
- [114] N. Casals, C. Miralpeix, A. Fosch, S. Zagmutt and D. Cota, "Progress in lipid research," *Research*, vol. 61, pp. 134-148, 2016.
- [115] J. Houmard, "Intramuscular lipid oxidation and obesity," *Am J Physiol Regul Integr Comp Physiol*, vol. 294, p. R1111–R1116, 2008.
- [116] D. Kelley, J. He, E. Menshikova and V. Ritov, "Diabetes," *Diabeter Journal*, vol. 51, no. 10, 2002.

- [117] M. Malandrino, R. Fucho, M. Weber, M. Calderon-Dominguez and J. Mir, "Endocrinology and Metabolism," *American Journal of Physiology*, vol. 308, no. 9, pp. E756-E769, 2015.
- [118] J. Monsénégo, "Enhancing liver mitochondrial fatty acid oxidation capacity in obese mice improves insulin sensitivity independently of hepatic steatosis" *Journal of hepatology*, vol. 56, no. 3, p. 32–39, 2012.
- [119] J. Orellana-Gavaldà, L. Herrero, M. I. Malandrino, A. Pañeda, M. S. Rodríguez-Peña, H. Petry, G. Asins, S. Van Deventer, F. Hegardt and D. Serra, "Molecular therapy for obesity and diabetes based on a long-term increase in hepatic fatty-acid oxidation," *Hepatology*, vol. 53, no. 3, pp. 821-832, 2010.
- [120] M. Stefanovic-Racic, "A moderate increase in carnitine palmitoyltransferase 1a activity is sufficient to substantially reduce hepatic triglyceride levels," *American journal of physiology Endocrinology and metabolism*, vol. 294, no. 5, 2008.
- [121] L. Herrero, "Alteration of the malonyl-CoA carnitine palmitoyltransferase I interaction in the beta-cell impairs glucose-induced insulin secretion" *Diabetes*, vol. 54, no. 2, p. 462–471, 2005.
- [122] B. Rubi, "Adenovirus-mediated overexpression of liver carnitine palmitoyltransferase I in INS1E cells: effects on cell metabolism and insulin secretion," *Biochem J*, vol. 364, no. 1, 2002.
- [123] M. Morillas, "The Journal of biological chemistry," vol. 278, no. 11, p. 9058–63., 2003.
- [124] H. Miller, "Gene Therapy for enhancement," *Lancet*, vol. 344, pp. 316-317, 1994.

- [125] C. Modesto, "Terapia génica en reumatología pediátrica," *An Esp Pediatr*, vol. 56, no. 6, pp. 515-20, 2002.
- [126] P. Thorpe, B. Stevenson and D. Porteous, "Optimising gene repair strategies in cell culture," 700-2, vol. 9, pp. 700-2, 2002.
- [127] C. A. Agudelo Vélez and L. M. Martínez Sánchez, "Terapia genica: una opción de tratamiento y una controversia etica," *Revista Salud Uninorte*, vol. 29, no. 2, 2013.
- [128] C. Jambrina Pallarés, "Tratamiento de la diabetes y la obesidad mediante una terapia génica con fgf21," Universidad Autónoma de Barcelona, 2017.
- [129] N. Nayerossadat, P. Ali and T. Maedeh, "Viral and nonviral delivery systems for gene delivery," *Adv. Biomed. Res*, vol. 1, no. 27, 2012.
- [130] J. Mount, R. Herzog, D. Tillson, S. Goodman, N. Robinson, M. McClelland, D. Bellinger, T. Nichols, V. Arruda and C. Lothrop, "Sustained phenotypic correction of hemophilia B dogs with a factor IX null mutation by liver-directed gene therapy," *Blood*, vol. 99, p. 2670–2676, 2002.
- [131] F. Mingozzi and K. High, "Therapeutic in vivo gene transfer for genetic disease using AAV: progress and challenges.," *Nat. Rev. Genet*, vol. 12, p. 341–355, 2011.
- [132] W. Hauswirth, "Retinal gene therapy using adeno-associated viral vectors: multiple applications for a small virus," *Hum Gene Ther*, vol. 25, no. 8, pp. 671-8, 2014.
- [133] B. China Rodríguez, "Gene therapy: Viral vectors and applications," *Psychologia Latina*, vol. Especial, pp. 67-69, 2018.
- [134] M. Gao and D. Liu, "Gene therapy for obesity: progress and prospects," *Discov Med*, vol. 96, pp. 319-28, 2014.

- [135] V. Jimenez, C. Jambrina , E. Casana , V. Sacristan, S. Muñoz, S. Darriba, J. Rodó, C. Mallol , M. Garcia, X. León, S. Marcó, A. Ribera, I. Elias, A. Casellas , I. Grass, G. Elias, T. Ferré , S. Motas, S. Franckhauser, F. Mulero, M. Navarro, V. Haurigot, J. Ruberte and F. Bosch, "FGF21 gene therapy as treatment for obesity and insulin resistance," *EMBO Mol Med*, vol. 10, no. 8, 2018.
- [136] M. Weber, P. Mera, J. Casas, J. Salvador, A. Rodríguez, S. Alonso, D. Sebastián, M. C. Soler-Vázquez, C. Montironi, S. Recalde, R. Fucho, M. Calderón-Domínguez, J. Francesc Mir, R. Bartrons, J. C. Escola-Gil, D. Sánchez Infantes, A. Zorzano, V. Llorente-Cortes, N. Casals, V. Valentí, G. Frühbeck, L. Herrero and D. Serra, "Liver CPT1A gene therapy reduces diet-induced hepatic steatosis in mice and highlights potential lipid biomarkers for human NAFLD," *The FASEB Journal*, vol. 34, p. 11816–11837, 2020.
- [137] M. Calderon-Dominguez, D. Sebastián, R. Fucho and L. Herrero, "Carnitine Palmitoyltransferase 1 Increases Lipolysis, UCP1 Protein Expression and Mitochondrial Activity in Brown Adipocytes," *PLoS one*, vol. 11, no. 7, 2016.
- [138] H. Lan, K. Teayoun , L. Qinqiang , L. Jian , W. Peiyong , Z. Yiqun , D. Yishu , P. Jeevan , P. Wood and Q. Yang, "Carnitine Palmitoyltransferase1b (CPT1b) Deficiency Aggravates Pressure-Overload-Induced Cardiac Hypertrophy due to Lipotoxicity," *PMC* , vol. 126, no. 14, pp. 1705-1716, 2012.
- [139] M. Pozo Ariza, "Role of CPT1C in the control of Energy Homeostasis," *Universitat Internacional de Catalunya*, 2015.
- [140] J. McGarry and S. Mills, "Observations on the affinity for carnitine, and malonyl-CoA sensitivity, of carnitine palmitoyltransferase I in animal and

- human tissues. Demonstration of the presence of malonyl-CoA in non-hepatic tissues of the rat," *Biochem J*, vol. 214, no. 1, p. 21–8, 1993.
- [141] C. Britton and D. Mackey, "Fine chromosome mapping of the genes for human liver and muscle carnitine palmitoyltransferase I (CPT1A and CPT1B)," *Genomics*, vol. 40, no. 1, p. 209–11, 1997.
- [142] SEBBM, "XXXIV Congreso de la Sociedad Española de Bioquímica y Biología Molecular," Sociedad Española de Bioquímica y Biología Molecular (SEBBM), Barcelona, 2011.
- [143] M. Morillas and P. Gómez–Puertas, "Structural model of the catalytic core of carnitine palmitoyltransferase I and carnitine octanoyltransferase (COT): mutation of CPT I histidine 473 and alanine 381 and COT alanine 238 impairs the catalytic activity," *J Biol Chem*, vol. 276, no. 48, p. 45001–8, 2001.
- [144] E. Park and R. Mynatt, "Insulin regulates enzyme activity, malonyl-CoA sensitivity and mRNA abundance of hepatic carnitine palmitoyltransferase-I," *Biochem J*, vol. 310, no. Pt 3, p. 853–8, 1995.
- [145] Z. Andrews and Z. Liu, "UCP2 mediates ghrelin's action on NPY/AgRP neurons by lowering free radicals," *Nature*, vol. 454, no. 7206, p. 846–51, 2008.
- [146] J. Brandt and F. Djouadi, "Fatty acids activate transcription of the muscle carnitine palmitoyltransferase I gene in cardiac myocytes via the peroxisome proliferator-activated receptor alpha," *J Biol Chem*, vol. 273, no. 37, p. 23786–92, 1998.
- [147] V. Zammit, "Carnitine palmitoyltransferase 1: central to cell function," *IUBMB Life*, vol. 60, no. 5, p. 347–54, 2008.

- [148] M. Guzmán and M. Kolodziej , "Evidence against direct involvement of phosphorylation in the activation of carnitine palmitoyltransferase by okadaic acid in rat hepatocytes," *Biochem J*, vol. 300, no. Pt 3, p. 693–9, 1994.
- [149] L. Badimon, B. Oñate and G. Vilahur, "Adipose-derived Mesenchymal Stem Cells and Their Reparative Potential in Ischemic Heart Disease," *Rev. Esp. Card.*, vol. 68, no. 7, pp. 599-611, 2015.
- [150] V. Jimenez, S. Muñoz, E. Casana, C. Mallol, I. Elias, C. Jambrina, A. Ribera, T. Ferre, S. Franckhauser and F. Bosch, "In vivo adeno-associated viral vector-mediated genetic engineering of white and brown adipose tissue in adult mice," *Diabetes*, vol. 62, no. 12, 2013.
- [151] V. Jimenez, E. Casana , C. Mallol , I. Elias and C. Jambrina , "In vivo adeno-associated viral vector-mediated genetic engineering of white and brown adipose tissue in adult mice.," *Diabetes*, vol. 62, no. 12, p. 4012–4022, 2013.
- [152] G. Suárez Román, A. J. Perera Calderín, S. Clapés Hernández, T. Fernández Romero and E. Egaña Morales, "Standardization of model to induce obesity in rats," *Instituto de Ciencias Básicas y Preclínica Victoria de Girón* , 2015.
- [153] M. Vargas, L. Lancheros and M. d. P. Barrera, "Energy expenditure in repose related to body composition in adults," *Rev Fac Med.*, vol. 59, no. (Supl 1), pp. S43-58, 2011.
- [154] Ministerio de Salud del Perú, "Guía de manejo y cuidado de animales de laboratorio: ratón," *Ministerio de Salud del Perú*, 2008.
- [155] Su Gao, Dolors Serra, Wendy Keung, Fausto G Hegardt, Gary D Lopaschuk, "Important role of ventromedial hypothalamic carnitine



palmitoyltransferase-1a in the control of food intake", *Am J Physiol Endocrinol Metab.* Vol. 305, pp 336-347.

- [156] MC. Soler Vázquez, Tesis Doctoral "Transplantation of a functional adipose tissue with enhanced lipid oxidation reduces obesity and glucose intolerance," Universitat de Barcelona, 2020.
- [157] E. Amengual Cladera, "Dimorfismo sexual en la función y biogénesis mitocondriales en el tejido adiposo blanco de rata. Respuesta a una dieta hiperlipídica," Universitat de les Illes Balears, Palma, 2012.
- [158] B. Colom, A. Alcolea, J. Valle, P. Oliver, Roca and F. Garcia-Palmer, "Skeletal muscle of female rats exhibit higher mitochondrial mass and oxidative-phosphorylative capacities compared to males," *Cell Physiol Biochem*, vol. 19, no. 1-4, pp. 205-212, 2007.
- [159] Justo, M. Frontera, E. Pujo, S. Rodriguez-Cuenca, I. Llado, F. Garcia-Palmer, P. Roca and M. Gianotti, "Gender-related differences in morphology and thermogenic capacity of brown adipose tissue mitochondrial subpopulations," *Life Sci*, vol. 76, no. 10, pp. 1147-1158, 2005.
- [160] R. Guevara, F. Santandreu, A. Valle, M. Gianotti, J. Oliver and P. Roca, "Sex dependent differences in aged rat brain mitochondrial function and oxidative stress," *Free Radic Biol Med*, vol. 46, no. 2, pp. 169-175, 2009.
- [161] S. Rodriguez-Cuenca, E. Pujol, R. Justo, M. Frontera, J. Oliver, M. Gianotti and P. Roca, "Sex-dependent thermogenesis, differences in mitochondrial morphology and function, and adrenergic response in brown adipose tissue," *J Biol Chem*, vol. 277, no. 45, pp. 42958-42963, 2002.
- [162] S. Zagmutt, Tesis Doctoral "Analysis of the in vivo effect of carnitine palmitoyltransferase 1A deletion in AgRP neurons," Universitat de Barcelona, 2020.

- [163] F. d. J. Díaz-Reséndiz, K. Franco-Paredes, A. G. Martínez-Moreno, A. López-Espinoza and V. G. Aguilera-Cervantes, "Effects of Environmental Variables on Eating Behavior in Rats: a Conceptual and Historical Review," *Univ. Psychol*, vol. 8, no. 2, pp. 519-532, 2009.
- [164] M. Stefanovic-Racic, G. Perdomo, B. Mantell, I. J. Sipula, N. Brown and R. M. O'Doherty, "Un aumento moderado de la actividad de la carnitina palmitoiltransferasa 1a es suficiente para reducir sustancialmente los niveles de triglicéridos hepáticos," *Am J Physiol Endocrinol Metab*, vol. 294, pp. E969-E977, 2008.
- [165] M. Alcalá, M. Calderon-Dominguez, E. Bustos, P. Ramos, N. Casals, D. Serra, M. Viana and L. Herrero, "Increased inflammation, oxidative stress and mitochondrial respiration in brown adipose tissue from obese mice," *Scientific Reports*, vol. 7, p. 16082, 2017.
- [166] A. Kuryłowicz and M. Puzianowska-Kuźnicka, "Induction of Adipose Tissue Browning as a Strategy to Combat Obesity," *Int J Mol Sci*, vol. 21, no. 17, p. 6241, 2020.
- [167] N. Longo, C. Amat di San Filippo and M. Pasquali, "Disorders of carnitine transport and the carnitine cycle," *Am J Med Genet C Semin Med Genet*, vol. 142C, p. 77–85, 2006.
- [168] J. Lee, J. Ellis and M. Wolfgang, "Adipose fatty acid oxidation is required for thermogenesis and potentiates oxidative stress induced inflammation," *Cell Rep*, vol. 10, no. 2, p. 266–279., 2015.
- [169] J. A. Ontko and M. L. Johns, "Evaluation of malonyl-CoA in the regulation of long-chain fatty acid oxidation in the liver. Evidence for an unidentified regulatory component of the system," *Biochem. J.*, vol. 192, p. 959–962, 1980.

- [170] L. Cao, E.-J. D Lin, M. C. Cahill, C. Wang, X. Liu and M. J. During, "Molecular therapy of obesity and diabetes by a physiological autoregulatory approach," *Nat Med*, vol. 4, pp. 447-54, 2009.
- [171] M. Gao, Y. Ma, R. Cui and D. Liu, "Hydrodynamic Delivery of FGF21 Gene Alleviates Obesity and Fatty Liver in Mice Fed a High-fat Diet," *J Control Release*, vol. 185, p. 1–11, 2014.
- [172] P. Boström, J. Wu, M. Jedrychowski, A. Korde, L. Ye, J. Lo, K. A. Rasbach, E. Almer Boström, J. Hyun Choi, J. Z. Long, S. Kajimura, M. C. Zingaretti, B. Vind, H. Tu, S. Cinti, K. Højlund, S. Gygi and B. Spiegelman, "A PGC1- $\alpha$ -dependent myokine that drives brown-fat-like development of white fat and thermogenesis," *Nature*, vol. 481, p. 463–468 , 2012.
- [173] V. Jimenez, S. Muñoz, E. Casana, C. Mallol, I. Elias, *et al.* "In vivo adeno-associated viral vector-mediated genetic engineering of white and brown adipose tissue in adult mice", *Diabetes*, vol. 62, pp. 4012-4022, 2003.
- [174] M. Pigeyre, F. Yazdi , Y. Kaur and D. Meyre , "Recent progress in genetics, epigenetics and metagenomics unveils the pathophysiology of human obesity," *Cin Sc* , vol. 130, no. 12, pp. 943-86, 2016.
- [175] A. Schwartz, D. Taras , K. Schafer , S. Beijer , N. Bos and C. Donus , "Microbiota and SCFA in lean and overweight healthy subjects.," *Obesity*, vol. 18, no. 1, pp. 190-95, 2010.
- [176] J. L. Kaar , T. Crume , J. T. Brinton , K. J. Bischoff , R. McDuffie and D. Dabelea , "Maternal obesity, gestational weight gain, and offspring adiposity: the exploring perinatal outcomes among children study," *J Peds*, vol. 165, no. 3, pp. 509-15, 2014.

- [177] L. Serra-Majem and I. Bautista-Castaño , "Etiology of obesity: two "key issues" and other emerging factors.," *Nutr Hosp*, vol. 28, no. supl 5, pp. 32-43, 2013.
- [178] "American Dietetic Association. Position of the American Dietetic Association: weight management," *J Am Diet Assoc*, vol. 109, no. 2, pp. 330-46, 2009.
- [179] M. Ibrahim, "Subcutaneous and visceral adipose tissue: structural and functional differences," *Obes Rev*, no. 11, pp. 11-8, s.f.
- [180] J. Kim, E. Van de Wall and M. Laplante, "Obesity-associated improvements in metabolic profile through expansion of adipose tissue," *J Clin Invest*, no. 2621-2637, p. 117, 2007.
- [181] P. Herranz , R. De Lucas, L. Perez-Espana and M. Mayor, "Lipodystrophy syndromes," *Dermatol Clin*, vol. 26, pp. 569-578, 2008.
- [182] Z. Guo, D. Hensrud, C. Johnson and M. Jensen, "Regional postprandial fatty acid metabolism in different obesity phenotypes," *Diabetes*, vol. 48, no. 1586-1592, 1999.
- [183] L. Fontana, J. Eagon, M. Trujillo, P. Scherer and S. Klein, "Visceral fat adipokine secretion is associated with systemic inflammation in obese humans," *Diabetes*, no. 1010-1013, p. 56, 2007.
- [184] H. Zhang and C. Zhang, "Adipose "talks" to distant organs to regulate insulin sensitivity and vascular function," *Obesity (Silver Spring)*, vol. 18, pp. 2071-6, 2007.
- [185] K. Spalding, E. Arner and P. Westermark, "Dynamics of fat cell turnover in humans," *Nature*, vol. 453, pp. 783-787, 2008.
- [186] J. Smith, M. Al-Amri, P. Dorairaj and A. Sniderman, "The adipocyte life cycle hypothesis," *Clin Sci (Lond)*, vol. 110, pp. 1-9, 2006.

- [187] R. Baker, M. Hayden and S. Ghosh, "NF-kappaB, inflammation, and metabolic disease," *Cell Metab*, vol. 13, pp. 11-22, 2013.
- [188] J. Ehses, A. Perren and E. Eppler, "Increased number of islet-associated macrophages in type 2 diabetes," *Diabetes*, vol. 56, pp. 2356-2370, 2007.
- [189] M. Pasarica, O. Sereda and M. Redman, "Reduced adipose tissue oxygenation in human obesity: evidence for rarefaction, macrophage chemotaxis, and inflammation without an angiogenic response," *Diabetes*, vol. 58, pp. 718-725, 2009.
- [190] S. Torrades, "Stem cell research," *Elsevier*, vol. 22, no. 3, pp. 90-94, 2003.
- [191] J. P. Giraldo, J. I. Madero, M. Avila, S. Cuneo, C. Lopez, M. Escobar, A. Aparicio and J. Ruiz, "Stem cells," *Revista colombiana de obstetricia y ginecologia*, vol. 54, no. 2, pp. 87-96, 2002.
- [192] B. Reubinoff, "The clinical potential of human embryonic stem cells. En reproductive medicine in the twenty-first century. Eds. D.L. Healy, G. Kovacs, R. McLachlan, O. Rodriguez Armas," *The Parthenon publishing group*, pp. 454-461, 2001.
- [193] S. Temple, "The development of neural stem cells," *Nature*, vol. 414, pp. 112-117, 2001.
- [194] A. Spradling, B. Drummond and T. Kai, "Stem cells find their niche," *Nature*, vol. 414, pp. 98-104, 2001.
- [195] F. Watt and B. Hogan, " Out of eden: stem cells and their niches," *Science*, vol. 287, pp. 1427- 1430, 2000.
- [196] S. Perrini, L. Laviola, A. Cignarelli, M. Melchiorre, F. De Stefano and C. Caccioppoli, "Fat depot-related differences in gene expression, adiponectin secretion, and insulin action and signalling in human

- adipocytes differentiated in vitro from precursor stromal cells," *Diabetologia*, vol. 51, pp. 155-164, 2008.
- [197] S. Majka, Y. Barak and D. Klemm, "Concise review: adipocyte origins: weighing the possibilities," *Stem Cells*, vol. 29, pp. 1034-1040, 2011.
- [198] R. Ferrer-Lorente, M. Bejar, M. Tous, G. Vilahur and L. Badimon, "Systems biology approach to identify alterations in the stem cell reservoir of subcutaneous adipose tissue in a rat model of diabetes: effects on differentiation potential and function," *Diabetologia*, vol. 57, no. 246-256, 2014.
- [199] V. Van Harmelen, T. Skurk, K. Rohrig, Y. Lee, M. Halbleib and I. Aprath-Husmann, "Effect of BMI and age on adipose tissue cellularity and differentiation capacity in women," *Int J Obes Relat Metab Disord*, vol. 27, pp. 889-895, 2003.
- [200] S. Nair, H. Lee, E. Rousseau, M. Cam, P. Tataranni and L. Baier, "Increased expression of inflammation-related genes in cultured preadipocytes/stromal vascular cells from obese compared with non-obese Pima Indians," *Diabetologia*, vol. 48, pp. 1784-1788, 2005.
- [201] M. Roldan, M. Macias-Gonzalez, R. Garcia, F. Tinahones and M. Martin, "Obesity short-circuits stemness gene network in human adipose multipotent stem cells," *FASEB J.*, vol. 25, pp. 4111-4126, 2011.
- [202] M. Pertea, A. Shumate, G. Pertea, A. Varabyou, F. Breitwieser and Y. Chang, "CHESS: a new human gene catalog curated from thousands of large-scale RNA sequencing experiments reveals extensive transcriptional noise," *Genome Biol*, vol. 19, no. 1, p. 208, 2018.
- [203] E. Speliotes, C. Willer, S. Berndt, K. Monda, G. Thorleifsson and A. Jackson, "Association analyses of 249,796 individuals reveal eighteen new loci

- associated with body mass index," *Nat Genet*, vol. 42, no. 11, pp. 937-48, 2010.
- [204] J. Hebebrand, A. Volckmar, N. Knoll and A. Hinney, "Chipping Away the 'Missing Heritability': GIANT Steps Forward in the Molecular Elucidation of Obesity – but Still Lots to Go," *Obes Facts*, vol. 3, no. 5, pp. 294-303, 2010.
- [205] H. Funato, S. Oda, J. Yokofujita, H. Igarashi and M. Kuroda, "Fasting and high-fat diet alter histone deacetylase expression in the medial hypothalamus," *PLoS One*, vol. 6, no. 4, 2011.
- [206] M. Marcovecchio, L. Patricelli, M. Zito, R. Capanna, M. Ciampani and F. Chiarelli, "Ambulatory blood pressure monitoring in obese children: role of insulin resistance," *J Hypertens*, vol. 24, no. 12, pp. 2431-6, 2006.
- [207] M. D. Marrodán Serrano, J. R. Martínez-Álvarez, M. Sánchez-Álvarez, N. López-Ejeda, I. Alférez and A. Villarino Marín, "Prevalencia del fenotipo metabólicamente sano entre españoles adultos con exceso de peso," *Rev. P. Card.*, vol. 69, no. 2, pp. 216-217, 2016.
- [208] J. Stern and P. Johnson, "Spontaneous activity and adipose cellularity in the genetically obese Zucker rat (fa/fa)," *Metabolism*, vol. 26, pp. 371-380, 1977.
- [209] J. Vasselli, M. Cleary, K. Jen and M. Greenwood, "Development of food motivated behavior in free feeding and food restricted Zucker fatty (fa/fa) rats," *Physiol Behav*, vol. 25, pp. 565-573, 1980.
- [210] J. Thornhill, B. Taylor, W. Marshall and K. Parent, "Central, as well as peripheral naloxone administration suppresses feeding in food-deprived Sprague-Dawley and genetically obese (Zucker) rats," *Physiol Behav*, vol. 29, pp. 841-846, 1982.

- [211] J. Grinker, A. Drewnowski, M. Enns and H. Kissileff, "Effects of damphetamine and fenfluramine on feeding patterns and activity of obese and lean Zucker rats," *Pharmacol Biochem Behav*, vol. 12, pp. 265-275, 1980.
- [212] J. Vasselli, E. Harackiewicz, C. Maggio and M. Greenwood, "Effects of a glucosidase inhibitor (acarbose, BAY g 5421) on the development of obesity and food motivated behavior in obese Zucker (fafa) rats," *Pharmacol Biochem Behav*, vol. 19, pp. 85-95, 1983.
- [213] C. Maggio, E. Harackiewicz and J. Vasselli, "Diet composition alters the satiety effect of cholecystokinin in lean and obese Zucker rats," *Physiol Behav*, vol. 43, pp. 485-491, 1988.
- [214] C. Maggio and M. Greenwood, "Adipose tissue lipoprotein lipase (LPL) and triglyceride uptake in Zucker rats," *Physiol Behav*, vol. 29, pp. 1147-1152, 1982.
- [215] M. Cleary, J. Vasselli and M. Greenwood, "Development of obesity in Zucker obese (fa/fa) rat in absence of hyperphagia," *Am J Physiol*, vol. 238, pp. E284-E292, 1980.
- [216] D. Hausman, J. Fine, K. Tagra, S. Fleming, R. Martin and M. DiGirolamo, "Regional fat pad growth and cellularity in obese Zucker rats: modulation by caloric restriction," *Obesity Res*, vol. 11, pp. 674-682, 2003.
- [217] J. Wardle, C. Llewellyn, S. Sanderson and R. Plomin, "The FTO gene and measured food intake in children," *Int J Obes (Lond)*, vol. 33, pp. 42-5, 2009.
- [218] T. Rendo, A. Molerés and A. Martí Del Moral, "Effects of the FTO gene on lifestyle intervention studies in children," *Obes Facts*, vol. 2, pp. 393-9, 2009.

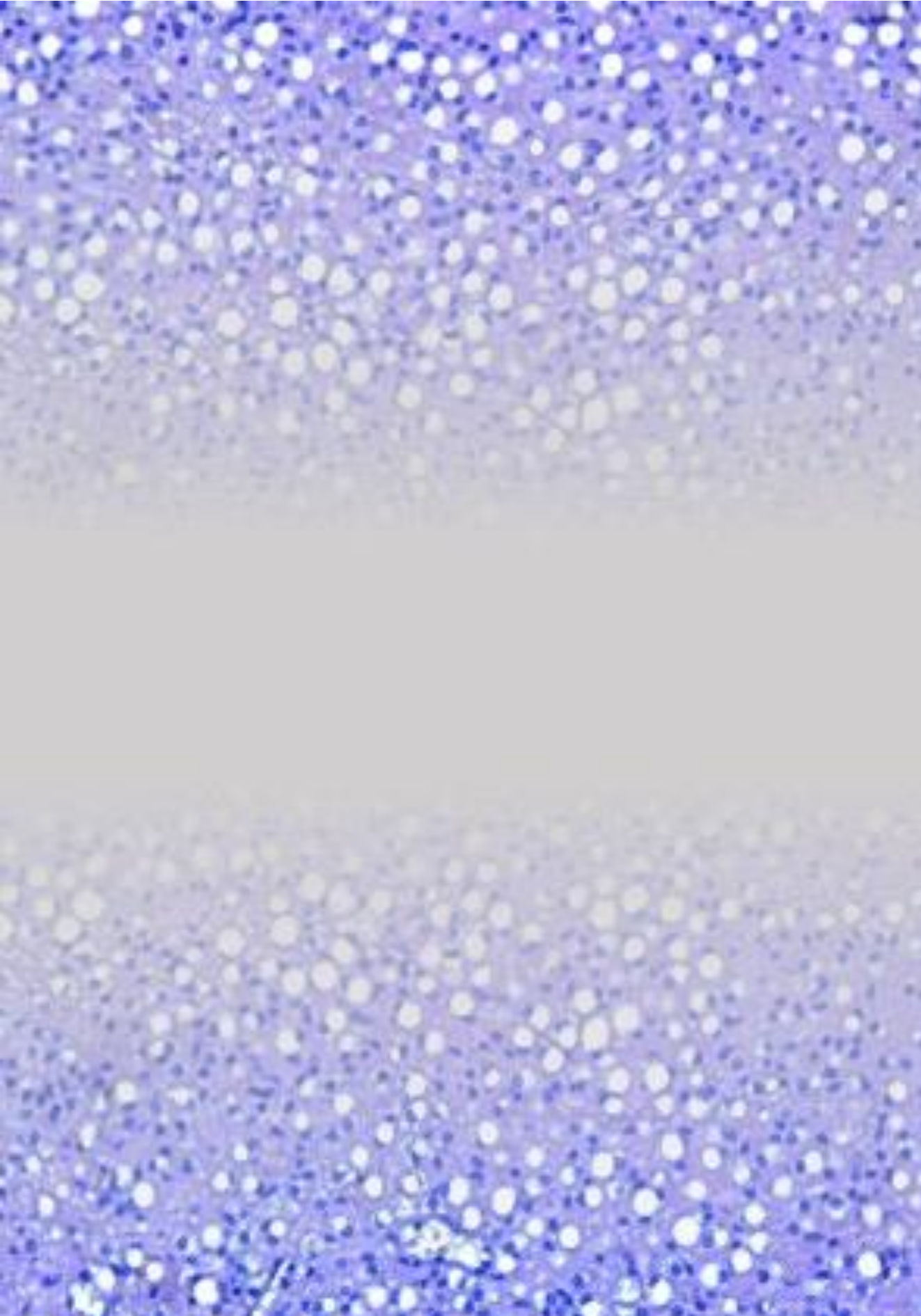


- [219] J. Bienertova-Vasku, L. Bienert P, Sablikova, L. Slo-vackova , M. Forejt, Z. Piskackova, L. Kucerova, K. Heczkova, Z. Brazdova and A. Vasku, "Effect of ID ACE gene polymorphism on dietary composition and obesity-related anthropometric parameters in the Czech adult population," *Genes Nutr*, vol. 4, pp. 207-13, 2009.
- [220] T. Rendo, A. Molerés and A. Martí Del Moral, "Effects of the FTO gene on lifestyle intervention studies in children," *Obes Facts*, vol. 2, pp. 393-9, 2009.
- [221] I. Arkadianos, A. Valdes, E. Marinós, A. Florou , R. Gill and K. Grimaldi, "Improved weight management using genetic information to personalize a calorie controlled diet," *Nutr J*, vol. 6, p. 29, 2007.
- [222] M. B. Silveira Rodríguez, L. . M. Piñeiro Muñoz and R. Carraro Casieri, "Nutrigenómica, obesidad y salud pública," *Rev. Esp. Salud Pública*, vol. 81, no. 5, pp. 475-487, 2007.
- [223] M. Moreno, "Definición y clasificación de la obesidad," *Revista Médica Clínica Las Condes*, vol. 23, no. 2, pp. 124-8, 2012.
- [224] A. Bonora Centelles, J. Castell and M. Gómez Lechón, "Células madre del tejido adiposo: plasticidad hepática," *Gastroenterol Hepatol*, vol. 31, no. 5, pp. 299-309, 2008.
- [225] J. Sánchez, C. Romero, L. Muñoz and R. Rivera, "Adipose organ, a metabolic and endocrine regulating rainbow," *Rev Cubana Endocrinol*, vol. 27, no. 1, pp. 105-19, 2016.
- [226] M. Legorreta-Herrera, F. Martínez-Flores, F. Hernández Sánchez and A. Zentella-Dehesa, "Los vectores virales y la transgénesis," *Vertientes Revista Especializada en Ciencias de la Salud*, vol. 15, no. 1, pp. 5-14, 2012.

- [227] L. Rodríguez, N. Gómez and D. Egaña, "El peso de lo social y la percepción del riesgo corporal," 27 Mayo 2021. [Online]. Available: <https://www.uchile.cl/noticias/176397/el-peso-de-lo-social-y-la-percepcion-del-riesgo-corpora>. [Accessed 02 agosto 2022].
- [228] V. Sacristán Fraile, "Ingeniería genética del tejido adiposo o del músculo esquelético mediante vectores aav-fgf21 para el tratamiento de la diabetes y la obesidad," Universitat Autònoma de Barcelona, Barcelona, 2018.
- [229] WHO, "Obesity and overweight," 9 July 2021. [Online]. Available: <https://www.who.int/news-room/fact-sheets/detail/obesity-and-overweight>.
- [230] M. Morillas, P. Gómez-Puertas and A. Bentebibel, "Identificación de residuos de aminoácidos conservados en carnitina palmitoiltransferasa I de hígado de rata críticos para la inhibición de malonil-CoA. La mutación de la metionina 593 suprime la inhibición de malonil-CoA," *J Biol Chem*, vol. 278, pp. 9058-9063, 2003.

The background of the slide is a microscopic image of plant tissue, likely a cross-section of a stem or root. It shows numerous small, circular cells with distinct cell walls, arranged in a somewhat regular pattern. The cells are stained, giving them a light purple or blue appearance. The overall texture is granular and cellular.

# **Scientific Production**



## 9 SCIENTIFIC PRODUCTION

1. **Implantation of CPT1AM-expressing adipocytes reduces obesity and glucose intolerance in mice. (submitted)** M Carmen Soler-Vázquez, Katia Delgado, Carles Calatayud, Paula Mera, Sebastián Zagmutt, Marianela Bastías-Pérez, Kevin Ibeas, Núria Casals, Antonella Consiglio, Dolors Serra, Laura Herrero.
2. **Cpt1a is required in AgRP neurons to control food intake and thirst in a sex-dependent manner. (submitted)** Sebastián Zagmutt, Paula Mera, Ismael González-García, Kevin Ibeas, Arnaud Obri, Beatriz Martin, Anna Esteve, M Carmen Soler-Vázquez, Marianela Bastías-Pérez, Laia Cañes, Elisabeth Augé, Carmen Pelegri<sup>1</sup>, Jordi Vilaplana, Xavier Ariza, Jordi García, José Martinez-González, Núria Casals, Miguel López, Elisenda Sanz, Albert Quintana, Laura Herrero, Dolors Serra.
3. **Dietary Options for Rodents in the Study of Obesity. Bastías-Pérez M, Serra D, Herrero L. Nutrients, 2020.**  
DOI: 10.3390/nu12113234.PMID: 33105762
4. **Impact of Adaptive Thermogenesis in Mice on the Treatment of Obesity. Bastías-Pérez M, Zagmutt S, Soler-Vázquez MC, Serra D, Mera P, Herrero L. Cells, 2020.**  
DOI: 10.3390/cells9020316.PMID: 32012991

\*Authors contributed equally to this work.





